

PUBLISHER :



Address of Publisher & Editor's Office :

GDAŃSK UNIVERSITY
OF TECHNOLOGY
Faculty
of Ocean Engineering
& Ship Technology

ul. Narutowicza 11/12
80-952 Gdańsk, POLAND
tel.: +48 58 347 13 66
fax: +48 58 341 13 66
e-mail : office.pmr@pg.gda.pl

Account number :
BANK ZACHODNI WBK S.A.
I Oddział w Gdańsku
41 1090 1098 0000 0000 0901 5569

Editorial Staff :

Kazimierz Kempa Editor in Chief
e-mail : kkempa@pg.gda.pl

Przemysław Wierchowski Scientific Editor
e-mail : e.wierchowski@chello.pl

Jan Michalski Editor for review matters
e-mail : janmi@pg.gda.pl

Tadeusz Borzęcki Editor for international relations
e-mail : tadbtor@pg.gda.pl

Piotr Bzura Managing Editor
e-mail : pbzura@pg.gda.pl

Cezary Spigarski Computer Design
e-mail : biuro@oficynamorska.pl

Domestic price :
single issue : 20 zł

Prices for abroad :
single issue :
- in Europe EURO 15
- overseas US\$ 20

ISSN 1233-2585



POLISH MARITIME RESEARCH

in internet

www.bg.pg.gda.pl/pmr/pmr.php



POLISH MARITIME RESEARCH

No 3(57) 2008 Vol 15

CONTENTS

- 3 **MAGDALENA KAUP**
Functional model of river-sea ships operating in European system of transport corridors. Part I. Methods used to elaborate functional models of river-sea ships operating in European system of transport corridors
- 12 **JANUSZ KOLENDA**
On the behaviour of viscoelastic solids under multiaxial loads
- 18 **KAZIMIERZ TRĘBACKI**
Modelling of vibrations of a liquid filled tank
- 28 **ZYGMUNT PASZOTA**
Graphical presentation of the power of energy losses and power developed in the elements of hydrostatic drive and control system. Part I. Rotational hydraulic motor speed series throttling control systems
- 38 **PIOTR KRZYŚLAK, MARIAN WINOWIECKI**
A method of diagnosing labyrinth seals in fluid-flow machines
- 42 **DAMIAN BOCHENSKI**
Investigations of operational driving loads of bucket chains and manoeuvre hoisting winches on multi-bucket dredgers
- 49 **LESZEK MATUSZEWSKI**
The application of magnetic fluids in sealing nodes designed for operation in difficult conditions and in machines used in sea environment
- 59 **ZYGMUNT SYCHTA**
Complex approach to selection and evaluation of the fire safety measures to be applied during repair of refrigerated holds
- 67 **RYSZARD KŁOS**
Removal of oxidizable contaminations contained in submarine atmosphere
- 70 **MIECZYŚLAW HANN**
Simulation method for determination of human reliability function taking stress into consideration
- 77 **IOURI N. SEMENOV**
The multidimensional approach to marine industry development. Part I. Obstacles and willingness to the EU marine industry reengineering
- 86 **ZBIGNIEW KORCZEWSKI**
Application of expert systems in diagnostics, management and logistics
- 92 **MARIA MELER-KAPCIA**
Algorithm for searching out similar ships within expert system of computer aided preliminary design of ship power plant

The papers published in this issue have been reviewed by:
Prof. J. Badur ; Prof. A. Balawender ; Prof. A. Brandowski
Prof. C. Dymarski ; Prof. J. Girtler ; Prof. M. Hann
Prof. I. N. Semenov ; Prof. J. A. Szantyr

Editorial

POLISH MARITIME RESEARCH is a scientific journal of worldwide circulation. The journal appears as a quarterly four times a year. The first issue of it was published in September 1994. Its main aim is to present original, innovative scientific ideas and Research & Development achievements in the field of :

Engineering, Computing & Technology, Mechanical Engineering,

which could find applications in the broad domain of maritime economy. Hence there are published papers which concern methods of the designing, manufacturing and operating processes of such technical objects and devices as : ships, port equipment, ocean engineering units, underwater vehicles and equipment as well as harbour facilities, with accounting for marine environment protection.

The Editors of POLISH MARITIME RESEARCH make also efforts to present problems dealing with education of engineers and scientific and teaching personnel. As a rule, the basic papers are supplemented by information on conferences , important scientific events as well as cooperation in carrying out international scientific research projects.

Scientific Board

Chairman : Prof. **JERZY GIRTLEK** - Gdańsk University of Technology, Poland

Vice-chairman : Prof. **ANTONI JANKOWSKI** - Institute of Aeronautics, Poland

Vice-chairman : Prof. **MIROSLAW L. WYSZYŃSKI** - University of Birmingham, United Kingdom

Dr **POUL ANDERSEN**
Technical University
of Denmark
Denmark

Dr **MEHMET ATLAR**
University of Newcastle
United Kingdom

Prof. **GÖRAN BARK**
Chalmers University
of Technology
Sweden

Prof. **SERGEY BARSUKOV**
Army Institute of Odessa
Ukraine

Prof. **MUSTAFA BAYHAN**
Süleyman Demirel University
Turkey

Prof. **MAREK DZIDA**
Gdańsk University
of Technology
Poland

Prof. **ODD M. FALTINSEN**
Norwegian University
of Science and Technology
Norway

Prof. **PATRICK V. FARRELL**
University of Wisconsin
Madison, WI
USA

Prof. **WOLFGANG FRICKE**
Technical University
Hamburg-Harburg
Germany

Prof. **STANISŁAW GUCMA**
Maritime University of Szczecin
Poland

Prof. **ANTONI ISKRA**
Poznań University
of Technology
Poland

Prof. **JAN KICIŃSKI**
Institute of Fluid-Flow Machinery
of PASci
Poland

Prof. **ZYGMUNT KITOWSKI**
Naval University
Poland

Prof. **JAN KULCZYK**
Wrocław University of Technology
Poland

Prof. **NICOS LADOMMATOS**
University College London
United Kingdom

Prof. **JÓZEF LISOWSKI**
Gdynia Maritime University
Poland

Prof. **JERZY MATUSIAK**
Helsinki University
of Technology
Finland

Prof. **EUGEN NEGRUS**
University of Bucharest
Romania

Prof. **YASUHIKO OHTA**
Nagoya Institute of Technology
Japan

Prof. **KRZYSZTOF ROSOCHOWICZ**
Gdańsk University
of Technology
Poland

Dr **YOSHIO SATO**
National Traffic Safety
and Environment Laboratory
Japan

Prof. **KLAUS SCHIER**
University of Applied Sciences
Germany

Prof. **FREDERICK STERN**
University of Iowa,
IA, USA

Prof. **JÓZEF SZALA**
Bydgoszcz University
of Technology and Agriculture
Poland

Prof. **TADEUSZ SZELANGIEWICZ**
Technical University
of Szczecin
Poland

Prof. **WITALIJ SZCZAGIN**
State Technical University
of Kaliningrad
Russia

Prof. **BORIS TIKHOMIROV**
State Marine University
of St. Petersburg
Russia

Prof. **DRACOS VASSALOS**
University of Glasgow
and Strathclyde
United Kingdom

Functional model of river-sea ships operating in European system of transport corridors

Part I.

Methods used to elaborate functional models of river-sea ships operating in European system of transport corridors

Magdalena Kaup, Ph. D.
Szczecin University of Technology

ABSTRACT



This paper presents a functional model of river-sea ships (shortly called: SRM) operating in European system of transport corridors. It is composed of two parts: Part I contains a descriptive model of functioning the SRM fleet with taking into account various shipping tasks as well as impact factors (external and internal factors, limitations and criteria). Also, a mathematical model of functioning the SRM fleet, including choice of relevant economic criteria (e.g. profit maximization, capital return period minimization etc), is presented. Results achieved on the basis of the functional model are presented in Part II of the paper.

Keywords: European system of transport, river-sea ships, river-sea transport system, water transport

INTRODUCTION

If current linear and point infrastructure of water transport over a given area and database of geography of cargo flows are at disposal, one can select such way of transport, out of those available, which will satisfy requirements of both cargo-providers and cargo-recipients at an accepted level of values of technical, economical, functional and environmental criteria. However various strategies of cargo shipping and loading should be considered. In order to select a concrete shipping strategy to be applied to river-sea transport system it is necessary to elaborate in advance a model of functioning the SRM fleet, that means:

- ❖ elaboration of possible schemes of the functioning of river-sea ships
- ❖ determination of permissible zone of operation of river-sea ships
- ❖ adjusting the selected shipping strategy to shipping route
- ❖ elaboration of a mathematical model for assessing the functioning of river-sea ships according to different scenarios
- ❖ elaboration of technical design assumptions for river-sea ships.

SHIPPING TASKS AND FUNCTIONING SCHEMES OF RIVER-SEA SHIPS

The functioning of river-sea ships has been always and still is subordinated to concrete shipping tasks, i.e. transport of a given amount of cargo over a given route within a given period. On them is dependent the functioning scheme and kind of assumed shipping strategies. Form of river-sea shipping tasks in European system of water transport corridors depends on:

- rate of cargo flows
- direction of cargo flows
- geography of inland waterways and sea routes
- traffic capacity of inland waterways
- functional parameters and location of ports.

Essence of a given shipping task depends on:

- length of shipping route
- number and traffic capacity of sea and inland ports, locks etc, planned to be used
- permissible speed of transport units on a given waterway,
- kind and amount of cargo shipment within a planned cargo flow
- traffic limitations on inland waterways, e.g. seasonal ones.

The following transport strategies should be taken into account for river-sea shipping:

- shuttle mode – consists in shipping between two terminal ports
- linear mode – consists in regular shipping between selected ports in compliance with a given schedule
- delivery (tender) mode – consists in shipping between two ports where one of them can be used as an intermediate port
- block – shipment mode – consists in shipping between two terminal ports which may be different depending on instantaneous demand on shipping services.


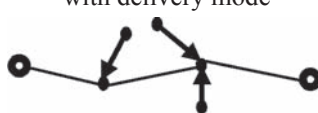

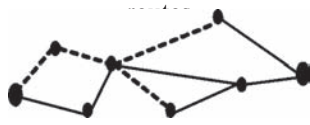
Among the strategies dependent on shipping task other types can be also distinguished. Some of them are given in Tab. 2. Characteristic features of the basic shipping strategies are presented in Tab. 1.

Tab. 1. Shipping strategies in river-sea transport

No.	Strategy type	Advantages	Disadvantages
1.	Shuttle mode	<ul style="list-style-type: none"> short transport time, regularity of connections certainty of shipping orders/ tasks 	<ul style="list-style-type: none"> necessity of having permanent cargo flows problems in ensuring full cargo load
2.	Linear mode	<ul style="list-style-type: none"> regularity of connections possible application to long distance routes possible tending small shipments, 	<ul style="list-style-type: none"> relatively long duration time of transport resulting from using intermediate ports
3.	Delivery (tender) mode	<ul style="list-style-type: none"> short transport time relatively high usage effectiveness possible supplementing the shipped cargo mass 	<ul style="list-style-type: none"> necessity of having additional shipping orders/tasks problems with ensuring full cargo load for ship a shipping coordination system is required
4.	Block-shipment mode	<ul style="list-style-type: none"> easy to use not requiring permanent cargo flows possible application to routes in a broad range of length. 	<ul style="list-style-type: none"> lack of regularity of connections necessity of shipping coordination.

Source: The author's concept

Tab. 2. Adjustment of permissible shipping strategies to shipping tasks in river-sea transport system

No.	Shipping tasks	Permissible shipping strategy
1.	Direct cargo shipping mode  (DCS group)	<ul style="list-style-type: none"> shuttle mode direct linear mode
2.	Cargo shipping in accordance with delivery mode  (CSDS group)	<ul style="list-style-type: none"> intermediate linear mode delivery mode (along supply sections) block - shipment mode (along supply sections)
3.	Cargo shipping in accordance with shipment consolidation mode  (CSSCS group)	<ul style="list-style-type: none"> „hub and arms” mode consolidation and decomposition mode
4.	Cargo shipping in accordance with multi-variant mode of  (CSMSR group)	<ul style="list-style-type: none"> linear mode with reserve connections Y-shuttle mode

Source: The author's concept

Assessment of the functional effectiveness of river-sea ships as to shipping tasks can be performed by adjusting the shipping strategies as well as functioning schemes to a given shipping task.

When the types of shipping tasks and strategies presented in Tab. 1, 2 and 3, are taken into account a set of possible solution variants of the functional model of river-sea ships can be formed. Each of them should be decomposed in order to obtain one preferable functioning scheme of river-sea ships which contains detail information resulting from a considered shipping task. For every permissible connection of ports through a water transport corridor it is possible to perform calculations on the basis of which optimum functioning strategies of river-sea ships as well as design assumptions for them can be determined.

From the information contained in Tab. 2 it results that different shipping tasks can be aggregated into 4 basic groups which correspond with 9 permissible strategies.

To each of the groups concrete shipping strategies can be attributed. This can be illustrated e.g. by CSDS group to which, by making use of the intermediate linear strategy, the shipping task given in the Scheme 2 of Tab. 3, corresponds, and in the case of DCS group and the shuttle strategy - the task given in Scheme 1 of Tab. 3.

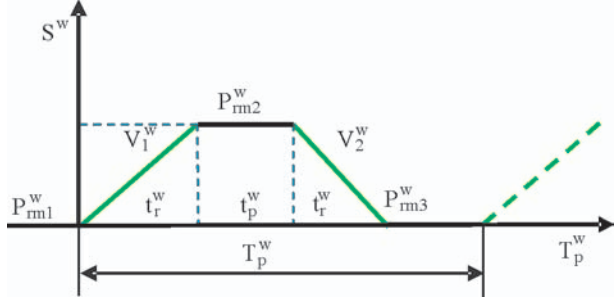
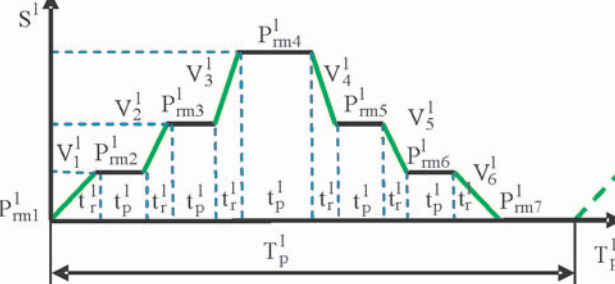
FACTORS WHICH FORM FUNCTIONAL MODEL OF THE FLEET OF RIVER-SEA SHIPS

The functional effectiveness of river-sea ships in European system of transport corridors in accordance with concrete shipping tasks depends – directly or indirectly- on many external and internal factors (Fig. 1). The factors, depending on a considered navigation zone and characteristics of cargo flows over a given area, contribute - in a positively (e.g. low shipping rates, social acceptance) or negatively (e.g. ship speed limitation, low class of waterways, low traffic capacity of ports and locks) to the effectiveness of fulfilling the shipping tasks.

Apart from the forming factors, also technological and financial limitations etc influence the functional effectiveness of river-sea ships. Therefore, is of a great importance to appropriately choose criteria (Fig. 2) according to which it will be possible to select the most effective system of functioning the SRM fleet in line with features of serviced cargo flows.

Models of functioning the river-sea ships in European system of water transport corridors greatly depend on changes in the external and internal factors. These constitute premises for building a multi-variant functional model of ships of the kind in question.

Tab. 3. Selected examples of functional schemes of river-sea ship accomplishing concrete shipping tasks

No.	Shipping strategy	Functioning scheme in accordance with a given shipping task
1.	<ul style="list-style-type: none"> ▪ shuttle mode 	 <p style="text-align: center;">Scheme 1</p>
2.	<ul style="list-style-type: none"> ▪ intermediate linear mode 	 <p style="text-align: center;">Scheme 2</p>

Source: The author's concept

where:

T_p^w – cargoload shipping period of river-sea ship [days]

S^p – assumed length of shipping route [km]

t_r – voyage period [days]

t_p – port lying period [days]

V – permissible service speed [km/h]

P_{rm} – particular river-sea ports.

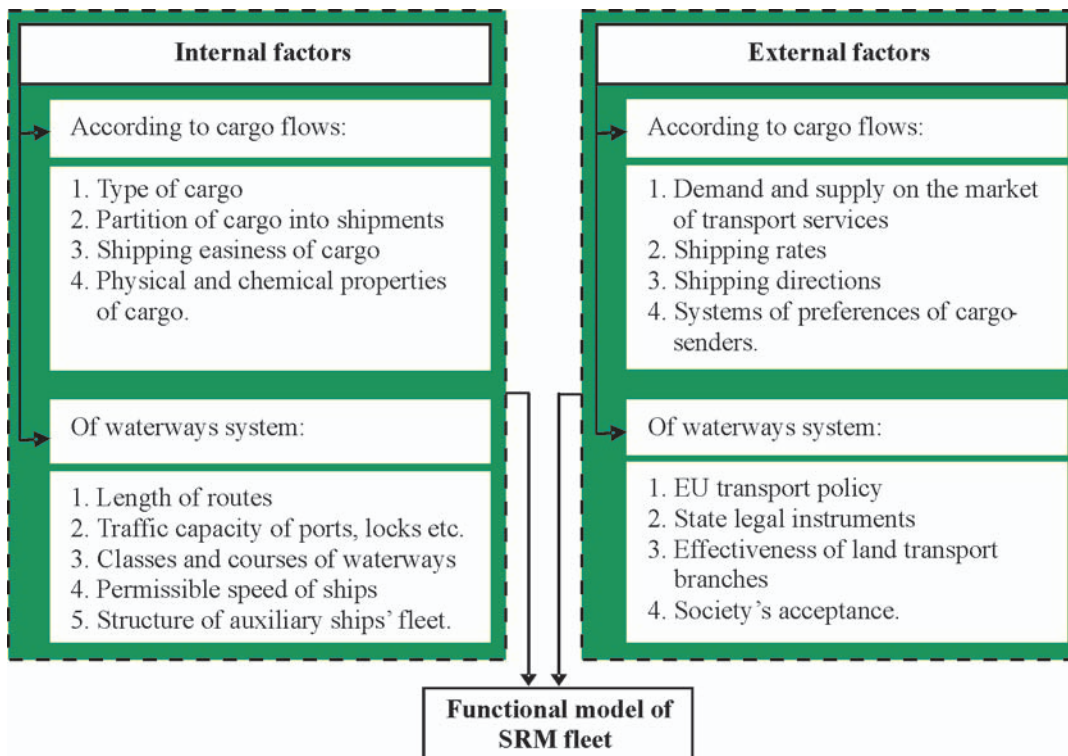


Fig. 1. Factors taken into account in assessing the SRM fleet shipping effectiveness.

Source: The author's concept

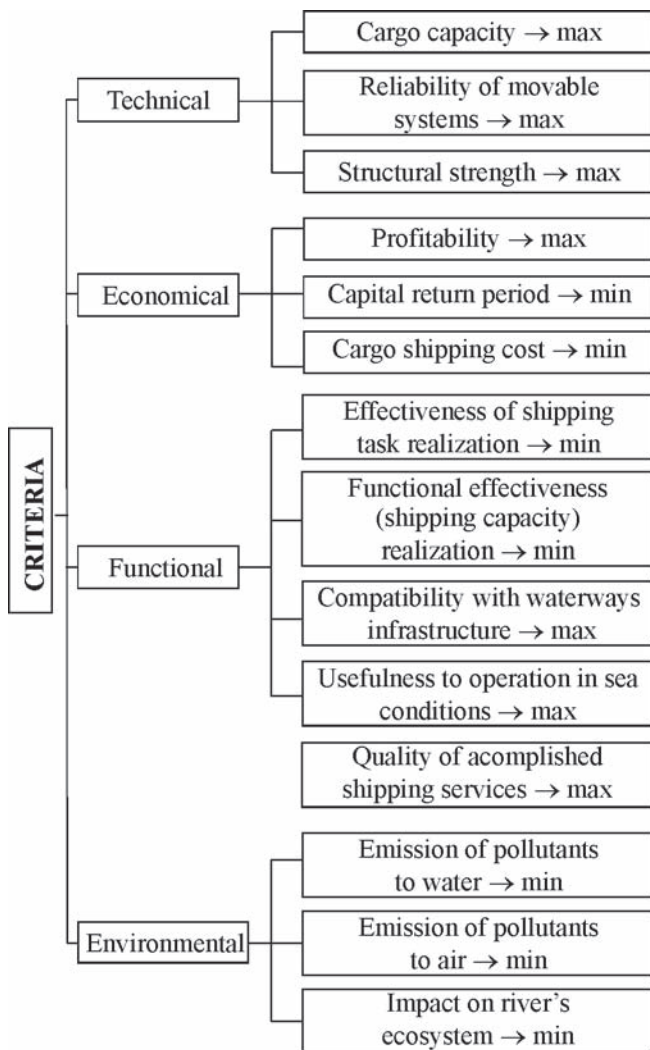


Fig. 2. Set of criteria for assessing the acceptability of SRM fleet structures.
Source: The author's concept

MATHEMATICAL MODEL OF FUNCTIONING THE FLEET OF RIVER-SEA SHIPS

Decision variables in the mathematical model of functioning the fleet of river-sea ships

The mathematical model of functioning the river-sea ships can be elaborated in compliance with the principles presented by Tarnowski [6]. The first step in building such model is to determine parameters and decision variables. In the case in question for each of the schemes of operation of such ships the following can be distinguished:

- Assumed parameters, namely:
 - ⤴ rate of cargo flow – W [mln t/year]
 - ⤴ length of shipping route – S [km]
 - ⤴ port cargo handling capacity – Z_p [t/day]
 - ⤴ season (of the year) – S_z [-].
- Searched decision variables, namely:
 - ⤴ type of ship (bulk cargo carrier, tanker, versatile river-sea ship)
 - ⤴ Cargo carrying capacity (permissible mass of shipped cargo) – M_{lad} [t]
 - ⤴ ship speed – V [km/h]
 - ⤴ number of ships necessary to cope with cargo flows on a given shipping route – n_{s_i} [units/year].

Limitations in the mathematical model of functioning the fleet of river-sea ships

In the mathematical model of functioning the river-sea ships - for the reason of a large number of investigated variants and a broad range of parameters of cargo flows – definite areas of planned investigations should be distinguished, including the following:

- possible solutions for SRM fleet
- permissible solutions for SRM fleet.

Geometry of area of possible solutions results from rates and directions of cargo flows. Geometry of area of permissible solutions results from real situation on both waterways and market of transport services.

Limitations of the mathematical model of functioning the river-sea ships can be divided into:

- qualitative ones,
- quantitative ones.

Qualitative limitations have been already systematized in Fig. 3, and quantitative ones are as follows:

- concerning SRM fleet:
 - maximum permissible shipping period, according to shipping task – T_{pmax} [days]
 - minimum possible frequency of ship arrivals to port, according to structure of the fleet – n_{wmin} [units/day]
 - maximum permissible ship deadweight on a given route, according to river bed parameters – DWT_{max} [t]
 - maximum permissible ship speed on a given waterway, according to navigation standards – V_{max} [km/h]
 - maximum permissible cargo shipping cost, according to requirements of orderers – KT_{max} [€/(t*km)].
- concerning cargo flows:
 - both maximum and minimum permissible amount of cargo shipments accepted on ship board, their masses and volumes, according to shipping tasks.

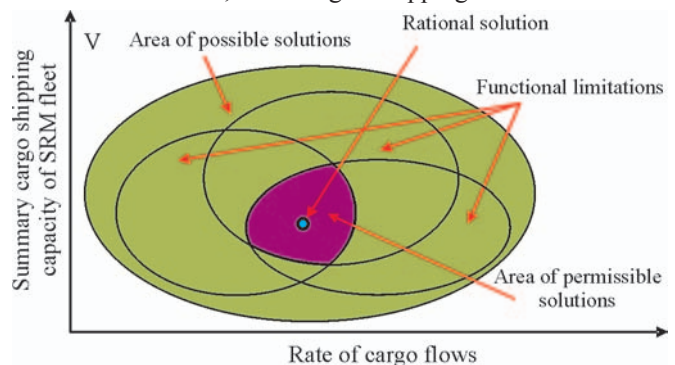


Fig. 3. Example geometry of areas of possible and permissible solutions of SRM fleet functioning.
Source: The author's concept

Mathematical description of functioning the SRM fleet. Functional criteria and their place in the model

The mathematical model of the river-sea ships' functioning consists in checking the effectiveness of the conditions for SRM fleet structure in compliance with the following functional criteria:

A. Functional effectiveness according to the „point-to-point” principle

General assumptions:

The functional effectiveness of every SRM group incorporated to the fleet's structure should be maximum:

$$\sum_i E_i \rightarrow \max \quad (1)$$

under the condition:

$$\sum_i E_i \geq W \quad (2)$$

where:

W – assumed cargo flow rate [mln t/year]
 $\sum_i E_i$ – functional effectiveness (shipping capacity) of SRM fleet [mln t/year].

And, necessary values of the criterion should be determined by using the following relationships:

$$\sum_i E_i = n_{s_i} \cdot n_{r_i} \cdot M_{lad_i} \quad (3)$$

$$n_{r_i} = \frac{(365 - t_{rm})}{T_{p_i}} \quad (4)$$

where:

n_{s_i} – number of river-sea ships of i-th group, necessary to cope with cargo flows on a given shipping route [ships/year]
 n_{r_i} – number of voyages possible to be performed by i-th group of ships during one year [voyages/year]
 M_{lad_i} – permissible mass of cargo shipped on board the ships of i-th group [t]
 t_{rm} – duration time of repairs, inspections [days]
 T_{p_i} – duration time of cargo shipping by the ships of i-th group [days].

Types of shipping tasks:

a) DCS and CSSCS group

$$T_p = (t_r + t_p) \quad (5)$$

where:

t_r – calculated period of river-sea ship's voyage [days]
 t_p – calculated period of river-sea ship's port lying [days].

And:

$$t_r = \frac{S}{V} \quad (6)$$

$$t_p = \frac{M_{lad}}{Z_p} \quad (7)$$

where:

S – assumed length of shipping route [km]
V – required service speed of river-sea ship [km/h]
 M_{lad} – permissible mass of shipped cargo [t]
 Z_p – assumed cargo handling capacity of port [t/day].

b) CSDS and CSMSR group

$$T_p = \sum_{i=1}^n (t_{r_i} + t_{p_i}) \quad (8)$$

where:

t_{r_i} – period of i-th voyage [days]
 t_{p_i} – period of i-th lying in i-th port [days].

And:

$$t_{r_i} = \frac{S_i}{V_i} \quad (9)$$

$$t_{p_i} = \frac{\Delta M_{lad_i}}{Z_{p_i}} \quad (10)$$

where:

S_i – length of i-th section of shipping route [km]
 V_i – ship speed over i-th section of shipping route [km/h]

ΔM_{lad_i} – mass of cargo handled in i-th port [t]
 Z_{p_i} – assumed cargo handling capacity of i-th port [t/day].

B. Effectiveness of shipping task accomplishment according to the „just-in-time” principle

General assumptions:

Effectiveness of shipping task accomplishment should be maximum provided it does not exceed the period given in the shipping agreement:

$$S_p \rightarrow \max \quad (11)$$

under the condition:

$$T_p \leq T_u \quad (12)$$

where:

S_p – effectiveness of shipping task accomplishment [-]
 T_p – cargo shipping period [days]
 T_u – cargo shipping period given in the shipping agreement [days].

Types of shipping tasks:

- For the groups: DCS and CSSCS T_p value should be determined on the basis of the relation (5).
- For the groups: CSDS and CSMSR T_p value should be determined on the basis of the relation (8).

C. „Shipping service quality” according to the ALARP principle

Quality of shipping service should be maximum:

$$Q \rightarrow \max \quad (13)$$

under the condition:

$$Q \geq Q_{wp} \quad (14)$$

where:

Q – shipping service quality (percentage of cargo mass accepted by cargo receivers without any claims as to its state) [%]
 Q_{wp} – required quality of shipping service [%].

The shipping service quality can be considered as a risk of non-fulfilment of client's demands contained in the shipping agreement. It should be lower than an acceptable risk level estimated by underwriters on the basis of the following factors: ship age, crew experience, crew certificates, date of survey, failure statistics etc. Risk is the product of failure probability and loss resulting from the failure.

Therefore:

$$R_{su} \geq R_{wp}^n \quad (15)$$

where:

R_{su} – risk level estimated by underwriters [mln €]
 R_{wp}^n – risk of non-fulfilment of client's demands [mln €]

hence:

$$P_{su} * S_{su} \geq P_{wp}^n * S_{wp}^n \quad (16)$$

where:

P_{su} – probability of failure occurrence during accomplishment of shipping service (estimated by underwriters) [%]
 S_{su} – possible financial loss suffered by underwriters [mln €]
 P_{wp}^n – probability of non-fulfilment of client's demands [%]
 S_{wp}^n – possible loss suffered due to non-fulfilment of client's demands [mln €].

And:

$$P_{su} > P_{wp}^n \quad (17)$$

$$S_{su} > S_{wp}^n \quad (18)$$

$$P_{wp}^n = P_{lad}^n * P_t^n * P_m^n \quad (19)$$

where:

P_{lad}^n – probability of not coping with demanded shipping service quality (cargo delivery associated with claims as to its state from the side of its receiver [%])

P_t^n – probability of non-delivery of cargo to its receiver within a given period [%]

P_m^n – probability of non-delivery of cargo to its receiver to a given place [%].

Each of the probabilities can be realized independently to other ones. Therefore the product (19) is valid.

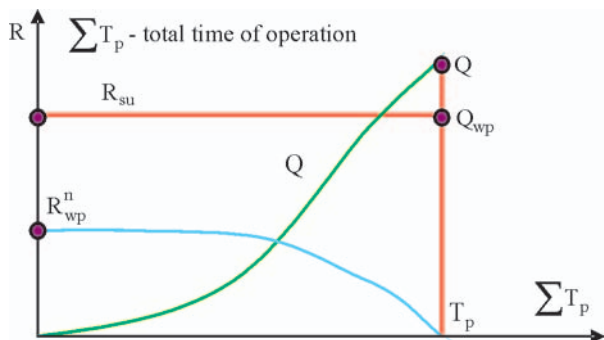
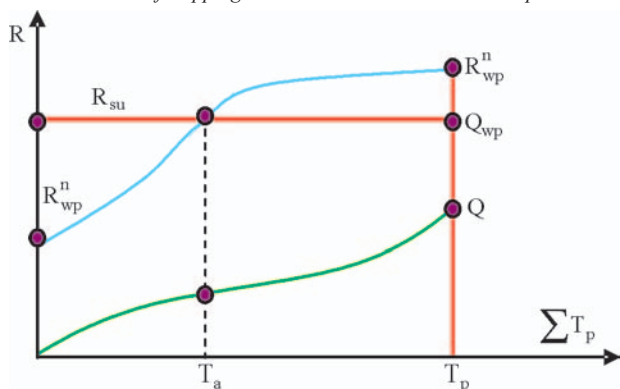


Fig. 4. Example of an acceptable shipping variant with a view of shipping risk. Source: The author's concept



T_a - instant of probable failure occurrence during ship service

ΣT_p - total time of service

Fig. 5. Example of an unacceptable shipping variant with a view of shipping risk. Source: The author's concept

Hence, the probability of fulfilment of conditions of demanded shipping service quality (P_{wp}) is equal to:

$$P_{wp} = 1 - P_{wp}^n \quad (20)$$

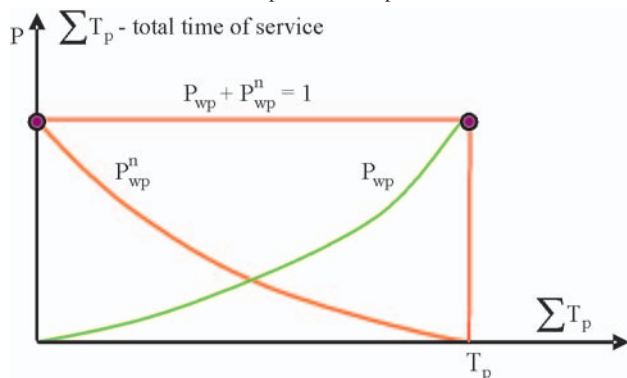


Fig. 6. Example of dynamic changes in probabilities of fulfilment or non-fulfilment of conditions of demanded shipping service quality. Source: The author's concept

The above presented kinds of probabilities are directly connected with safety of river-sea ships. According to J. Semenov [5], in order to determine their values, it is necessary to apply - to failure risk estimation practice - such characteristics which would be capable of ensuring objective control of shipping service quality to the ships in question. Statistical indices are suitable to solve the problem. They are formulated on the basis of statistical information and characterize a safety level of existing river-sea ships regarding causes which have led to failure of any particular ship. They can be divided into absolute and relative ones.

Absolute statistical indices

Such indices are formed to estimate safety level of transport units within a given period of their operation (year, month etc). These are a.o.:

- ▲ number of failures of a considered type of ships, and associated casualties
- ▲ number and deadweight of lost ships of a considered type, and associated loss of property
- ▲ number and value of lost cargo, and associated loss of profits
- ▲ size of pollution resulting from failures and associated cost of its liquidation etc.

Relative statistical indices

Such indices are formed to estimate safety level related to absolute statistical data. These are a. o. as follows:

- ✦ number of voyages of failed river-sea ships versus their total number
- ✦ amount of cargo shipments accepted with claims as to their state versus their total amount
- ✦ duration time and length of voyages of failed ships versus total period of their service.

The relative failure frequency indices can be used to assess the achieved levels of:

- ★ safety of operation of river-sea ships
- ★ service life of ships of a considered type
- ★ technical perfectness of shipboard, power and technological devices installed on river-sea ships
- ★ professional preparedness and discipline of crews of river-sea ships
- ★ organization and support of rescue actions.

The main value of the specified statistical indices is its objectiveness. Though they possess many important drawbacks, e.g.:

- ✦ they reflect only past events
- ✦ they can not be fully used for solving distant-future tasks.

To analyze causes of failure frequency is necessary because of possible multiple factors disturbing safe navigation modes.

Failure frequency characteristics according to causes of failure occurrence

On the basis of such characteristics it is possible to objectively assess navigation safety of river-sea ships as compared with other types of failure frequency due to a given cause during a given period (year, month etc). A set of such characteristics should be formed on the basis of the following principles:

- ✦ every characteristic is represented by probability distributions of its parameters in all modes of functioning the SRM
- ✦ probability of passing the river-sea ship into failure functioning mode is reflected by occurrence of endangering factors which can be of subjective or objective character

- possibility of recovering the safe functioning modes of river-sea ships should be assessed depending on adequacy of resources planned to be used for normalizing the functioning mode of a given type of ships (such resources can be of technical, organizational, social and legal character).

Economic criteria used in the functional model of the SRM fleet

In order to select one rational solution, out of possible variants, it is necessary to perform an economical analysis in which economic criteria will be taken into account. For the reason of reaching the information certainty level which has been usually faced, the following criteria seem to be most effective:

- expected profitability of shipping services - Z [mln €], and $Z \rightarrow \max$
- predicted return period of invested capital - PBP [years], and PBP $\rightarrow \max$
- cargo shipping cost -KT [€/t*km], and $KT \rightarrow \min$.

A. The profitability of river-sea ships can be determined on the basis of the following relationship:

$$Z = WE - KE \quad (21)$$

where:

- WE – expected incomes from the SRM fleet operation [mln €/year]
- KE – operational cost of the SRM fleet [mln €/year].

The above mentioned incomes can be determined on the basis of the relationships:

$$WE = n_{s_i} * M_{lad_i} * n_{r_i} * f_r \quad (22)$$

$$f_r = S * f_{r_j} \quad (23)$$

where:

- f_r – freight rate [€/t]
- f_{r_j} – unit shipping rate [€/t*km].

The quantities: n_{s_i} , M_{lad_i} , n_{r_i} have been already defined in page 7 (3).

Yearly operation cost of the SRM fleet can be determined on the basis of the relationship:

$$KE = (KZ + KB) * n_{s_i} \quad (24)$$

where:

- KZ – cost of invested capital return [mln €/year]
- KB – current maintenance costs of one river-sea ship [mln €/year].

The cost of invested capital return can be determined from the following relationship:

$$KZ = CR[KI - KZL(1 - i)^e] \quad (25)$$

$$CR = \frac{(1+i)^e \cdot i}{(1+i)^e - 1} \quad (26)$$

$$KI = 4.12 + 0.010369 \cdot DWT^{0.717338} \pm \Delta_1 \quad (27)$$

where:

- CR – coefficient of invested capital return period [-]
- KI – investment cost of river-sea ship [mln €/year]
- KZL – price of a ship excluded from service, equivalent to its scrapping value [mln €]
- i – credit interest per year [%]
- e – credit payback period [years]
- Δ_1 – correction for specificity of river sea ship ($\Delta_1 = \pm 0.14$) [mln €].

Eq. (27) was elaborated on the basis of worldwide prices of cargo ships of main types [CTO (Ship Design and Research Center, Poland) Market information].

On the basis of information published in the *Shiprepair* journal in the years 1999-2006 it can be assumed that:

$$KZL = 0.1 \cdot KI \pm 0.007 \quad (28)$$

The current costs can be determined from the following relationship:

$$KB = KBZ + KBK + KBU + KR \quad (29)$$

where:

- KBZ – personnel costs (crew wages and boarding) [mln €/year]
- KBK – repair and maintenance costs [mln €/year]
- KBU – ship and cargo insurance costs [mln €/year]
- KR – ship operation expenditures [mln €/year].

It can be assumed that:

$$KBZ = \frac{k_1 \cdot n_{zal} \cdot w}{10^6} \quad (30)$$

$$KBK = k_2 \cdot KI \quad (31)$$

$$KBU = 0.022 \cdot (KI)^{0.99} \quad (32)$$

$$KR = KRP + KRO \quad (33)$$

where:

- k_1 – number of month of labour of one crew member [months]
- n_{zal} – required number of crew members [persons]
- w – mean monthly wage of one crew member [€]
- k_2 – coefficient of repair and maintenance costs [-]
- KRP – costs of propulsion fuel oil [mln €/year]
- KRO – costs of ship servicing in ports (including: charges for: cargo handling, port servicing and agent's servicing) [mln €/year].

And:

$$KRP = \frac{t_r \cdot n_r \cdot h_{pal} \cdot C_{pal}}{10^6} \quad (34)$$

$$KRO = \frac{t_p \cdot n_p \cdot \beta \cdot GT + \chi \cdot M_{lad}}{10^6} \quad (35)$$

where:

- t_r – calculated period of voyage of river-sea ship [days]
- t_p – calculated period of port lying of river-sea ship [days]
- n_r – number of voyages of river-sea ship per year [units/year]
- h_{pal} – assumed fuel consumption per hour [t/h]
- C_{pal} – assumed fuel price [€/t]
- n_p – number of port-lyings of river-sea ship per year [units/year]
- β – assumed port service charge [€/t]
- GT – designed gross register tonnage of river-sea ship [t] (Fig. 7)
- χ – assumed cargo handling charge [€/t].

It can be assumed that:

$$n_p = k_3 \cdot n_r \quad (36)$$

$$h_{pal} = N \cdot h_{pal}^j \cdot 10^{-6} \quad (37)$$

$$N = \frac{D^{\frac{2}{3}} \cdot V^3}{C} \quad (38)$$

where:

- k_3 – coefficient of shipping task complexity [-]
- N – designed output of river-sea ship power plant [kW]
- D – designed displacement of river-sea ship [t]
- V – required service speed of river-sea ship [km/h]
- h_{pal}^j – assumed specific fuel oil consumption during ship voyage [g/kWh]
- C – Admiralty coefficient [-] (Fig. 8).

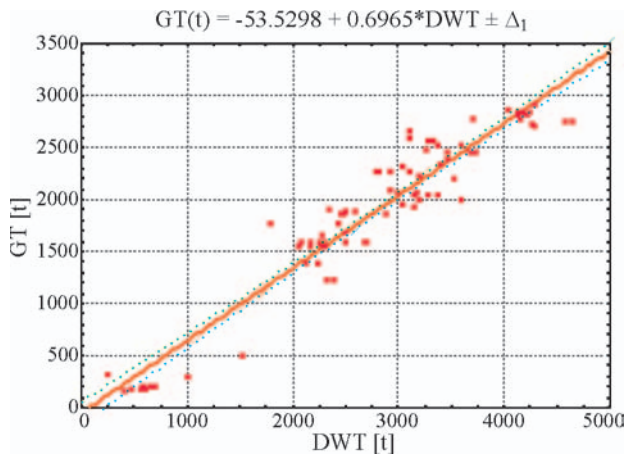


Fig. 7. The relationship: $GT = f(DWT)$. Source: the author's elaboration

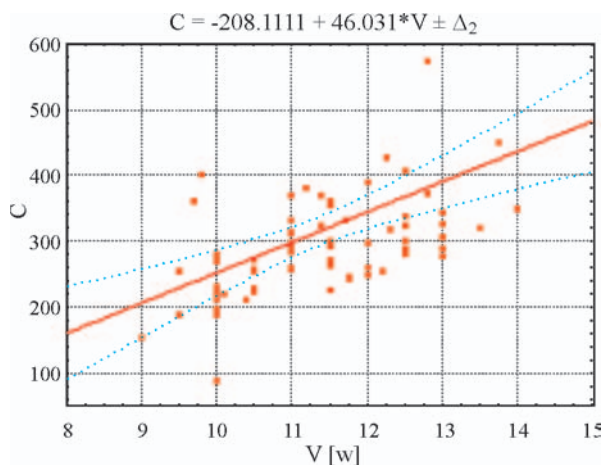


Fig. 8. The relationship: $C = f(V)$. Source: the author's elaboration

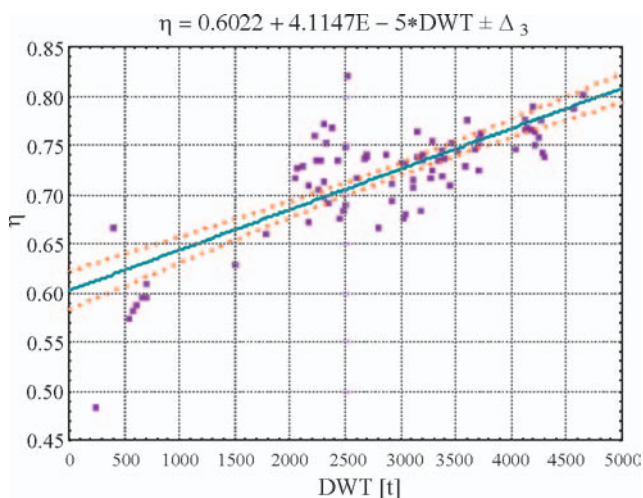


Fig. 9. The relationship: $\eta = f(DWT)$. Source: the author's elaboration

The ship displacement D can be determined on the basis of the following relationship:

$$D = \eta \cdot DWT \quad (39)$$

where:

- η – deadweight factor of river-sea ship (Fig.9)
- DWT – designed deadweight of river-sea ship [t].

And:

$$DWT = q \cdot M_{lad} \quad (40)$$

$$DWT \leq DWT_{max} \quad (41)$$

where:

- q – a calculation coefficient: $q = 1.10 \div 1.20$ [-]
- DWT_{max} – maximum permissible deadweight of ship on a given shipping route [t].

B. The second economic criterion, i.e. the invested capital return period PBP [years], can be determined from the relationship:

$$PBP = \frac{KI}{Z} \quad (42)$$

Values of the quantities Z and KI can be determined by using the relation (21) and (27).

Values of the capital return period parameters show investment profitability levels.

The period should be as short as possible and not exceed 5 – 7 years.

C. The third criterion, i.e. the cargo shipping cost KT [€/t*km], can be determined on the basis of the following relationship:

$$KT = \frac{KE}{n_s \cdot M_{lad_r} \cdot S_r} \quad (43)$$

where:

- n_s – number of ships necessary to cope with cargo flows on a given shipping route [ships/year]
- M_{lad_r} – mass of cargo shipped by one ship during one year [t]
- S_r – length of route covered by one ship during one year [km/year].

And:

$$M_{lad_r} = M_{lad} \cdot n_r \quad (44)$$

$$S_r = S \cdot n_r \quad (45)$$

CONCLUSIONS

In order to select a concrete shipping strategy which has to be used in river-sea shipping system it is necessary to elaborate in advance a functional model of fleet of river-sea ships. Its elaboration allows to preform simulations which can serve for assessing and checking the following items:

- parameters of functioning the ships on a given route in compliance with a shipping task elaborated in line with current rate of cargo flow along the considered route
- flexibility of the functional model regarding changes in rates and directions of cargo flows according to their short-term and long-term predictions.

The elaboration and analysis of such model can be applied to:

- An appropriate choice and adjustment of:
 - ✓ shipping task depending on market demand considered in the form of cargo flows
 - ✓ rational scheme of SRM fleet functioning, depending on selected shipping tasks and waterways infrastructure parameters.

- Determination of design assumptions for river-sea ships intended for operation in European system of water transport corridors, including:
 - ✓ number of ships necessary for realization of shipping tasks, i.e. structure of the ships' stock
 - ✓ service speed values of the ships of particular types
 - ✓ cargo capacity values (volume of holds) of the ships of particular types.
- Choice of cargo shipments for a selected shipping scheme, depending on operational features of the ships, season of the year etc.

Investigation of the functional model results in determination of technical assumptions for design of particular river-sea ships.

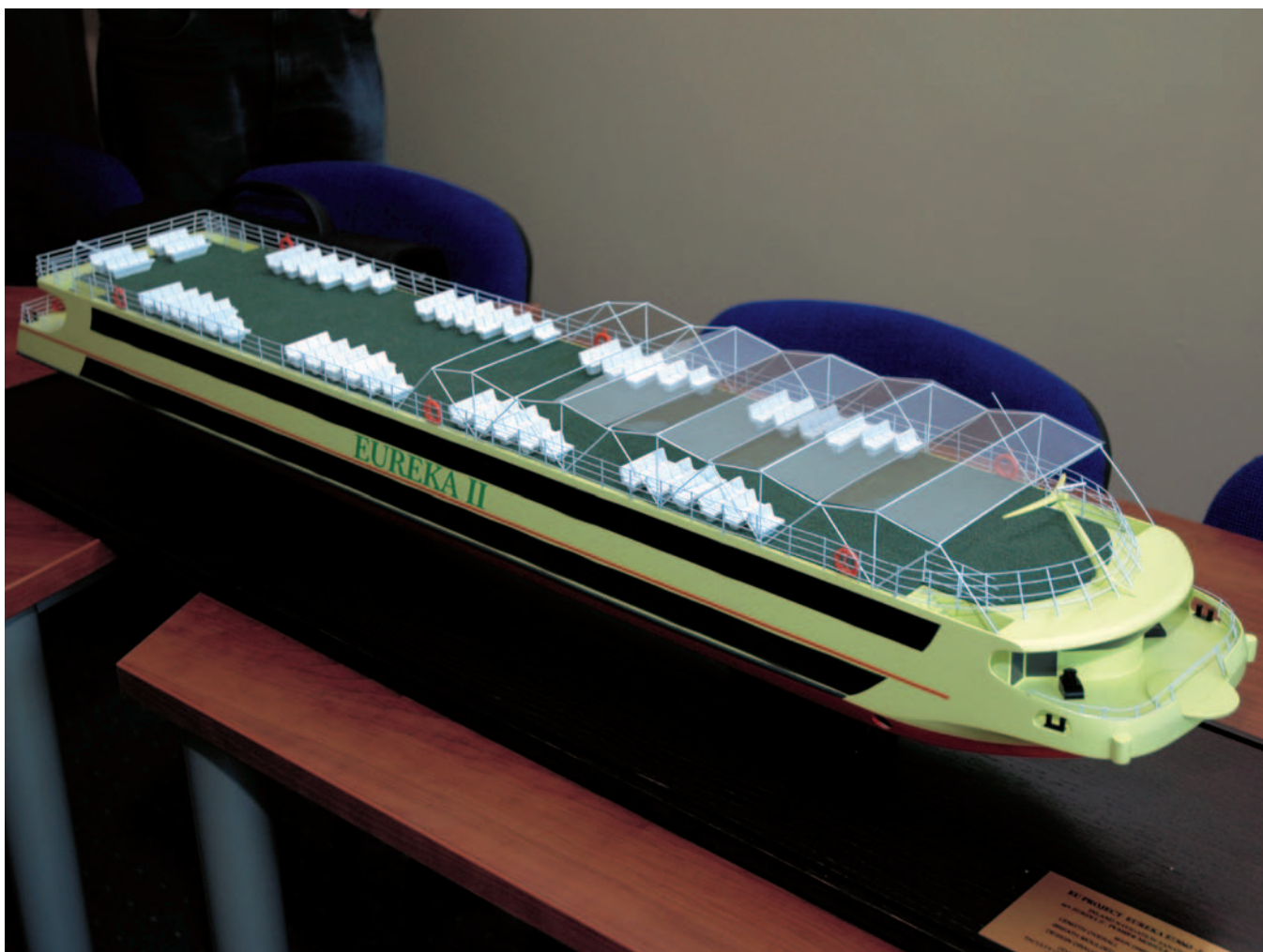
BIBLIOGRAPHY

1. Charlier J. & Ridolfi G.: *Intermodal transportation in Europe: of modes, corridors and nodes*, Maritime Policy and Management, 21 (3), 1994
2. Kaup M.: *Importance of river-sea fleet for development of the Baltic Sea region* (in Polish). Materials of 2nd International Scientific Conference on „ Operation of Polish Liner and Ferry Fleet in 2004”, Szczecin 2004

3. Kaup M., Kaup J.: *Design model of river-sea ships operating on European waterways*, Marine Technology Transactions, Vol.16, Polish Academy of Sciences – Branch in Gdańsk, Gdańsk 2005
4. Kreutzberger I.E.: *Innovative Networks and New-generation Terminals for Intermodal Transport*, Delft 1999
5. Semenov I. N.: *Innovative Conceptions Impacts on Development system of Inland Shipping Network*. Materials of 1st International Conference on “Inland Shipping 2005”, Szczecin Maritime University, Szczecin 2005
6. Semenov I. N.: *Risk management in maritime economy. Safety management of transport ships and floating units* (in Polish). Vol. I, Publishing House of Szczecin University of Technology, Szczecin 2003
7. Tarnowski W.: *CAD CAM computer aiding. Essentials of technical design* (in Polish). Scientific Technical Publishers (Wydawnictwo Naukowo-Techniczne), Warszawa 1997
8. Winnikow W.W.: *Sea shipping economy* (in Russian), Odessa, Latstar, 2001.

CONTACT WITH THE AUTHOR

Magdalena Kaup, Ph. D.
 Faculty of Marine Technology
 Szczecin University of Technology
 AL. Piastów 41,
 71-065 Szczecin, POLAND
 e-mail: mkaup@ps.pl
 phone: (091) 449 - 47 - 50



On the behaviour of viscoelastic solids under multiaxial loads

Janusz Kolenda

Naval Academy of Gdynia
 Gdańsk University of Technology

ABSTRACT



On the basis of modified Hooke's law for multiaxial stress in viscoelastic solids, three-dimensional constitutive equations for strains have been derived. It is shown that after application or removal of triaxial static load, normal and shear strain components vary in course of time proportionally to each other and that in-phase stress components produce in-phase strain components. Harmonic out-of-phase stress as well as multiaxial periodic and stationary random stresses are also considered. The matrix of dynamical flexibility of viscoelastic materials is determined which depends on three material constants (Young modulus, Poisson's ratio and coefficient of viscous damping of normal strain) and load circular frequency.

Keywords: viscoelastic material, multiaxial stress, constitutive equations, static load, vibratory load

INTRODUCTION

Deformation of solids is accompanied by internal friction [1]. Consequently, even in the region below the proportionality limit metals are not perfectly elastic [2]. If tensile strain has occurred in an anelastic rod, the complete removal of the load will be followed by a gradual decrease in length. When the length does decrease with time after unloading, the shortening is called "creep recovery". The anelastic strain, which occurs during long-time creep, is basically the same as that which occurs during vibratory load, and in both cases the anelastic behaviour can be expressed in the same terms [2].

There are various models of anelastic materials and damping mechanisms in use [1-3]. When the Kelvin-Voigt's model (spring and dashpot in parallel) of viscoelastic material is applied to the rod, its behaviour is easy to deduce. In particular, it is obvious that:

- * creep recovery at a given time, following partial or complete unloading from a given prior load of a given duration, is proportional to the stress decrement
- * after creep recovery, deformation should cease and the dimensions should remain constant.

The governing differential equation that relates stress σ and strain ε , the creep compliance $I(t)$ and the relaxation modulus $G(t)$ read [3]:

$$\sigma = q_0 \varepsilon + q_1 \dot{\varepsilon} \quad (1)$$

$$I(t) = \frac{1}{q_0} \left(1 - e^{-\frac{q_0 t}{q_1}} \right) \quad (2)$$

$$G(t) = q_0 + q_1 \delta(t) \quad (3)$$

where:

- q_0, q_1 – material constants in the Kelvin-Voigt's model
- $I(t)$ – response of strain due to a unit step input of stress
- $G(t)$ – response of stress due to a unit step input of strain
- $\delta(t)$ – Kronecker delta.

As the relaxation modulus is known, the stress response can be determined under any strain loading condition through a convolution integral. These equations are:

$$\sigma(t) = \varepsilon(0)G(t) + \int_0^t G(t-\tau) \frac{d\varepsilon(\tau)}{d\tau} d\tau \quad (4)$$

or

$$\sigma(t) = \varepsilon(t)G(0) + \int_0^t \varepsilon(\tau) \frac{dG(t-\tau)}{d\tau} d\tau \quad (5)$$

with a similar equation for the strain response due to arbitrary stress input:

$$\varepsilon(t) = \sigma(0)I(t) + \int_0^t I(t-\tau) \frac{d\sigma(\tau)}{d\tau} d\tau \quad (6)$$

or

$$\varepsilon(t) = \sigma(t)I(0) + \int_0^t \sigma(\tau) \frac{dI(t-\tau)}{d\tau} d\tau \quad (7)$$

The one-dimensional constitutive equations can be extended to three-dimensional constitutive equations. A general and most common form of these are [3]:

$$\sigma_{ij}(t) = G_{ijkl}(t)\varepsilon_{kl}(0) + \int_0^t G_{ijkl}(t-\tau) \frac{d\varepsilon_{kl}(\tau)}{d\tau} d\tau \quad (8)$$

$$\sigma_{ij}(t) = G_{ijkl}(0)\varepsilon_{kl}(t) + \int_0^t \varepsilon_{kl}(\tau) \frac{dG_{ijkl}(t-\tau)}{d\tau} d\tau \quad (9)$$

The stress σ_{ij} and the strain ε_{kl} are second-order tensor quantities, and G_{ijkl} are the four-order relaxation modulus. A set of similar constitutive equations for strains, when the stress history is known, can be obtained.

The aim of the present paper is to derive three-dimensional constitutive equations for strains by means of the modified Hooke's law for multiaxial stress in viscoelastic solids [4] because its simplicity in the case of homogeneous isotropic materials may be advantageous.

STRAIN RESPONSE OF VISCOELASTIC SOLIDS TO REMOVAL AND APPLICATION OF MULTIAXIAL STATIC LOAD

After a long period of static load resulting in normal and shear components σ_{j0} and τ_{k0} ($j = x, y, z; k = xy, yz, zx$), the normal and shear strain components ε_{j0} and γ_{k0} in a viscoelastic material can be calculated as those in elastic materials [3,5]:

$$\begin{aligned} \varepsilon_{x0} &= \frac{1}{E} [\sigma_{x0} - \nu(\sigma_{y0} + \sigma_{z0})] \\ \varepsilon_{y0} &= \frac{1}{E} [\sigma_{y0} - \nu(\sigma_{x0} + \sigma_{z0})] \\ \varepsilon_{z0} &= \frac{1}{E} [\sigma_{z0} - \nu(\sigma_{x0} + \sigma_{y0})] \\ \gamma_{k0} &= \frac{1}{G} \tau_{k0} \end{aligned} \quad (10)$$

where E is the Young modulus, ν is the Poisson's ratio and

$$G = \frac{E}{2(1+\nu)} \quad (11)$$

is the shear modulus. If at $t = 0$ the load is removed, in accordance with the modified Hooke's law [4], the following equations can be applied:

$$\begin{aligned} E\varepsilon_j + \eta\dot{\varepsilon}_j &= 0 \\ G\gamma_k + \lambda\dot{\gamma}_k &= 0 \end{aligned} \quad (12)$$

and solved with the initial conditions:

$$\varepsilon_j(0) = \varepsilon_{j0}, \quad \gamma_k(0) = \gamma_{k0} \quad (13)$$

In Eqs (12), η is the coefficient of viscous damping of normal strain and [4]:

$$\lambda = \frac{\eta}{2(1+\nu)} \quad (14)$$

is the coefficient of viscous damping of shear strain.

The solutions of Eqs (12) have the form:

$$\varepsilon_j(t) = A_j e^{-rt}, \quad \gamma_k(t) = B_k e^{-st} \quad (15)$$

where A_j, B_k, r and s are constants. Substitution of Eqs (15) into Eqs (12) yields:

$$E - r\eta = 0, \quad G - s\lambda = 0 \quad (16)$$

so that:

$$r = \frac{E}{\eta}, \quad s = \frac{G}{\lambda} = \frac{E}{\eta} = r \quad (17)$$

From Eqs (13) and (15) one obtains:

$$A_j = \varepsilon_{j0}, \quad B_k = \gamma_{k0} \quad (18)$$

Hence:

$$\begin{aligned} \varepsilon_j(t) &= \varepsilon_{j0} e^{-\frac{E}{\eta}t} \\ \gamma_k(t) &= \gamma_{k0} e^{-\frac{E}{\eta}t} \end{aligned} \quad (19)$$

It is also easy to prove that sudden application of a multiaxial static load producing stress components σ_{j0} and τ_{k0} to viscoelastic solids evokes their dimensional changes and distortions described by equations:

$$\begin{aligned} \varepsilon_j(t) &= \varepsilon_{j0} \left(1 - e^{-\frac{E}{\eta}t} \right) \\ \gamma_k(t) &= \gamma_{k0} \left(1 - e^{-\frac{E}{\eta}t} \right) \end{aligned} \quad (20)$$

It is noteworthy that in conformity with Eqs (19) and (20), after removal or application of multiaxial static loads, the strain components in viscoelastic solids vary in course of time proportionally to each other.

Eqs (19) and (20) apply to creep recovery following a long period at constant stress, or to creep at a particular stress level following a long period of zero stress. These, of course, are very special cases, but with the modified Hooke's law we are able to handle effectively also other load patterns. Some of them are considered below.

THE CASE OF HARMONIC IN-PHASE STRESS

The relations between stress and strain in viscoelastic materials subjected below the yield point to time-dependent loads are governed by the modified Hooke's law [4]:

$$\begin{aligned} E\varepsilon_x + \eta\dot{\varepsilon}_x &= \sigma_x - \nu(\sigma_y + \sigma_z) \\ E\varepsilon_y + \eta\dot{\varepsilon}_y &= \sigma_y - \nu(\sigma_x + \sigma_z) \\ E\varepsilon_z + \eta\dot{\varepsilon}_z &= \sigma_z - \nu(\sigma_x + \sigma_y) \\ G\gamma_k + \lambda\dot{\gamma}_k &= \tau_k; \quad k = xy, yz, zx \end{aligned} \quad (21)$$

Under in-phase stress components:

$$\begin{aligned} \sigma_j &= \sigma_{ja} \sin \omega t; \quad j = x, y, z \\ \tau_k &= \tau_{ka} \sin \omega t \end{aligned} \quad (22)$$

the strain components take the form:

$$\begin{aligned} \varepsilon_j &= \varepsilon_{j1} \sin \omega t + \varepsilon_{j2} \cos \omega t \\ \gamma_k &= \gamma_{k1} \sin \omega t + \gamma_{k2} \cos \omega t \end{aligned} \quad (23)$$

In Eqs (22), σ_{ja} and τ_{ka} are the amplitudes of stress components and ω is their circular frequency. With Eqs (22) and (23), Eqs (21) become:

$$\begin{aligned} E(\varepsilon_{x1} \sin \omega t + \varepsilon_{x2} \cos \omega t) + \eta\omega(\varepsilon_{x1} \cos \omega t - \varepsilon_{x2} \sin \omega t) &= [\sigma_{xa} - \nu(\sigma_{ya} + \sigma_{za})] \sin \omega t \\ E(\varepsilon_{y1} \sin \omega t + \varepsilon_{y2} \cos \omega t) + \eta\omega(\varepsilon_{y1} \cos \omega t - \varepsilon_{y2} \sin \omega t) &= [\sigma_{ya} - \nu(\sigma_{xa} + \sigma_{za})] \sin \omega t \\ E(\varepsilon_{z1} \sin \omega t + \varepsilon_{z2} \cos \omega t) + \eta\omega(\varepsilon_{z1} \cos \omega t - \varepsilon_{z2} \sin \omega t) &= [\sigma_{za} - \nu(\sigma_{xa} + \sigma_{ya})] \sin \omega t \\ G(\gamma_{k1} \sin \omega t + \gamma_{k2} \cos \omega t) + \lambda\omega(\gamma_{k1} \cos \omega t - \gamma_{k2} \sin \omega t) &= \tau_{ka} \sin \omega t \end{aligned} \quad (24)$$

Eqs (24) are satisfied if:

$$\begin{aligned} E\varepsilon_{x1} - \eta\omega\varepsilon_{x2} &= \sigma_{xa} - \nu(\sigma_{ya} + \sigma_{za}) \\ E\varepsilon_{y1} - \eta\omega\varepsilon_{y2} &= \sigma_{ya} - \nu(\sigma_{xa} + \sigma_{za}) \\ E\varepsilon_{z1} - \eta\omega\varepsilon_{z2} &= \sigma_{za} - \nu(\sigma_{xa} + \sigma_{ya}) \\ \eta\omega\varepsilon_{j1} + E\varepsilon_{j2} &= 0, \quad G\gamma_{k1} - \lambda\omega\gamma_{k2} = \tau_{ka}, \quad \lambda\omega\gamma_{k1} + G\gamma_{k2} = 0 \end{aligned} \quad (25)$$

Eqs (23) and (25) lead to the constitutive equations for strains as follows:

$$\begin{aligned} \varepsilon_x &= \frac{\sigma_{xa} - \nu(\sigma_{ya} + \sigma_{za})}{\sqrt{E^2 + (\eta\omega)^2}} \sin(\omega t - \alpha), \quad \alpha = \arctg \frac{\eta\omega}{E} \\ \varepsilon_y &= \frac{\sigma_{ya} - \nu(\sigma_{xa} + \sigma_{za})}{\sqrt{E^2 + (\eta\omega)^2}} \sin(\omega t - \alpha) \\ \varepsilon_z &= \frac{\sigma_{za} - \nu(\sigma_{xa} + \sigma_{ya})}{\sqrt{E^2 + (\eta\omega)^2}} \sin(\omega t - \alpha) \end{aligned} \quad (26)$$

and

$$\gamma_k = \frac{\tau_{ka}}{\sqrt{G^2 + (\lambda\omega)^2}} \sin(\omega t - \beta), \quad \beta = \arctg \frac{\lambda\omega}{G} \quad (27)$$

Through Eqs (11) and (14), Eqs (27) become:

$$\gamma_k = \frac{2(1+\nu)\tau_{ka}}{\sqrt{E^2 + (\eta\omega)^2}} \sin(\omega t - \alpha), \quad \beta = \alpha \quad (28)$$

It means that in-phase stress components produce in homogeneous, isotropic viscoelastic materials in-phase strain components.

Introducing the strain vector:

$$\boldsymbol{\varepsilon} = [\varepsilon_x \varepsilon_y \varepsilon_z \gamma_{xy} \gamma_{yz} \gamma_{zx}]^T \quad (29)$$

and the vector of amplitudes of the stress components:

$$\boldsymbol{\sigma}_a = [\sigma_{xa} \sigma_{ya} \sigma_{za} \tau_{xya} \tau_{yza} \tau_{zxa}]^T \quad (30)$$

Eqs (26) and (28) can be rewritten in a matrix form:

$$\boldsymbol{\varepsilon} = \mathbf{H}\boldsymbol{\sigma}_a \sin(\omega t - \alpha) \quad (31)$$

where:

$$\mathbf{H} = \mathbf{H}(\omega) = \frac{1}{\sqrt{E^2 + (\eta\omega)^2}} \begin{bmatrix} 1 & -\nu & -\nu & 0 & 0 & 0 \\ -\nu & 1 & -\nu & 0 & 0 & 0 \\ -\nu & -\nu & 1 & 0 & 0 & 0 \\ 0 & 0 & 0 & 2(1+\nu) & 0 & 0 \\ 0 & 0 & 0 & 0 & 2(1+\nu) & 0 \\ 0 & 0 & 0 & 0 & 0 & 2(1+\nu) \end{bmatrix} \quad (32)$$

is the matrix of dynamical flexibility of the viscoelastic material at the load circular frequency ω .

THE CASE OF HARMONIC OUT-OF-PHASE STRESS

When the stress components are given by:

$$\begin{aligned}\sigma_j &= \sigma_{ja} \sin(\omega t + \varphi_j) \\ \tau_k &= \tau_{ka} \sin(\omega t + \varphi_k)\end{aligned}\quad (33)$$

where φ_j and φ_k are the phase angles, it is convenient to introduce the complex stress components:

$$\begin{aligned}\bar{\sigma}_j &= \sigma_{ja} e^{i(\omega t + \varphi_j)} = \bar{\sigma}_{ja} e^{i\omega t} \\ \bar{\tau}_k &= \tau_{ka} e^{i(\omega t + \varphi_k)} = \bar{\tau}_{ka} e^{i\omega t}\end{aligned}\quad (34)$$

Here i is the imaginary unity and

$$\bar{\sigma}_{ja} = \sigma_{ja} e^{i\varphi_j}, \quad \bar{\tau}_{ka} = \tau_{ka} e^{i\varphi_k}\quad (35)$$

are the complex amplitudes of the stress components. Then the real stress components are represented by the imaginary parts of the complex stress components:

$$\sigma_j = \text{Im} \bar{\sigma}_j, \quad \tau_k = \text{Im} \bar{\tau}_k\quad (36)$$

Consequently, in view of Eq. (31) the strain response of the viscoelastic material to the stress (33) can be calculated as:

$$\boldsymbol{\varepsilon} = \mathbf{H} \text{Im} \left[\bar{\boldsymbol{\sigma}}_a e^{i(\omega t - \alpha)} \right]\quad (37)$$

where:

$$\bar{\boldsymbol{\sigma}}_a = \left[\bar{\sigma}_{xa} \bar{\sigma}_{ya} \bar{\sigma}_{za} \bar{\tau}_{xya} \bar{\tau}_{yza} \bar{\tau}_{zxa} \right]^T\quad (38)$$

is the vector of complex amplitudes of the stress components.

STRAIN RESPONSE OF VISCOELASTIC SOLIDS TO MULTIAXIAL PERIODIC AND STATIONARY RANDOM LOADS

The solution (37) can be utilized for determination of behaviour of viscoelastic materials under multiaxial periodic loads. The resulting stress components can be expanded in Fourier series:

$$\begin{aligned}\sigma_j &= \sigma_{j0} + \sum_n \sigma_{jn} \sin(n\omega t + \varphi_{jn}) \\ \tau_k &= \tau_{k0} + \sum_n \tau_{kn} \sin(n\omega t + \varphi_{kn})\end{aligned}\quad (39)$$

where:

- σ_{j0}, τ_{k0} – mean stress components
- $\sigma_{jn}, \varphi_{jn}$ – amplitude and phase angle of n -th term in Fourier expansion of j -th stress component
- τ_{kn}, φ_{kn} – amplitude and phase angle of n -th term in Fourier expansion of k -th stress component
- ω – fundamental circular frequency.

Since Eqs (21) are linear, the principle of superposition can be applied. For this purpose we define:

* the vector of mean stress components:

$$\boldsymbol{\sigma}_0 = \left[\sigma_{x0} \sigma_{y0} \sigma_{z0} \tau_{xy0} \tau_{yz0} \tau_{zx0} \right]^T\quad (40)$$

* the vector of mean strain components:

$$\boldsymbol{\varepsilon}_0 = \left[\varepsilon_{x0} \varepsilon_{y0} \varepsilon_{z0} \gamma_{xy0} \gamma_{yz0} \gamma_{zx0} \right]^T\quad (41)$$

* the vector of complex amplitudes of n -th terms of the stress components:

$$\bar{\boldsymbol{\sigma}}_n = \left[\bar{\sigma}_{xn} \bar{\sigma}_{yn} \bar{\sigma}_{zn} \bar{\tau}_{xyn} \bar{\tau}_{yzn} \bar{\tau}_{zxn} \right]^T\quad (42)$$

with

$$\bar{\sigma}_{jn} = \sigma_{jn} e^{i\varphi_{jn}}, \quad \bar{\tau}_{kn} = \tau_{kn} e^{i\varphi_{kn}}\quad (43)$$

* the matrix of dynamical flexibility of the viscoelastic material at the load circular frequency $n\omega$:

$$\mathbf{H}_n = \mathbf{H}(n\omega)\quad (44)$$

* the phase angle of n -th terms of the strain components:

$$\alpha_n = \text{arctg} \frac{\eta n \omega}{E}\quad (45)$$

Under assumption that the material remains viscoelastic, its strain response to the stress (39) is described by the following equation:

$$\boldsymbol{\varepsilon} = \boldsymbol{\varepsilon}_0 + \sum_n \mathbf{H}_n \text{Im} \left[\bar{\boldsymbol{\sigma}}_n e^{i(n\omega t - \alpha_n)} \right]\quad (46)$$

where the elements of the vector $\boldsymbol{\varepsilon}_0$ are given in Eqs (10).

As the stress is increased above the yield point, the linear behaviour of viscoelastic material expressed by the modified Hooke's law (21) is terminated by the onset of plastic flow. In the case of uniaxial static tension, the part will yield if the uniaxial stress equals the yield strength of the material. For biaxial or triaxial static stress, various theories of failure by yielding have been developed, for example the distortion-energy strength theory [3, 5]. This theory is an important one because it comes closest of all to verifying experimental results [3]. Therefore in [6] an attempt was made to extend its use also to the case of multiaxial periodic stress and to model the stress components (39) by the reduced uniaxial stress:

$$\sigma_e(t) = \sigma_{e0} + \sigma_{ea} \sin \omega_e t\quad (47)$$

The mean value σ_{e0} , amplitude σ_{ea} and circular frequency ω_e of the reduced stress are determined in [6]. Such an approach suggests that under multiaxial periodic stress the yield strength is not exceeded at a given point if the following condition is met:

$$\sigma_{e0} + \sigma_{ea} < R_e\quad (48)$$

where R_e is the tensile yield strength of the material.

Similar condition of avoiding plastic flow in viscoelastic solids can be postulated in the cases of multiaxial random loads if a uniaxial reduced random stress [6, 7] is taken under consideration.

As far as the strain response of viscoelastic solids to random loads is concerned, we shall confine ourselves to the solution in frequency domain [8, 9]. When the stress components represent zero mean stochastic processes that are stationary and stationary correlated with each other, and when their power spectral densities are given, the power spectral densities of the strain components can be calculated from the following equation:

$$\mathbf{S}_\varepsilon = \mathbf{H} \mathbf{S}_\sigma \mathbf{H}\quad (49)$$

where \mathbf{H} is the matrix (32) of dynamical flexibility of the material, and:

$$\mathbf{S}_\varepsilon = \begin{bmatrix} S_{\varepsilon_x \varepsilon_x} & S_{\varepsilon_x \varepsilon_y} & S_{\varepsilon_x \varepsilon_z} & S_{\varepsilon_x \gamma_{xy}} & S_{\varepsilon_x \gamma_{yz}} & S_{\varepsilon_x \gamma_{zx}} \\ S_{\varepsilon_y \varepsilon_x} & S_{\varepsilon_y \varepsilon_y} & S_{\varepsilon_y \varepsilon_z} & S_{\varepsilon_y \gamma_{xy}} & S_{\varepsilon_y \gamma_{yz}} & S_{\varepsilon_y \gamma_{zx}} \\ \dots & \dots & \dots & \dots & \dots & \dots \\ S_{\gamma_{zx} \varepsilon_x} & S_{\gamma_{zx} \varepsilon_y} & S_{\gamma_{zx} \varepsilon_z} & S_{\gamma_{zx} \gamma_{xy}} & S_{\gamma_{zx} \gamma_{yz}} & S_{\gamma_{zx} \gamma_{zx}} \end{bmatrix}\quad (50)$$

$$S_{\sigma} = \begin{bmatrix} S_{\sigma_x \sigma_x} & S_{\sigma_x \sigma_y} & S_{\sigma_x \sigma_z} & S_{\sigma_x \tau_{xy}} & S_{\sigma_x \tau_{yz}} & S_{\sigma_x \tau_{zx}} \\ S_{\sigma_y \sigma_x} & S_{\sigma_y \sigma_y} & S_{\sigma_y \sigma_z} & S_{\sigma_y \tau_{xy}} & S_{\sigma_y \tau_{yz}} & S_{\sigma_y \tau_{zx}} \\ \hline S_{\tau_{zx} \sigma_x} & S_{\tau_{zx} \sigma_y} & S_{\tau_{zx} \sigma_z} & S_{\tau_{zx} \tau_{xy}} & S_{\tau_{zx} \tau_{yz}} & S_{\tau_{zx} \tau_{zx}} \end{bmatrix} \quad (51)$$

where:

- $S_{\varepsilon_x \varepsilon_x}, S_{\varepsilon_y \varepsilon_y}, S_{\varepsilon_z \varepsilon_z}$ – power spectral densities of the strain components $\varepsilon_x, \varepsilon_y, \dots, \varepsilon_z$
- $S_{\varepsilon_x \varepsilon_y}, S_{\varepsilon_x \varepsilon_z}, S_{\varepsilon_y \varepsilon_z}$ – cross power spectral densities of the strain components ε_x and $\varepsilon_y, \varepsilon_x$ and $\varepsilon_z, \dots, \varepsilon_y$ and ε_z
- $S_{\sigma_x \sigma_x}, S_{\sigma_y \sigma_y}, S_{\tau_{zx} \tau_{zx}}$ – power spectral densities of the stress components $\sigma_x, \sigma_y, \dots, \tau_{zx}$
- $S_{\sigma_x \sigma_y}, S_{\sigma_x \sigma_z}, S_{\tau_{zx} \tau_{yz}}$ – cross power spectral densities of the stress components σ_x and σ_y, σ_x and $\sigma_z, \dots, \tau_{zx}$ and τ_{yz} .

Within the static, purely mechanical theory of continua there are two numbers which may be associated with the deformed state of a structure: its mass and its stored energy [10]. This association provides the criteria for the comparison of various designs. Apart from these numbers, in dynamic problems the load frequency and in fatigue design the stress range and number of cycles also play an important role. In this context it is clear that the physical models of structural materials should incorporate their mass density. As a result of application of the two-parameter Kelvin-Voigt's model, the relationships derived in the foregoing ignore inertia forces which in many cases may not be negligible in comparison with external loads and internal forces due to the viscoelastic properties of the material. However, the problems dealt with in the present paper have been aimed at gaining additional information on the influence of dissipative properties on the behaviour of structural materials and mathematical solutions within the assumed simpler model. Three-parameter models and more comprehensive stress-strain relations in viscoelastic materials are discussed, e.g., in [1, 3, 11, 12].

As to the behaviour of engineering details under vibratory loads with inertia forces taken into account, this problem has been widely addressed in the literature on vibration of continuous systems by exact mathematical treatment and numerical methods (see, e.g., [1, 13-15]) and will not be considered here.

CONCLUSIONS

- Three-dimensional constitutive equations for strains in homogeneous, isotropic viscoelastic solids have been derived by means of the modified Hooke's law.
- Owing to the fact that for homogeneous, isotropic viscoelastic materials the ratio of moduli E and G is equal to the ratio of damping coefficients η and λ , after sudden change of multiaxial static loads the strain components vary in time proportionally to each other because the time function of normal and shear creep is the same.
- If the stress components in a homogeneous, isotropic viscoelastic material are in phase, there are no phase shifts between the strain components.

- The matrix of dynamical flexibility of the homogeneous, isotropic viscoelastic material has been determined which depends on three material constants (Young modulus, Poisson's ratio, coefficient of viscous damping of normal strain) and load circular frequency.

NOMECLATURE

E	– Young modulus
G	– shear modulus, relaxation modulus
H	– matrix of dynamical flexibility of the viscoelastic material at the load circular frequency ω
H_n	– matrix of dynamical flexibility of the viscoelastic material at the load circular frequency $n\omega$
i	– imaginary unity
I	– creep compliance
Im	– imaginary part
n	– natural number
$q_0 = E, q_1 = \eta$	– material constants in the Kelvin-Voigt's model of the viscoelastic material
R_c	– tensile yield strength
S_{ε}	– matrix of power spectral densities of the strain components
S_{σ}	– matrix of power spectral densities of the stress components
t	– time
α	– phase angle of the strain components
α_n	– phase angle of n -th terms of the strain components
γ	– shear strain
γ_k	– k -th strain component ($k = xy, yz, zx$)
γ_{k0}	– k -th strain component at the static load, mean value of k -th strain component
ε	– normal strain
ε	– vector of the strain components
ε_j	– j -th strain component ($j = x, y, z$)
ε_{j0}	– j -th strain component at the static load, mean value of j -th strain component
ε_0	– vector of mean values of the strain components
η	– coefficient of viscous damping of normal strain
λ	– coefficient of viscous damping of shear strain
ν	– Poisson's ratio
σ	– normal stress
σ_a	– vector of the amplitudes of stress components
σ_{e0}	– mean value of the reduced stress
σ_{ea}	– amplitude of the reduced stress
σ_j	– j -th stress component
σ_j^a	– amplitude of j -th stress component
σ_j^{in}	– amplitude of n -th term in Fourier expansion of σ_j
σ_{j0}	– j -th stress component at the static load, mean value of j -th stress component
$\bar{\sigma}_n$	– vector of complex amplitudes of n -th terms in Fourier expansions of the stress components
σ_0	– vector of mean values of the stress components
τ	– shear stress
τ_k	– k -th stress component
τ_{ka}	– amplitude of k -th stress component
τ_{kn}	– amplitude of n -th term in Fourier expansion of τ_k
τ_{k0}	– k -th stress component at the static load, mean value of k -th stress component
φ_j	– phase angle of j -th stress component
φ_j^{in}	– phase angle of n -th term in Fourier expansion of σ_j
φ_k	– phase angle of k -th stress component
φ_{kn}	– phase angle of n -th term in Fourier expansion of τ_k
ω	– circular frequency, fundamental circular frequency
ω_c	– circular frequency of the reduced stress
$(\bar{\tau})$	– complex quantity

BIBLIOGRAPHY

1. Panovko J.G.: *Internal Friction at Vibrations of Elastic Systems* (in Russian). Fizmatgiz, Moscow, 1960
2. Lubahn J.D., Felgar R.P.: *Plasticity and Creep of Metals*. J. Wiley & Sons, New York, 1961
3. Blake A. (Ed.): *Handbook of Mechanics, Materials and Structures*. J. Wiley & Sons, New York, 1985
4. Kolenda J.: *Modification of Hooke's law for multiaxial stress in viscoelastic solids*. Polish Maritime Research, 2, 2007
5. Haslach H.W., Jr., Armstrong R.W.: *Deformable Bodies and Their Material Behaviour*. J. Wiley & Sons, 2004
6. Kolenda J.: *Criteria in design for finite fatigue life under multiaxial static and dynamic loadings*. Marine Technology Transactions, Vol. 10, 1999
7. Kolenda J.: *A modification of distortion-energy theory at static-dynamic random loading*. Polish Maritime Research, 2, 1999
8. Papoulis A.: *Probability, Random Variables and Stochastic Processes*. McGraw-Hill, New York, 1984
9. Preumont A.: *Vibrations aléatoires et analyse spectrale*. Presses Polytechniques et Universitaires Romandes, CH-1015, Lausanne, 1990
10. Stadler W.: *Natural structural shapes (the static case)*. Quarterly Journal of Mechanics and Applied Mathematics, Vol. XXXI, Pt. 2, 1978
11. Pisarenko G.S., Lebedev A.A.: *Resistance of Materials to Deformation and Failure in Complex Stress State* (in Russian). Izd. Naukova Dumka, Kiev, 1969
12. Nashif A.D., Jones D.I.G., Henderson J.P.: *Vibration Damping*. J. Wiley & Sons, New York, 1985
13. Osiński Z.: *Damping of Mechanical Vibrations* (in Polish). PWN, Warszawa, 1979
14. Giergiel J.: *Damping of Mechanical Vibrations* (in Polish). PWN, Warszawa, 1990
15. Kruszewski J., Wittbrodt E., Walczyk Z.: *Vibrations of Mechanical Systems in Computer-Based Approach* (in Polish). Vol. 2, WNT, Warszawa, 1993.

CONTACT WITH THE AUTHOR

Prof. Janusz Kolenda
Mechanic-Electric Faculty,
Polish Naval Academy
Śmidowicza 69
81-103 Gdynia POLAND
phone : +48 58 626 27 89



Photo: Cezary Spigarski

Modelling of vibrations of a liquid filled tank

Kazimierz Trębacki, Ph. D.
 Gdansk University of Technology

ABSTRACT



Kinematic excitations provoke the motion and vibrations of the construction, which in turn considerably affects hydrodynamic loads generated on the walls of liquid cargo tanks. The issues of hydrodynamics also refer to the constructions fixed to the bottom, and those half-immersed, fully immersed, and floating (drilling platforms). They mainly concern ship tanks and oceanotechnical tanks. The theoretical and numerical analysis for long and short tanks, fully or partially filled with liquid has been performed. The determined hydrodynamic loads directly refer to the strength of the tank structure, which provides opportunities for determining the constructional strength of the entire hull. Extremely severe requirements are to be met by tanks used for carrying radioactive liquids, as an extremely high safety level is to be secured on all cargo carriers used in marine and land transport.

Keywords: modelling, vibrations, hydroelasticity, ship tanks for liquid fuels and liquefied gases

PROBLEM FORMULATION

A long tank filled with liquid can be modelled by a beam of rectangular cross-section and dimensions $l \times b \times h$, with articulated supports at two points. The supports reveal flexibility to vertical movements and rotation [9 ÷ 12] (see Fig.1).

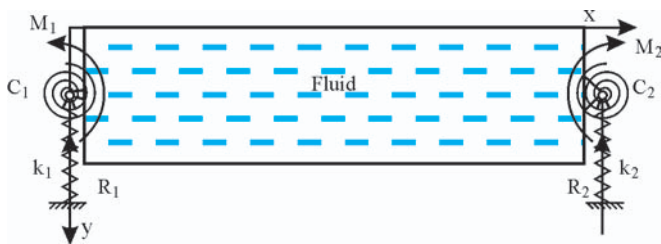


Fig. 1. Scheme of a model liquid-filled tank

where:

- k_1, k_2 – axial spring constants
- C_1, C_2 – spiral spring constants
- R_1, R_2, M_1, M_2 – support reactions and reaction moments, respectively.

When analysing free vibrations of the liquid-filled beam we assume that the functions of beam deflection w and velocity potential φ have the following harmonic form:

$$w = \tilde{w}(x) \sin \omega t \quad (1)$$

$$\varphi = \tilde{\varphi}(x, y, z) \cos \omega t \quad (2)$$

The differential equation for the liquid-filled beam is the following [11]:

$$EI \frac{\partial^4 w}{\partial x^4} - (N_h + N_d) \frac{\partial^2 w}{\partial x^2} + \rho_b A \frac{\partial^2 w}{\partial t^2} = q(x) + \int_0^b (p_2 - p_1) dz \quad (3)$$

where:

- EI – flexural stiffness
- ρ_b – beam material density,
- A – cross-section area,
- p_2, p_1 – wall pressures for $y = h$ and $y = 0$,
- N_h, N_d – longitudinal forces from hydrostatic and hydrodynamic pressure, respectively, acting on top walls for $x = 0$ and $x = l$.

These forces are determined using the formulas:

$$N_h = \frac{1}{2} \rho g b h^2 \quad (4)$$

$$N_d = \int_0^h p_d b dy \quad (5)$$

where:

- ρ – liquid density
- $g = -9.81 \text{ ms}^{-2}$ – Earth gravitation.

The hydrodynamic pressure is calculated from the Bernoulli equation:

$$p_d = -\rho \frac{\partial \varphi}{\partial t} = \rho \omega \tilde{\varphi} \sin \omega t \quad (6)$$

After putting (6) into relation (5) we get the formula for N_d :

$$N_d = \rho b \omega \sin \omega t \int_0^h \tilde{\varphi}|_{x=1} dy \quad (7)$$

After putting (4) and (5) into the differential equation (3) and, as a substitution for pressures p_2 and p_1 , into the linear part of the Cauchy-Lagrange integral we arrive at:

$$EI \frac{\partial^4 w}{\partial x^4} - \left(\frac{1}{2} \rho g b h^2 - \rho b \int_0^h \frac{\partial \varphi}{\partial t} \Big|_{x=1} dy \right) \frac{\partial^2 w}{\partial x^2} + \rho_b A \frac{\partial^2 w}{\partial t^2} = q(x) - \rho b \left(\frac{\partial \varphi}{\partial t} \Big|_{y=h} - \frac{\partial \varphi}{\partial t} \Big|_{y=0} \right) + \rho g b h \quad (8)$$

This is the non-linear differential equation for transverse vibrations of a long model tank filled with liquid.

For the liquid inside the tank the Laplace equation is solved

$$\nabla^2 \varphi = 0 \quad (9)$$

with the following boundary conditions for the liquid velocity potential:

❖ in the z-axis direction:

$$\frac{\partial \varphi}{\partial z} = 0 \text{ dla } z = -\frac{b}{2} \text{ i } z = \frac{b}{2} \quad (10)$$

❖ in the y-axis direction:

$$\frac{\partial \varphi}{\partial y} = \frac{\partial w}{\partial t} \text{ for } y = 0 \text{ and } y = h \quad (11)$$

❖ in the x-axis direction:

$$\frac{\partial \varphi}{\partial x} = -\left(y - \frac{h}{2} \right) \frac{\partial^2 w}{\partial x \partial t} \text{ for } x = 0 \text{ and } x = 1 \quad (12)$$

After dividing equation (8) by stiffness EI, neglecting the small non-linear term and assuming that $q(x) = 0$ we arrive at the following new form of the differential equation:

$$\frac{\partial^4 w}{\partial x^4} - B \frac{\partial^2 w}{\partial x^2} + B_1 \frac{\partial^2 w}{\partial t^2} = B_2 - B_3 \left(\frac{\partial \varphi}{\partial t} \Big|_{y=h} - \frac{\partial \varphi}{\partial t} \Big|_{y=0} \right) \quad (13)$$

where:

$$B \equiv \frac{\rho g b h^2}{2EI} ; B_1 \equiv \frac{\rho_b A}{EI} ; B_2 \equiv \frac{\rho g b h}{EI} ; B_3 \equiv \frac{\rho b}{EI}$$

This equation includes the deflection function w and the flow velocity potential φ . In order to get the partial differential vibration equation which only includes the flow velocity potential, equation (13) is to be differentiated with respect to time t , and then the boundary condition (11) for velocity is to be adopted. Then we get:

$$\frac{\partial^5 \varphi}{\partial x^4 \partial y} - B \frac{\partial^3 \varphi}{\partial x^2 \partial y} + B_1 \frac{\partial^3 \varphi}{\partial t^2 \partial y} = -B_3 \left(\frac{\partial^2 \varphi}{\partial t^2} \Big|_{y=h} - \frac{\partial^2 \varphi}{\partial t^2} \Big|_{y=0} \right) \text{ for } y = 0 \quad (14)$$

As we can see, this is the fifth order linear partial differential equation which only includes the velocity potential function $\varphi(x, y, z, t)$.

The boundary conditions for the supports have the form:

$$\begin{aligned} \frac{\partial^3 w}{\partial x^3} \Big|_{x=0} &= -\frac{k_1}{EI} w(0) ; \frac{\partial^3 w}{\partial x^3} \Big|_{x=1} = -\frac{k_0}{EI} w(l) \\ \frac{\partial^2 w}{\partial x^2} \Big|_{x=0} &= \frac{C_1}{EI} \frac{\partial w}{\partial x} \Big|_{x=0} - \frac{\rho g b h^3}{12EI} + \frac{\rho b}{EI} \int_0^h \frac{\partial \varphi}{\partial t} \Big|_{x=0} y dy \\ \frac{\partial^2 w}{\partial x^2} \Big|_{x=1} &= \frac{C_2}{EI} \frac{\partial w}{\partial x} \Big|_{x=1} - \frac{\rho g b h^3}{12EI} + \frac{\rho b}{EI} \int_0^h \frac{\partial \varphi}{\partial t} \Big|_{x=1} y dy \end{aligned} \quad (15)$$

The above support boundary conditions are also to be differentiated with respect to time t , and the condition (11) is to be adopted. Then we get:

$$\begin{aligned} \frac{\partial^4 \varphi}{\partial x^3 \partial y} \Big|_{x=0} &= -\frac{k_1}{EI} \frac{\partial \varphi}{\partial y} \Big|_{x=0}; & \frac{\partial^4 \varphi}{\partial x^3 \partial y} \Big|_{x=1} &= \frac{k_2}{EI} \frac{\partial \varphi}{\partial y} \Big|_{x=1} \\ \frac{\partial^3 \varphi}{\partial x^2 \partial y} \Big|_{x=0} &= \frac{C_1}{EI} \frac{\partial^2 \varphi}{\partial x \partial y} \Big|_{x=0} + \frac{\rho b}{EI} \int_0^h \frac{\partial^2 \varphi}{\partial t^2} y dy & (16) \\ \frac{\partial^3 \varphi}{\partial x^2 \partial y} \Big|_{x=1} &= \frac{-C_2}{EI} \frac{\partial^2 \varphi}{\partial x \partial y} \Big|_{x=1} + \frac{\rho b}{EI} \int_0^h \frac{\partial^2 \varphi}{\partial t^2} y dy \end{aligned}$$

Additionally we have:

$$\frac{\partial \varphi}{\partial y} \Big|_{y=0} = \frac{\partial \varphi}{\partial y} \Big|_{y=h} \quad (17)$$

The transverse vibration of a beam fully filled with liquid and supported at two points in an arbitrary way is completely defined by the differential equation (14) with the support conditions (16) and the Laplace equation (9) with the boundary conditions (17) ÷ (19) for the liquid velocity:

$$\frac{\partial \varphi}{\partial z} = 0 \quad \text{for } z = \pm \frac{b}{2} \quad (18)$$

$$\frac{\partial \varphi}{\partial x} = -\left(y - \frac{h}{2}\right) \frac{\partial^2 \varphi}{\partial x \partial y} \quad \text{for } x = 0 \text{ and } x = 1 \quad (19)$$

For free vibrations, taking into account (2) we arrive at the following form of equation (14):

$$\begin{aligned} \frac{\partial^5 \tilde{\varphi}}{\partial x^4 \partial y} \Big|_{y=0} - B \frac{\partial^3 \tilde{\varphi}}{\partial x^2 \partial y} \Big|_{y=0} &= \\ = \omega^2 \left[B_1 \frac{\partial \tilde{\varphi}}{\partial y} \Big|_{y=0} + B_3 \left(\tilde{\varphi} \Big|_{y=h} - \tilde{\varphi} \Big|_{y=0} \right) \right] & (20) \end{aligned}$$

with the boundary conditions for the velocity potential $\tilde{\varphi}(x, y, z)$:

$$\begin{aligned} \frac{\partial^4 \tilde{\varphi}}{\partial x^3 \partial y} \Big|_{x=0} &= -\frac{k_1}{EI} \frac{\partial \tilde{\varphi}}{\partial y} \Big|_{x=0}; & \frac{\partial^4 \tilde{\varphi}}{\partial x^3 \partial y} \Big|_{x=1} &= \frac{k_2}{EI} \frac{\partial \tilde{\varphi}}{\partial y} \Big|_{x=1} \\ \frac{\partial^3 \tilde{\varphi}}{\partial x^2 \partial y} \Big|_{x=0} &= \frac{C_1}{EI} \frac{\partial^2 \tilde{\varphi}}{\partial x \partial y} \Big|_{x=0} - \omega^2 B_3 \int_0^h \tilde{\varphi} \Big|_{x=0} y dy & (21) \\ \frac{\partial^3 \tilde{\varphi}}{\partial x^2 \partial y} \Big|_{x=1} &= \frac{-C_2}{EI} \frac{\partial^2 \tilde{\varphi}}{\partial x \partial y} \Big|_{x=1} - \omega^2 B_3 \int_0^h \tilde{\varphi} \Big|_{x=1} y dy \end{aligned}$$

For the liquid inside the tank, the liquid velocity potential equation holds:

$$\frac{\partial^2 \tilde{\varphi}}{\partial x^2} + \frac{\partial^2 \tilde{\varphi}}{\partial y^2} = 0 \quad (22)$$

with boundary conditions for the velocity:

$$\frac{\partial \tilde{\varphi}}{\partial y} \Big|_{y=0} = \frac{\partial \tilde{\varphi}}{\partial y} \Big|_{y=h} \quad (23)$$

$$\frac{\partial \tilde{\varphi}}{\partial z} = 0 \quad \text{for } z = \pm \frac{b}{2} \quad (24)$$

$$\frac{\partial \tilde{\varphi}}{\partial x} = -\left(y - \frac{h}{2}\right) \frac{\partial^2 \tilde{\varphi}}{\partial x \partial y} \quad \text{for } x = 0 \text{ and } x = 1 \quad (25)$$

Let us introduce the „ u ” function defined as:

$$u \equiv \frac{\partial \tilde{\varphi}}{\partial y} \quad (26)$$

Then the vibration equation (20) can be written as:

$$\frac{d^4 u}{dx^4} \Big|_{y=0} - B \frac{d^2 u}{dx^2} \Big|_{y=0} = K(x; t) \quad (27)$$

where:

$$K(x; t) \equiv \omega^2 \left[B_1 \frac{\partial \tilde{\varphi}}{\partial y} \Big|_{y=0} + B_3 \tilde{\varphi} \Big|_{y=0}^{y=h} \right] \quad (28)$$

Solving equation (27) is reduced to the search for the general integral of the homogeneous equation and a particular integral of the non-homogeneous equation. The general integral of the associate homogeneous equation is the following [13]:

$$u_0 = D_1 + D_2 x + D_3 \text{sh}ax + D_4 \text{ch}ax \quad (29)$$

where:
 $a \equiv \sqrt{B}$.

The particular integral of the non-homogeneous equation is searched for using the method of variation of constants. Finally, the integral of the non-homogeneous equation gets the form :

$$\begin{aligned} u &= \tilde{D}_1 + \tilde{D}_2 x + \tilde{D}_3 \text{sh}ax + \tilde{D}_4 \text{ch}ax + \\ &+ \frac{1}{a^2} \left[\int_0^x \xi K(\xi, t) d\xi - x \int_0^x K(\xi, t) d\xi \right] + \\ &+ \frac{1}{a^3} \left[\text{sh}ax \int_0^x \text{ch}a\xi K(\xi, t) d\xi - \text{ch}ax \int_0^x \text{sh}a\xi K(\xi, t) d\xi \right] \end{aligned} \quad (30)$$

Now, the boundary conditions (21) for the potential function will refer to the introduced function $u \equiv u(x, t)$. These conditions will allow the constants $D_i (i = 1, 2, 3, 4)$ to be determined. Then, these constants are to be put into the general integral (30), after which we get the solution in the form:

$$\begin{aligned} u(x, 0; t) &\equiv \frac{\partial \tilde{\varphi}}{\partial y} \Big|_{y=0} = F_1(x) \int_0^1 \xi K d\xi + \frac{1}{a^2} \int_0^x \xi K d\xi + \\ &+ F_2(x) \int_0^1 K d\xi - \frac{x}{a^2} \int_0^x K d\xi + \omega^2 F_3(x) \int_0^h \tilde{\varphi} \Big|_{x=1} y dy + \\ &+ F_4(x) \omega^2 \int_0^h \tilde{\varphi} \Big|_{x=0} y dy + \\ &+ F_5(x) \int_0^1 \text{sh}a\xi K d\xi - \frac{\text{ch}ax}{a^3} \int_0^x \text{sh}a\xi K d\xi + \\ &+ F_6(x) \int_0^1 \text{ch}a\xi K d\xi + \frac{\text{sh}ax}{a^3} \int_0^x \text{ch}a\xi K d\xi \end{aligned} \quad (31)$$

$$F_i(x) \equiv u_i + \eta_i x + \alpha_i \text{shax} + \beta_i \text{chax} \quad (32)$$

for $i = 1, 2, 3, 5, 6$

and

$$F_4(x) \equiv \mu_4 + \left(\eta_4 + \frac{\rho b}{C_1} \right) x + \alpha_4 \text{shax} + \beta_4 \text{chax} \quad (33)$$

The abovenamed coefficients: $u_i, \eta_i, \alpha_i, \beta_i$ (for $i = 1, 2, 3, 4, 5, 6$) are numeric constants calculated from the following formulas:

$$\mu_i \equiv -\beta_i - \frac{a^3 EI}{k_1} \alpha_i ; \eta_i \equiv \frac{EI a^2}{C_1} \beta_i - a \alpha_i \quad (34)$$

and

$$\beta_1 \equiv \frac{1}{Q} \left[\frac{k_2}{EI} \text{shal} + \frac{C_2 k_2 (\text{chal} - 1)}{a(EI)^2} \right]$$

$$\beta_2 \equiv -\frac{1}{Q} \left[\frac{k_2 l}{EI} \text{shal} + \frac{C_2 k_2 l \cdot \text{chal}}{a(EI)^2} - \frac{C_2 k_2 l \cdot \text{shal}}{(a \cdot EI)^2} + \frac{C_2 a}{EI} \left(\text{chal} + \frac{k_2}{k_1} \right) \right]$$

$$\beta_3 \equiv \frac{1}{Q} \left[\frac{\rho b a^3}{EI} \left(\text{chal} + \frac{k_2}{k_1} \right) + \frac{\rho b k_2}{(EI)^2} (a l - \text{shal}) \right] \quad (35)$$

$$\beta_4 \equiv \frac{1}{Q} \left[\frac{k_2 l \rho b a^2 \text{shal}}{C_1 EI} + \frac{C_2 \rho b a^3}{C_1 EI} \left(\text{chal} + \frac{k_2}{k_1} \right) + \frac{C_2 k_2 \rho b}{C_1 (EI)^2} (a l \text{chal} - \text{shal}) \right]$$

$$\beta_5 \equiv \frac{1}{Q} \left[-a^2 + \frac{C_2 k_2}{(aEI)^2} (\text{chal} - 1) - \frac{C_2 a \cdot \text{shal}}{EI} - \frac{C_2 k_2 l \cdot \text{shal}}{(aEI)^2} - \frac{k_2 l \text{chal}}{EI} - \frac{a^2 k_2 \text{chal}}{k_1} - \frac{C_2 k_2 a \text{shal}}{k_1 \cdot EI} \right]$$

$$\beta_6 \equiv \frac{1}{Q} \left[\frac{C_2 a \text{chal}}{EI} - \frac{C_2 k_2 \text{shal}}{(aEI)^2} + \frac{k_2 l \text{shal}}{EI} + \frac{k_2 a \text{shal}}{k_1} + \frac{C_2 k_2 l \text{chal}}{a(EI)^2} + \frac{C_2 k_2 a \text{chal}}{k_1 EI} \right]$$

Here, Q is equal to:

$$Q \equiv \frac{C_2 k_2 a}{(EI)^2} (2\text{chal} - a l \text{shal} - 2) + \frac{C_2 a^4}{(EI)} \left[\frac{k_2 l}{a C_1} (1 - \text{chal}) - \text{shal} \left(1 + \frac{k_2}{k_1} \right) \right] + \quad (36)$$

$$+ \frac{k_2 a^2}{EI} \left[\text{shal} \left(1 + \frac{C_2}{C_1} \right) - a l \left(\text{chal} + \frac{C_2}{C_1} \right) \right] - a^5 \left[\frac{k_2 l}{a C_1} \text{shal} + \text{chal} \left(\frac{k_2}{k_1} + \frac{C_2}{C_1} \right) + \frac{C_2 k_2}{C_1 k_1} + 1 \right]$$

$$\alpha_1 \equiv -\frac{1}{Q} \left[\frac{k_2 \text{chal}}{EI} + \frac{C_2 k_2}{EIC_1} + \frac{C_2 k_2 \text{shal}}{a(EI)^2} \right]$$

$$\alpha_2 \equiv \frac{1}{Q} \left[\frac{C_2 k_2}{(aEI)^2} (1 - \text{chal}) + \frac{C_2 a \text{shal}}{EI} + \frac{k_2 l \text{chal}}{EI} + \frac{C_2 k_2 l \text{shal}}{a(EI)^2} \right]$$

$$\alpha_3 \equiv \frac{1}{Q} \left[\frac{\rho b k_2}{(EI)^2} (\text{chal} - 1) + \frac{\rho b a^2}{EI} \left(\frac{k_2 l}{C_1} - a \text{shal} \right) \right] \quad (37)$$

$$\alpha_4 \equiv \frac{1}{Q} \left[\frac{C_2 k \rho b}{C_1 (EI)^2} (\text{chal} - 1 - a l \text{shal}) - \frac{\rho b a^2}{C_1 EI} (C_2 a \text{shal} + k_2 l \text{chal}) \right]$$

$$\alpha_5 \equiv \frac{1}{Q} \left[\frac{k_2}{EI} \left(\frac{C_2 \text{shal}}{a^2 EI} + \frac{\text{chal}}{a} \right) - \frac{k_2 l}{C_1} \left(\frac{C_2 \text{shal}}{EI} + \frac{a \text{chal}}{1} \right) + \frac{C_2}{C_1} \left(\frac{k_2 \text{chal}}{aEI} - a^2 \text{shal} \right) \right]$$

$$\alpha_6 \equiv \frac{1}{Q} \left[\frac{C_2 k_2}{(aEI)^2} (1 - \text{chal}) - \frac{k_2 \text{shal}}{aEI} + a^2 \left(1 + \frac{C_2}{C_1} \text{chal} \right) + \frac{C_2 k_2}{EIC_1} \left(1 \text{chal} - \frac{\text{shal}}{a} \right) + \frac{k_2 a l \text{shal}}{C_1} \right]$$

The free vibration problem of the liquid-filled beam has been finally reduced to solving the Laplace equation (22) with boundary conditions (23) + (25) for the velocity potential and conditions (31) and (32), in which numeric coefficients are defined by formulas (33) + (37).

From the general boundary conditions for the velocity potential we can derive all particular cases referring to different cases of beam fixing at its both ends. An exception here is rigid fixing, for which the constants for axial and spiral springs (Fig. 1) $k, C \rightarrow \infty$.

FREE VIBRATION OF A TANK COMPLETELY FILLED WITH LIQUID

Let us return to equation (20), which is the free vibration equation for the liquid-filled beam. Neglecting the constant, the equation has the following form:

$$\frac{\partial^5 \tilde{\varphi}}{\partial x^4 \partial y} \Big|_{y=0} = \omega^2 \left[A_1 \cdot \frac{\partial \tilde{\varphi}}{\partial y} \Big|_{y=0} + B \left(\tilde{\varphi} \Big|_{y=h} - \tilde{\varphi} \Big|_{y=0} \right) \right] \quad (38)$$

For the liquid inside the beam the Laplace equation (22) holds.

After integrating equation (38) four times with respect to the "x" variable we get:

$$\frac{\partial \tilde{\varphi}}{\partial y} \Big|_{y=0} = \omega^2 \int_0^1 K(x, \xi) F(\xi, 0) d\xi \quad (39)$$

where:

$$F(\xi, 0) \equiv A_1 \cdot \frac{\partial \tilde{\varphi}}{\partial y} \Big|_{(\xi, 0)} + B [\tilde{\varphi}(\xi, h) - \tilde{\varphi}(\xi, 0)] \quad (40)$$

and $K | x, \xi |$ is a symmetrical kernel, i.e.

$$K | x, \xi | = K | \xi, x |$$

The kernel $K | x, \xi |$ defined in the two-dimensional domain, see Fig. 2, has the following polynomial form:

$$K(x, \xi) = \begin{cases} -\frac{\xi^3}{6} + \frac{x\xi^2}{2} - \frac{x^2\xi^2}{1} + \frac{x^2\xi^2(x+\xi)}{2l^2} - \frac{x^3\xi^3}{3l^3} & \text{for } 0 \leq \xi \leq x \\ -\frac{x^3}{6} + \frac{\xi x^2}{2} - \frac{\xi^2 x^2}{1} + \frac{\xi^2 x^2(\xi+x)}{2l^2} - \frac{\xi^3 x^3}{3l^3} & \text{for } x \leq \xi \leq l \end{cases} \quad (41)$$

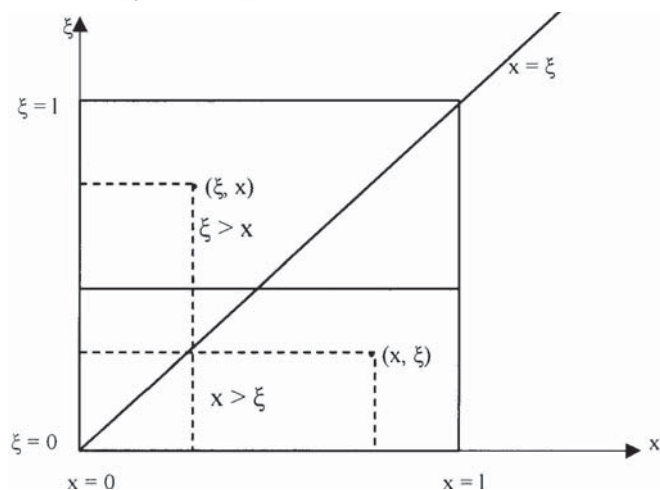


Fig. 2. Graphical representation of the symmetrical kernel

Finally, the free vibration problem for a beam fixed at both sides and filled with liquid within the linear range has been reduced to solving the Laplace equation in the two-dimensional domain D defined as (Fig. 3)

$$D \equiv \begin{cases} 0 \leq x \leq l \\ 0 \leq y \leq h \end{cases} \quad (42)$$

$$\frac{\partial^2 \tilde{\varphi}}{\partial x^2} + \frac{\partial^2 \tilde{\varphi}}{\partial y^2} = 0 \quad (43)$$

with differential conditions, and a differential-integral condition.

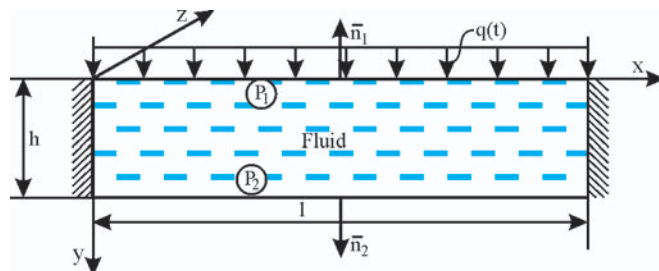


Fig. 3. Liquid-filled beam fixed at both sides

Let us assume that the liquid velocity potential function $\tilde{\varphi} \equiv \tilde{\varphi}(x, y)$ is the product of two functions with separated variables in the form of the sum of an infinite series

$$\tilde{\varphi}(x, y) = \sum_{n=0}^{\infty} \cos \frac{n\pi x}{l} g_n(y) \quad (44)$$

The assumed potential has to fulfil the Laplace equation.

This way we arrive at the equation system determining free vibration frequencies and related modes. It is an infinite system of homogeneous algebraic equations. The problem of determining the free vibration frequency spectrum and modes is therefore reduced to the eigenvalue and eigenvector problem, written in the following matrix notation:

$$[A\omega^2 - D] [CX] = [0] \quad (45)$$

where:

$A \equiv [a_{jn}]$ - symmetrical matrix of coefficients of kernel decomposition into the Fourier series, (formulas 46).

$$a_{jn} = \frac{l^4}{(jn\pi^2)^4} [(j\pi)^4 \delta_{jn} + 24(\cos n\pi)(1 - \cos j\pi)] \quad \text{for } j, n \geq 1$$

$$a_{00} = \frac{l^4}{720} \quad \text{for } j, n = 0 \quad (46)$$

$$a_{j0} = \frac{1}{2} a_{0n} = \frac{-l^4(1 + \cos j\pi)}{2(j\pi)^4} \quad \text{for } j \geq 1, n = 0$$

The matrices in the matrix equation (45) represent:

$D \equiv [d_{jj}]$ - diagonal matrix, the element of which are calculated using the formula

$$d_{jj} = \left[A_1 + \frac{2l}{j\pi} B \operatorname{th} \frac{j\pi h}{2l} \right]^{-1} \quad \text{for } j \geq 1 \quad (47)$$

$$d_{00} = [A_1 + Bh]^{-1} \quad \text{for } j = 0 \quad (48)$$

$CX \equiv [C_j X_j]$ - single-column matrix, in which C_j are unknown constants $\neq 0$

and X_j are calculated using formulas (49) and (50):

$$X_0 \equiv A_1 + Bh \text{ for } j = 0 \quad (49)$$

$$X_j \equiv \frac{j\pi}{1} \left(e^{\frac{j\pi h}{1}} + 1 \right) A_1 + 2B \left(e^{\frac{j\pi h}{1}} - 1 \right) \text{ for } j \geq 1 \quad (50)$$

In a special case when **the liquid is absent**, i.e. when $\rho = 0$, and $B = 0$ the elements of the abovenamed matrices are determined using the following relations:

$$d_{jj} = \frac{1}{A_1} \text{ for } j \geq 0 \quad (51)$$

and

$$X_0 = A_1 \text{ for } j = 0$$

$$X_j = \frac{j\pi}{1} \left(e^{\frac{j\pi h}{1}} + 1 \right) A_1 \text{ for } j \geq 1 \quad (52)$$

In this case the matrix equation (45) describes free vibrations of the system without liquid.

Behaviour of the liquid inside the beam during free vibrations.

Having known the liquid velocity potential we can determine the velocity field for the liquid:

$$\vec{V} = \frac{\partial \tilde{\varphi}}{\partial x} \vec{i} + \frac{\partial \tilde{\varphi}}{\partial y} \vec{j} \quad (53)$$

where:

\vec{i}, \vec{j} – unit vectors of the Cartesian coordinate system Oxy

and

$$\frac{\partial \tilde{\varphi}}{\partial x} = -\sum_{n=1}^{\infty} C_n \frac{n\pi}{1} \sin \frac{n\pi x}{1} \left[e^{\frac{n\pi y}{1}} - e^{\frac{n\pi(h-y)}{1}} \right] \quad (54)$$

$$\frac{\partial \tilde{\varphi}}{\partial y} = C_0 + \sum_{n=1}^{\infty} C_n \frac{n\pi}{1} \cos \frac{n\pi x}{1} \left[e^{\frac{n\pi y}{1}} + e^{\frac{n\pi(h-y)}{1}} \right] \quad (55)$$

Having determined components of the liquid velocity field we can find the equation for the family of streamlines as:

$$\psi(x, y) = -C_0 x - \sum_{n=1}^{\infty} C_n \sin \frac{n\pi x}{1} \left[e^{\frac{n\pi y}{1}} + e^{\frac{n\pi(h-y)}{1}} \right] \quad (56)$$

From the condition $\psi = \text{const}$ we obtain the family of streamlines.

The pressure is calculated from the following Bernoulli relation:

$$p(x, y, t) = -\rho \left(\frac{\partial \varphi}{\partial t} \right) \quad (57)$$

or taking into account the velocity term [12]:

$$p(x, y, t) = -\rho \left(\frac{\partial \varphi}{\partial t} + \frac{1}{2} \text{grad}^2 \varphi \right) \quad (58)$$

Taking only into account the amplitude of the dynamic pressure we arrive at:

$$\tilde{p}(x, y) = \rho \omega \left\{ C_0 \left(y - \frac{h}{2} \right) + \sum_{n=1}^{\infty} C_n \cos \frac{n\pi x}{1} \cdot \left[e^{\frac{n\pi y}{1}} - e^{\frac{n\pi(h-y)}{1}} \right] \right\} \quad (59)$$

FREE VIBRATION OF A BEAM PARTIALLY FILLED WITH LIQUID

A case which most often happens in practice is when the tank is partially filled with liquid. A thin-wall prismatic beam of dimensions $l \times b \times h$ is assumed, with the liquid of density ρ inside it. The height to which the beam is filled with the liquid is smaller than the h dimension of the beam.

For the $Oxyz$ system assumed as in Fig. 4, the free surface of the liquid has a wavy shape described by the equation $y=Y(x, z, t)$.

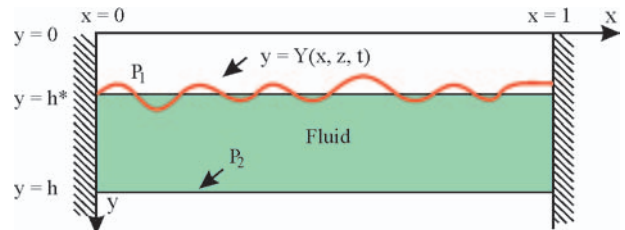


Fig. 4. Beam partially filled with liquid

Like in the previous case, we have to adopt model assumptions for the beam and the liquid. The liquid velocity potential $\varphi(x, y, z, t)$ fulfils the Laplace equation:

$$\nabla^2 \varphi = 0 \quad (60)$$

as, by default, the flow of incompressible liquid in the beam is irrotational within the entire domain D defined as:

$$D \equiv \left\{ \begin{array}{l} 0 \leq x \leq 1 \\ -\frac{b}{2} \leq z \leq \frac{b}{2} \\ Y(x, z) \leq y \leq h \end{array} \right\} \quad (61)$$

Assuming two-dimensional waves, we introduce a constant average height of filling $H \equiv h - h^*$. After further transformations of equation (45) we arrive at infinite homogeneous equation system, which can be written in the matrix form:

$$[A\omega^2] [CX] = [0] \quad (62)$$

where:

$A \equiv [a_{jn}]$ – symmetrical matrix of coefficients of kernel expansion into the Fourier series, the elements of which are calculated using formulas (38)
 $CX \equiv [C_j X_j]$ – single-column matrix, in which C_j are constant unknowns $\neq 0$; and X_j are calculated in the following way:

$$X_j = A_1 s \left[(gs + \omega^2) e^{s(h-h^*)} - (gs - \omega^2) e^{s(h^*-h)} \right] + B \left[(gs + \omega^2) e^{s(h-h^*)} + (gs - \omega^2) e^{s(h^*-h)} - 2gs \right] \quad (63)$$

and

$$X_0 = A_1 + B(h - h^*) \quad (64)$$

$D \equiv [d_{jj}]$ – diagonal matrix, the elements of which are determined using the following formulas:

$$\text{for } j = 0 \quad d_{00} = \frac{1}{A_1 + B(h - h^*)}$$

$$d_{jj} = \left[A_1 + \frac{B}{s} \frac{gs \text{th} \frac{s}{2} (h - h^*) + \omega^2}{gs + \omega^2 \text{cth} s (h - h^*)} \right]^{-1} \text{ for } j \geq 1 \quad (65)$$

$$s = \frac{j\pi}{1}$$

Here we can make distinction between two limiting cases of liquid filling, which are :

- I. where $h^* \rightarrow h$ – liquid is absent
- II. where $h^* \rightarrow 0$ – full filling.

Case I:

$\rho = 0$ i.e. $B = 0$ and then:

$$X_0 = A_1 ; X_j = \frac{2j\pi}{l} A_1 \omega^2 \text{ for } j \geq 1 \quad (66)$$

$$d_{00} = d_{jj} = \frac{1}{A_1} \quad (67)$$

Case II:

$\rho \neq 0$; $h - h^* \rightarrow h$, then:

$$X_j = A_1 s \left[(gs + \omega^2) e^{sh} - (gs - \omega^2) e^{-sh} \right] + B \left[(gs + \omega^2) e^{sh} + (gs - \omega^2) e^{-sh} - 2gs \right] \quad (68)$$

$$d_{00} = \frac{1}{A_1 + Bh} \quad \text{for } j = 0$$

$$d_{jj} = \left[A_1 + \frac{B \left(gs \operatorname{th} \left(\frac{sh}{2} \right) + \omega^2 \right)}{s (gs + \omega^2 \operatorname{cth}(sh))} \right]^{-1} \quad \text{for } j \geq 1 \quad (69)$$

In all above formulas A_1 and B are the constants equal, respectively, to:

$$A_1 \equiv \frac{\rho_b A}{EI} ; B \equiv \frac{\rho b}{EI} \quad (70)$$

Case II is not included in the earlier obtained relations, as there was no free surface in those cases.

NUMERICAL SOLUTIONS

The equation systems (45) and (62) were solved numerically using an in-home code written on PC computer. An infinite system of algebraic equations was obtained, which is fully regular. According to a theorem, a method of successive sections can be applied in this case. For the assumed section dimension “n” the code creates system matrices and solves the eigenvalue and eigenvector problem. The code calculates and prints the liquid pressure and velocity fields at a selected point of the area occupied by the liquid. For partial filling, the code additionally prints the deflection and the shape of the free surface. For this case dynamic pressure amplitudes are also calculated. Along with hydrodynamic frequencies in the deformable tank, the frequencies of the same volume of liquid in a rigid tank are determined as well.

CONCLUSIONS FROM THE OBTAINED SOLUTIONS

For four height-to-length ratios, i.e.

$$h/l \in \{0.02, 0.1, 0.5, 1\}$$

transverse vibration frequency spectra were obtained, making use of the here presented theory and a simplified formula, for the tank filled with liquid.

Figs (5) ÷ (6) show the frequency spectra for six first frequencies and that for the tank without liquid (curves marked $\rho = 0$ in the figures).

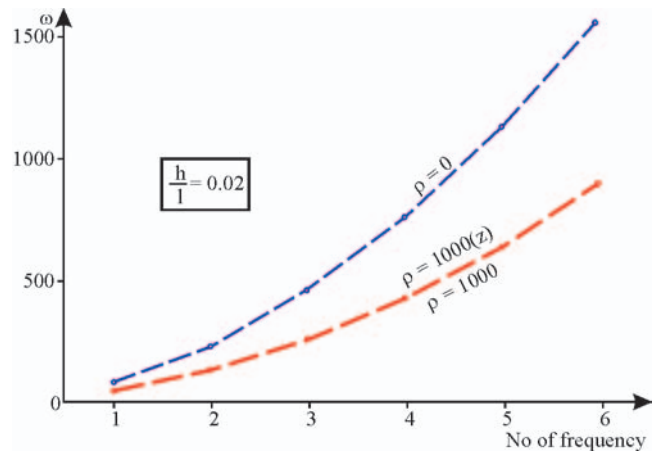


Fig. 5. Vibration frequency spectrum for the tank fully filled with liquid: $h/l = 0.02$

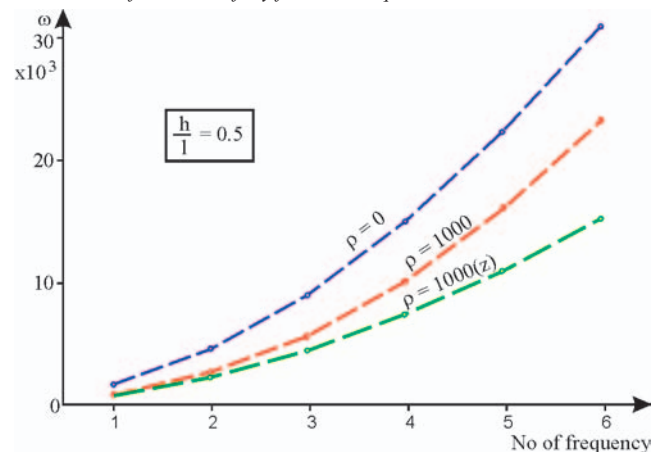


Fig. 6. Vibration frequency spectrum for the tank fully filled with liquid: $h/l = 0.5$

Dynamic pressure amplitudes and velocity field components were determined at all nodes of the grid of the dimensions $1/40 \times h/10$.

This made the basis for preparing diagrams of dynamic pressure distributions on tank walls for each of six first modes and for three h/l ratios. The pressure diagrams refer to the half-length of the tank and the fixed top wall. Sample cases are shown in Figs. (7÷8).

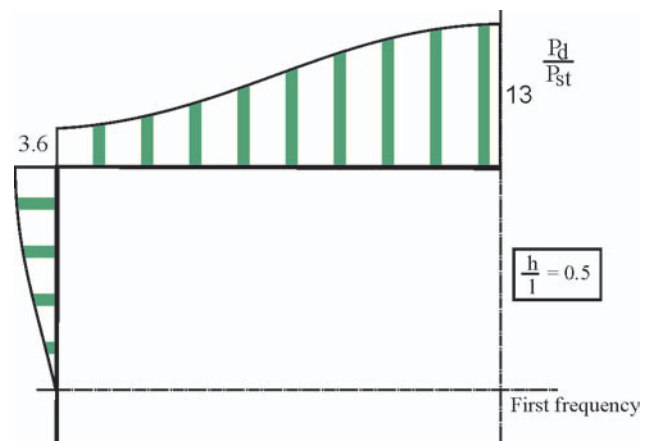


Fig. 7. Pressure distribution on tank walls for the first frequency and $h/l = 0.5$

In the case of the tank partially filled with liquid, frequency spectra are shown for each of the above named h/l ratios and four cases of liquid filling, i.e.

$$H/h \in \{0.25, 0.5, 0.75, 1\}$$

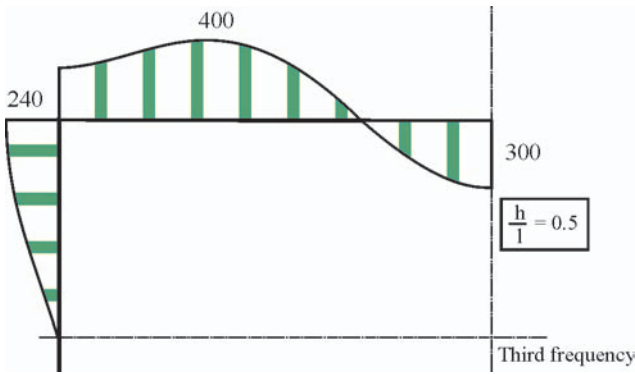


Fig. 8. Pressure distribution on tank walls for the third frequency and $h/l = 0,5$

where:

H – liquid column height.

Additionally, sample diagrams shown in Figs. (9÷10) present, as a comparison, frequency spectra which neglect the dynamic condition on the free surface of the liquid (curves marked "I").

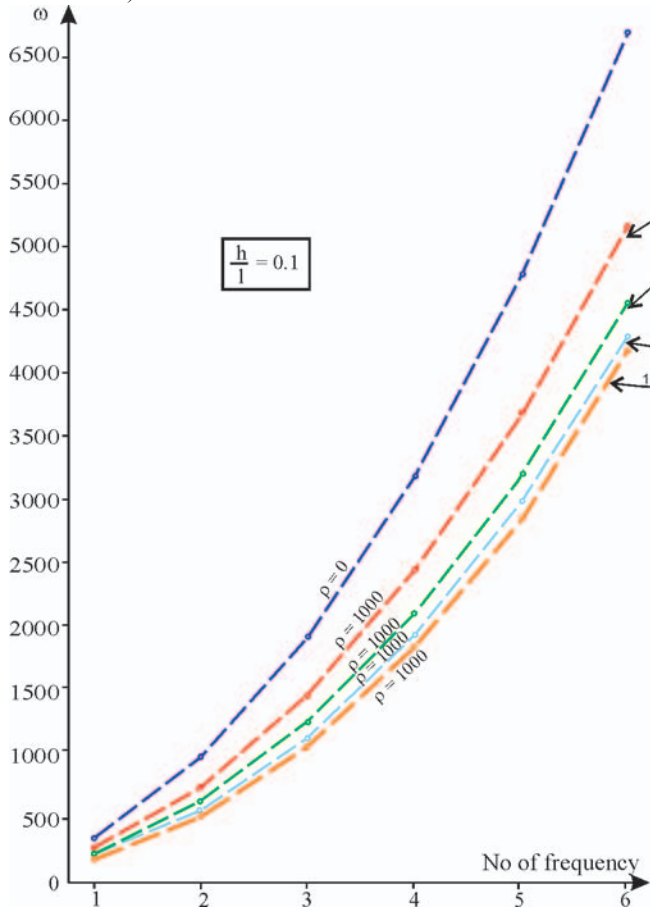


Fig. 9. Vibration frequency spectrum for the tank partially filled with liquid: $h/l = 0.1$

Figures (11) show beam frequency diagrams for the first frequencies. The diagrams present the beam frequencies according to the present theory (marked "B"), those calculated as the reduced frequencies (marked "z"), the hydrodynamic or "liquid" frequencies (marked "c") and the frequencies of the liquid itself in a rigid tank (marked "w").

Then, for two frequencies and four h/l ratios, Figs. (12÷13) show dynamic pressure distributions for the bottom and top walls, for all four fillings. These diagrams refer to the half-length of the tank. Obviously, the point symmetry is observed for even frequencies and the axial symmetry for odd frequencies.

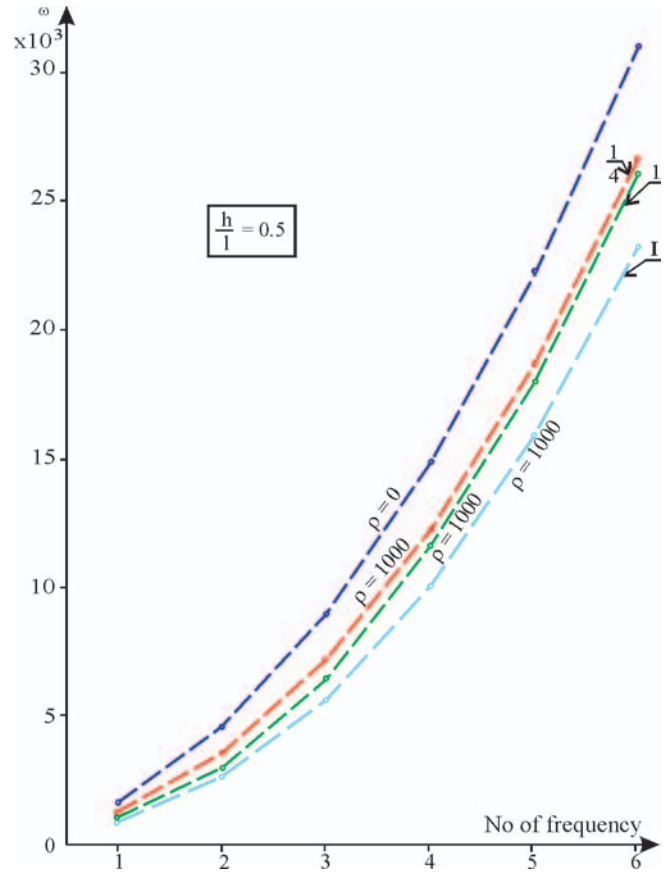


Fig. 10. Vibration frequency spectrum for the tank partially filled with liquid: $h/l = 0.5$

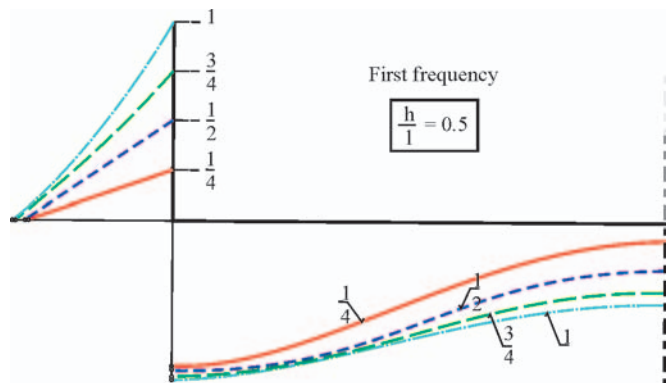


Fig. 12. Dynamic pressure distribution for tank bottom and top walls: $h/l = 0.5$, the first frequency

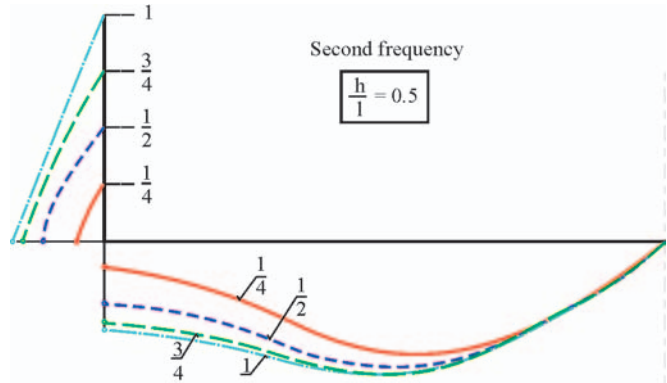


Fig. 13. Dynamic pressure distribution for tank bottom and top walls: $h/l = 0.5$, the second frequency

The next figures, Figs. (14÷15), show tank bottom deflection amplitudes and the shape of the liquid free surface for the first three frequencies, and for different h/l ratios and tank fillings.

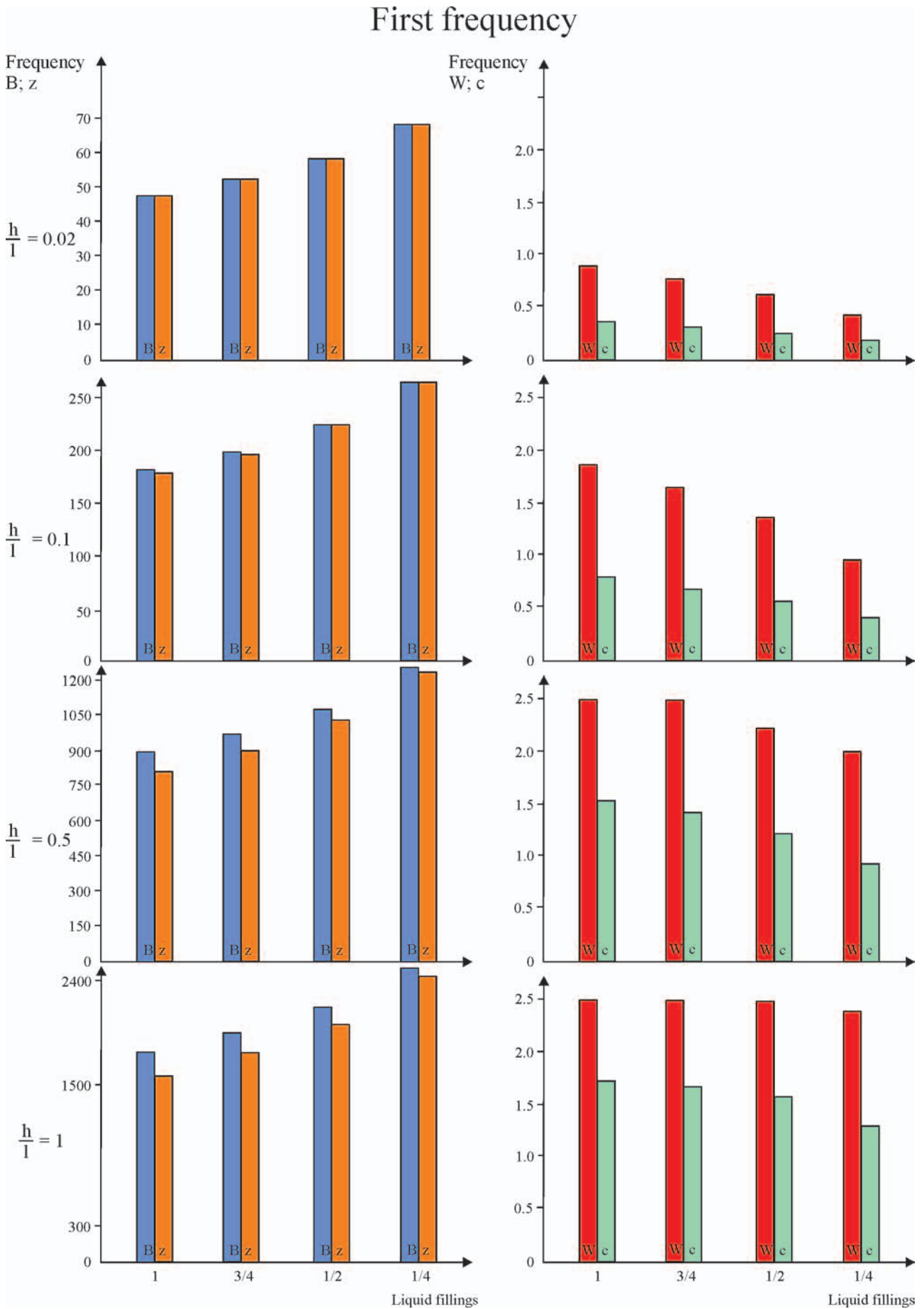


Fig. 11. Beam frequency diagram for different liquid fillings: the first frequency

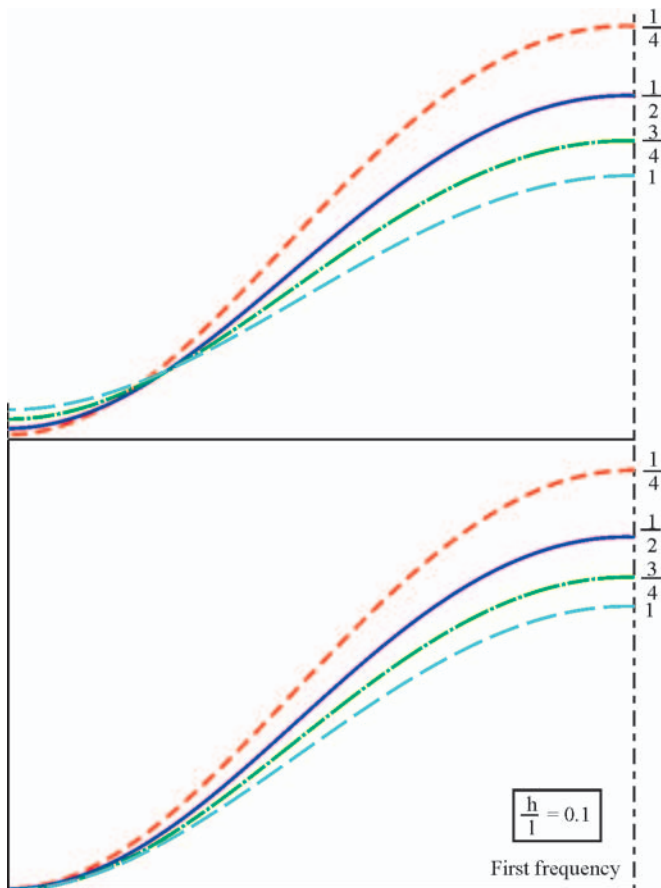


Fig. 14. Tank bottom deflection amplitudes and free surface shapes: $h/l = 0.1$; the first frequency

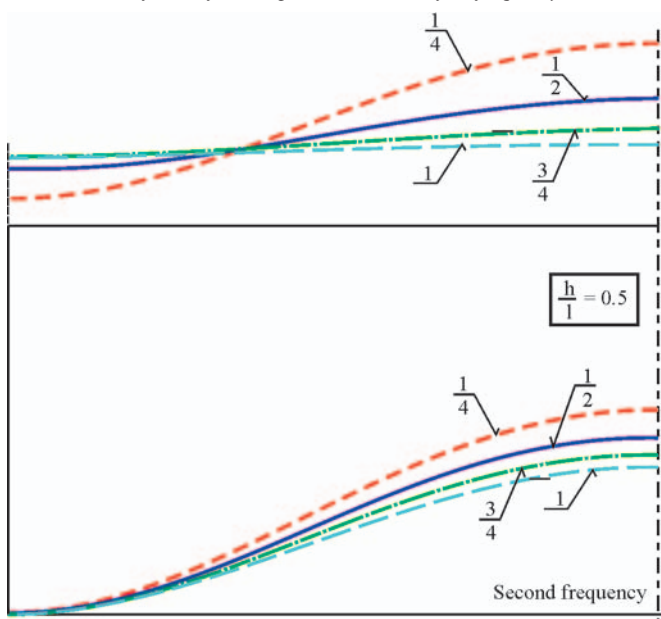


Fig. 15. Tank bottom deflection amplitudes and free surface shapes: $h/l = 0.5$; the second frequency

CONCLUSIONS

- The presence of the liquid in the beam decreases vibration frequencies, compared to the frequency spectrum of the beam without liquid.
- The spectrum levels determined based on the here presented theory depend on the h/l ratio, and are above those calculated using a simplified formula.

- Reducing the volume of the liquid in the beam leads to the reduction in percentage differences between the abovementioned spectra, and in the limiting case of the absence of the liquid the frequency spectra are identical with each other.
- Taking into account the dynamic condition on the free surface moves the spectrum towards higher values. For low beams $h/l < 0.1$ this effects is negligible.
- When h/l increases, the flow of the liquid in the vicinity of the tank walls becomes more intensified. Vertical velocities of the liquid particles in the central layer and on the surface of the moistened tank bottom differ significantly, starting from the second and higher frequencies. For beams fully filled with liquid and the ratio $h/l = 1$ the motion of the liquid reflects the membrane principle.
- Horizontal velocity components of the liquid particles move the hydrodynamic pressure distribution towards tank tops, which increases the loads of the top walls with increasing h/l .

BIBLIOGRAPHY

1. Cho J.R., Lee H.W. and Kim K.W.: *Free vibration analysis of baffled liquid-storage tanks by the structural-acoustic finite element formulation*, J.Sound and Vibration, 258, 847, 2002
2. Kekana M. and Badur J.: *Modeling of beams using the reduced integration technique-statics and free vibration*, Res.Dev.J., 16, 9, 2000
3. Kobayashi E., Asai S.: *A study on a mathematical model for maneuvering motions at low speed* (in Japanese), J Kansai Soc. Nav. Archit., 193, 27-37, 1984
4. Lamb H.: *Hydrodynamics*, Cambridge University Press, 1975
5. Liu W. K., Ma D. C.: *Computer implementation aspects for fluid-structure interaction problems*, Comp. Meth. in Applied Mech. and Eng., 31, 2, 129-148, 1982
6. Morand H. J. P., Ohayon R.: *Fluid Structure Interaction*, J. Wiley & Sons, Chichester, 1995
7. Parszewski Z.: *Drgania i dynamika maszyn*, WNT Warszawa, 1982
8. Sawicki A.: *Mechanika Kontinuum – Wprowadzenie*, IBW PAN, Gdańsk, 1994
9. Trębacki K.: *Drgania swobodne cieczy w sztywnych i odkształconych zbiornikach wypełnionych cieczą*, Pr. IO nr 2268/MR-1141/85, Gdańsk, 1985
10. Trębacki K.: *Algorytm obliczania drgań swobodnych zbiornika wypełnionego cieczą*, PB IO nr 223/CPBR 9.5-231/87, Gdańsk, 1987
11. Trębacki K.: *Drgania swobodne zbiorników wypełnionych cieczą. Cz. I – Analiza teoretyczna*, Zeszyty Naukowe Politechniki Gdańskiej nr 418, Budownictwo Okrętowe XLVII, ss. 197-210, 1990
12. Trębacki K.: *Wpływ bezwładności obrotowej ścian szczytowych zbiornika z cieczą na widmo częstości drgań*, Polish Academy of Sciences, Branch in Gdańsk, Marine Technology Transaction Vol. 4, pp. 224-246, 1993
13. Trębacki K.: *Hydrodynamika zbiornika wypełnionego częściowo cieczą*, XXI Sesja Naukowa Okrętowców, Gdańsk, 2004
14. Zienkiewicz O.C. and Taylor R.L.: *The Finite Element Method*, McGraw-Hill, NY, 1991.

CONTACT WITH THE AUTHOR

Kazimierz Trębacki, Ph. D.
 Faculty of Ocean Engineering
 and Ship Technology
 Gdansk University of Technology
 Narutowicza 11/12
 80-952 Gdansk, POLAND
 e-mail : katre@pg.gda.pl

Graphical presentation of the power of energy losses and power developed in the elements of hydrostatic drive and control system

Part I

Rotational hydraulic motor speed series throttling control systems

Zygmunt Paszota, Prof.

Gdansk University of Technology

ABSTRACT



Paper proposes and justifies a diagram of the direction of increase of power stream from the shaft or piston rod of a hydraulic motor to the pump shaft, power increasing as an effect of the imposed power of energy losses in the hydrostatic drive and control system elements. Graphical interpretation of the power of energy losses in the hydrostatic drive and control system elements and also of the power developed by those elements is presented. An individual system with the rotational hydraulic motor speed series throttling control fed by a constant capacity pump cooperating with an overflow valve in a constant pressure system $p = cte \approx pn$ is analyzed and also an individual system with the rotational hydraulic motor speed series throttling control fed by a constant capacity pump cooperating with an overflow valve controlled in a variable pressure system: $p = var$; an individual system with the rotational hydraulic motor speed series throttling control fed by a variable capacity pump cooperating with a pressure regulator in a constant pressure system $p = cte \approx pn$ and an individual system with the rotational hydraulic motor speed series throttling control fed by a variable capacity pump cooperating with the Load Sensing regulator in a variable pressure $p = var$ system.

Keywords: hydrostatic drive and control system, power of energy losses, energy efficiency

INTRODUCTION

The graphic presentation, by means of fields with specific areas, of the power of energy losses generated in the elements of a hydrostatic drive and control system and of power processed in the hydraulic displacement machines used in the system, becomes a tool facilitating comparison of the size of losses.

Fig. 1 presents (as an example of a system with the hydraulic motor speed series throttling control fed by a constant capacity pump cooperating with an overflow valve) a diagram of the direction of increase of power stream from the shaft or piston rod of a hydraulic motor to the pump shaft, power increasing as an effect of the imposed power of energy losses in the hydrostatic drive and control elements.

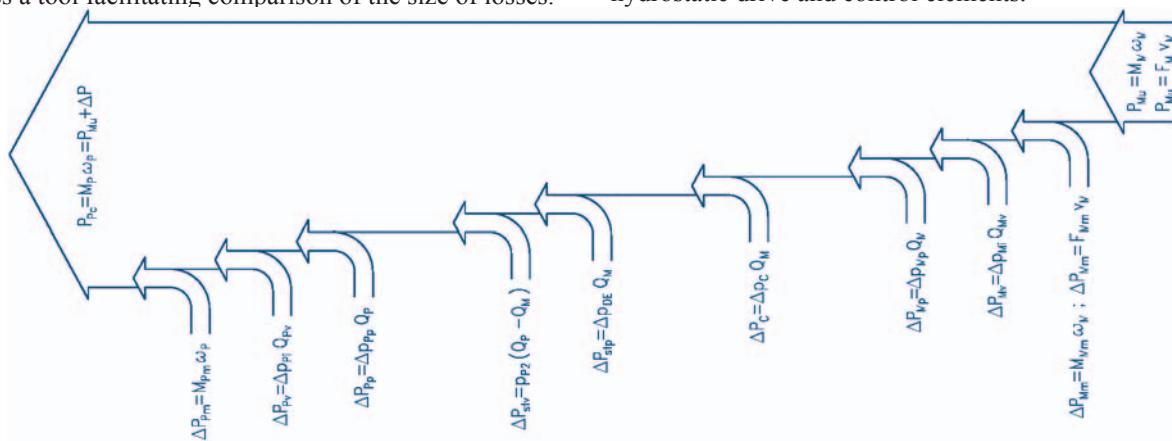


Fig. 1. The diagram presenting the direction of increase of power stream from the useful power P_{Mu} on the shaft or piston rod of the hydraulic motor to the power P_{pc} consumed on the pump shaft as an effect of the power of losses generated in the hydrostatic drive and control system elements. Power P_{pc} on the pump shaft is a function (a sum) of the power P_{Mu} on the shaft or piston rod of the hydraulic motor and the sum ΔP of power of losses in the elements (example of a system with the hydraulic motor speed series throttling control fed by a constant capacity pump cooperating with an overflow valve) $P_{Mu} = M_M \omega_M$ – motor useful power on the rotational motor shaft; $P_{Mu} = F_M v_M$ – motor useful power on the linear motor piston rod, $\Delta P_{Mm} = M_{Mm} \omega_M$ – power of mechanical losses in the rotational motor; $\Delta P_{Mm} = F_{Mm} v_M$ – power of mechanical losses in the linear motor; $\Delta P_{Mv} = \Delta p_{Mv} Q_{Mv}$ – power of volumetric losses in the motor; $\Delta P_{Mp} = \Delta p_{Mp} Q_M$ – power of pressure losses in the motor; $\Delta P_c = \Delta p_c Q_M$ – power of pressure losses in the system conduits, $\Delta P_{sp} = \Delta p_{DE} Q_M$ – power of structural pressure losses in the throttling control assembly (in servo-valve, directional proportional valve, set throttling valve or set two-way flow regulator), $\Delta P_{sv} = p_{sp} (Q_p - Q_M)$ – power of structural volumetric losses in the throttling control assembly (in overflow valve), $\Delta P_{pp} = \Delta p_{pp} Q_p$ – power of pressure losses in the pump, $\Delta P_{pv} = \Delta p_{pv} Q_p$ – power of volumetric losses in the pump, $\Delta P_{pm} = M_{pm} \omega_p$ – power of mechanical losses in the pump, $P_{pc} = M_p \omega_p$ – power consumed on the pump shaft

The useful power $P_{Mu} = M_M \omega_M$ determined on the rotational hydraulic motor shaft or $P_{Mu} = F_M v_M$ determined on the linear hydraulic motor piston rod, changing in the work field ($0 \leq M_M \leq M_{Mmax}$ and $0 \leq \omega_M \leq \omega_{Mmax}$) or ($0 \leq F_M \leq F_{Mmax}$ and $0 \leq v_M \leq v_{Mmax}$) of the motor driven device, is a result of instantaneous requirements of the device toward motor both as regards load M_M (F_M) and speed ω_M (v_M). Therefore, the instantaneous useful power P_{Mu} is independent of the structure of hydraulic system (used for changing the motor speed ω_M (v_M)) and of the power ΔP of losses in the system elements. However, this does not apply to the upper limits of the device parameter ranges, i.e. maximum load M_{Mmax} (F_{Mmax}) and maximum speed ω_{Mmax} (v_{Mmax}).

The upper limits of work field, determined by the $M_{Mmax} = f(\omega_{Mmax})$ and $\omega_{Mmax} = f(M_{Mmax})$ or $F_{Mmax} = f(v_{Mmax})$ and $v_{Mmax} = f(F_{Mmax})$ lines, of the hydraulic motor driving the device, depend on the theoretical capacity Q_{pt} of the pump in the system, on the nominal pressure p_n level of the system operation (the product $Q_{pt} p_n$ is the reference power), on the motor speed control structure used, and also on the sum ΔP of power of losses in the system elements. The upper limits of the motor work field differ in systems with different motor speed control structures.

On the other hand, the instantaneous power $P_{pc} = M_p \omega_p$, absorbed (consumed) by the pump from the drive (electric, internal combustion) motor, determined on the pump shaft, is a sum of the instantaneous useful power P_{Mu} of the hydraulic motor and instantaneous sum ΔP of power of losses in the hydraulic system elements: $P_{pc} = P_{Mu} + \Delta P$.

Power P_{pc} on the pump shaft is equal to the sum ΔP of power of energy losses in the system elements ($P_{pc} = \Delta P$) during the operation with unloaded motor (when $M_M = 0$ or $F_M = 0$) or with the stopped motor (when $\omega_M = 0$ or $v_M = 0$). The useful power P_{Mu} of the motor and energy efficiency η of the system are then equal to zero ($P_{Mu} = 0$, $\eta = 0$). The information on the level of power P_{pc} absorbed then by the pump and entirely lost in the system is particularly important at the system operation with unloaded motor (when $M_M = 0$ or $F_M = 0$). Power P_{pc} of the pump operating with hydraulic motor stopped (when $\omega_M = 0$ or $v_M = 0$) may be minimized by simultaneous cutting of the pump discharge conduit from the hydraulic motor and connecting this conduit with the tank, i.e. unloading the pump. However, this is only possible in an individual system, when the pump feeds only one hydraulic motor.

In references [1 – 6] and other dealing with energy aspects of the hydrostatic transmission operation a need is discussed of determining the energy efficiency of those transmissions in terms of the power of the mechanical, volumetric and pressure losses in them.

In references [7 – 10] an approach is presented to the problems of energy losses in the hydrostatic drive system elements. It has been concluded, that the often practiced method of presenting the energy losses as a function of parameters depending on those losses should be abandoned.

Reference [10] ends with the following conclusions:

- * the energy losses in the elements and also power of those losses should be presented as a function of parameters independent of those losses
- * definition of the efficiency of system elements as a relation of the respective hydraulic and mechanical powers increasing in the power stream from the shaft or piston rod of a hydraulic motor to the pump shaft is a form of precise description of the value of those efficiencies
- * description of the power of losses and energy efficiencies (presented in references [7 – 10]) is based on the principle of equality of the power absorbed by the pump with the sum of hydraulic motor useful power and power of losses in the

system elements, and also on the principle of equality of the system energy efficiency, expressed as a relation of the motor useful power to the pump absorbed power, with the product of the system element energy efficiencies

- * comparing the power of losses in the system elements gives an information facilitating the system design
- * presenting the fields of the power of losses in the system elements allows to draw conclusions about e.g. minimization of the power of structural volumetric and pressure losses in the motor speed throttling control assembly elements, in the proportional control systems and in the hydraulic servomechanism systems
- * graphical interpretation, by means of the field areas of the power of the energy losses in the hydrostatic drive system elements and of power developed by the elements, allows to compare powers of those losses with the area of the field of reference power given by the product $Q_{pt} p_n$ of theoretical pump capacity and the system nominal pressure
- * graphical interpretation of the power of losses allows to evaluate directly the energy savings after introducing the energy – saving solutions, allows to compare directly the energy losses due to change of the working medium viscosity or replacing the oil by oil – water emulsion or water.

References [8,10] present an example (without any comment) of the graphical interpretation of the power of losses in a system with the hydraulic motor speed series throttling control fed by a constant capacity pump cooperating with an overflow valve in a constant pressure system.

This publication presents and analyses the field areas of the power of energy losses in the hydraulic system elements with different rotational hydraulic motor speed control structures. Deliberations allow to realise the rules deciding of the size of fields of power losses in the instantaneous motor operation parameters required by the motor driven device, i.e. instantaneous load M_M and speed ω_M (n_M). Deliberations allow to draw conclusions on achieving high energy efficiency η of a system with selected structure and also conditions that must be fulfilled in order to achieve that high efficiency. Deliberations allow also to compare the power of losses connected with the used hydraulic motor speed control structure and the power P_{pc} absorbed (consumed) by the pump from the drive (electric or internal combustion) motor, the power necessary to ensure the required useful power $P_{Mu} = M_M \omega_M$ of the pump driven hydraulic motor.

The paper consists of two parts. This Part I presents graphical interpretation of the power of energy losses and power developed in the elements of systems of the rotational hydraulic motor speed series throttling control, Part II – the same problems but related to the systems with parallel throttling control and volumetric control of the rotational hydraulic motor speed.

SYSTEM OF THE MOTOR SPEED SERIES THROTTLING CONTROL FED BY A CONSTANT CAPACITY PUMP COOPERATING WITH AN OVERFLOW VALVE IN CONSTANT PRESSURE CONDITIONS

Fig. 2 presents graphical interpretation of the power of energy losses in elements of an individual system with the rotational hydraulic motor speed series throttling control, fed by a constant capacity pump cooperating with an overflow valve in a constant pressure system $p = cte \approx p_n$.

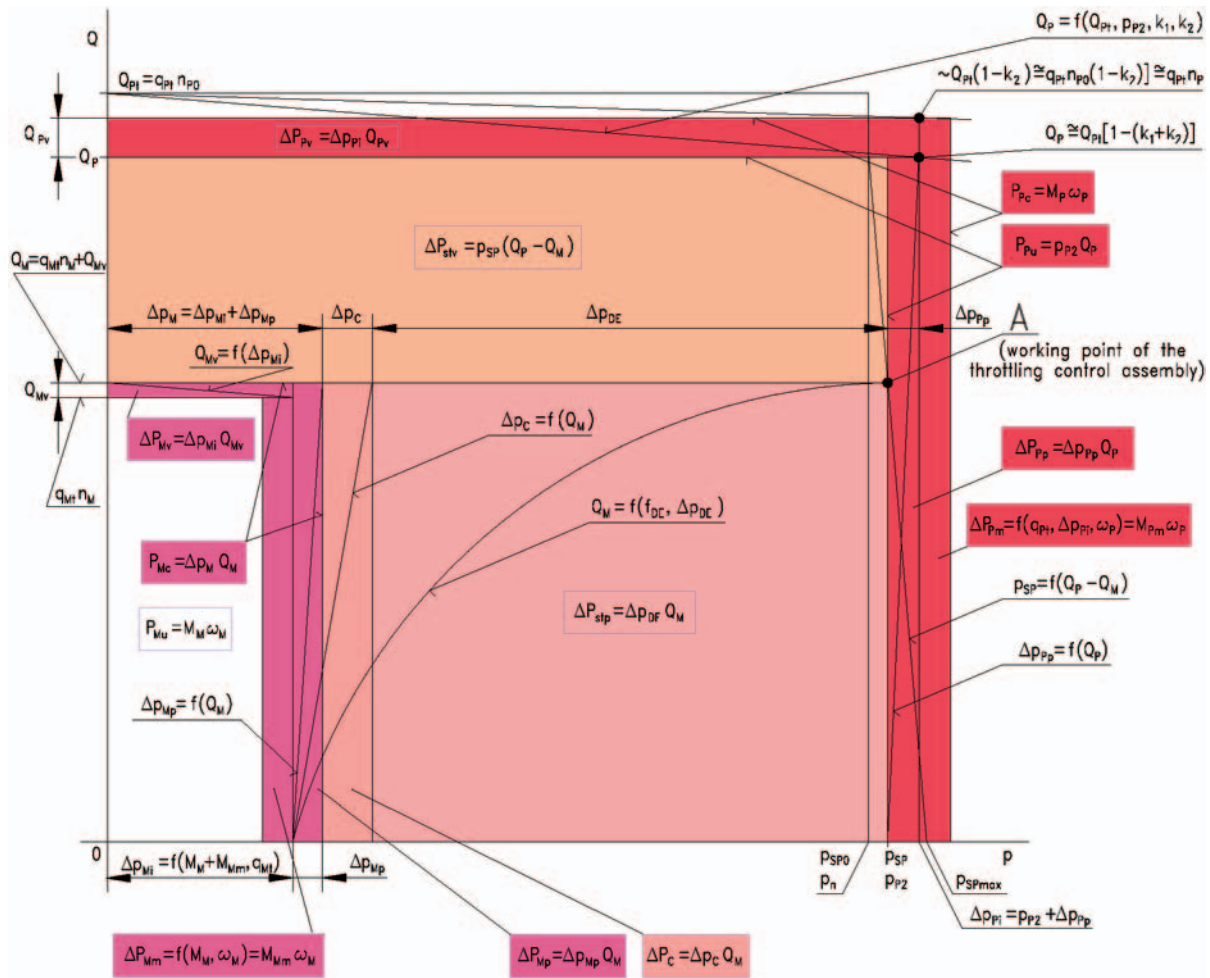


Fig. 2. Graphical interpretation of power losses in a hydrostatic drive and control system elements. Individual system with rotational hydraulic motor speed series throttling control fed by a constant capacity pump cooperating with an overflow valve in a constant pressure system: $p = cte \approx p_n$ (coefficient „a” of pressure increase in the overflow valve $a > 0$); the series throttling control assembly in the form of: 1. servo-valve, 2. proportional directional valve, 3. set throttling valve, 4. set two – way flow regulator; k_1 – coefficient of the intensity Q_{Pv} of volumetric losses in the pump; k_2 – coefficient of the decrease of pump shaft rotational speed n_p compared with speed n_{p0} of unloaded pump

The series throttling control assembly used in the system may be a servo-valve or proportional directional valve (Fig. 3) or else a set throttling valve or a set two – way flow regulator placed at the motor inlet (Fig. 4).

Graphical interpretation (Fig. 2) of the power of energy loss (in the system elements) field area and field area of power developed in those elements allows to compare the losses with **the field area of reference power determined by the product $p_n Q_{Pt}$ of the system nominal pressure p_n** (assumed here as opening pressure p_{Sp0} of the overflow valve) **and the theoretical capacity $Q_{Pt} = q_{Pt} n_{p0}$ of the pump.**

Nominal pressure p_n of the pump operation corresponds to the need of assuring maximum decrease Δp_{Mmax} of the hydraulic motor pressure guaranteeing (with a given capacity q_{M1} per one motor revolution) meeting the maximum torque M_{Mmax} that the motor may be loaded with, from time to time, by the driven device.

The theoretical pump capacity Q_{Pt} , on the other hand, meets the need of assuring maximum hydraulic shaft angular speed ω_{Mmax} (rotational speed n_{Mmax}) required by the driven device.

It has to be noted that assumption of an equal field $p_n Q_{Pt}$ of reference power in all the control structures leads to slightly different ranges of the change of speed $0 \leq \omega_M \leq \omega_{Mmax}$ and load $0 \leq M_M \leq M_{Mmax}$ of the hydraulic motor controlled by those structures.

The actual hydraulic motor useful power $P_{Mu} = M_M \omega_M$ is a result of the product of current torque M_M , which the hydraulic motor is loaded with by the driven device, and the current motor

shaft angular speed ω_M , also required at a given moment by the driven device.

Therefore, the motor useful power P_{Mu} depends on the current requirements of the driven device and is independent of the control structure and of the losses in elements of the hydrostatic drive system with a defined structure.

But powers ΔP of losses in the hydraulic system elements are a function of the current value of useful power P_{Mu} , i.e. a function of current torque M_M and current motor shaft speed ω_M . Besides, it depends on the structure of the motor speed control system and on the quality of the hydraulic system components (the level of energy losses in them).

In Fig. 2, the actual hydraulic motor useful power $P_{Mu} = M_M \omega_M$, transmitted to the driven device by the motor shaft, is presented as the field of the white rectangular, with the following fields „added” to it:

- ▲ field $\Delta P_{Mm} = M_{Mm} \omega_M$ of the power of mechanical losses in the hydraulic motor
- ▲ field $\Delta P_{Mv} = \Delta p_{Mv} Q_{Mv}$ of the power of volumetric losses in the hydraulic motor
- ▲ field $\Delta P_{Mp} = \Delta p_{Mp} Q_M$ of the power of pressure losses in the hydraulic motor
- ▲ field $\Delta P_C = \Delta p_C Q_M$ of the power of pressure losses in the system conduits
- ▲ field $\Delta P_{stp} = \Delta p_{DE} Q_M$ of the power of structural pressure losses in the throttling control assembly (in servo-valve, directional proportional valve, set throttling valve or set two – way flow regulator)

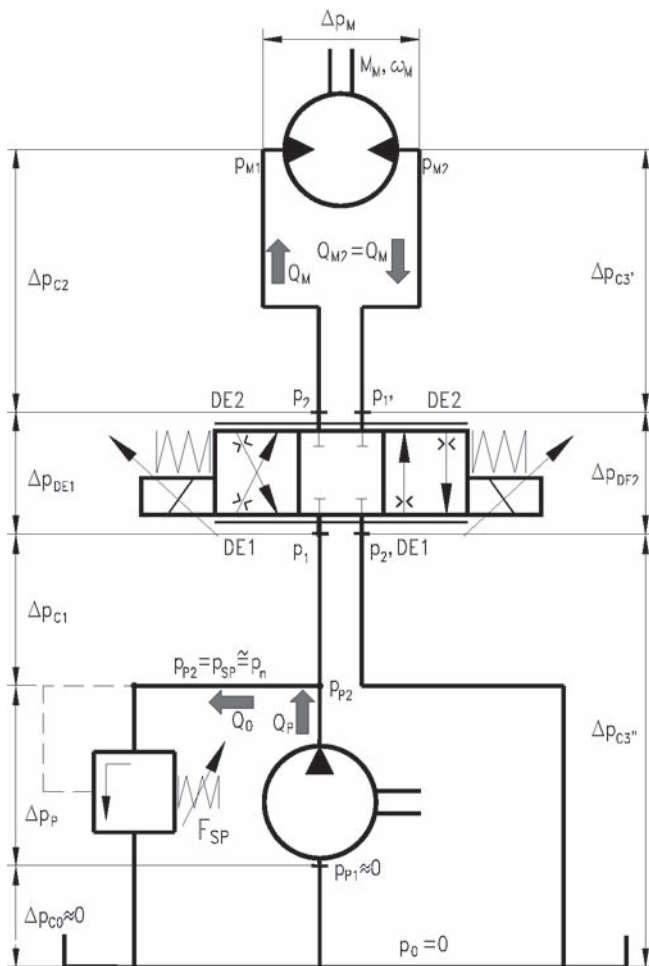


Fig. 3. Individual system of the rotational hydraulic motor speed series throttling control fed by a constant capacity pump cooperating with an overflow valve in constant pressure conditions $p_{p2} = cte \approx p_n$; the throttling control assembly in the form of servo-valve or proportional directional valve

- ▲ field $\Delta P_{stv} = p_{SP} (Q_p - Q_M)$ of the power of structural volumetric losses in the throttling control assembly (in overflow valve)
- ▲ field $\Delta P_{pp} = \Delta p_{pp} Q_p$ of the power of pressure losses in the pump
- ▲ field $\Delta P_{pv} = \Delta p_{pi} Q_{pv}$ of the power of volumetric losses in the pump
- ▲ field $\Delta P_{pm} = M_{pm} \omega_p$ of the power of mechanical losses in the pump.

The sum of the field areas of the hydraulic motor current useful power P_{Mu} rectangle and the field areas of rectangles ΔP representing the power of individual losses occurring at a given moment of work in the hydrostatic drive and control system elements constitutes the rectangle field area corresponding to the actual power P_{pc} absorbed (consumed) by the pump from the electric or internal combustion driving motor, resulting from the product of current torque M_p and current pump shaft angular speed ω_p ($P_{pc} = M_p \omega_p$).

Power P_{pc} absorbed by the pump from its drive motor is greater than the reference power $p_n Q_{pt}$ resulting from the product of nominal pressure p_n and theoretical pump capacity Q_{pt} .

The required level of nominal pressure p_n of pump operation and the required level of pump theoretical capacity Q_{pt} during the system operation, as well as the current small loading torque M_M and current small hydraulic motor shaft angular speed ω_M are decisive in that motor speed throttling control structure of

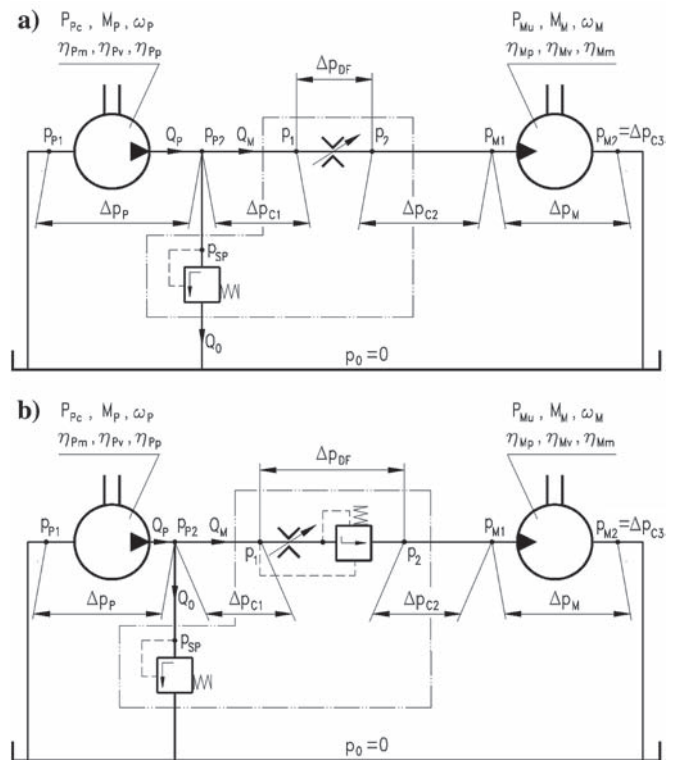


Fig. 4. Individual system of the rotational hydraulic motor speed series throttling control fed by a constant capacity pump cooperating with an overflow valve in constant pressure conditions $p_{p2} = cte \approx p_n$; the throttling control assembly in the form of: a) set throttling valve, b) set two-way flow regulator

temporary power ΔP_{stp} of structural pressure losses and power ΔP_{stv} of structural volumetric losses. This is then accompanied by a very low value of the overall energy efficiency η of the system.

The power ΔP_{stp} of the structural pressure losses in the throttling control assembly may be reduced almost to zero during the hydraulic motor operation at the maximum shaft load M_{Mmax} .

The power ΔP_{stv} of the structural volumetric losses in the throttling control assembly may be reduced almost to zero in a situation when the hydraulic motor operates with maximum angular speed ω_{Mmax} (rotational speed n_{Mmax}).

The hydraulic motor operation with maximum load M_{Mmax} and simultaneous maximum speed ω_{Mmax} (n_{Mmax}) may cause minimization of the power of losses connected with the motor speed throttling control and the sum of energy losses in the system consists of the hydraulic motor losses, the conduit losses and pump losses. The overall system efficiency η reaches then a high value η_{max} , close to the value of energy efficiency η_{max} of a system with the motor speed volumetric control (by a variable capacity pump).

However, in order to be able, in a system with series throttling control, to load the hydraulic motor with a maximum torque M_{Mmax} close to the maximum load M_{Mmax} of the motor in a system with volumetric speed control, the throttling slot of the throttling proportional control valve (or of the throttling valve) has to be increased to the size requiring a small decrease $\Delta p_{DEmin} \approx 0$ of pressure at the maximum flow intensity $Q_{Mmax} \approx Q_p$.

On the other hand, in order to be able, in a system with series throttling control, to set, with a throttling proportional control valve or a throttling valve, the maximum intensity $Q_{Mmax} \approx Q_p$ i.e. close to the pump capacity, an overflow valve has to be used in the system to stabilize the pressure level $p_{SP} \approx p_n$ of the pump operation at the flow intensity $Q_p - Q_M \approx 0$ (i.e. close to zero).

System of the motor speed series throttling control fed by a constant capacity pump cooperating with an overflow valve controlled in variable pressure conditions

Fig. 5 presents graphical interpretation of the power of energy losses in the elements of an individual system with the rotational hydraulic motor speed series throttling control, fed by a constant capacity pump cooperating with an overflow valve controlled in a variable pressure system: $p = \text{var}$. The series throttling control assembly used in the system may have a form of servo-valve or proportional directional control valve (Fig. 6) or else a set throttling valve (creating, with the controlled overflow valve, a set three – way flow regulator) or a set two – way flow regulator placed at the motor inlet (Fig. 7).

The pump operation pressure p_{p2} , controlled by the overflow valve with remote pilot control (SPS), is set to a level higher by a value $\Delta p_{SPS} = \Delta p_{DE1|f_{DE1max}, Q_{Pt}} + \Delta p_{C1max} = \text{cte}$ than the current pressure p_2 in the throttling proportional valve outlet conduit to the hydraulic motor. The pressure difference $\Delta p_{SPS} = p_{p2} - p_2$ must allow to achieve, through the throttling proportional valve slot DE1, controlling the hydraulic motor feed flow intensity Q_M , the flow intensity Q_M equal to the theoretical pump capacity Q_{Pt} ($Q_M = Q_{Pt}$). The area of DE1 slot reaches then the maximum value f_{DE1max} , with a possibility of achieving the pressure decrease $\Delta p_{DE1|f_{DE1max}, Q_{Pt}}$ required by the throttling proportional valve structure, with simultaneous ability to overcome the maximum flow resistance value Δp_{C1max} in the segment between the pump and the throttling proportional valve. Pressure p_1 before the throttling proportional valve slot DE1 equals $p_1 = p_{p2} - \Delta p_{C1}$.

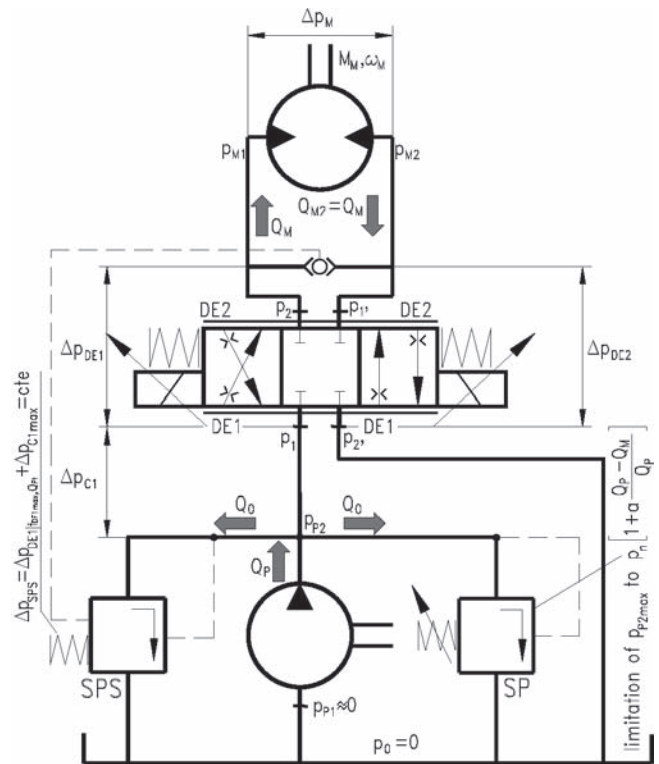


Fig. 6. Individual system of the rotational hydraulic motor speed series throttling control fed by a constant capacity pump cooperating with an overflow valve controlled in variable pressure conditions $p_{p2} = \text{var}$; the throttling control assembly in a form of servo – valve or directional proportional valve

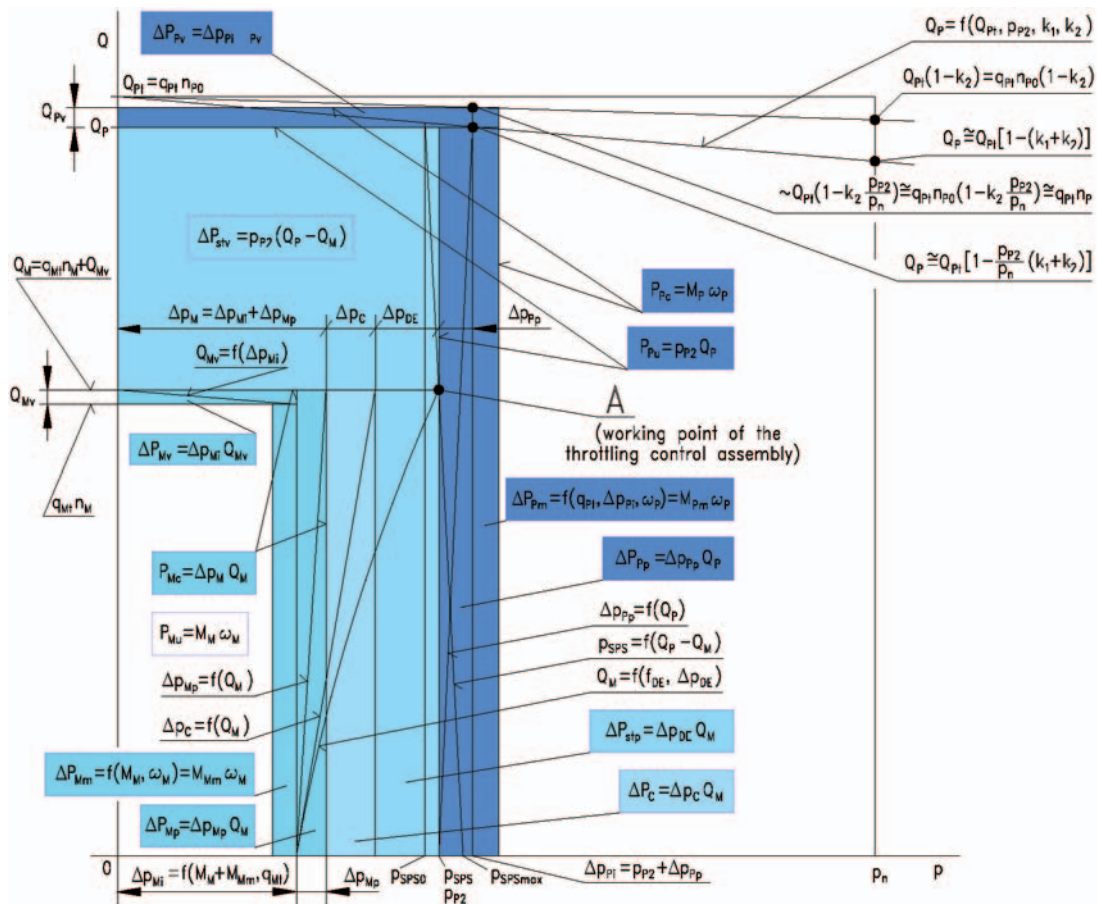


Fig. 5. Graphical interpretation of power losses in a hydrostatic drive and control system elements. Individual system with rotational hydraulic motor speed series throttling control fed by a constant capacity pump cooperating with a controlled overflow valve in a variable pressure system – $p = \text{var}$ (coefficient „a” of pressure increase in the controlled overflow valve $a > 0$); the series throttling control assembly in the form of: 1. servo-valve, 2. proportional directional valve; 3. set throttling valve (together with controlled overflow valve forming a three – way set flow regulator)

The current value of pump discharge pressure p_{p2} , higher by Δp_{SPS} than the current value of the throttling proportional valve outlet (to the hydraulic motor) pressure p_2 , is a result of the pressure p_{M1} required by the motor at its inlet. The maximum limit value p_{p2max} of pressure in the pump discharge conduit is determined by the overflow valve SP with opening pressure p_{SP0} equal to the system nominal pressure p_n .

This solution significantly reduces (compared with the constant pressure feeding system) the power $\Delta P_{stp} = \Delta p_{DE} Q_M$ of structural pressure losses in the throttling control assembly, occurring during the hydraulic motor loading with a decreasing torque M_M .

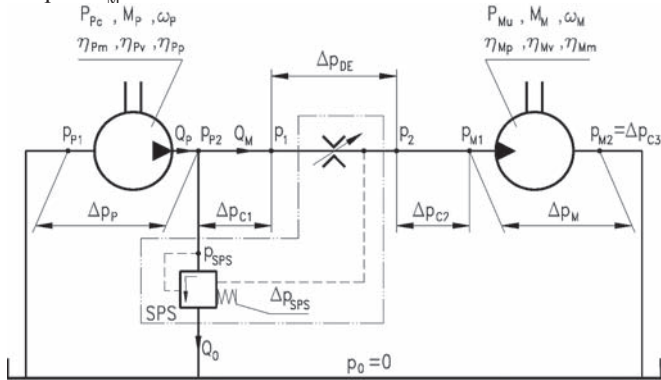


Fig. 7. Individual system of the rotational hydraulic motor speed series throttling control fed by a constant capacity pump cooperating with an overflow valve controlled in variable pressure conditions $p_{p2} = \text{var}$; the throttling control assembly in a form of three-way flow regulator

The power $\Delta P_{stv} = p_{SPS} (Q_p - Q_M)$ of structural volumetric losses in the controlled overflow valve is then also reduced, although the flow intensity $Q_0 = Q_p - Q_M$ of volumetric losses in that valve increases slightly compared with the constant pressure feeding system (Fig. 2) due to a higher pump capacity Q_p (at a lower pump operating pressure p_{p2}).

In a rotational hydraulic motor operating in both systems ($p = \text{cte}$ and $p = \text{var}$) the three values of power of energy losses (ΔP_{Mm} , ΔP_{Mv} and ΔP_{Mp}) are practically the same (with a slight tendency to lower the power ΔP_{Mm} of mechanical losses and power ΔP_{Mv} of volumetric losses in a motor operating in a $p = \text{var}$ system).

Power $\Delta P_c = \Delta p_c Q_M$ of pressure losses in the $p = \text{var}$ system conduits is the same as in a $p = \text{cte}$ system.

In a pump, due to its operation in a variable pressure feeding system, the power $\Delta P_{pp} = \Delta p_{pp} Q_p$ of pressure losses is slightly increased, power $\Delta P_{pv} = \Delta p_{pv} Q_{pv}$ of volumetric losses is decreased and power $\Delta P_{pm} = M_{pm} \omega_p$ of mechanical losses is also decreased.

In effect, when the hydraulic motor is loaded with a small torque M_M , the power $\Delta P_{pc} = M_p \omega_p$ absorbed by the pump from the drive (electric or internal combustion) motor is also significantly reduced, which, with an unchanged hydraulic motor useful power $P_{Mm} = M_M \omega_M$, increases the overall system energy efficiency η compared with the constant pressure feeding system efficiency η .

Both structures ($p = \text{cte}$ and $p = \text{var}$) of the hydraulic motor speed series throttling control, fed by a constant capacity pump, may achieve, during maximum motor load M_{Mmax} and simultaneous maximum speed ω_{Mmax} (n_{Mmax}), the same maximum overall system efficiency η_{max} . It is close to the maximum energy efficiency η_{max} of a system with volumetric control (by a variable capacity pump) of hydraulic motor speed. The $p = \text{var}$ system becomes then a $p = \text{cte}$ system, therefore the operating conditions of both systems are the same and structural losses ΔP_{stp} and ΔP_{stv} in the throttling control assembly may be practically eliminated. However, similarly as in the constant

capacity pump system $p = \text{cte}$, it requires increased area of the f_{DEmax} slot in the throttling directional control valve (throttling valve) to a size requiring slight pressure decrease $\Delta p_{DEmin} \approx 0$ at the maximum flow intensity $Q_{Mmax} = Q_p$. It requires also the use of a controlled overflow valve stabilizing the value $\Delta p_{SPS} = p_{p2} - p_2 = \text{cte}$ also at the flow intensity $Q_p - Q_M \approx 0$ (close to zero) and an overflow valve stabilizing the pressure level $p_{SP} \approx p_n$ at the flow intensity $Q_p - Q_M \approx 0$.

SYSTEM OF THE MOTOR SPEED SERIES THROTTLING CONTROL FED BY A VARIABLE CAPACITY PUMP COOPERATING WITH REGULATOR IN THE CONSTANT PRESSURE CONDITIONS

Fig. 8 describes the power of energy losses in the elements of an individual system with the rotational hydraulic motor speed series throttling control, fed by a variable capacity pump cooperating with a pressure regulator in a constant pressure system $p = \text{cte} \approx p_n$. The series throttling control assembly used in the system may have a form of servo-valve or proportional directional control valve (Fig. 9) or else a set throttling or a set two-way flow regulator placed in the motor inlet (Fig. 10 – example of a central system with parallelly situated motors and with variable capacity pump cooperating with pressure regulator $p_{p2} = \text{cte} \approx p_n$ – during one motor operation).

The use, as a source of supply of the hydraulic motor series throttling control system, an assembly consisting of a variable capacity pump and a constant pressure $p_{p2} = \text{cte} \approx p_n$ regulator entirely eliminates structural volumetric losses. The current pump capacity Q_p is adjusted by the pressure regulator to the current flow intensity Q_M set by the throttling assembly, therefore the pump capacity Q_p is equal to the hydraulic motor absorption capacity Q_M ($Q_p = Q_M$) and the power $\Delta P_{stv} = p_{p2} (Q_p - Q_M) = 0$.

Power $\Delta P_{stp} = \Delta p_{DE} Q_M$ of structural pressure losses in the series throttling control assembly fed at a constant pressure by a variable capacity pump fitted with a pressure regulator is close to the power of structural pressure losses when the assembly is fed by pressure $p_{p2} = \text{cte} \approx p_n$ of a constant capacity pump cooperating with an overflow valve (Fig. 2).

Power of mechanical losses ΔP_{Mm} , volumetric losses ΔP_{Mv} and pressure losses ΔP_{Mp} occurring in the rotational hydraulic motor remains practically unchanged.

Power $\Delta P_c = \Delta p_c Q_M$ of pressure losses in the system conduits is not changed here compared with the above described systems with a constant capacity pump.

In the variable capacity pump feeding (together with the pressure regulator) the throttling control assembly at the pressure $p_{p2} = \text{cte} \approx p_n$, the power of pressure losses $\Delta P_{pp} = \Delta p_{pp} Q_p$ is reduced (due to decrease of Q_p and Δp_{pp}). Power $\Delta P_{pv} = \Delta p_{pv} Q_{pv}$ of volumetric losses in the pump is practically the same as in a constant capacity pump operating at pressure $p_{p2} = \text{cte} \approx p_n$. However, the power $\Delta P_{pm} = M_{pm} \omega_p$ of mechanical losses in the pump is reduced compared with a constant capacity pump operating in the $p_{p2} = \text{cte} \approx p_n$ system (due to decrease of M_{pm}).

The use, as a hydraulic motor speed series throttling speed control system feeding source, a variable capacity pump with pressure regulator, operating at pressure $p_{p2} = \text{cte} \approx p_n$, allows, during the motor run with small speed ω_M (n_M), to reduce significantly the power $P_{pc} = M_p \omega_p$ absorbed by the pump from the drive electric or internal combustion motor. With the unchanged useful power $P_{mu} = M_M \omega_M$ of the hydraulic motor, the entire system energy

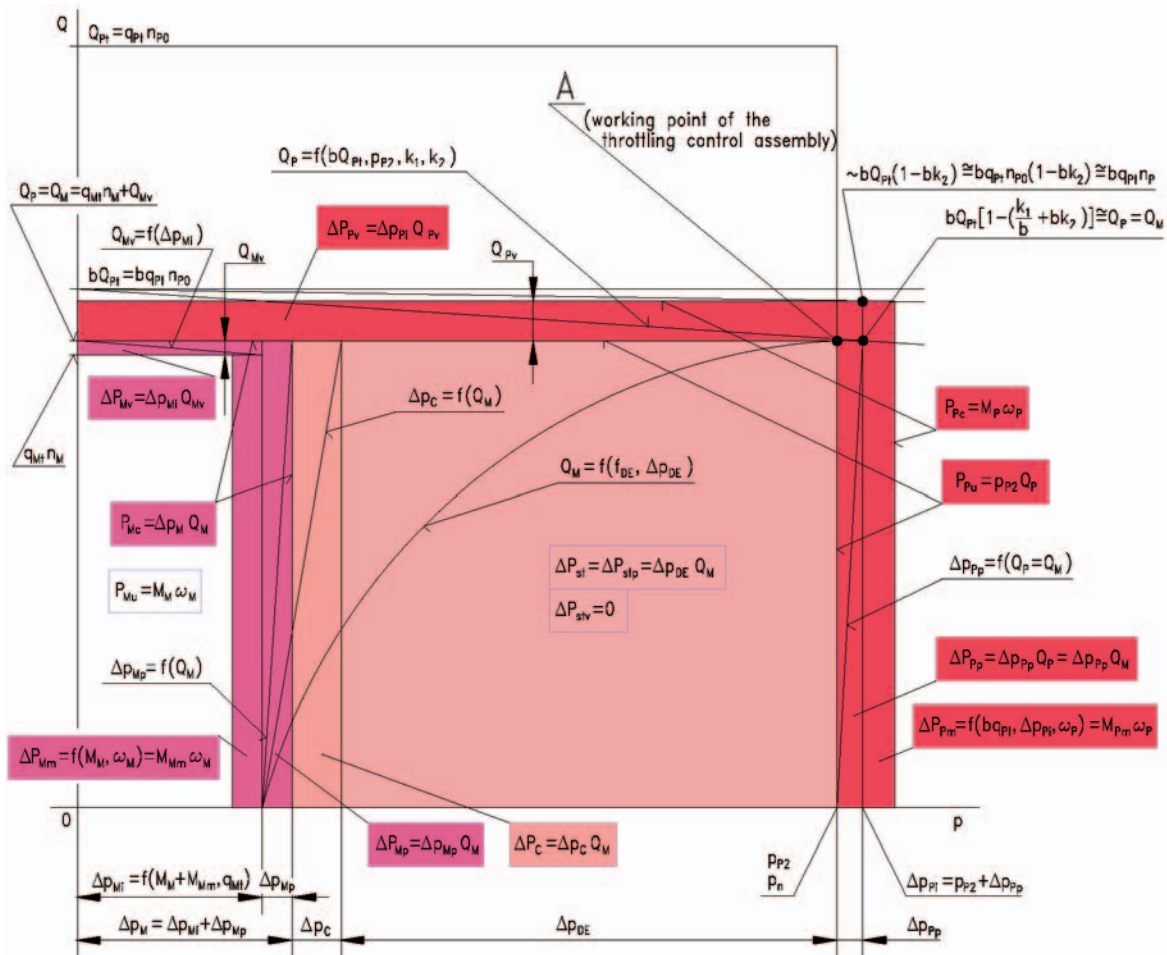


Fig. 8. Graphical interpretation of power losses in a hydrostatic drive and control system elements. Individual system with rotational hydraulic motor speed series throttling control fed by a constant capacity pump cooperating with pressure regulator in a constant pressure system: $p = cte \approx p_n$ (coefficient „ a_1 ” of pressure increase in the regulator $a_1 = 0$); the series throttling control assembly in the form of: 1. servo-valve, 2. proportional directional valve, 3. set throttling valve, 4. set two – way flow regulator

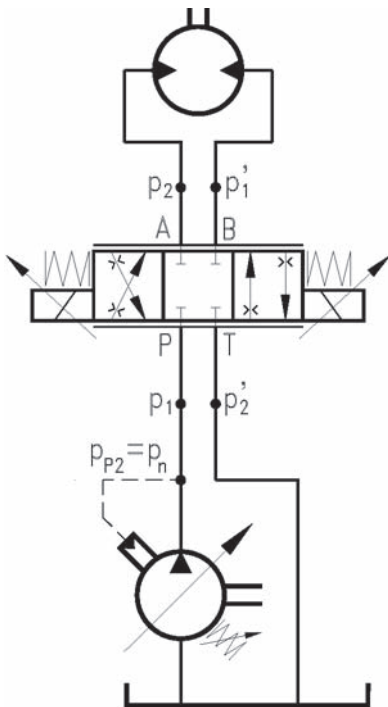


Fig. 9. Individual system with the rotational hydraulic motor speed series throttling control fed by a variable capacity pump cooperating with regulator in the constant pressure conditions $p_{p2} = cte \approx p_n$; the throttling control assembly in the form of servo-valve or proportional directional valve

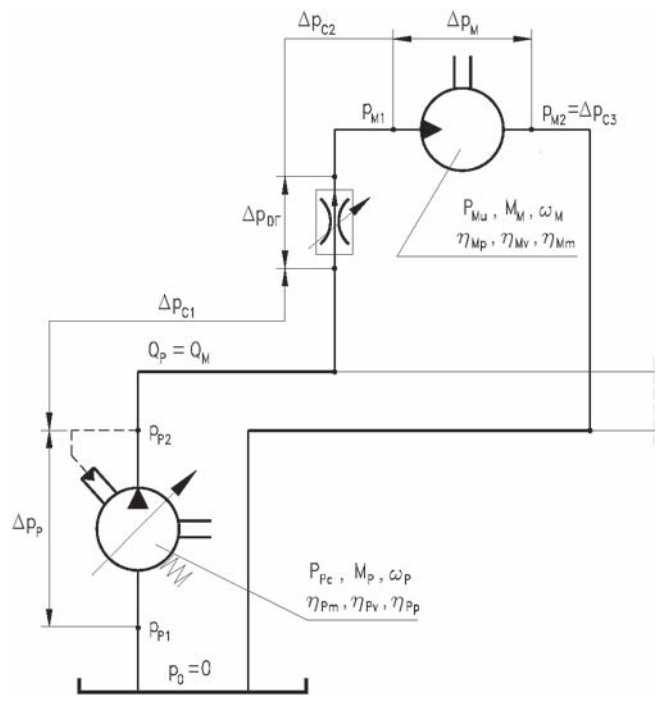


Fig. 10. Central system with parallelly situated motors and with variable capacity pump cooperating with pressure regulator in the constant pressure conditions $p_{p2} = cte \approx p_n$ – during one motor operation

efficiency η is significantly higher compared with efficiency η of a constant pressure ($p = \text{cte}$) throttling assembly constant capacity pump feeding system.

The considered system may achieve, during the maximum hydraulic motor load $M_{M_{\text{max}}}$ and in the whole range of the motor speed change $0 \leq \omega_M \leq \omega_{M_{\text{max}}}$, the overall efficiency η close to the value of energy efficiency η of a system with the motor speed volumetric control (by a variable capacity pump). The power $\Delta P_{\text{stp}} = \Delta p_{\text{DE}} Q_M$ of the structural pressure losses is then minimalized. It requires, in a system with the hydraulic motor speed series throttling control, an increased area of the f_{DEmax} slot in the throttling directional control valve (or the throttling valve) to a size requiring slight pressure decrease $\Delta p_{\text{DEmin}} \approx 0$ at the maximum flow intensity $Q_{M_{\text{max}}} = Q_{p_{\text{max}}}$, i.e. equal to the full pump capacity. It requires also correct operation of the pump pressure regulator stabilizing the pump discharge pressure p_{p2} at the level $p_{p2} = \text{cte} \approx p_n$ in the whole range $0 \leq Q_p \leq Q_{p_{\text{max}}}$ of the pump capacity variation.

In a situation of simultaneous maximum load $M_{M_{\text{max}}}$ and maximum speed $\omega_{M_{\text{max}}}$ of a hydraulic motor controlled by series throttling, the maximum achievable energy efficiency η_{max} of a system is close to the value η_{max} of a system with hydraulic motor speed volumetric control i.e. directly by a variable capacity pump.

The greatest energy savings in the considered series throttling control system, compared with a series control system fed by a constant pressure constant capacity pump, are obtained during the hydraulic motor operation at small speed $\omega_M (n_M)$.

SYSTEM OF THE MOTOR SPEED SERIES THROTTLING CONTROL FED BY A VARIABLE CAPACITY PUMP COOPERATING WITH A LOAD SENSING REGULATOR IN THE VARIABLE PRESSURE CONDITIONS

Fig. 11 illustrates the fields of power of energy losses in elements of an individual system with the rotational hydraulic motor speed series throttling control, fed by a variable capacity pump cooperating with the Load Sensing regulator in a variable pressure $p = \text{var}$ system. The series throttling control assembly may have a form of servo-valve or proportional directional valve (Fig. 12) or else a set throttling valve or a set two-way flow regulator placed at the motor inlet (Fig. 13 – example of a central system with parallelly situated motors and with variable capacity pump cooperating with Load Sensing regulator – during one motor operation).

The use, as a supply source of the hydraulic motor speed series throttling control assembly, of a set consisting of a variable capacity pump cooperating with a Load Sensing (LS) regulator, totally eliminates the structural volumetric losses in a system. Similarly as in the series throttling control system fed by a variable capacity pump cooperating with the $p_{p2} = \text{cte} \approx p_n$ regulator, i.e. at the constant pressure feeding, the structural volumetric losses are eliminated here. Power ΔP_{stv} of those losses is equal to zero ($\Delta P_{\text{stv}} = p_{p2} (Q_p - Q_M) = 0$),

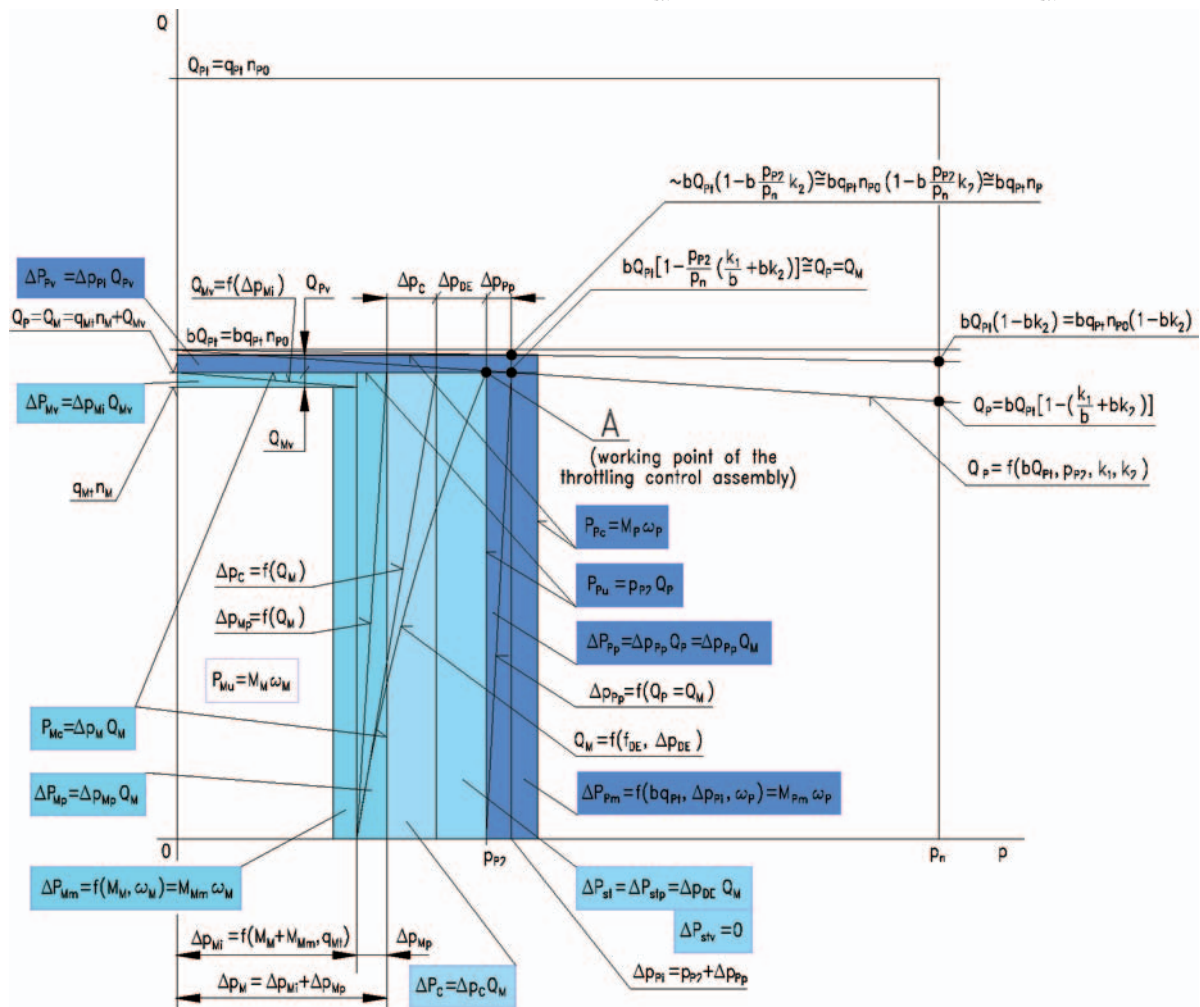


Fig. 11. Graphical interpretation of power losses in a hydrostatic drive and control system elements. Individual system with rotational hydraulic motor speed series throttling control fed by a variable capacity pump cooperating with the Load Sensing regulator in a variable pressure system: $p = \text{var}$ (coefficient „ a_1 ” of pressure increase in the regulator $a_1 = 0$); the series throttling control assembly in the form of:
 1. servo-valve, 2. proportional directional valve, 3. set throttling valve, 4. set two-way flow regulator

because the current pump capacity Q_p is adjusted, by the LS regulator, to the current flow intensity Q_M set by the throttling assembly (i.e. $Q_p = Q_M$).

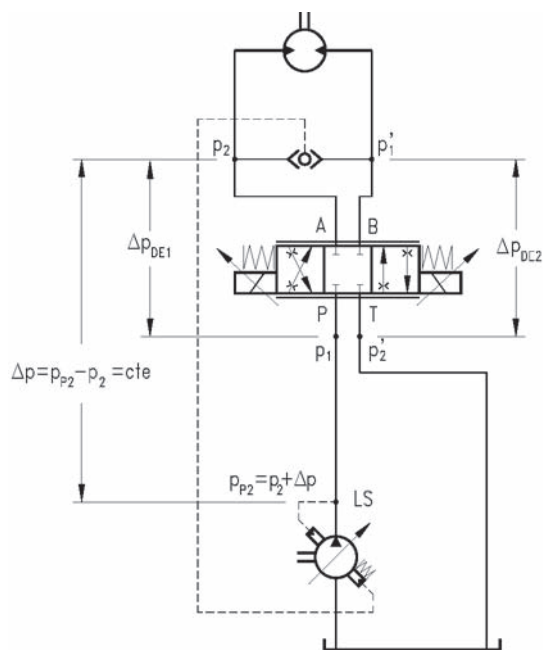


Fig. 12. Individual system with rotational hydraulic motor speed series throttling control fed by a variable capacity pump cooperating with Load Sensing regulator in the variable pressure conditions $p_{p2} = \text{var}$; the throttling control assembly in the form of servo-valve or proportional directional valve

Pressure p_{p2} of the pump operation, adjusted by the LS regulator, is, as in the series throttling control assembly feeding system with the constant capacity pump cooperating with an SPS variable pressure overflow valve (Fig. 6), set at a level higher by the value of $\Delta p_{LS} = \Delta p_{DE1|f_{DE1max}, Q_{Pt}} + \Delta p_{C1max} = \text{cte}$ than the current pressure p_2 in the throttling proportional control valve outlet conduit to the hydraulic motor. The value $\Delta p_{LS} = p_{p2} - p_2$ of the pressure difference must allow to obtain, through the throttling proportional valve slot DE1 (controlling the flow intensity Q_M feeding the hydraulic motor), the flow intensity Q_M equal to DE1 slot area reaches then the maximum size f_{DE1max} and a possibility of pressure decrease $\Delta p_{LS} = \Delta p_{DE1|f_{DE1max}, Q_{Pt}}$ required by the throttling proportional design, with simultaneous capability of overcoming the maximum flow resistance value Δp_{C1max} which may occur in the conduit between the pump and the directional valve.

Like in the series throttling control system fed by the constant capacity pump cooperating with a variable pressure overflow valve SPS, the current value of the pump discharge pressure p_{p2} , higher by a value of Δp_{LS} than the current pressure value p_2 at the throttling proportional directional valve outlet to the hydraulic motor, adjusts itself to the pressure value p_{M1} required by the motor at its inlet. The maximum limit pressure value p_{p2max} in the pump discharge conduit also here is determined by the overflow valve SP, whose opening pressure p_{SP0} is equal to the system nominal pressure p_n .

Therefore, in the hydraulic motor speed series throttling control assembly *Load Sensing* feeding system, the power $\Delta P_{stp} = \Delta p_{DE} Q_M$ of structural pressure losses occurring in the throttling control assembly during loading the hydraulic motor with a smaller torque will be considerably reduced (compared with the situation in a system fed by a variable capacity pump with a pressure regulator $p = \text{cte} \approx p_0$ (Fig. 3)). With a simultaneous elimination of the power ΔP_{stv} of the structural volumetric losses in the throttling control assembly,

the LS system allows to decrease to a negligible value the sum of power ΔP_{st} of structural energy losses resulting from the use of series throttling as a form of precise hydraulic motor speed control.

In a rotational hydraulic motor operating in an LS system, practically the same three values of power of energy losses (ΔP_{Mm} , ΔP_{Mv} and ΔP_{Mp}) occur as in the above mentioned systems (with a tendency to slight decrease of the power ΔP_{Mm} of mechanical losses and power ΔP_{Mv} of volumetric losses in the motor operating in a $p = \text{var}$ system, in this case in the LS system).

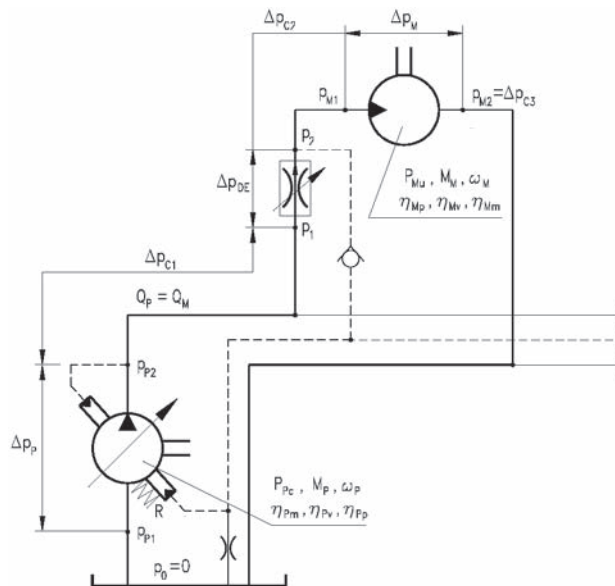


Fig. 13. Central system with parallelly situated motors and with variable capacity pump cooperating with Load Sensing regulator in the variable pressure conditions $p_{p2} = \text{var}$ – during one motor operation

Power $\Delta P_C = \Delta p_C Q_M$ of the pressure losses in the conduits of a system with LS feeding of the throttling control assembly remains unchanged at a given motor speed ω_M (n_M), i.e. equal to the ΔP_C values in the above mentioned systems.

In a variable capacity pump cooperating with a *Load Sensing* regulator of the variable pressure ($p = \text{var}$) feeding system of a hydraulic motor series throttling speed control assembly occurs (compared with three above mentioned series throttling control systems and with unchanged useful power $P_{Mu} = M_M \omega_M$ of the motor) decrease of the power $\Delta P_{pp} = \Delta p_{pp} Q_p$ of pressure losses in the pump (due to decrease of Q_p and Δp_{pp}), decrease of the power $\Delta P_{pv} = \Delta p_{pv} Q_{pv}$ of volumetric losses in the pump (due to decrease of Δp_{pv} and Q_{pv}) and decrease of power $\Delta P_{pm} = M_{pm} \omega_p$ of mechanical losses in the pump (due to decrease of M_{pm} with slight increase of ω_p).

The use, as a feeding source of the hydraulic motor series throttling speed control system, of a variable capacity pump with the *Load Sensing* regulator operating at a pressure $p_{p2} = \Delta p_{LS} + p_2 \approx \Delta p_{LS} + p_{M1}$, i.e. slightly higher than the current pressure p_{M1} required by the hydraulic motor at its inlet (which is accompanied by decrease to a small value of the power ΔP_{st} of structural energy losses in the throttling control assembly), reduces the sum of power of energy losses in the system to a value only slightly higher than the sum of power of losses in the elements of a system with volumetric control of the motor speed (directly by a variable pump capacity). Power $P_{pc} = M_p \omega_p$ absorbed by the pump from the electric or internal combustion drive motor is only slightly higher here than the power P_{pc} of a variable capacity pump directly driving the hydraulic motor.

The considered LS system operates in the whole range $0 \leq M_M \leq M_{Mmax}$ of the hydraulic motor load and in the whole

range $0 \leq \omega_M \leq \omega_{Mmax}$ of its speed with the energy efficiency η only slightly lower than the efficiency η of a volumetric control system (directly by a variable capacity pump). The difference between overall efficiencies η of both systems will be inversely dependent on the capability of increase of the area of throttling proportional valve (or throttling valve) slot f_{DEmax} . The increase of f_{DEmax} allows to decrease $\Delta p_{DEmin} \approx 0$ at a maximum flow intensity $Q_{Mmax} = Q_{Pmax}$ (i.e. equal to a full pump capacity). It also requires correct operation of the pump LS regulator adjusting, in the whole range $0 \leq Q_p \leq Q_{Mmax}$ of the pump capacity, the discharge pressure p_{p2} at the level higher by a value $\Delta p_{LS} = p_{p2} - p_2 = cte$ then the p_2 pressure in the discharge conduit from the throttling proportional control valve (throttling valve) to the hydraulic motor.

To be continued in the next issue

BIBLIOGRAPHY

1. Paszota Z.: *Aspects énergétiques des transmissions hydrostatiques*, Monograph, 2002
2. Paszota Z.: Model of losses and efficiency of an energy – saving hydraulic servomechanism system, Marine Technology Transactions, Polish Academy of Sciences, Branch in Gdansk, Vol. 18, 2007
3. Paszota Z.: *Energy saving in a hydraulic servomechanism system*, Proc. 17th Symposium on Theory and Practice of Shipbuilding in memoriam prof. Leopold Soria, Opatija, 19 – 21 October 2006
4. Skorek G.: *Energy characteristics of the hydraulic systems with proportionally controlled cylinder fed in a constant or variable pressure* (in Polish), Doctor dissertation, Gdansk University of Technology, continuation
5. Paszota Z.: *Energy Saving in a Hydraulic Servomechanism System – Theory and Examples of Laboratory Verification*, Brodogradnja, Journal of Naval Architecture and Shipbuilding Industry, Vol. 58, No 2, Zagreb, June 2007
6. Paszota Z.: *Hydraulic Servomechanism System. Examples of Reduction of Power Losses in the Variable Pressure Power Supply*, International Scientific – Technical Conference “Hydraulics and Pneumatics’2007”, Wrocław, 10 – 12 October 2007
7. Paszota Z.: *Power of energy losses in the hydrostatic drive system elements – definitions, relations, range of changes, energy efficiencies*. Part I – Hydraulic motor. Chapter in the monograph: „*Research, design, production and operation of hydraulic systems*” (in Polish), Andrzej Meder and Adam Klich editors. „Cylinder” Library. Komag Mining Mechanisation Centre, Gliwice 2007
8. Paszota Z.: *Power of energy losses in the hydrostatic drive system elements – definitions, relations, range of changes, energy efficiencies*. Part II – Conduits, throttling control assembly, pump. Chapter in the monograph: „*Research, design, production and operation of hydraulic systems*” (in Polish), Andrzej Meder and Adam Klich editors. „Cylinder” Library. Komag Mining Mechanisation Centre, Gliwice 2007
9. Paszota Z.: *Power of energy losses in the hydrostatic drive system elements – definitions, relations, range of changes, energy efficiencies* (in Polish). Part I – Hydraulic motor. Napędy i sterowanie, scientific monthly, No 11 (103), November 2007
10. Paszota Z.: *Power of energy losses in the hydrostatic drive system elements – definitions, relations, range of changes, energy efficiencies* (in Polish). Part II – Conduits, throttling control assembly, pump. Napędy i sterowanie, scientific monthly, No 12 (104), December 2007
11. Paszota Z.: *Graphical presentation of the power of energy losses and power developed in the elements of hydrostatic drive and control system* (in Polish). Part I – Rotational hydraulic motor speed series throttling control systems. To be presented at the Cylinder’2008 Conference in September 2008
12. Paszota Z.: *Graphical presentation of the power of energy losses and power developed in the elements of hydrostatic drive and control system* (in Polish). Part II – Rotational hydraulic motor speed parallel throttling control and volumetric control systems. To be presented at the Cylinder’2008 Conference in September 2008

CONTACT WITH THE AUTHOR

Prof. Zygmunt Paszota
Faculty of Ocean Engineering
and Ship Technology
Gdansk University of Technology
Narutowicza 11/12
80-952 Gdansk, POLAND
e-mail: zpaszota@pg.gda.pl



Photo: Cezary Spigarski

A method of diagnosing labyrinth seals in fluid-flow machines

Piotr Krzyślak, Ph. D.
Gdańsk University of Technology
Marian Winowiecki
Techmaw

ABSTRACT

Steam turbines constitute fluid flow machines which are used for driving engines of power plants, merchant and naval ships. They are commonly applied in power industry to driving electric generators. One of the important elements which affect efficiency of steam turbines used in power industry and for ship propulsion is state of labyrinth sealings whose aim is to minimize losses associated with steam leakage within turbine casing. Until now to assess state of labyrinth sealings has been only possible after stopping the turbine and its dismantling in order to determine values of clearances in the sealings. This paper presents a method which makes it possible to assess state of labyrinth sealings without the necessity of stopping and dismantling the machine. This is the method which allows to assess on-line state of machine sealings during its operation.

Keywords: labyrinth sealings, steam turbines, sealing diagnostics

INTRODUCTION

Steam turbines are fluid-flow machines which are used for driving power machines, and merchant and battle ships. In power engineering they are commonly used for driving electric current generators. The efficiency of those machines strongly depends on numerous factors, the main of which are the initial steam pressure and temperature [3]. That is why higher and higher initial steam parameters are used in thermal cycles with steam turbines, both stationary and used for driving ships, to obtain higher efficiency and, consequently, to reduce the costs of electric current production or ship maintenance [3].

On the other hand, increasing initial steam parameters in the turbine leads to serious problems with sealing the turbine casing. Usually this problem is solved using systems of labyrinth seals to reduce the steam leakage [1]. Additionally, some turbine producers introduce a double turbine casing in the regions of extremely high parameters of the steam. The use of this construction reduces stresses in the casing and temperature gradients in casing material. However, both the inner casing and the outer casing are still to be sealed in a proper way to eliminate excessive steam leakages. For this purpose labyrinth seals are used in the both casings [3].

METHOD OF DIAGNOSING THE SEALINGS

Fig. 1 shows schematically a supply system for a 215 MW turbine, along with the inner and outer casings.

Thus, the use of extremely high initial steam parameters in the thermal cycle has an impact on turbine construction.

The condition of the labyrinth seals in a fluid-flow machine considerably affects parameters of its performance. Therefore the information on the current state of these seals is of high

importance from two mutually related points of view, which are [3]:

- ★ possible efficiency losses caused by poor condition of the seals
- ★ ability to plan repair actions.

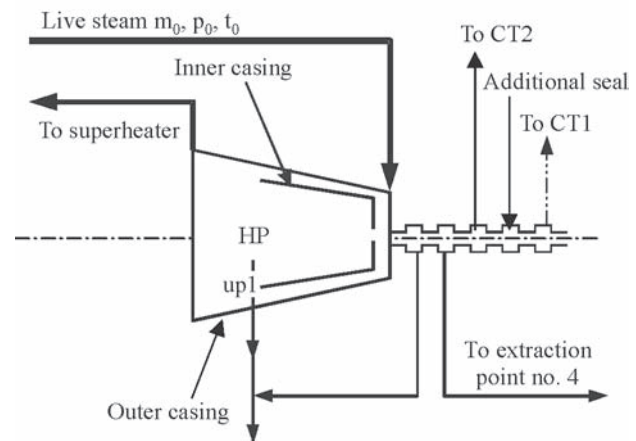


Fig. 1. Scheme of HP casing of 13K215 turbine with inner casing

In the past, assessing the state of such a seal was connected with stopping the machine and opening it to do necessary geometry measurements, which in case of seals situated inside the turbine (for instance in the turbine with the inner casing) required uncovering both the outer and inner casing. This, in practice, was only possible during large machine overhauls. Current information on the condition of the seal of interest during machine operation makes it possible to plan the date and range of the future machine repair.

The basic geometrical parameter used for describing the size of clearances in the labyrinth seal is the averaged clearance, defined as [1, 2]:

$$s = \sqrt{\frac{z}{\sum_{i=1}^z \frac{1}{s_i^2}}} \quad (1)$$

where:

- s – averaged seal clearance
- s_i – sizes of clearances in successive gaps of the seal
- z – number of teeth in the seal.

The mass flow rate through the seal can be modelled using the equation in which the scale of leakage is related to the averaged clearance. The basic equation describing the mass flow rate through the seal is that proposed by Stodola in the form [1, 2]:

$$m = \mu \rho_1 \frac{F}{\sqrt{z}} \sqrt{\frac{p_1}{\rho_1} [1 - (p_2/p_1)^2]} \quad (2)$$

where:

- m – mass flow rate through the seal
- μ – flow coefficient for the seal
- ρ_1 – density of the medium at seal inlet
- p_1 – pressure in front of the seal
- p_2 – pressure behind the seal
- $F = \pi Ds$ – flow area inside the seal (corresponding to the parameters)
- z – number of teeth in the seal
- D – seal diameter.

The above formula relates the averaged clearance to the mass flow rate through the seal. These two quantities are closely coupled by the above equation and cannot be separated from each other in this system. As a result, pressure or temperature measurements performed in front of and behind the seal do not provide opportunities for unique assessment of the mass flow rate through the seal in the situation when the averaged clearance s is not known. Determining losses attributed to the leakage flow through the seal requires the information on the geometry of the seal. During turbine operation, when the turbine casing is closed, we do not have the information of the current condition of the seal, as the sizes of clearances in successive gaps can change with time. A single mass flow rate equation does not provide opportunities for determining the mass flow rate when the scale s of the clearance changes during machine operation. This can be described using the following equation:

$$m = f(p_1, p_2, \rho_1, s, z) \quad (3)$$

where:

- m – mass flow rate through the seal
- p_1 – pressure in front of the seal
- p_2 – pressure behind the seal
- ρ_1 – steam density in front of the seal
- s – averaged clearance in the seal
- z – number of teeth in the seal.

The role of the averaged clearance s is of high importance when assessing the scale of power losses in the turbine. This can be seen in Fig. 2 showing the diagram of power loss recorded in the 215 MW turbine HP casing as a function of the averaged clearance s in the labyrinth seal situated in the inner casing. Increasing the size of the clearance in the inner casing leads to the increase of the volume of steam flowing through the seal, which in turn decreases the mass flow rate of the medium flowing through the turbine blade system. The calculations shown in Fig. 2 were done assuming the nominal averaged clearance as equal to $s = 0.7$ mm.

To sum up, the above discussed system is incalculable - its makes the calculation of the mass flow rate through the seal impossible when the averaged clearance s is not known.

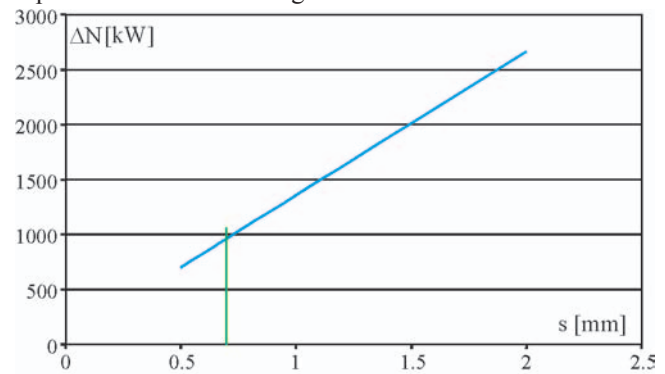


Fig. 2. Power loss in 13K215 turbine HP casing vs. averaged clearance

The solution presented in the article provides opportunities for on-line diagnostics of those seals, without interfering into the mechanical system of the machine. It also does not require stopping the machine to do clearance geometry measurements in the seal [4].

The essence of the new solution consists in introducing a disturbance in the flow of steam through the seal in such a way that the changes in pressure distribution in the seal which are related to this disturbance describe the current seal clearance geometry. This disturbance can have a form of an extraction system installed in the seal, through which a small but well-known volume of steam is extracted [4].

In the static element of the seal, at a selected distance from its end at least one opening is made to communicate this area with the space behind the seal, and at least one opening for measuring the pressure in the extraction area, see Fig. 3 and 4. The geometry of the communication openings and their location along the seal length are formed in such a way that the extraction flow disturbs the flow through the seal in a way sufficiently large to obtain satisfying resolution of the method, and, on the other hand, the volume of the flow leaving the seal in this way is sufficiently small to make resultant efficiency loss increase negligible [4].

Fig. 3 shows a longitudinal section of the labyrinth seal, while Fig. 4 presents its cross section.

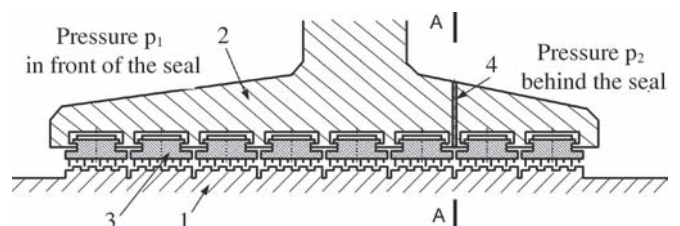


Fig. 3. Longitudinal section of the seal with diagnostic system

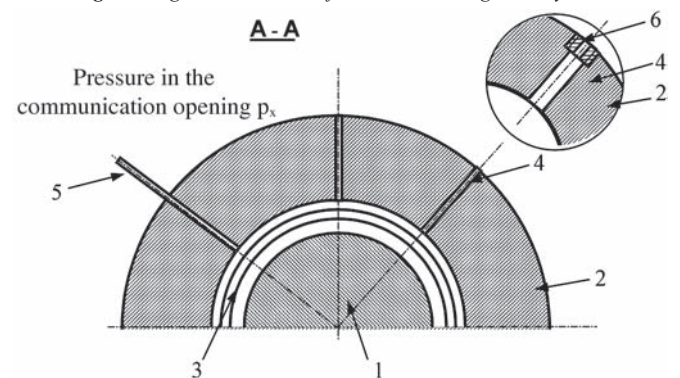


Fig. 4. Cross section of the seal with diagnostic system

The labyrinth seal 3 (having the form of a series of sealing segments) is situated between the shaft 1 and the static element 2 (gland clamping ring). In the clamping ring 2 a number of communication openings 4 are made to connect the inside of the seal 3 with the space behind it (the element disturbing the flow through the seal), along with the pulse opening 5 situated in the plane of communication openings 4 for measuring the pressure in the flow disturbance area.

The role of the communication openings 4 is to execute the throttling process, which can be obtained by designing relevant geometry of the opening, or, for instance, by introducing a reducing pipe 6. The locations of the communication openings (steam extraction) 4 and the pulse opening 5 are optimised using thermodynamic and flow calculations until the maximum diagnosing sensitivity/accuracy is obtained.

The first segment of the seal, marked A, is the segment between the seal inlet and the plane of communication openings (section A-A). The second segment, marked B, is the segment between the plane of openings and the seal exit.

For the seal with an extraction system (4, 6), defined as in Figs. 3 and 4, the set of equations can be written in the following form:

$$\begin{aligned} m_A &= f_1(p_1, h_1, p_x, s, z_A) \\ m_B &= f_2(p_x, h_1, p_2, s, z_B) \\ m &= m_B - m_C \end{aligned} \quad (4)$$

where:

- m_A – mass flow rate through seal segment A
- m_B – mass flow rate through seal segment B
- m_C – mass flow rate through communication openings in the seal
- p_1 – pressure in front of the seal
- p_2 – pressure behind the seal
- p_x – pressure in the communication opening
- h_1 – enthalpy of the medium in front of the seal
- s – averaged clearance in the seal
- z_A – number of teeth in seal segment A
- z_B – number of teeth in seal segment B
- Φ – diameter of nozzles in communication openings.

An essential assumption of the entire methodology is that the nozzle diameter Φ is known. As a consequence, the mass flow rate m_C through the nozzle is known as well.

$$m_C = f_3(p_x, h_1, p_2, \Phi) \quad (5)$$

When the quantities p_1, p_2, p_x, h_1 and Φ are known, we have a set of three equations with three unknowns: m_A, m_B , and s .

This set of equations can be solved, thus allowing us to determine the size of clearance s and the volumes of leakage flows in segments A and B. We assume that the nozzle geometry does not change during seal operation. Both the communication openings and the nozzles installed in them can be distributed along the entire perimeter of the seal, composing a system of openings with nozzles. In that case selecting the parameter Φ (diameter of a single nozzle) should take into account the number of communication openings over the entire perimeter.

A limiting case is the situation in which the sum of areas of the nozzles installed in the communication openings tends to zero. In this case, when m_C tends to zero, we get a seal which can be described using one equation only. As a consequence, diagnosing the state of this seal is not possible anymore.

The second limiting case is the situation in which the total area of the nozzles increases to infinity. In that case the mass flow rate through the seal segment B tends to zero. As a consequence, like in the first limiting case, diagnosing the state of the seal is impossible, as we have only one equation for the seal segment A.

Thus we can write two conditions for which the seal state diagnosis cannot be done:

$$m_C = 0 \quad \text{or} \quad m_B = 0 \quad (6)$$

In this situation, the size of the nozzles is the parameter responsible for the sensitivity of the entire methodology. Introducing the additional flow channel in the form of communication openings increases the mass flow rate of the medium flowing through the first seal segment. Selecting the size of the nozzles, i.e. the area through which the flow m_C affects, on the one hand, the ability to diagnose the state of the seal, and, on the other hand, the total volume m_A of the medium flowing through the entire seal. Increasing the nozzle area corresponds to increasing the mass flow rate m_C and the resultant mass flow rate m_A . This, in turn, will decrease the volume of the medium flowing through the turbine blade system. Therefore the basic criterion in selecting the size of the nozzles is optimisation of the system from the point of view of two aspects, the first of which is diagnosing sensitivity, and the second - extra power loss generated by the increased mass flow rate m_A of the medium flowing through the entire seal.

Practical realisation of the labyrinth seal diagnosis consists in pressure measurements in front of and behind the seal, and in the pulse opening(s). For the changing clearance s we will have the changing pressure p_x at the point x in the seal. This fact makes it possible to define a diagnostic parameter indicating the state of the seal and the size of the averaged clearance s .

Based on three measured pressures p_1, p_2, p_x a diagnostic variable P_{diag} can be defined, which can be considered a parameter indicating the level of seal degradation in time:

$$P_{diag} = (p_x - p_2)/(p_1 - p_2) \quad (7)$$

Then the recorded change of this parameter is compared to its reference value obtained during initial calibration of the diagnostic system, with possible corrections taking into account referential thermodynamic parameters. This correction compensates pressure and temperature changes of the medium in front of the seal and pressures behind the seal when the conditions of turbine operation change.

This diagnostic system was implemented in one of Polish power plants on the seal in the inner HP casing of the 105 MW turbine [4]. The theoretical distribution of the diagnostic parameter, calculated for nominal conditions of turbine operation as a function of the averaged seal clearance s , is given in Fig. 5 [4]. The size of the averaged clearance was assumed as equal to $s = 0.6$ mm.

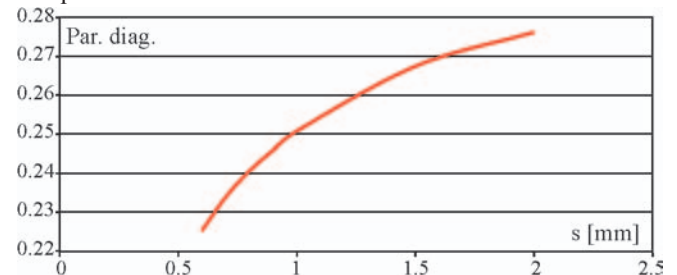


Fig. 5. Diagnostic parameter vs. averaged clearance

During the initial start-ups of the turbine after its overhaul, the system was calibrated and the value of the diagnostic parameter was determined as equal to 0.223 for the nominal mass flow rate 450 t/h of the steam flowing through the turbine (this value is presented in Fig. 6). Another value of the diagnostic parameter from Fig. 5 which was expected by the theory was equal to 0.225.

A few weeks after the start of the diagnostic system the failure of the generator took place. It caused rapid shutdown

of the turbine, which resulted, as a consequence, in relatively large eccentricity of the shaft. This, in turn, led to the failure of the inner gland in the HP turbine.

The data obtained from turbine operation records included:

- ❖ mass flow rate of the steam entering the turbine
- ❖ live steam pressure
- ❖ steam temperature in front of the gland
- ❖ pressures in front of the gland
- ❖ pressure behind the gland
- ❖ pressure in the pulse opening.

Comparing the data obtained directly after installing the diagnostic system and directly after the failure have made it possible to assess the scale of damage, and, at the same time, confirm the efficiency of the here presented method (Fig. 6).

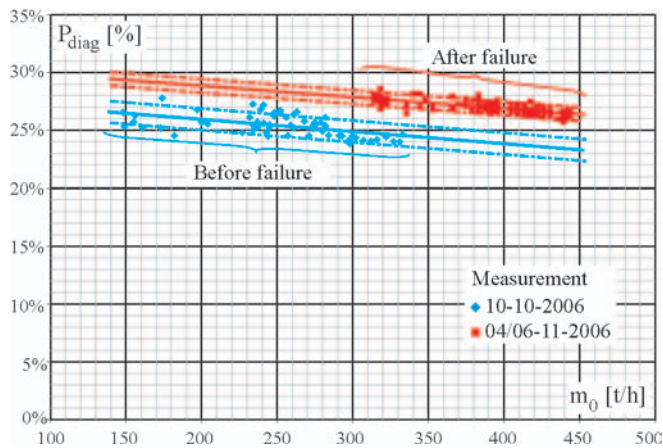


Fig. 6. Diagnostic parameter of the gland before and after failure

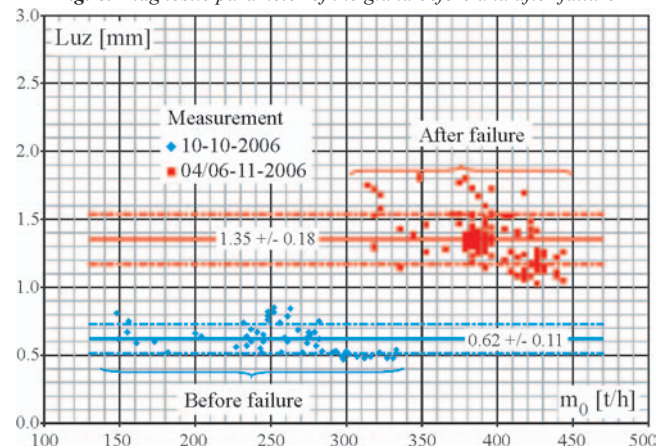


Fig. 7. Averaged clearances in the gland before and after failure

Processing of the obtained data has made it possible to reconstruct the averaged clearances in the gland before and after the failure, Fig. 7. In the both figures, Figs. 6 and 7, the quantities are presented as functions of the mass flow rate m_0 of the live steam entering the turbine.

As results from Fig. 7, the failure has led to the increase of averaged clearances in the gland from the nominal value of 0.6 mm up to about 1.35 mm, i.e. by about 0.7 to 0.8 mm. The average standard deviations of the spread of results are marked in the figure.

Such an increase of clearance size in the gland results in power loss by an order of 250-300 kW in this turbine, which gives the loss of an order of 2000 MWh per year (assuming each day of turbine operation at nearly nominal load).

Introducing the above described seal diagnostics methodology requires drilling communication openings in the gland casing and installing nozzles in those openings. Additionally, a duct for pressure measurements in the plane of communication openings is to be prepared. As mentioned

before, all this increases the leakage flow through the entire gland. However, this increase is very small. The volume of the leakage flow through the seal in the 105 MW turbine is approximately equal to 2.2 kg/s for the case without diagnostic system, while installing it increases the leakage flow to $m_A = 2.4$ kg/s. The volume of the medium flowing through the nozzles is equal to about 0.2 kg/s.

CONCLUSIONS

- The essence of the here presented method is introducing a disturbance to the flow through the seal. This disturbance has a form of additional flow of steam through nozzles in communication openings. Since the nozzle does not come into direct contact with rotating elements of the turbine, its geometry does not change during turbine operation.
- Changes of the averaged clearance s in the seals, caused by possible contact between the shaft and the turbine casing, lead to differences in pressure distributions in the seal in which the extraction system was installed. When the mass flow rate of the steam through the seal is constant, i.e. without steam extraction, the pressure distribution in the seal is constant for different averaged clearances. In that case pressure measurements inside the seal do not provide opportunities for its diagnosis. The role of the steam extraction is to change the pressure distribution in the seal.
- Measurements of three pressures: in front of the seal, behind the seal, and in the plane of communication openings with nozzles, makes it possible to determine the diagnostic parameter. As a consequence, the current size s of the clearance can be assessed on-line during machine operation, without disassembling it. A necessary component of this diagnostic system is performing the three above mentioned pressure measurements. In the version implemented in the 105 MW turbine the diagnostic parameter was introduced to the controlling and measuring system of the block. Its value can be controlled during normal operation of the block, thus providing opportunities for the assessment of the current condition of the inner turbine seal [4].
- The method and principle of the above diagnostics were submitted by the authors to the RP Patent Office [5].

BIBLIOGRAPHY

1. K. Trutnowski: *Berührungsfreie Dichtungen*. VDI Verlag Dusseldorf, 1964
2. T. Dębicki, R. Puzyrewski: *Analysing flow through circumferential gaps* (in Polish). XI Fluid Mechanics Conference, Warsaw, 1993
3. T. Chmielniak: *Thermal Turbines* (in Polish). Publishers of the Silesian University of Technology, 1998
4. P. Krzyślak, M. Winowiecki: *Diagnosing the state of the HP gland in turbine 13UC105* (in Polish). Alstom report, 2006
5. RP Patent Office: *P-379431 – acknowledgement of patent submission. Flow seal in a fluid-flow machine and method of its diagnostics* (in Polish). Warsaw, 2006.

CONTACT WITH AUTHORS

Piotr Krzyślak, Ph. D.
Faculty of Mechanical Engineering
Gdansk University of Technology
Narutowicza 11/12
80-952 Gdansk, POLAND
e-mail : pkrzysla@pg.gda.pl

Marian Winowiecki
Marynarki Polskiej 3/3
82-220 Stare Pole, POLAND
e-mail: techmaw@op.pl

Investigations of operational driving loads of bucket chains and manoeuvre hoisting winches on multi-bucket dredgers

Damian Bocheński, Ph. D.
Gdansk University of Technology

ABSTRACT



The paper concerns problems of preliminary designing of bucket dredgers' power plants. This paper presents results of investigations of six bucket dredgers in service. The operational investigations consisted in measuring the parameters which characterize working conditions of two main receivers of mechanical energy: bucket chains and swing winches. In the paper characteristics of disposition of loading of bucket chains and swing winches are presented. They covered average value, standard deviation and coefficient of variance of loading disposition mutability. Examples of load distributions of chains' and group of swing winches on chosen dredgers during some period of time were given. Conclusions in view to average values of main receivers of mechanical energy and coefficients of variance of loadings spread were formulated. Results of investigations of dependence of average loadings of main receivers on their nominal power were presented. The results of work will be used in creation of random models describing real conditions of operation of power plant elements of dredgers.

Keywords: Bucket ladder dredgers, main receivers of mechanical energy, ship power plants, bucket chain, swing winches

INTRODUCTION

The main mechanical energy consumers on dredgers, regardless of their type, are intended for realizing the following technological processes [2]:

- ⇒ loosening, dredging and transporting the soil
- ⇒ positioning, manoeuvring and possible propelling the dredger.

Bucket chains and set of manoeuvre hoisting winches are the main consumers in question on multi-bucket dredgers in their basic design solution [7]. Knowledge of operational loads of main consumers is crucial problem in preliminary designing the dredger power plant. This paper presents results of service investigations dealing with driving loads of bucket chains and set of manoeuvre hoisting winches on multi-bucket dredgers. The investigations constituted a part of a greater research project on energy consumption of technological processes on dredgers of three basic types, performed in the years 2000÷2003 and 2005÷2006 [5, 8]. As to the multi-bucket dredgers, five such dredgers were subjected to the investigations and their results were supplemented with results of the tests carried out on the dredger *Ivan Bachvalov* by a measuring team of RCP-KB design office in Rostov upon Don [10].

The main technical data of the dredgers, concerning the parameters of bucket chains and manoeuvre hoisting winches, are presented in Tab. 1.

On all the investigated dredgers the bucket chains and manoeuvre hoisting winches were driven by diesel-electric power systems. The measurements were performed with the use

of specially designed measuring systems consisted of electronic digital multimeters co-operating with computer [4, 5]. The multimeters were used to measure and record versus time electric current (indirect measurement by shunt-voltage measuring) and voltage (direct measurement). This way value of the power consumed by electric motors driving a given consumer, was determined. By making use of the results and knowing efficiency characteristics of power transmission systems, instantaneous power values at drive coupling of a given main consumer, were determined. Operational loads of bucket chain are subjected to great and frequent changes, that results from character of consumer's working mode. The changeability of loads is associated mainly with cutting-in successive buckets to the soil (every 3 ÷ 4 sec on average). How large is the changeability can be illustrated by the mean value of the coefficient $N_{LC}^{max} / N_{LC}^{min}$ equal to 4.5 calculated for several loadings of a hopper barge during preliminary service measurements [5]. For the reason of the highly changeable character of bucket chain loads it was assumed that the measurements of the loads of the bucket chains and set of manoeuvre hoisting winches, will be performed every second [5].

In order to determine the driving load characteristics of bucket chains and manoeuvre hoisting winches it is necessary to know changes of the loads occurring for a long time. Large number of instantaneous values of loads makes it possible to properly perform their statistical estimation. The mean duration time of dredging work carried out by multi-bucket dredgers at sea amounts to about 2500 h/year [5]. Because of limited possibility of carrying out the measurements for such a long period on each of the investigated dredgers it was planned to

perform the service investigations for at least 5% of the working period of each of the investigated dredger, i.e. for about 125 h. As a rule the service investigations were carried out in 24 h cycle. Overall, the measurements were carried out for 732 h [8]. Number of samples for every investigated dredger was greater than 300000 and significantly exceeded the minimum number of samples [9].

Tab. 1. Main technical data of the multi-bucket dredgers subjected to the investigations in service

Dredger's name	Bucket-chain drive parameters		Drive parameters of set of manoeuvre hoisting winches			Q _{PW}
	N _{LC} ^{nom}	N _{LC}	T _{WM}	v _{WM}	number	
	kW	n. bckts/min	kN	m/min	-	
<i>Małż II</i>	88	24	57	10	4	250
<i>Rozgwiazda</i>	300	19	90	12	4	640
<i>Inż. T. Wenda</i>	310	19	90	12	4	640
<i>Usedom</i>	420	25	155 81.5	17.5 17.5	2 2	840
<i>Kategats</i>	400	25	155 81.5	17.5 17.5	2 2	800
<i>Ivan Bachvalov</i>	400	25	155 81.5	17.5 17.5	2 2	800

where:

- N_{LC}^{nom} – bucket chain nominal power
- N_{LC} – bucket chain speed
- T_{WM} – hoisting winch pull
- v_{WM} – hauling speed of manoeuvre hoisting winch
- Q_{PW} – design dredging rate of a dredger.

The performed investigations made it possible to determine the driving load distribution characteristics for bucket chains and set of manoeuvre hoisting winches during soil dredging operations, namely these of:

- N_{LC}^{sr}/N_{WM}^{sr} – mean load of bucket chain and manoeuvre hoisting winches, respectively
- σ_{LC}, σ_{WM} – standard deviations of load distributions of bucket chain and manoeuvre hoisting winches, respectively
- v_{LC} = $\frac{\sigma_{LC}}{N_{LC}^{sr}}$ – coefficient of variation of bucket chain load distribution
- v_{WM} = $\frac{\sigma_{WM}}{N_{WM}^{sr}}$ – coefficient of variation of load distribution of manoeuvre hoisting winches
- λ_{LC}^{cz}, λ_{WM}^{cz} – coefficients which determine participation of working period of bucket chain and manoeuvre hoisting winches during dredging, respectively.

OPERATIONAL LOADS OF BUCKET CHAINS

The investigations of load distribution characteristics of bucket chains were performed with taking into account kind of dredged soil. During the performed operational investigations the following kinds of soil were dredged:

- medium soils of the in- the- site density of 1.7 ÷ 1.95 t/m³, which can be additionally divided into:
 - non-cohesive soils, fine- and medium- grain, medium-compacted sandy soils
 - cohesive soils, medium sandy and plastic silts
- light soils of the in- the- site density of 1.4 ÷ 1.6 t/m³
- warps with loose sands or quick clays.

The operational measurement results for bucket chains supplemented with those performed on the dredger *Ivan Bachvalov* [10] are shown in Tab. 2, and in Fig. 1 – the example histograms of the operational loads for selected dredgers. The loads were grouped into 10 left-sidedly-opened intervals of quantization which covered the range (N_{LC}^{min} – N_{LC}^{max}); the values of N_{LC}^{min} and N_{LC}^{max} were taken into account as integers most close to real measurement results.

Tab. 2. Characteristics of bucket chain load distributions for multi-bucket dredgers

Kind of soil	Name of dredger	N _{LC} ^{nom}	N _{LC} ^{sr}	$\overline{N_{LC}^{sr}}$	σ _{LC}	v _{LC}	λ _{LC} ^{cz}	Source of information
		kW	kW	-	kW	-	-	
Medium	<i>Małż II</i>	88	28.16 ¹⁾ 28.92 ²⁾	0.32 0.329	9.67 10.76	0.343 0.372	0.97 0.94	the author's investigations
	<i>Inż. T. Wenda</i>	310	105.19 ¹⁾ 99.32 ²⁾	0.339 0.32	34.74 42.95	0.331 0.432	0.98 0.95	ditto
	<i>Rozgwiazda</i>	300	99.78 ¹⁾ 92.37 ²⁾	0.333 0.308	30.96 33.79	0.31 0.366	0.98 0.97	ditto
	<i>Usedom</i>	420	183.44 ¹⁾	0.437	41.62	0.227	0.99	ditto
	<i>Kategats</i>	400	195.68 ¹⁾	0.489	42.35	0.216	0.98	ditto
	<i>Ivan Bachalov</i>	400	186.64 ¹⁾	0.467	46.84	0.251		[10]
	Mean values			0.398 ¹⁾		0.281 ¹⁾	0.97	
Light	<i>Małż II</i>	88	21.22	0.241	4.03	0.189	0.96	the author's investigations
	<i>Inż. T. Wenda</i>	310	92.73	0.299	14.28	0.154	0.98	ditto
	<i>Rozgwiazda</i>	300	90.98	0.303	16.91	0.186	0.97	ditto
	<i>Usedom</i>	420	158.93	0.378	29.93	0.188	0.99	ditto
	<i>Kategats</i>	400	172.86	0.432	21.48	0.124	0.99	ditto
	<i>Ivan Bachalov</i>	400	165.91	0.415	28.67	0.173		[10]
	Mean values			0.345		0.169	0.98	

¹⁾ – medium sands, ²⁾ – medium silts

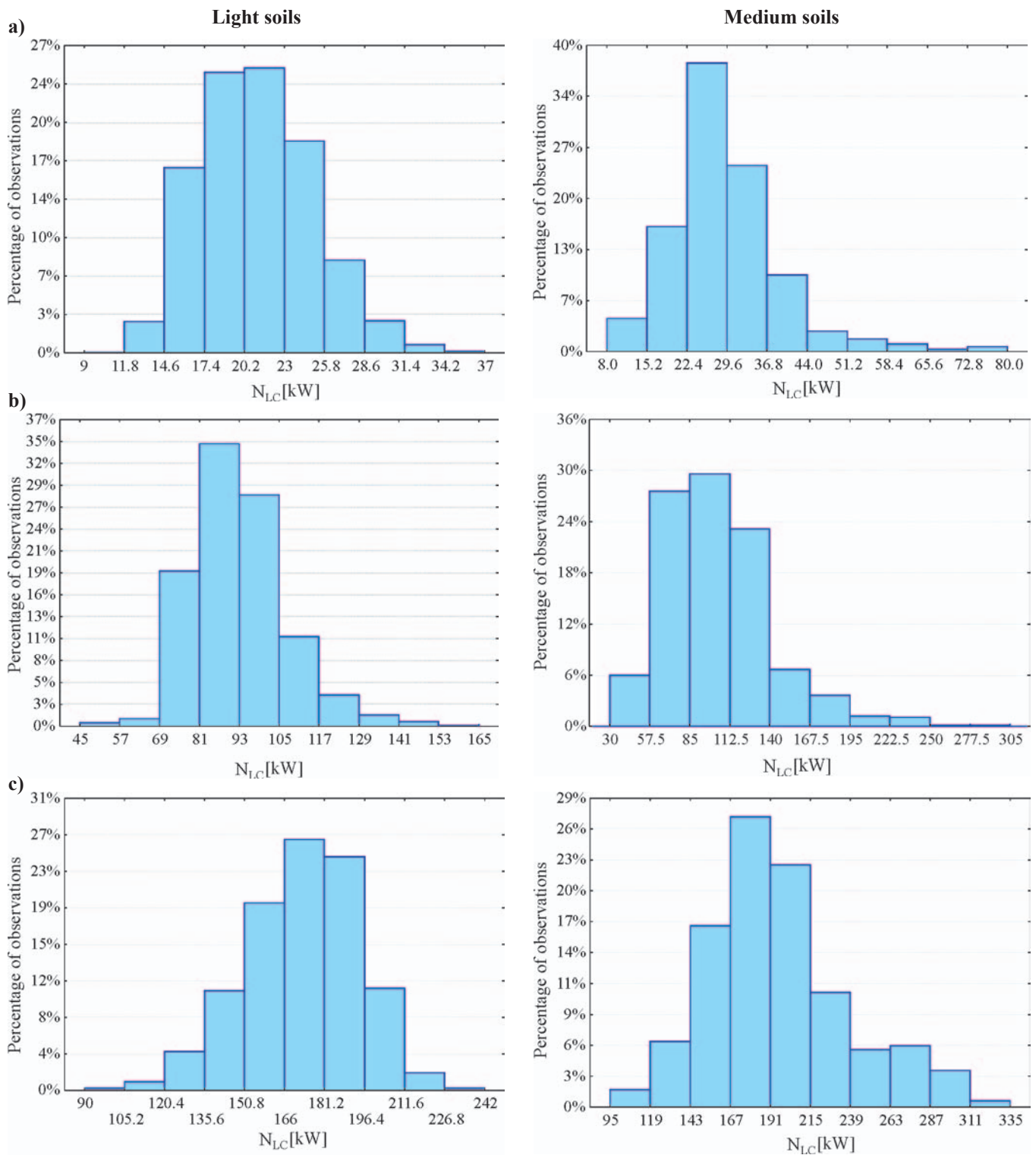


Fig. 1. Histograms of operational bucket chain loads on the multi-bucket dredgers: a) Małż II, b) Inż. T. Wenda, c) Kategats

The measurement results confirm the influence of kind of soil on operational characteristics of bucket chains. Distinct difference can be observed in values of the bucket chain load distribution parameters of the same dredger working in light and medium soils. The values of the mean relative bucket chain loads N_{LC}^{sr} for medium soils are greater by about 15-20% than those for light soils of the same dredger. Differences in values of the variation coefficients of the bucket chain load distribution, v_{LC} , are significant: for medium soils they are contained in the interval of (0.216÷0.432), and for light soils – in the interval of (0.124÷0.189).

The differences in the bucket chain load distribution parameters during dredging the medium soils – regardless

non-cohesive and cohesive – are practically neglectable. The differences in the mean relative bucket chain load values are rather small: in two cases – a little greater during dredging the non-cohesive soils, and in one case – during dredging the cohesive soils. The differences concerning values of variation coefficient of bucket chain load distribution seem a little more significant. In all the three cases the values were greater for dredging the cohesive soil. They amounted respectively to (0.366÷0.432) in the case of dredging the cohesive soils and (0.31÷0.343) - in the case of dredging the non-cohesive ones.

Analyzing the results of Tab. 2 one can clearly observe the differences in values of N_{LC}^{sr} , v_{LC} - especially at dredging medium soils - for the three first dredgers as compared with

three next ones. This situation can be explained by kind of work realized by a given dredger. Generally two types of dredging can be distinguished: investment work and maintenance work. The investment work, as compared with maintenance work, is characterized by a higher effectiveness and in consequence - higher bucket chain loads. Medium and small size dredgers are generally intended for maintenance work. Large dredgers are much more engaged in investment work [5, 6]. Among the investigated dredgers only one, the smallest dredger *Małż II*, was characterized by almost 80% participation in maintenance work; the larger ones: *Rozgwiazda* and *Inż. T. Wenda* were engaged by about 50-60% in investment work. The three largest ones performed only investment operations and for this reason they were characterized by the largest values of the mean relative loads of bucket chains. The carrying-out of investment operations probably results also in somewhat smaller values of variation coefficient of bucket chain load distribution. Worth stressing that the above mentioned percentage values of duration time of carrying-out investment and maintenance work are typical for the multi- bucket dredgers of the investigated size [5,6].

Values of the coefficient λ_{LC}^{cz} are contained in the interval of 0.94÷0.99 and they do not depend on kind of dredged soil.

OPERATIONAL LOADS OF SET OF MANOEUVRE HOISTING WINCHES

The investigations of operational loads of manoeuvre hoisting winches concerned the set of four winches. In manoeuvres also two other winches took part, however they were not considered to be main consumers because of their short-lasting period of work [6].

The results of operational measurements of the set of manoeuvre hoisting winches are presented in Tab.3. They relate to operation of the entire set hence they represent the total load of all hoisting winches in operation. Fig. 2 presents the histograms of operational loads of sets of manoeuvre hoisting winches on two selected dredgers. Like in the case of bucket chains the loads in question were grouped in 10 quantification intervals covering the range ($N_{WM}^{min} - N_{WM}^{max}$).

In Tab. 3 are given the values of distribution parameters of loads of the sets of manoeuvre hoisting winches regardless of kind of soil. The earlier made investigations [6] did not confirm any significant influence of kind of soil on loads of set of manoeuvre hoisting winches.

The performed calculations of the load distribution parameters of the sets of manoeuvre hoisting winches showed that for particular dredgers the mean loads were contained within the interval of 0.072÷0.158 with the mean value of

0.117 and the variation coefficient values in the interval of 0.254÷0.43 with the mean value of 0.372. For greater dredgers a noticeable increase of the mean relative load value can be observed. The fact results from greater values of relative effectiveness (i.e. the ratio of the operational effectiveness and design effectiveness) of greater dredgers as a result of their participation in investment operations. The influence of dredger effectiveness on demanded power of manoeuvre hoisting winches is known and described in many publications, e.g. [11, 12]; this author described his own investigations on the theme in [6]. Values of the coefficients λ_{WM}^{cz} are contained in the interval of 0.94÷0.99 and they are practically identical to those of the coefficient λ_{LC}^{cz} .

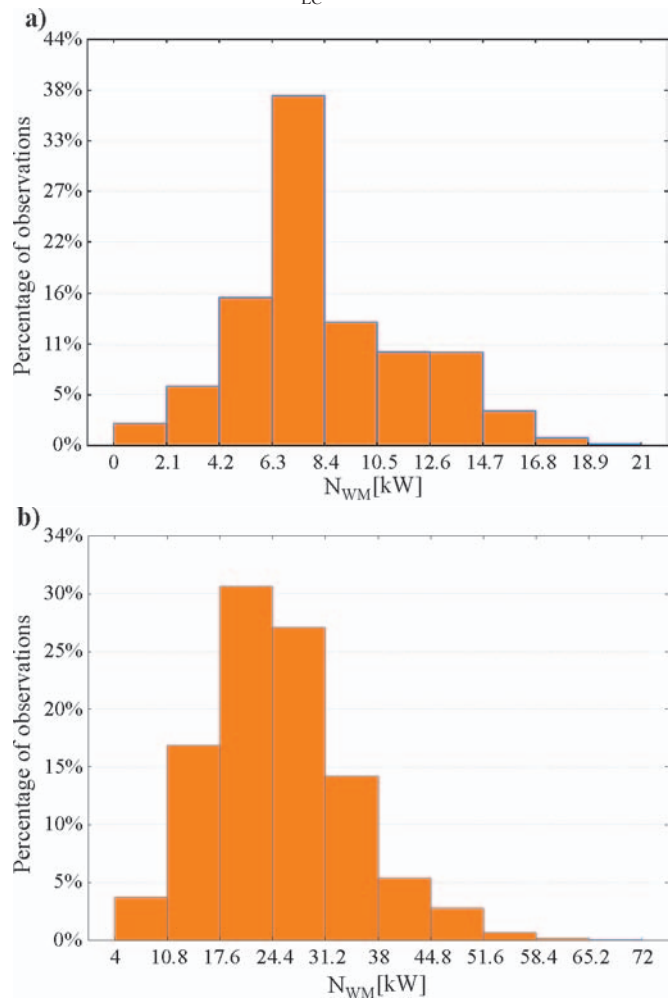


Fig. 2. Histograms of operational loads of sets of manoeuvre hoisting winches on the multi-bucket dredgers: a) *Inż. T. Wenda*, b) *Kategats*

Tab. 3. Characteristics of load distributions of sets of manoeuvre hoisting winches on multi-bucket dredgers

Name of dredger	$\sum N_{WM}^{nom}$	N_{WM}^{sr}	\bar{N}_{WM}^{sr}	σ_{WM}	v_{WM}	λ_{WM}^{cz}	Source of information
	kW	kW	-	kW	-	-	
<i>Małż II</i>	44	3.16	0.072	1.36	0.43	0.96	the author's investigations
<i>Inż. T. Wenda</i>	86	8.33	0.097	3.48	0.418	0.98	ditto
<i>Rozgwiazda</i>	86	7.21	0.084	1.83	0.254	0.97	ditto
<i>Usedom</i>	168	23.18	0.138	8.91	0.384	0.99	ditto
<i>Kategats</i>	168	25.37	0.151	9.23	0.364	0.99	ditto
<i>Ivan Bachalov</i>	168	26.47	0.158	10.04	0.379		[10]
Man values			0.117		0.372	0.98	

The coefficients λ_{LC}^{cz} and λ_{WM}^{cz} given in Tab. 2 and 3 determine duration of working time of bucket chain and set of manoeuvre hoisting winches during dredging the soil onto hopper barge (or silting-up the soil directly to land), respectively. To obtain time relation of the operational state „dredging” it is necessary to use additionally the coefficient λ_{cz}^{sp} (participation of time of dredging only in overall time of dredging operations). For this coefficient the value equal to 0.9 can be approximately assumed [5].

INVESTIGATIONS OF THE RELATIONS BETWEEN MEAN DRIVING LOADS OF MAIN CONSUMERS AND THEIR NOMINAL EFFECTIVE OUTPUT POWER VALUES

The investigations of the relations between the mean operational driving loads of main consumers, N_{GO}^{sr} , and their nominal effective output power values ($N_{GO}^{sr})^{nom}$ is very important for later possible use of their results in preliminary design stages of ship power plant.

As to the main consumers, the effective flux of energy of consumers, being in each case the product of the so called „generalized potential” and the „generalized flow rate”, can be considered [1].

The investigations of the relations between the mean driving loads of main consumers and their nominal effective output power values were already performed for industrial trawlers and typical transport ships (dry cargo ships, bulk carriers) [1, 3].

The performed investigations showed that for all types of main power consumers installed on the considered ships the following linear relation is valid [1,3]:

$$N_{GO}^{sr} = a + b (N_{GO}^{uz})^{nom} \quad (1)$$

where:

a, b – constants

The statement that the relation (1) appear to be linear and the possible determination of the constants a, b is of great importance as it can be used to estimate output power of main engines of ships of the considered types during the offer or preliminary design phase [1, 3, 5, 9].

The effective bucket chain power is determined by the relation:

$$N_{LC}^{uz} = M_{LC} \cdot \omega_{LC} \quad (2)$$

where:

M_{LC} – upper turas torque,

ω_{LC} – upper turas angular speed.

As bucket chain motion is forced by a prismatic rotary drum (called turas) cooperating with the bucket chain, located on a bucket tower, the bucket chain torque is assumed equal to the torque of the above mentioned upper turas. In the case of bucket chains, instead the angular speed, the bucket chain speed expressed by number of buckets passing the upper turas per one minute, as given in technical manuals of dredgers, is used.

In Tab. 4 are presented values of the nominal parameters of the bucket chains on the investigated dredgers as well as parameters of operational driving load distributions for the chains during dredging (on the basis of the data of Tab. 1 and 2). As stated earlier, there are no significant differences between mean values of bucket chain loads during dredging the medium sands and medium silts. Therefore the investigations of the relation (1) were carried out generally for medium soils, without distinguishing non-cohesive from cohesive ones. The investigations in question were performed for bucket chains by using the data of Tab. 4. Their results are presented in Tab. 5 and Fig. 3. The permissible intervals for independent variables of the equations given in Tab. 5, result from the data contained in Tab. 4.

Tab. 4. Nominal parameters of bucket chains and characteristics of their operational loads during dredging for 6 investigated dredgers

Name of dredger	Nominal parameters of bucket chains			Characteristics of operational loads					
	M_{LC}	n_{LC}	N_{LC}^{uz}	Medium soils			Light soils		
				N_{LC}^{sr}	σ_{LC}	v_{LC}	N_{LC}^{sr}	σ_{LC}	v_{LC}
kNm	n.bekts/ min	kNm · n.bekts/ min	kW	kW	-	kW	kW	-	
<i>Małż II</i>	85	24	2040	28.37	9.92	0.349	21.22	4.03	0.189
<i>Inż. T. Wenda</i>	370	19	7030	104.09	37.06	0.353	92.73	14.28	0.154
<i>Rozgwiazda</i>	360	19	6840	96.77	32.92	0.34	90.98	16.91	0.186
<i>Usedom</i>	400	25	10000	183.44	41.62	0.227	158.93	29.93	0.188
<i>Kategats</i>	380	25	9500	195.68	42.35	0.216	172.86	21.48	0.124
<i>Ivan Bachalov</i>	380	25	9500	186.64	46.84	0.251	165.91	28.67	0.173

Tab. 5. Linear regression equations which describe mean loads of bucket chains during dredging the soil of two kinds

Kind of soil	Form of relation	Statistical estimation parameters				
		R	σ [kW]	F	$F_{kr}; \alpha = 0.05$	m
medium	$(N_{LC}^{sr}) = 0.0216(N_{LC}^{uz}) - 29.44$	0.965	23.16	55.35	7.71	6
light	$(N_{LC}^{sr}) = 0.0194(N_{LC}^{uz}) - 27.84$	0.973	18.28	71.15	7.71	6

where: R – coefficient of correlation, σ – standard deviation

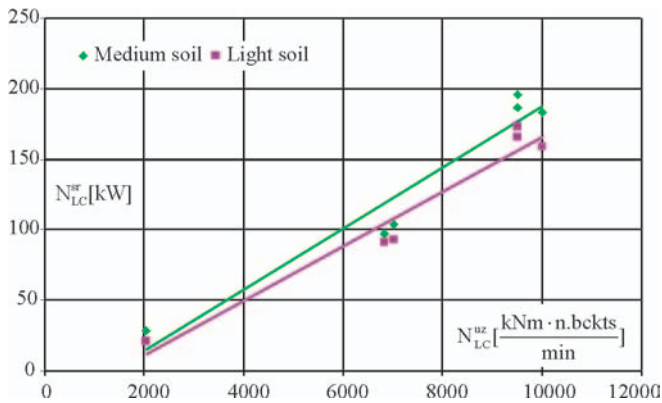


Fig. 3. The relation: $N_{LC}^{sr} = f(N_{LC}^{uz})$ for multi-bucket dredgers

To investigate significance level of correlation coefficient the F test of Snedecor distribution was used. Statistical significance is confirmed if: $F > F_{kr}$ for the assumed significance level α (usually $\alpha = 0.05$) and the degrees of freedom: s_1 and s_2 ($s_1 = 1, s_2 = m - 1 - 1$, where: 1 - number of independent variables, m - number of population).

The nominal effective output power of set of manoeuvre hoisting winches, N_{WM}^{uz} , is described by the relation:

$$N_{WM}^{uz} = \sum_{i=1}^4 (T_{WM} \cdot v_{WM})_i \quad (3)$$

where:

T_{WM} – hoisting winch torque,
 v_{WM} – hoisting winch speed.

In Tab. 6 are given the nominal parameters of manoeuvre hoisting winches on the investigated dredgers as well as parameters of operational load distributions of sets of the winches during dredging (on the basis of the data given in Tab. 1 and 3). The investigations of the relation (1) were performed jointly for the whole duration time of the state „dredging” regardless of kind of soil dredged by a given dredger.

By making use of the data of Tab. 6 the following relation was obtained (Fig. 4):

$$N_{WM}^{sr} = 0.2343(N_{WM}^{uz}) - 7.65 \quad (4)$$

for which the values of: the correlation coefficient $R = 0.986$, the standard deviation $\alpha = 2.06$ kW, the test $F = 148.64$ at the population number $m = 6$, and $F_{kr} = 7.71$ for $\alpha = 0.05$, were calculated. The relation is applicable within the range: $38 \leq N_{WM}^{uz} \leq 138$ kW.

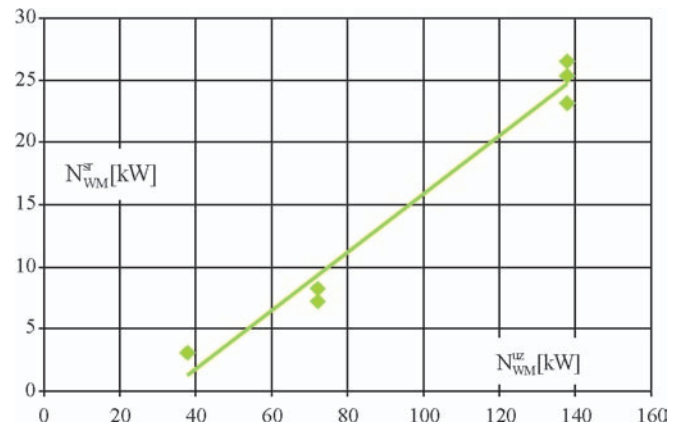


Fig. 4. The relation: $N_{WM}^{sr} = f(N_{WM}^{uz})$ for multi-bucket dredgers

SUMMARY

The performed investigations of operational loads of bucket chains and sets of manoeuvre hoisting winches on multi-bucket dredgers make it possible to offer the following remarks and conclusions:

- the averaged load distribution parameters of bucket chains and sets of manoeuvre hoisting winches, given in Tab. 2 and 3, can be deemed typical for the entire population of multi-bucket dredgers because of the long-lasting period of measurements as well as the broad range of size of the tested dredgers
- the characteristics of operational bucket chain loads, given in Tab. 2, confirm the necessity of taking into account kind of dredged soil
- in both the cases, i.e. of bucket chains and set of manoeuvre hoisting winches, the linearity of the relation (1) was confirmed as in all the considered relations large values (over 0.95) of the correlation coefficient R were obtained
- the achieved results can be used for predicting load distributions of bucket chains and manoeuvre hoisting winches; the relations given in Tab. 5 can be used to determine mean load of bucket chains; the relation (4) can be used to determine mean load of set of manoeuvre hoisting winches; the values of variation coefficients of load distributions of bucket chains and set of manoeuvre hoisting winches given in Tab. 2 and 3, can be used to estimate standard deviations of operational loads of the above mentioned main power consumers
- the presented results can be useful in solving problems during preliminary design phases of power plants for multi-bucket dredgers.

Tab. 6. Nominal effective power of set of manoeuvre hoisting winches and their operational load characteristics during dredging for 6 investigated dredgers

Name of dredger	Nominal effective power	Characteristics of operational loads of set of manoeuvre hoisting winches		
	N_{WM}^{uz}	N_{WM}^{sr}	σ_{WM}	v_{WM}
	kW	kW	kW	-
<i>Małż II</i>	38	3.16	1.36	0.43
<i>Inż. T. Wenda</i>	72	8.33	3.48	0.418
<i>Rozgwiazda</i>	72	7.21	1.83	0.254
<i>Usedom</i>	138	23.18	8.91	0.384
<i>Kategats</i>	138	25.37	9.23	0.364
<i>Ivan Bachalov</i>	138	26.47	10.04	0.379

BIBLIOGRAPHY

1. Balcerski A.: *Probabilistic models in the theory of design and operation of ship power plants* (in Polish). Fundacja Promocji Przemysłu Okrętowego i Gospodarki Morskiej (Foundation for promotion of shipbuilding industry and maritime economy), Gdańsk 2007
2. Balcerski A., Bocheński D.: *Proposal of a new structure of notions associated with ship power system* (in Polish). Materiały XXIII Sympozjum Siłowni Okrętowych SymSO 2002 (Proceedings of 23rd Symposium on ship power plants SymSO 2002), Gdynia 2002
3. Balcerski A., Bocheński D.: *Investigations of relations of mean driving loads of technological consumers on industrial floating units* (in Polish). Zeszyty Naukowe Wyższej Szkoły Morskiej w Szczecinie (Scientific Bulletins of Szczecin Maritime University), Szczecin 2003
4. Bocheński D., Kubiak A., Jurczyk L.: *Measurements of the parameters which characterize operation of technological systems on dredgers* (in Polish). Materiały XXII Sympozjum Siłowni Okrętowych SymSO 2001 (Proceedings of 22nd Symposium on ship power plants SymSO 2001), Szczecin 2001
5. Bocheński D. (Supervisor) et al.: *Research on identification energy consumption and parameters of dredging as well as winning transport on selected types of dredgers and pumping dredgers. Final report of the research project KBN no. 9T12C01718* (in Polish). Prace badawcze WOIO PG nr 8/2002/PB (Research report No.8/2002/PB, Faculty of Ocean Engineering and Ship Technology, Gdańsk University of Technology), Gdańsk 2002
6. Bocheński D.: *Analysis of operational loads of main power consumers on multi-bucket dredgers* (in Polish). Zeszyty Naukowe Akademii Marynarki Wojennej nr 162. XXVI (Scientific Bulletins of Polish Naval University, No. 162, XXVI), Sympozjum Siłowni Okrętowych SymSO 2005 (Proceedings of 26th Symposium on ship power plants SymSO 2005), Gdynia 2005
7. Bocheński D.: *Analysis of design solutions and relations which determine parameters of power systems of multi-bucket dredgers* (in Polish). Wybrane problemy projektowania i eksploatacji siłowni okrętowych (Selected problems of design and operation of ship power plants), XXVII Sympozjum Siłowni Okrętowych SymSO 2006, (Proceedings of 27th Symposium on ship power plants SymSO 2006), Szczecin 2006
8. Bocheński D.: *Operational loads of power system of bucket dredgers in main service states*. Journal of Polish CIMAC, Energetic aspects vol. 2, no 1, Gdańsk 2007
9. Bobrowski D.: *Probabilistics in engineering applications* (in Polish). WNT (Scientific Technical Publishing House), Warszawa 1986
10. *Kompleksyjne technologiczne issledowanija sudov popolnienija instrukcija po effektivnoj eksploatacji ziemsnarjada „Ivan Bachalov”* (in Russian). GDK, Rostow upon Don, 1985
11. Roorda A., Vertregt J.J.: *Floating dredgers*. De Technische Uitgeverij H. Stam, Haarlem, 1963
12. Vlasblom W. J.: *Designing dredging equipment*. Lecture notes, TUDelft 2003-05
13. Girtler J.: *Deterministic and probabilistic interpretation of operation of technical systems with regard to their reliability*. Polish Maritime Research, No 3/2003
14. Bocheński D.: *Design solutions and working conditions of power systems for trailing suction hopper dredgers*. Polish Maritime Research, No 2/1999
15. Girtler J.: *A probabilistic concept of load assessment of self-ignition engines*, Polish Maritime Research, No 2/2008

CONTACT WITH THE AUTHOR

Damian Bocheński, Ph. D.
Faculty of Ocean Engineering
and Ship Technology
Gdansk University of Technology
Narutowicza 11/12
80-952 Gdansk, POLAND
e-mail : daboche@pg.gda.pl



Photo: Cezary Spigarski

The application of magnetic fluids in sealing nodes designed for operation in difficult conditions and in machines used in sea environment

Leszek Matuszewski, Ph.D.
Gdansk University of Technology

Zbigniew Szydło, Ph.D.
AGH University of Science and Technology

ABSTRACT

Presented in article MF seals are being researched for sea technology purposes due to their excellent tightness and low resistance of motion. These features are most valuable for ring propellers and ship's main propeller shaft. There are more reasons why technologists pay significant attention for various MF seals applications in their difficult operating conditions. For instance, an advanced pumping systems are designed with contactless (screw or centrifugal) fluid seal used as the first stage seal and then the MF seal as the main seal. Further parts of the article contain discuss of the properties of magnetic fluids in the construction of MF seals. Sample of the few systems of magnetic fluid seals are presented, which have been researched lately in our laboratory including sea conditions. The magnetic fluids used in our seals are colloidal suspensions of magnetic nanoparticles. Undertaken earlier various systems selection for sea-water purposes forced us to focus on double sealing systems, in which the MF seal is used as the second seal following a conventional system especially adapted to co-operation with MF systems. This solution successfully limits direct contact of the sealed liquid with the magnetic fluid, and the entire sealing construction secures absolute tightness of the system. Using this solution we also can reduce costs by elements high accuracy avoidance. Research and design activities are carried out in the AGH Laboratory of Seals and Magnetic Fluid Applications together with Deep Water Department of Technical University of Gdansk over the use of magnetic fluid seals in sea water environment. These activities are oriented on working out MF seals able to work effectively in machines in which low-pressure water flow takes place. The objects of experimental investigations are seals having two different nominal diameters: 50 mm and 220 mm and two research rigs of different construction had to be built up. Works are scheduled to be continued.

Keywords: FM seal, sealing, magnetic fluids, sea technology, propellers

INTRODUCTION

Sealing rotating shafts, bearings, and other mechanical systems with the aid of the magnetic fluid, which creates a sealing partition kept steady by magnetic forces, is the technique which has been successfully used in machines working in gas environment at pressures up to, approximately, 1.0 MPa. These seals also provide opportunities for solving sealing problems in fixed and moving passages in vacuum machines.

In the worldwide technical literature and publications issued by companies producing magnetic fluids and machines in which they are applied the following names are used for the magnetic fluid seals:

- ✦ FerroMagnetic Seal (acronym: FM Seal)
- ✦ Magnetic Fluid Seal (acronym: MF Seal)
- ✦ FerroFluidic Seal (acronym: FF Seal).

In further parts of the article the names: "Magnetic Fluid Seal" or "MF Seal" will be most frequently used.

As a result of numerous experimental and theoretical studies oriented on investigating distributions of the magnetic field in the seals and rheological properties of the magnetic fluids, complemented by the development of technologies for production of these fluids, certain principles have been

formulated on magneto-mechanical shaping of the MF seal, selecting the type of fluid appropriate for expected conditions of machine operation, and calculating geometrical parameters of the sealing lips [1, 2, 3, 4].

Since the mechanism that keeps the MF seal tight differs considerably from that observed in other types of seals, opinions can be found that the use of MF seals is limited mainly to precise machines. These opinions are claimed to be justified by specific properties of magnetic fluids, the necessity of use of high-energy permanent magnets, and relatively high precision required during production of the MF seals. These factors decrease the permissible pressure limit to about 1.0 MPa, at the corresponding critical temperature of the magnetic fluid not exceeding, approximately, 200°C. Moreover, extremely high prices of high-dispersion magnetic fluids (nanomagnetic fluids) and the abovementioned required precision of machining are the reasons why MF seals are not in common use at present.

However, despite the above difficulties, obvious advantages of these seals, including excellent tightness and low resistance of motion, are the reasons why growing interest is observed towards their use in difficult operating conditions, where they are mainly used as so-called protective seals. This refers to such machines as reactors used in the chemical, biochemical,

and pharmaceutical industry, machines and systems used in the refining industry, and driving systems working in partial or total immersion in a liquid. Those machines frequently work in difficult conditions, which include non-uniformity of motion, oscillations and/or vibrations, high temperature and the action of aggressive environment having the form of vapours and aerosols. In the case of machines like floodable pump drives or sea-going vessel driving systems, which are immersed in liquids, certain problems connected with the contact of the magnetic fluid with the water are to be solved. The use of MF seals in those conditions requires special constructional designs and special magnetic fluids, which is of particular importance for machines used in liquids environment.

It is well known from available publications and patent solutions that the magnetic fluids applied in those conditions should reveal strong hydrophobic properties - here the most often described designs are hybrid sealing systems, in which the MF seal is used as the second seal following a conventional seal in a row arrangement. This design limits direct contact of the sealed liquid with the magnetic fluid, while the MF seal secures absolute tightness of the entire system.

For instance, some rotor pump sealing systems are designed in the above way, with the front seal or contactless (screw or centrifugal) fluid seal used as the first seal and the MF seal as the second seal.

In the case of high-amplitude vibrations, elastic systems are used which provide opportunities for stabilisation of the seal within certain range of its positions, despite the presence of oscillations of the sealed shaft. When high temperatures of operation are expected, the applied magnetic fluids should reveal increased temperature resistance, and intensive cooling of the system of magnets and the magnetic fluid is to be provided.

The next parts of the article discuss the properties of magnetic fluids, along with basic problems in the construction of MF seals. Sample designs of magnetic fluid seals are presented, which have been used in objects operating in difficult conditions, such as those observed, for instance, on sea-going vessels.

MAGNETIC AND MAGNETORHEOLOGICAL FLUIDS

The magnetic fluids used in seals are colloidal suspensions of magnetic nanoparticles (for instance magnetite – Fe_2O_3), of about 10 nm in diameter, in the carrier liquid (for instance, synthetic oil, silicone liquid, water). Particles having those dimensions are kept in constant motion by internal energy of the carrier liquid and create stable structures. In the production process, a surface active substance (oleic acid, for instance) is introduced to the carrier liquid to cover the surfaces of the magnetic particles and thus protect against their aggregation and sedimentation of the created multi-particle magnetic aggregates under the influence of gravitation and magnetic forces.

Magnetic fluids revealing those properties bear the name of nanomagnetic fluids. A basic advantage of the nanomagnetic fluids is high stability and durability of the colloidal system - which for many liquids can last as long as about 10 years.

Using a similar procedure to the described above, magnetic fluids are produced in with the suspensions of magnetic microparticles (magnetite – Fe_2O_3) have from 0.5 do 8 μm in diameter. Their percentage content in the liquid is from 20% to 80% [6].

To make distinction between them and the nanomagnetic fluids, these liquids are called micromagnetic fluids, although in producers' catalogues and the professional literature they are more often referred to as magnetorheological fluids.

The micromagnetic fluids are not stable – when the magnetic particles remain in rest from several to several hundred hours,

they are subject to sedimentation. However, if the energy from outside is delivered to this liquid, in the form of vibrations of motion of a mechanical system for instance, then the magnetic microparticles compose a homogeneous suspension, the behaviour of which is similar to that presented by the colloidal suspension of nanomagnetic particles. The main advantage of the micromagnetic fluids is high range of magnetic saturation – many times higher than that for nanomagnetic fluids, which increase their resistance to the action of external agents. Another important property is their rheological characteristic: strong and repeatable relation between the viscosity and the magnetic field strength – hence the frequently used name of a “magnetorheological fluid”.

With respect to magnetic interactions, the magnetic (nanomagnetic and micromagnetic) fluids belong to the group of so-called superparamagnetic materials, i.e. materials which do not reveal, in practice, any magnetic hysteresis.

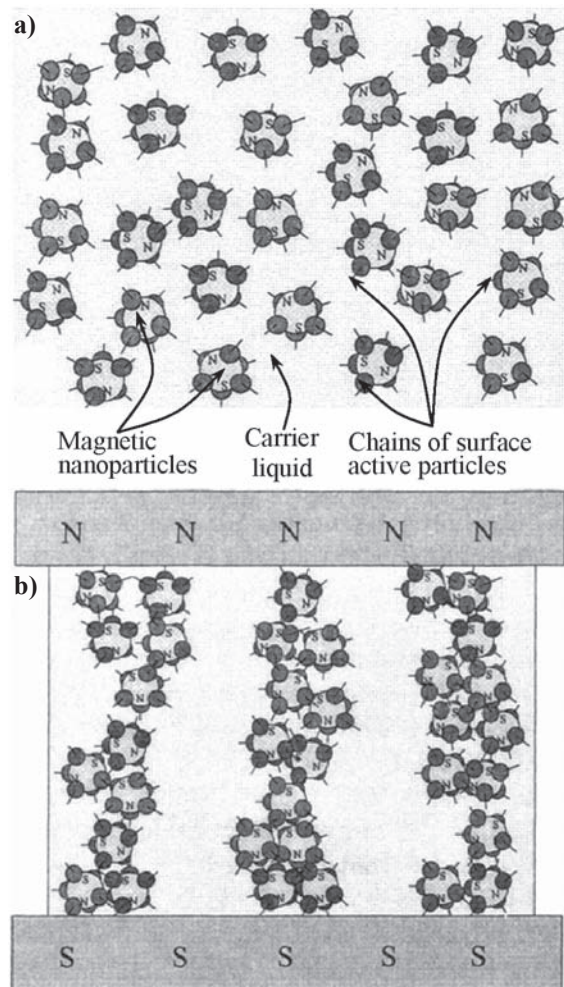


Fig. 1. Structure of the magnetic fluid and distribution of particles - magnetic dipoles: **a)** disordered distribution of magnetic dipoles in the absence of magnetic field, **b)** ordered chains of particles with oriented directions of magnetic dipoles in the presence of magnetic field [6].

Fig. 1a shows the disordered structure of the magnetic fluid in the absence of the magnetic field. The particles compose magnetic dipoles of arbitrary orientation, which makes the resultant magnetic force equal zero.

Fig. 1b, in turn, shows the ordered structure of the magnetic fluid in the presence of a constant or varying magnetic field. In these circumstances the particles compose chains of magnetic dipoles oriented along the direction of the magnetic lines of force.

High flexibility and speed of response (from 0,01 s to 0,0001 s) of the magnetic fluid to the presence of the magnetic field make the process of making order in particle orientations very short.

This property provides opportunities for using magnetic fluids not only in seals and lubricating technology, but also in controlled vibration dampers and couplings, and in measuring instruments. Due to remarkable advancement in technology of colloids, the magnetic fluids can be manufactured based on carrier liquids adapted to the planned type of application and conditions of magnetic fluid operation, with various content and properties of the magnetic phase (nanoparticles or microparticles). All this provides good opportunities for controlling parameters of the magnetic fluid and adapting them to actual needs.

Basic physical properties of the magnetic fluids, which decide on their possible applications, include magnetic saturation, dynamic viscosity, and operating temperature range. The magnetic saturation of the liquid determines the permissible pressure level (critical pressure) of the seal, while the viscosity affects the resistance of motion, and the range of temperatures in which the magnetic fluid can be used is to be adapted to operating conditions of a given machine.

At present, magnetic fluids are produced which reveal magnetic saturation up to 70 kA/m and dynamic viscosity ranging from 2 to 15000 mP·s.

The micromagnetic fluids reveal much higher, from five to ten times, magnetic saturation, which is connected with much larger dimensions of the magnetic particles used in those liquids.

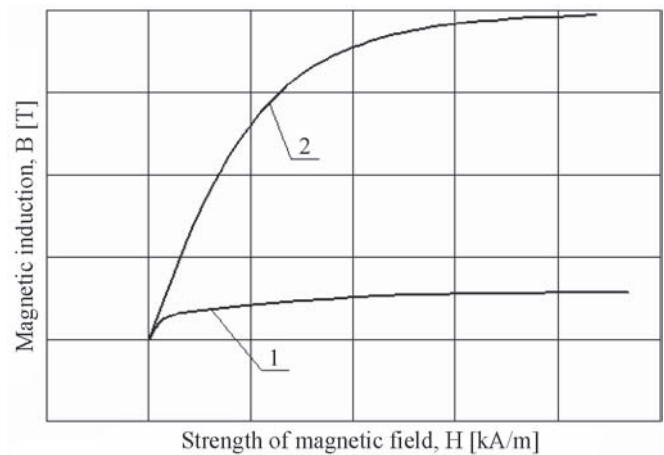


Fig. 2. Magnetic induction vs. magnetic field strength: nanomagnetic fluid (1) and magnetorheological fluid (2)

Fig. 2 shows the dependence of the magnetic induction B in the nanomagnetic and micromagnetic (magnetorheological) liquids on the strength H of the external magnetic field [6].

Tab. 1 collects basic properties of the nanomagnetic fluids produced by FerroLabs, Russia, while in Tab. 2 basic properties of the magnetorheological (micromagnetic) fluids produced by

Tab. 1. Properties and applications of magnetic (nanomagnetic) fluids produced by FerroLabs, Russia, and used in sealing and lubricating technology

Type of fluid	Carrier liquid	Operating temperature range. °C	Density g/cm ³	Viscosity Pa·s @25°C	Magnetic saturation. kA/m	Applications
FLS 300.020	Silicone liquid	-50...+90	1.2...1.4	0.5...0.8	20...30	Vacuum machines: - plasma coating - semiconductor technology devices
FLS 040.040	Silicone liquid	-70...+150	1.0...2.0	0.3...0.8	40...50	High-speed shafts: - chemical reactors - CD and DVD drives
FLS 250.020	Silicone liquid	-60...+100	1.1...2.2	...1.0	20...30	Dustproof seals: - precise devices - measuring instruments
FLF 750.030	Perfluoropolyether	-30...+130	2.05	...15	30...40	Seals against aggressive gases and liquids: - industrial chemical reactors - petrochemical facilities
FLW 250.020	Water	0...+90	1.2	...0.02	5...30	Facilities in biotechnology and medicine: - medical instruments - production machines
FLC 002.050	Kerosene	-50...+50	1.2	0.002...0.02	30...70	Magnetic sensors and separators: - position and acceleration sensors - separation of materials
FLC 050.025	Synthetic oil	-50...+150	1.0...2.0	...0.3	25...50	Lubricating magnetic fluid: - hermetic bearing units lubricated with magnetic fluid

Tab. 2. Properties and applications of magnetorheological (micromagnetic) liquids produced by FerroLabs, Russia, and Lord, USA, and used in controlled vibration dampers, couplings, brakes, and in abrasive machining of materials

Type of fluid	Carrier liquid	Operating temperature range. °C	Density g/cm ³	Viscosity Pa·s @25°C	Magnetic saturation. kA/m	Applications
FLS 040.600/ FerroLabs	Silicone liquid	-50...+150	3.28	...10	600...700	Controlled brakes, couplings, dampers, vibration insulators
FLW 001.300/ FerroLabs	Water	0...+90	3.42	...10	300...600	Magnetic abrasive machining of materials
MRF-132ED/ Lord	Synthetic oil	-40...+150	3.06	0.33...0.94	-	Controlled brakes, couplings, dampers, vibration insulators
MRF-240BS/ Lord	Water	0...+70	3.82	5.0...13.6	-	Educational purposes. demonstration of magnetorheological effects

FerroLabs and Lord, USA, are given. According to FerroLabs, the magnetic saturation of the magnetorheological fluids reaches up to 700 kA/m. The American company Lord does not publish the level of magnetic saturation of the magnetorheological liquids produced by them.

THE STRUCTURE AND PRINCIPLE OF OPERATION OF MAGNETIC FLUID SEALS

Of particular importance among technical applications of the magnetic fluids are MF seals for rotating shafts. The magnetic fluid seals (MF seals) compose a separate class of contactless seals, revealing absolute tightness (leakage at the level of 10^{-6} Pa·l/s) within the range from very high vacuum (10^{-6} Pa) do the pressures of an order of 1.0 MPa, at relatively small power losses generated by liquid friction. For the time being, the MF seals have been used mainly in gas environment: as protective seals for rolling bearings, seals for passages of rotating shafts in vacuum technology machines, and as shaft seals in fans, mixers, and chemical and biochemical reactors.

Fig. 3 shows the structure and principle of operation of the rotating shaft MF seal. A permanent magnet is fixed in the casing made of non-magnetic material. The magnet has the shape of a cylinder with an opening. The NS magnetisation direction of the cylinder is parallel to the axis of the sealed shaft. One cylindrical pole shoe made of magnetic material is situated on each side of the permanent magnet. Between the shaft made of magnetic material and the inner surface of the pole shoe openings there is a gap filled with the magnetic fluid. The fluid is kept in place by magnetic forces generated by the permanent magnet closed in the circuit composed by pole shoes, shaft and the magnetic fluid. The thickness of the gap with the magnetic fluid ranges, generally, between 0.1 mm and 0.3 mm.

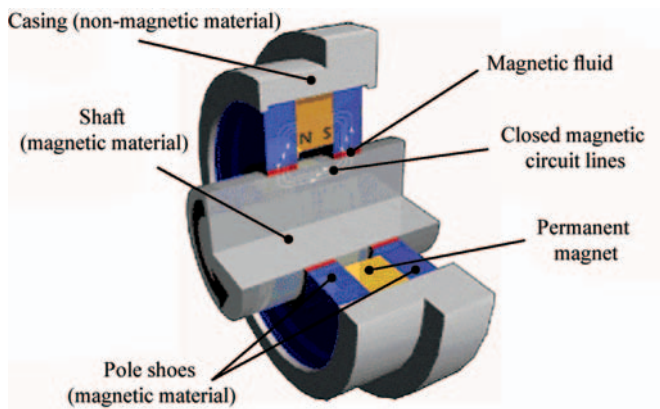


Fig. 3. Basic components of rotating shaft MF seal [7]

Despite simple principle of operation and construction of MF seals, designing them properly requires special knowledge due to specific properties of the magnetic fluid and its behaviour in the magnetic field. This refers in particular to large-dimension rotating shafts in high-speed machines revealing complex kinetics of motion.

MF seal's ability to keep tightness is defined by a so-called limiting perforation pressure, which is the maximum pressure kept by the seal, above which the magnetic fluid is ejected out from the gap and the tightness is lost. The ability to keep the seal tight depends on magnetic saturation of the liquid, the level of filling the gap with the magnetic fluid, the geometry of the seal, and pressure difference between two sides of the seal.

Fig. 4 shows the volumetric deformation of the magnetic fluid in the magnetic field in the gap of a single sealing lip.

The deformation is generated by the pressure difference between areas 4 and 1.

The pressure difference Δp which provokes the perforation of a single sealing lip filled with the magnetic fluid was determined from the Bernoulli equation for the flow of liquid in the magnetic field [2]. This equation takes into account only the magnetic saturation M_s of the magnetic fluid and the difference between the maximum and minimum values, H_{\max} and H_{\min} , of the magnetic field in the working gap.

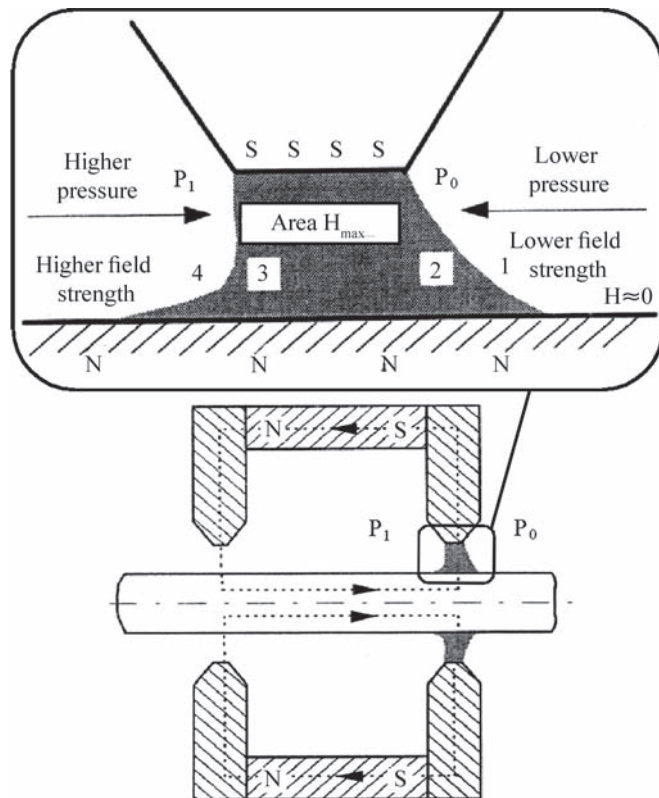


Fig. 4. Principle of operation of the magnetic fluid seal. 1 - lower pressure area, 2 - lower magnetic field strength area, 3 - higher magnetic field strength area, 4 - higher-pressure area

The distribution of the magnetic field (induction) within the gap, and consequently H_{\max} and H_{\min} , depend on the geometry of the sealing lip, the height of the working gap, and the energy of the magnetic system.

After assuming $H_{\min} = 0$ we arrive at the relation which will allow us to determine Δp for a single sealing lip in static conditions (μ_0 - magnetic permeability of the vacuum):

$$\Delta p = \mu_0 M_s H_{\max} = M_s B_{\max}$$

Determining the critical pressure for the MF seal in dynamic conditions is much more difficult, as the magnetic fluid in the working gap is subject to the action of not only the magnetic forces, but also flow processes, rotation (spin) of particles, their mutual interactions, and the centrifugal force which affects the position of the magnetic fluid in the gap and changes the seal perforation pressure. This pressure depends on the position of the sealing lips, which are mounted either on the rotating shaft, or on the pole shoes steadily fixed in the casing. These phenomena are clearly visible at higher rotational speeds of the shaft - above 10m/s.

The results of the experimental investigations suggest that the critical perforation pressure for a single sealing lip in the arrangement shown in Fig.3 is approximately equal to 0.05 MPa. A similar pressure level per one sealing lip can be assumed for a symmetrical two-lip arrangement, which is

more rational than a single lip from the technical point of view. However, for multi-lip seals (in symmetrical arrangements with four, six and more lips) the permissible working pressure for a single sealing lip is to be assumed from within the range between 0.03 MPa and 0.04 MPa.

MAGNETIC FLUID SEALS FOR ROTATING SHAFTS WITH RADIAL AND AXIAL RUNOUT

Using magnetic fluid seals for sealing rotating shafts with axial and radial runout requires special designs. When the axial and/or radial runout is relatively small, the applied sealing constructions are flexibly mounted on the machine casing using elastic rings. In the case of large axial and radial runout, the sealing constructions are mounted on elastic bellows fixed to the machine casing.

Fig. 5 shows the construction of a sealing passage with the magnetic fluid used in chemical reactors, in which extremely high tightness of the process chamber is required [7].

The sealing unit consists of a permanent magnet 5 with axial polarisation, the pole shoes 1, and a sleeve 11 with sealing lips, fixed to the bearing casing 3 on surface 15. The sleeve 11 is made of magnetic material, while the casing 3 is made of non-magnetic material. As a result, the magnetic circuit is closed through the magnetic fluid 10. The pole shoes 1 are placed inside the sleeve 4, which is rotationally mounted in the casing 3 using the rolling bearings 2. The sleeve 4 is connected with the shaft 8 via a moving sleeve 6. Loose connections between the shaft 8, the sleeve 6, and the sleeve 4, along with the application of elastic sealing O-rings 7 and 9 in those connections, provide opportunities for good transmission of vibrations, at the same time keeping the thickness of the gap 10 with the magnetic fluid constant. Loose fixing of the casing 3 in the flange 13, done with the aid of the sealing O-ring 12, also makes it possible to transmit axial displacements of the shaft.

This construction makes it possible to keep the seal tight even when drive shaft vibrations reach as much as 0.7 mm.

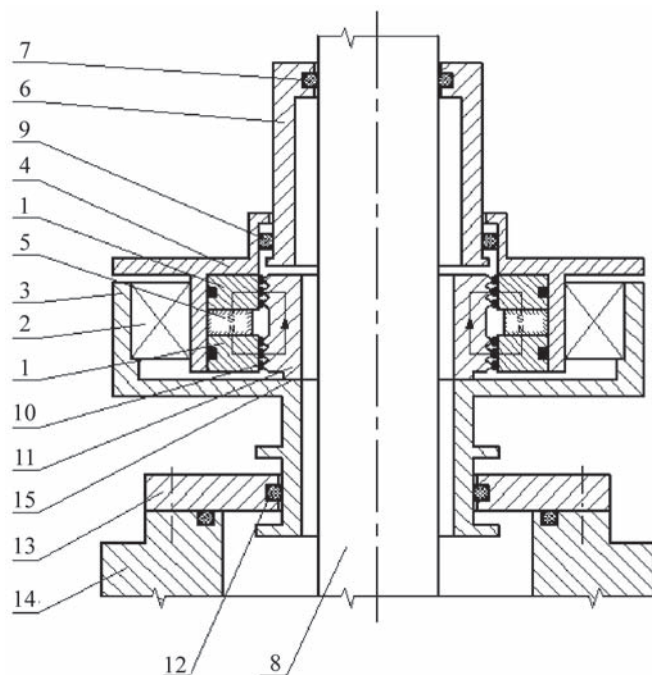


Fig. 5. Magnetic fluid seal for vertical shaft with limited axial runout: 1 – pole shoe; 2 – thrust bearing; 3 – bearing casing; 4 – intermediate sleeve; 5 – permanent magnet; 6 – moving sleeve; 7, 9, 12 – sealing O-rings; 8 – shaft; 10 – magnetic fluid; 11 – sleeve with sealing lips; 13 – flange; 14 – casing; 15 – fixing of sleeve 11 with sleeve 3.

Fig. 6 shows the magnetic fluid seal for a shaft with small axial and radial runout [9]. This seal consists of an axially polarised permanent ring magnet 1, pole shoes 2, 3 mounted on the shaft 5, and two self-adjusting rings 9, 10. The shaft 5 is made of non-magnetic material. The casing 8, the permanent magnet 1 with the pole shoes 2, 3, the self-adjusting rings 9, 10 and the magnetic fluid 12 filling the radial gaps δ_1 , δ_2 and the axial gaps δ_3 , δ_4 compose a closed magnetic circuit with magnetic flux Φ . The magnetic flux generates a radial force, which moves the self-adjusting rings 9, 10 closer to the casing 8, and a radial force which presses the self-adjusting rings, via rolling elements 11, to the pole shoes 2, 3. The magnetic force keeps the magnetic fluid 12 in the radial and axial gaps, thus securing tightness of the entire sealing structure.

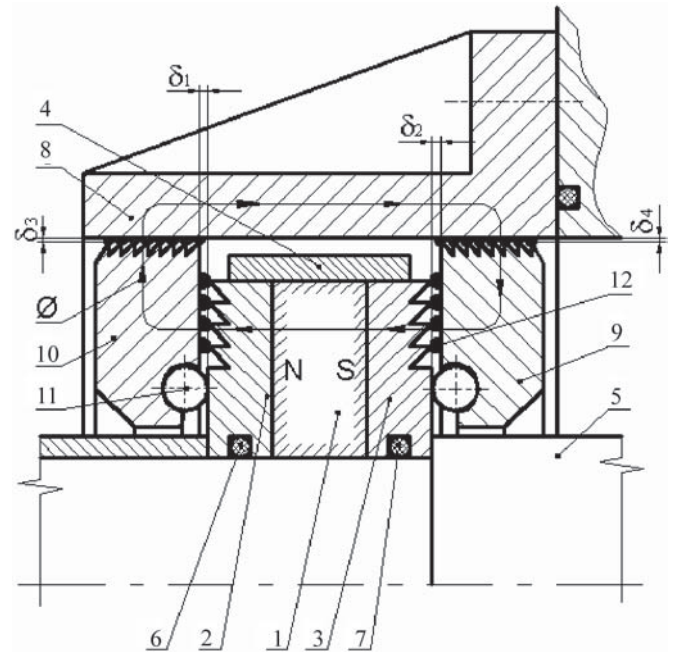


Fig. 6. Magnetic fluid seal for a shaft with limited axial and radial runout: 1 – permanent magnet; 2, 3 – pole shoes; 4 – clamping ring; 5 – shaft; 6, 7 – sealing O-rings; 8 – casing; 9, 10 – self-adjusting rings; 11 – rolling element; 12 – magnetic fluid

Fig. 7 shows the magnetic fluid seal for a shaft with large axial runout. In this construction two MF seals, consisting of magnets 7, pole shoes 8 and the magnetic fluid 9, are mounted in the carrying sleeves 5. The flange 3 is mounted between the casing elements 1, 2.

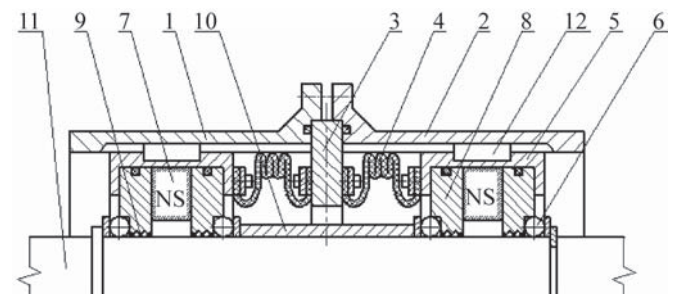


Fig. 7. Magnetic fluid seal for a shaft with large axial runout: 1, 2 – casing elements; 3 – flange; 4 – elastic bellows; 5 – carrying sleeve; 6 – rolling element; 7 – permanent magnet; 8 – pole shoe; 9 – magnetic fluid; 10 – distance sleeve; 11 – shaft; 12 – key

The carrying sleeves 5 are connected with the flange 3 via elastic bellows 4. The sleeves 5 can move in axial direction along the casing elements 1, 2. The rolling elements 6 allow the shaft 11 to rotate at constant dimensions of the working gaps between the lips of the pole shoes 8 and the shaft, with

the magnetic fluid 9 filling these gaps. Axial dislocations of the shaft 11 are totally compensated by the deformations of the bellows 4.

Fig. 8 shows a construction of the magnetic fluid seal for a vertical shaft with large axial and radial runout. The seal consists of the casing 3, a magnetic sleeve 2, a radially polarised permanent magnet 6, a pole shoe 9 and the magnetic fluid 8. The magnet 6 and the pole shoe 9 are mounted in the recess in the casing 3. The closed magnetic circuit is composed by the casing 3, the magnet 3, the pole shoe 9, the sleeve 2, and the magnetic fluid 8. The working gap between the sealing lips of the casing 3 and the pole shoe 9, and the sleeve 2 fixed on the shaft 1, is approximately equal to 0.5-0.6 mm and is filled with the magnetic fluid 8, which creates sort of a liquid gland and secures tightness of the centre. Axial and radial runout of the shaft 1 is compensated by the elastic bellows 13 mounted to the casing 3 and the machine body.

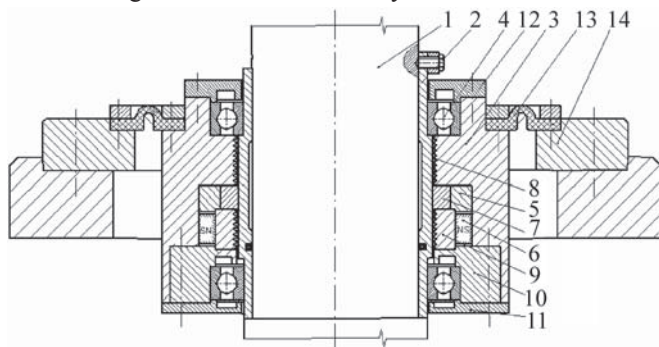


Fig. 8. Magnetic fluid seal for a vertical shaft with large axial and radial runout: 1 – shaft; 2 – magnetic sleeve; 3 – casing; 4 – rolling bearing; 5 – non-magnetic ring; 6 – permanent magnet; 7 – felt ring; 8 – magnetic fluid; 9 – pole shoe; 10 – non-magnetic retaining ring; 11 – lower cover; 12 – upper cover; 13 – elastic bellows; 14 – flange

Fig. 9 shows other designs of magnetic fluid seals for shafts revealing large axial and radial runout [9]. In the seal shown in Fig. 9a the shaft 2 transmits the rotational motion with radial and axial runout to the sleeve 6 via an elastic element (bellows 7), which fully compensates those dislocations by own deformation. The elastic bellows 7 secures tight joint of the shaft 2 with the sleeve 6. The rolling bearings 5 allow the sleeve 6 to rotate at constant working gap with respect to the fixed pole shoes 8 mounted in the casing 1, independently of radial and axial dislocations of the shaft 2. The magnetic fluid 4 is situated in radial gaps between the lips of the pole shoes 8 and the outer surface of the sleeve 6, and is kept inside by magnetic forces. In the design shown in Fig. 9b the MF seal is placed, along with the rolling bearings 5, in the casing 1 and mounted on the shaft 2. The casing 1 is connected via elastic bellows 7 with the stationary housing of the device. The above design also includes the system which cools the MF seal by delivering the cooling medium to the channels in the pole shoes.

MAGNETIC FLUID SEALS USED IN HIGH-TEMPERATURE OPERATION CONDITIONS

The lifetime of a magnetic fluid seal used in higher temperatures mainly depends on the temperature of intensive evaporation of the carrying liquid. The magnetic fluids used in these conditions are produced on the basis of specially silicone liquids or synthetic oils (Tab. 1, Tab. 2) which secure correct operation of the seal at temperatures up to 150°C, with the critical temperature approximately equal to 200°C.

Intensive heating of the magnetic fluid takes place in seals which operate in high temperature environment, and when

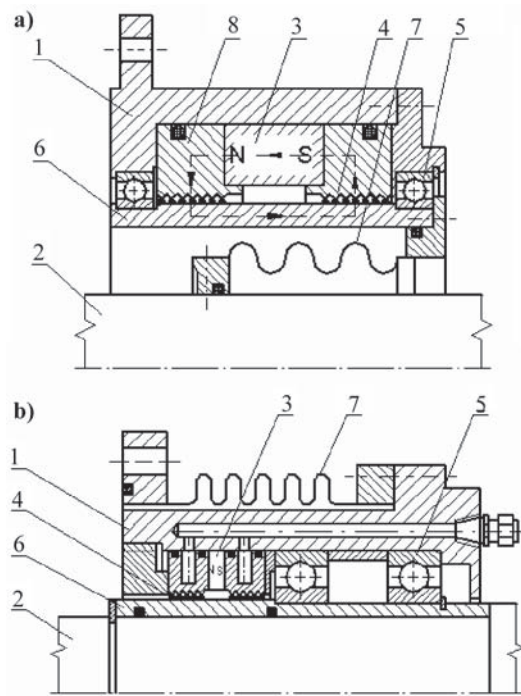


Fig. 9. Magnetic fluid seal for a shaft with large axial and radial runout: a), b) – design variants: 1 – casing, 2 – shaft, 3 – permanent magnet, 4 – magnetic fluid, 5 – rolling bearing, 6 – sleeve, 7 – elastic bellows, 8(a) – pole shoe

they seal shafts with extremely high rotational speed, where the produced heat is provoked by internal friction in the fluid. In those cases seals with extra cooling systems are used.

Fig. 10 shows a multi-lip sealing culvert with magnetic fluid, produced by FerroLabs (Russia) [7], which is used in industrial high-temperature bioreactors. The culvert is mounted on the shaft 1 using a rotating sleeve 2 linked with the shaft via the clamping ring 6. The sealing magnetic system is composed of the permanent magnet 7 and the pole shoes 8 mounted in the stationary sleeve 3, the lips of the rotating sleeve 2, and the magnetic fluid 9 in the gaps between the lips and the pole shoes. The geometry of the gap filled with the magnetic fluid is kept constant by the rolling bearings 4 and 5.

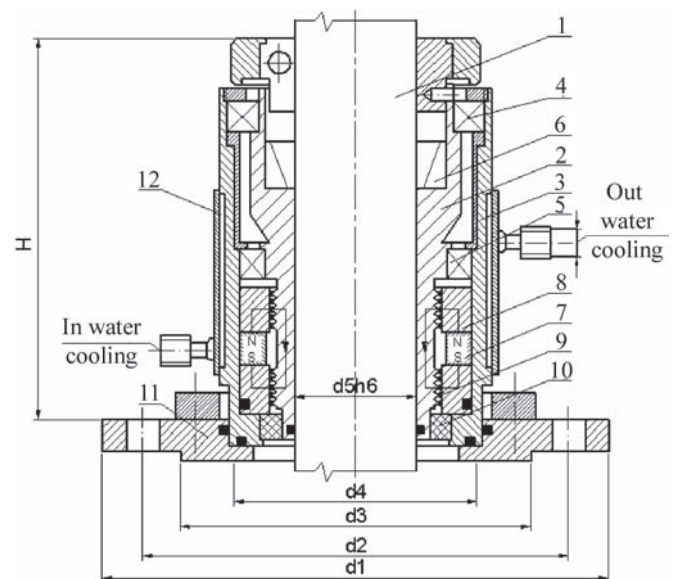


Fig. 10. Magnetic fluid seal for vertical shaft with external cooling system, made by FerroLabs: 1 – shaft; 2 – rotating sleeve; 3 – stationary sleeve; 4, 5 – rolling bearings; 6 – clamping ring; 7 – permanent magnet; 8 – pole shoe; 9 – magnetic fluid; 10 – sliding ring; 11 – flange; 12 – water jacket

A large part of length of the stationary sleeve 3 is surrounded by the water jacket 12 which protects the seal against the action of the ambient temperature. At the same time the water carries away the heat generated in the magnetic liquid during high-speed operation of the shaft.

According to the catalogue data given by the producer, this seal can work at ambient temperatures up to 1200°C and at maximum peripheral speed 15 m/s, when the pressure does not exceed 0.3 MPa. This culvert, produced for shafts with diameters ranging from 40 to 100 mm, can also work at the presence of lateral vibrations of the shaft, the amplitude of which does not exceed do 0.7 mm.

Fig. 11 shows a magnetic fluid seal designed for high-speed shaft with external and internal cooling system [9]. In this design the cooling liquid (water) is delivered to the seal by channels 9 made in the pole shoes 5, 6 and in the hollow shaft 2.

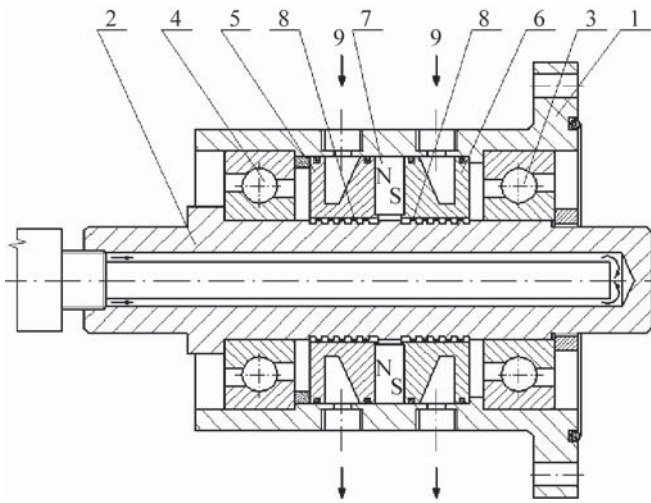


Fig. 11. Magnetic fluid seal for high-revolution shaft with external and internal cooling system: 1 – casing; 2 – hollow shaft; 3, 4 – rolling bearing; 5, 6 – pole shoes; 7 – permanent magnet; 8 – magnetic fluid; 9 – channel

MAGNETIC FLUID SEALS USED IN LIQUID ENVIRONMENT

Magnetic fluid seals which are used for sealing rotating shafts in liquid environment require double sealing systems, in which the MF seal is used as the second seal following a conventional seal in a one-by-one arrangement. This solution limits direct contact of the sealed liquid with the magnetic fluid, and the entire sealing construction secures absolute tightness of the system.

Fig. 12 presents a hybrid seal for an impeller pump shaft. This seal consists of a centrifugal seal and a magnetic fluid seal. The first sealing stage is the centrifugal seal 4 having the form of a disc mounted on the shaft 1. The second sealing stage is the magnetic fluid seal, consisting of the permanent magnet 5, the pole shoe 6 and the magnetic fluid 7. On the shaft 1 made of material revealing good magnetic permeability, two sealing lips 1a are mounted under the pole shoe 6. The magnetic fluid 7 fills small ring gaps between the pole shoe 6 and the sealing lips 1a, and is kept in there by magnetic forces to create additional sealing obstacle for the working medium. The chamber 8 filled with the compressed neutral gas protects the sealed medium (water, for instance) against coming into direct contact with the magnetic fluid, eliminating this way an unfavourable effect of the working medium on the magnetic fluid.

Fig. 13 presents a hybrid magnetic fluid seal for a vertical shaft of a deep-well pump [11]. This seal is a composition of

a centrifugal seal with two MF seals, out of which one MF seal is situated above the centrifugal seal and the other - below. The centrifugal seal consists of a rotor, having the form of the flange 9 mounted on the shaft 1 situated in the chamber 11, and the barrier fluid 10. In dynamic conditions the sealing function is performed by the centrifugal seal while in static conditions - by two MF seals, which counteract the leakage of the barrier fluid from the chamber and the penetration of impurities to pump inside.

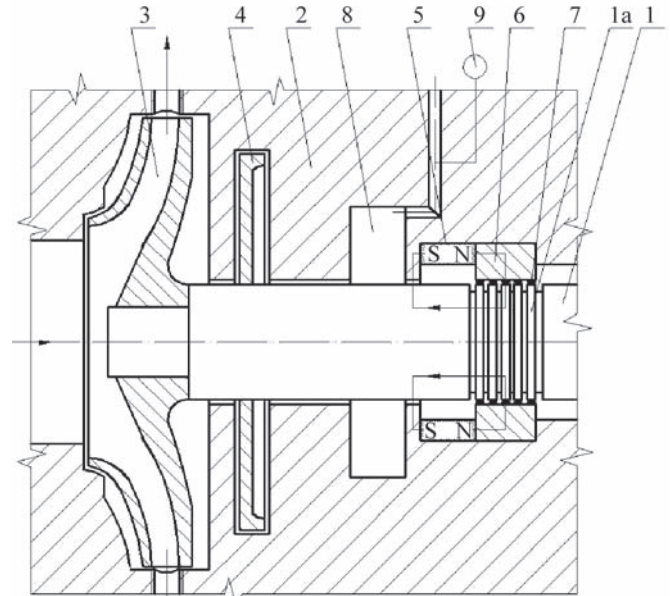


Fig. 12. Hybrid seal of impeller pump shaft: 1 – shaft, 1a – sealing lip, 2 – casing, 3 – impeller; 4 – centrifugal seal, 5 – permanent magnet, 6 – pole shoe, 7 – magnetic fluid, 8 – chamber filled with neutral gas, 9 – manometer

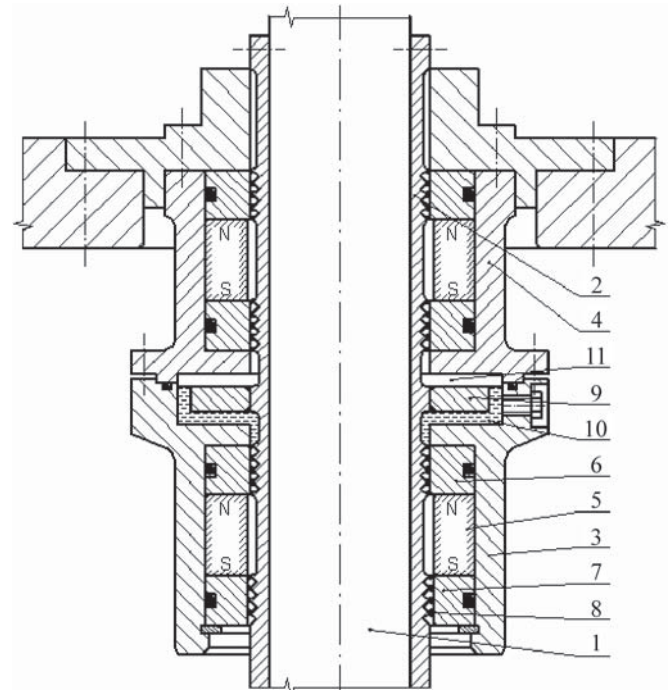


Fig. 13. Hybrid magnetic fluid seal for a vertical pump shaft : 1 – shaft; 2 – sleeve with sealing lips; 3, 4 – casing elements; 5 – permanent magnet; 6, 7 – pole shoes; 8 – magnetic fluid; 9 – flange; 10 – barrier fluid; 11 – chamber

Fig. 14 presents the double rotating shaft seal consisting of the primary liquid seal, the screw seal (Fig.14a) or the centrifugal seal (Fig.14b) for instance, and the secondary magnetic fluid seal situated behind the primary seal [9]. In this case the basic sealing function in dynamic conditions is

performed by the conventional liquid, while the role of the MF seal is to keep the working medium inside the machine in steady-state conditions and at low shaft rotations.

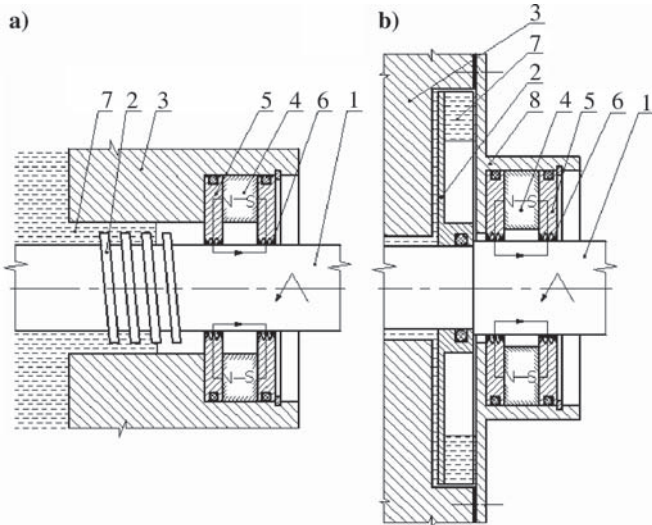


Fig. 14. Double rotating shaft seal: **a)** composed of screw seal and magnetic fluid seal; **b)** composed of centrifugal seal and magnetic fluid seal: 1 – shaft, 2 – screw groove or rotor, 3 – casing, 4 – permanent magnet, 5 – pole shoe, 6 – magnetic fluid, 7 – sealed liquid, 8(b) – cover

Fig. 15a presents a general view of a sea-going vessel with marked the position of the propeller drive system, while in Fig. 15b the drive system itself is schematically shown with marked the position of the passage that seals the propeller shaft. Fig. 15c shows a typical packing seal with soft packing,

normally used for ship propeller shafts. This seal consists of a package of sealing rings 6 made of a woven cord which are placed in the packing chamber and pressed by the gland 5. A disadvantage of this solution is the need for periodical pressing of the gland to compensate the relaxation of stresses in the packing.

Fig. 15d shows the construction of a magnetic fluid seal for the propeller shaft, which protects against the penetration of the seawater inside the ship's hull [12]. This seal consists of two axially polarised permanent magnets 6, 7, separated by multi-edge pole shoes 8, 9 and the magnetic fluid 10. The magnets 6, 7 and the pole shoes are mounted in the non-magnetic sleeve 5 fixed in the seal casing 4. Two closed magnetic circuits are composed by the magnets 6, 7, the pole shoes 8, 9, the magnetic fluid 10 and the shaft 1 made of material revealing good magnetic permeability. The magnetic fluid 10 is kept by the magnetic forces inside small ring gaps between the sealing lips of the pole shoes 8, 9 and the shaft 1, thus creating the sealing barriers for the working medium.

Fig. 16 shows the construction of a two-stage seal for a ship propeller shaft. The seal consists of a number of lip seals and the magnetic fluid seal [13]. The first sealing stage consists of two sealing lip rings 4 mounted in the casing 2. The second stage is the magnetic fluid seal which consists of the axially polarised permanent magnet 5, two pole shoes 6 and the magnetic fluid 7. The closed magnetic circuit is composed by the magnet 4, the pole shoes 6, the magnetic fluid 7 and the sleeve 3, made of material revealing good magnetic permeability, which is mounted on the shaft 1. The magnetic forces keep the magnetic fluid inside the small ring gaps 8, thus composing additional barriers for the sealed medium.

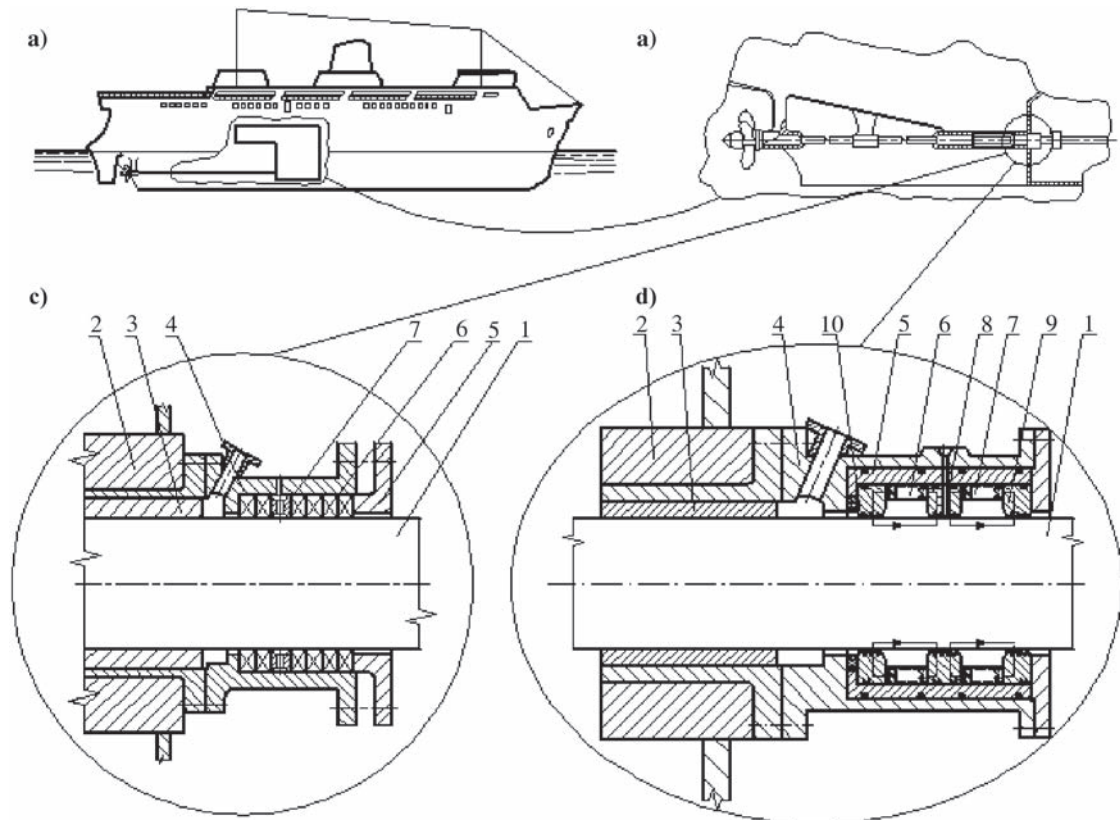


Fig. 15. Seal for ship propeller shaft: **a)** sea-going vessel with marked position of the propeller drive system; **b)** scheme of propeller drive system; **c)** typical packing seal for propeller shaft: 1 – propeller shaft, 2 – body, 3 – slide bearing, 4 – seal casing, 5 – gland, 6 – package of sealing rings, 7 – distance ring; **d)** magnetic fluid seal: 1 – propeller shaft; 2 – body; 3 – slide bearing; 4 – seal casing; 5 – non-magnetic sleeve; 6, 7 – permanent magnets; 8, 9 – multi-edge pole shoes; 10 – magnetic fluid

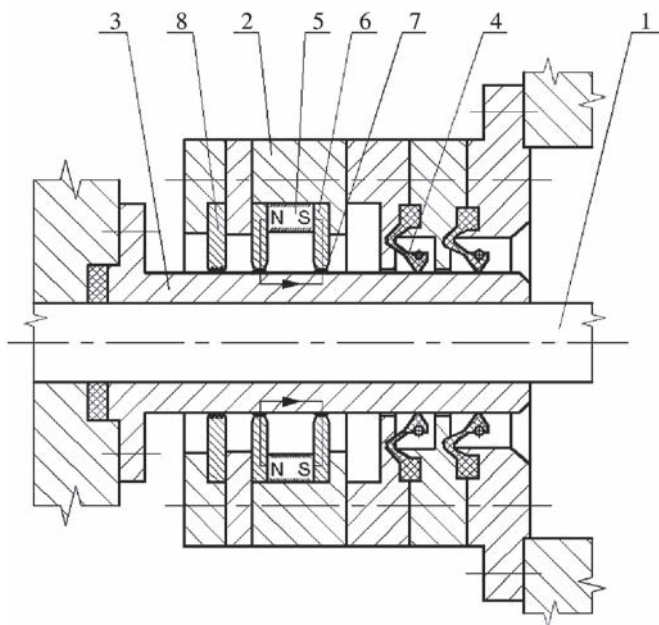


Fig. 16. Two-stage seal for ship propeller shaft, composed of lip seals and magnetic fluid seal: 1 – ship propeller shaft, 2 – casing, 3 – protecting sleeve, 4 – sealing lip ring, 5 – permanent magnet, 6 – pole shoe, 7 – magnetic fluid, 8 – sealing groove/gap ring

RESEARCH ACTIVITIES CARRIED OUT IN THE AGH LABORATORY OF SEALS AND MAGNETIC FLUID APPLICATIONS OVER THE USE OF MAGNETIC FLUIDS FOR SEALING ROTATING SHAFTS IN WATER ENVIRONMENT

Research and design activities are carried out in the AGH Laboratory of Seals and Magnetic Fluid Applications over the use of magnetic fluid seals in water environment. These activities are oriented on working out MF seals able to work effectively in machines in which low-pressure water flow takes place.

The objects of experimental investigations are seals having two different nominal diameters: 50 mm and 220 mm. This situation forced building two research rigs of different construction.

The experimental investigations of the seal of 50 mm in diameter, performed in water at pressure equal to 0.1 MPa and rotational speed equal to 3000 rev/min, have proved that this seal can continuously work during 200 hours, the least, without any traces of worsening of the assumed initial parameters. Tests performed on different constructional versions of this seal have revealed potential for increasing the critical speed of the shaft by using additional protecting elements in the sealing unit.

For the investigations of the magnetic fluid seal of 220 mm in nominal diameter, a special research rig was built which made it possible to measure the torque on the propeller shaft, the temperature of the seal, and its tightness in the presence, or absence, of the flow of the process liquid (water, in the examined case) through the sealed research chamber.

Fig. 17 shows a cross-section of the research head used in this rig. The basic elements of this head include the collapsible chamber 1, 2, 3, 4, with a set of magnets 7 with pole shoes 5. In the chamber the rotating disc 13 is placed, on which the rim 14 with sealing lips is mounted. The disc is fixed on the shaft 9 using the clamping ring 16.

After the magnetic fluid is introduced to the gaps between the pole shoes 5 and the sealing lips of the rotating disc 13, the chamber is divided into space A filled with the examined

medium, and space B used for disposing of leakages through the opening E drilled in the lower part of the chamber.

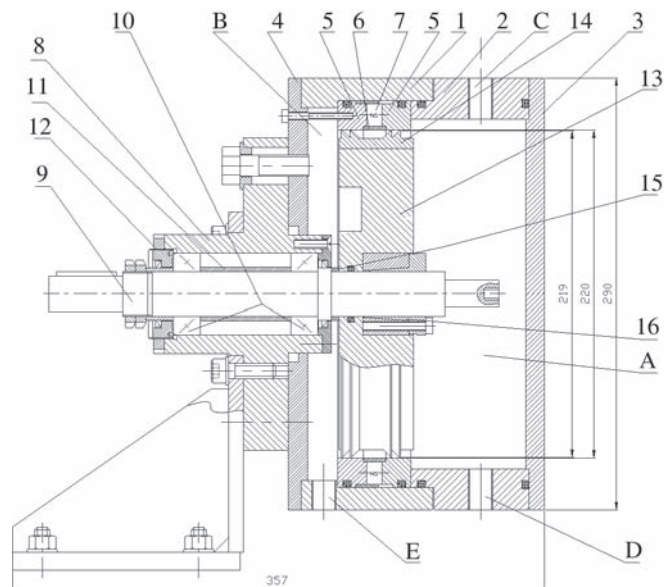


Fig. 17. Research head used on the rig for examining large-dimension magnetic fluid seals in water environment – MFLPI: 1, 2, 3, 4 – components of the collapsible research chamber; 5 – pole shoes; 6 – non-magnetic distance sleeve; 7 – replaceable set of permanent magnets; 8 – shaft body; 9 – rotating shaft; 10 – cone bearings; 11 – distance sleeve; 12 – adjusting nut; 13, 14 – two-part disc with sealing lips; 15 – positioning sleeve; 16 – clamping sleeve.

The openings C and D in the chamber are used for filling the space A, or for generating the flow of the examined medium with the aid of an external hydraulic system.

A basic condition for correct action of the magnetic fluid seal is securing uniform thickness of the gap along the entire perimeter of the seal.

Meeting this condition is difficult on the research rig designed for examining large-diameter objects, as the examination of different geometric versions of the seal would require a rig construction in which particular elements could be changed, at the same time securing the repeatability of the obtained results.

The research rig under discussion was tested in conditions in which the sealed chamber was filled with gas (air) and with liquid (water) under pressure 0,05 MPa and without flow.

The performed investigations and geometrical measurements have revealed high influence of the magnetic field generated by the set of permanent magnets on the axial alignment of the rotating and fixed elements of the seal when the magnetic circuit was closed by the magnetic fluid. This phenomenon was a source of leakages through the sealing magnetic fluid, and resultant difficulties in keeping the required pressure in the research chamber, which was particularly visible at low rotational speed ranges.

That was why additional elements were to be machined and installed in the rig to centre the set of pole shoes with respect to the rotating disc with sealing lips.

The measurements and investigations performed in the presence of additional centring elements have confirmed high efficiency of the introduced constructional changes.

The investigations did not take long, as their main goal was to check the operation of the research rig. Half-hour tests were performed with the water under pressure 0.03 MPa in the chamber and at shaft rotational speeds equal to 250 rev/min, 500 rev/min and 600 rev/min.

The modernised construction has confirmed the ability of the magnetic fluid seal with the working gap having

the nominal thickness of 0.5 mm to keep pressure in the abovementioned time interval and at the abovementioned working conditions.

BIBLIOGRAPHY

1. Berkovsky B.M., Medvedev V.F., Krakov M.S.: *Magnetic fluids - engineering applications*, Oxford Science Publications, 1993
2. Rosensweig R.E.: *Ferrohydrodynamics*, Cambridge University Press, Cambridge, MA, 1985
3. Orlov D.W., Podgorkov W.S.: *Magnitnyje židkosti w maszynostrojenii*, Izd. Maszynostrojenije, Moskwa, 1993
4. Kamiyama S., Oyama T., Htwe J. : *Basic study on the performance of magnetic fluid seals*, pp. 985–990. Proc. of JSLE Int Tribology Conf. 1985
5. J. Kurfess, H.K. Müller : *Sealing liquids with magnetic fluids*, Journal of Magnetism and Magnetic Materials, 85, 1990
6. Ławniczak A., Milecki A.: *Electro- and magnetorheological fluids and their technical applications*, Publishing House of Poznan University of Technology, Poznań, 1999 (in Polish)
7. Catalogue: *Ferrofluid-based seals*, Ferrolabs Inc. (Rosja)
8. Product Bulletin: *Magneto-Rheological Fluids*, LORD Corp. (USA)
9. Tietze W.: *Handbuch Dichtungspraxis*, 3.Auflage, Vulkan-Verlag, Essen 2003
10. USA patent, Int.Cl. F16J15/40, no 4681328, Magnetic fluid shaft seal
11. USA patent, Int.Cl. F 16J15/42, no 4054293, Hybrid magnetic fluid shaft seal
12. USA patent, Int.Cl. F16J15/54, no 4436313, Device for sealing a propeller shaft against invasion of sea water
13. JP patent, Int.Cl. F16J15/16, no 62178498, Stern pipe sealing device

CONTACT WITH THE AUTHORS

Leszek Matuszewski, Ph. D.
Faculty of Ocean Engineering
and Ship Technology
Gdansk University of Technology
Narutowicza 11/12
80-952 Gdansk, POLAND
e-mail : leszekma@pg.gda.pl

Zbigniew Szydło, Ph.D.
AGH University of Science and Technology
Faculty of Mechanical Engineering and Robotics
Al. Mickiewicza 30
31-069 Kraków, POLAND
zbszydlo@agh.edu.pl

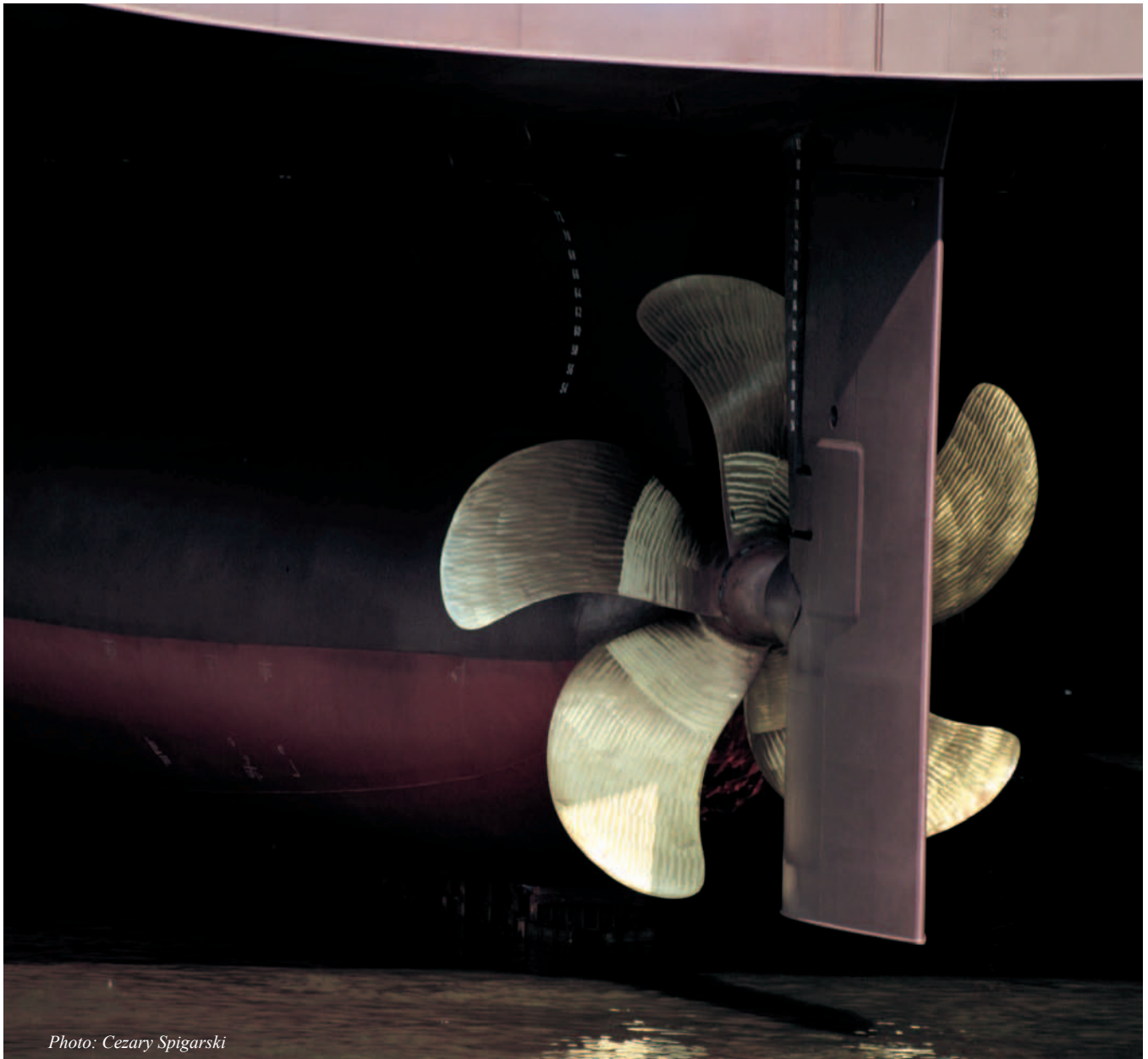


Photo: Cezary Spigarski

Complex approach to selection and evaluation of the fire safety measures to be applied during repair of refrigerated holds

Zygmunt Sychta, Prof.
Szczecin University of Technology

ABSTRACT



This paper presents an analysis of fire hazard during repair work of refrigerated hold with a view of specificity of its equipment and construction, as well as the algorithm of the system of analysis and evaluation of safety measures and their effectiveness. The assessment of effectiveness was based on the applied fire safety measures. Selected actions and technical measures for fire safety must make it possible to prevent fire ignition in hardly accessible spaces behind the boarding of hold walls and in air cooling chambers as unnoticed fire may very fast propagate to the next holds and ship compartments due to flue drafts.

Keywords: refrigerated hold, ship repair work, fire safety

CONSTRUCTION AND EQUIPMENT OF REFRIGERATED HOLDS

Refrigerated vessels constitute a special group of ships. Palettization of cargo has caused major changes in construction of refrigerated vessel holds. A modern refrigerated vessel has the refrigerated holds with vertical walls parallel to ship centreline. Thermal insulation made of mineral or glass wool is placed directly on metal surfaces of hold walls. A water-resistant lacquered plywood or aluminium sheet serves as a timbering of insulation.

Old versions of refrigerated ships or other ships adapted to transport palettized refrigerated cargo have been fitted with

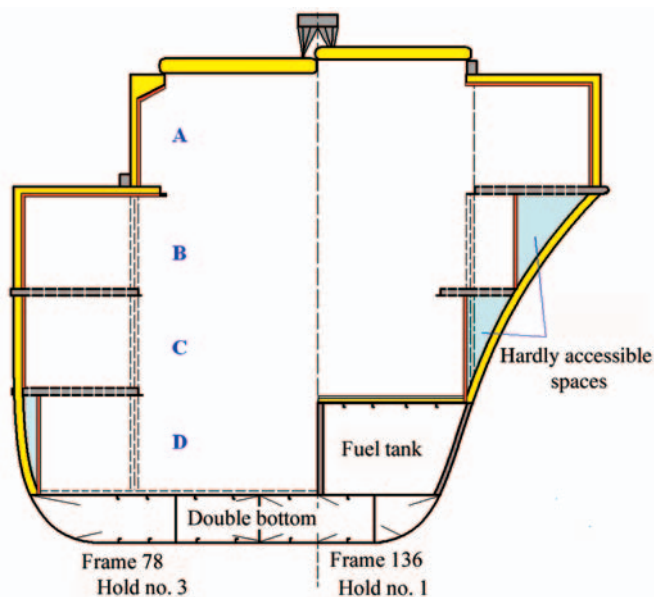


Fig. 1. An example of old version of thermal insulation of refrigerated holds

the different thermal insulation system of refrigerated holds as shown in Fig. 1.

A hard polyurethane foam and mineral wool are the thermal insulation placed directly on steel surface of ship's side structure. The refrigerated hold walls are made of water-resistant lacquered plywood fixed to vertical steel construction. A perforated steel tweendeck construction forms the ceiling of hardly accessible spaces. As a result of that construction hardly accessible spaces made of flammable materials have been created along refrigerated holds. Cross-section area of hardly accessible side spaces varies from 0 to about 2 m² depending on hull curvature of refrigerated vessel. Such spaces located between the holds are separated by steel bulkheads.

A ventilation system ensures an appropriate temperature required for shipped cargo. Forced air circulation in refrigerated holds is initiated by axial fans combined with coolers. They force the air to flow under gratings across the whole width of the hold (Fig. 2). The intake air flows into cargo space through grating holes. Then the air flows back to cold room through ducts placed under hold ceiling.

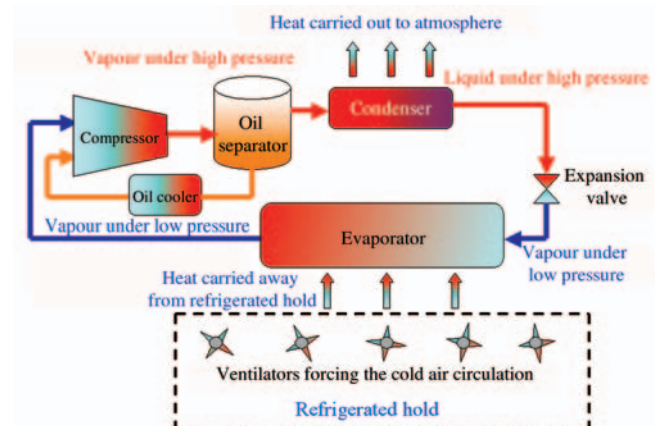


Fig. 2. Schematic diagram of air cooling system

Another function of the refrigerated hold ventilation system is to freshen up the air in refrigerated holds (by applying two air changes per hour [ACH]) that has to limit concentration of the gases released from cargo as to not exceed its maximum permissible level (e.g. for bananas, citrus fruits). The ventilation system also controls air humidity in the hold.

Every refrigerated hold usually consists of four air-cooling units: two of them placed on the hold bottom and the other two - above the tweendeck. Air coolers with direct evaporation of refrigerant are used most often. The coolers together with fans are located in separate rooms whose walls are made of water-resistant lacquered plywood.

A number of air changes (rate) in refrigerated hold depends on type of cargo and it varies between $30 \div 120$ [ACH]. Air circulation rate is adjusted to requirements of shipped cargo by switching on an appropriate number of fans installed in the unit or by switching-on a suitable gear if two-gear fan is used.

The air circulation is used if to dry thermal insulation of the hold in hardly accessible spaces in refrigerated holds is necessary in order to protect the insulation from loss of its insulating features, that may be caused by moisture. A very dry air flowing slowly through ducts of hold insulation, absorbs the moisture which penetrates from hold by diffusion, and then releases it by condensation in the cooler.

Piston, screw and rotary compressors require to be lubricated by liquid oil which decreases friction, carries away heat, seals piston in cylinder and stuffing-box, dampens vibrations and reduces noise. To decrease amount of oil in installation, high-efficiency oil separators located close to the compressor, are applied (Fig. 3). The separated oil re-circulates immediately to crankcase of compressor, that is performed either continuously or periodically depending on type of compressor.

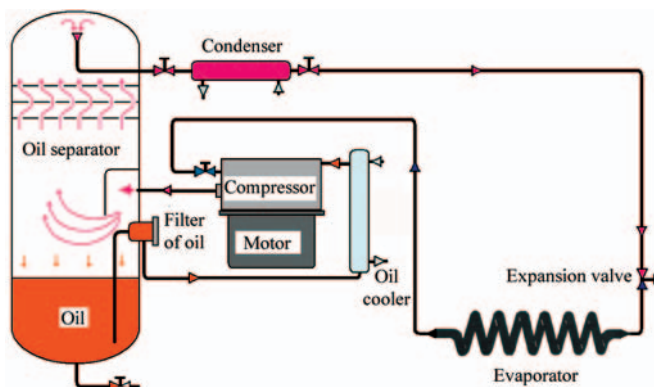


Fig. 3. Schematic diagram of cooling system

3 to 10 % amount of the oil which seeps into the cooling system, brings in additional problems of design and operational character. During operation of cooling device, apart from refrigerant circulation, the oil must flow without obstacles. The following measures must be undertaken to achieve it:

- ☆ all horizontal sections of conduits must be sloped in direction of refrigerant flow
- ☆ diameters of conduits must be appropriately selected so that refrigerant velocity in vertical sections would cause oil convection
- ☆ design of the installation must prevent oil gravitational drift to compressor during its standstill
- ☆ oil filling-up must be possible also during motion
- ☆ design of the installation must prevent oil accumulation during motion and standstill.

Every technical system has an acceptable emergency range of operational parameters within which it is capable of working.

Then it should be possible to perform effective corrections and repairs, and setting of automatic safety systems etc. Loss of control of progress of a hazardous situation occurs when the control and safety systems and repair personnel are not capable of correcting a dangerous trend in values of the parameters that indicate the area of safe operation of an installation or device, that may lead to damage, escalation of accident and release of hazardous substances or amount of energy. Fire, an uncontrolled combustion of materials in time and space, is a frequent effect of loss of control of progress of an emergency situation.

THE COMPLEX APPROACH TO ANALYSIS AND EVALUATION OF EFFECTIVENESS OF APPLIED SAFETY MEASURES

The above presented description of construction and equipment of refrigerated holds reveals major problems of fire safety during operation and repair work. The fire accidents are mainly triggered by frequently underestimated factors which cause dynamic progress of fire. Knowledge of the factors may reduce consequences and financial losses caused by fire accidents.

The process of identification of a level of knowledge of technical requirements, environmental protection and external factors is used to determine purposeful and planned actions which have to contribute in maintaining the high level of fire safety (Fig. 4). The process is controlled by current assessing the results of implementation of the established schedule. The process is characterized by multi-stage character, continuity and dynamics, logic and time sequence, complex approach to tasks and a wide range of performance options.

The basic features of the system are as follows:

- it is a social and technical creative action including scientific and technical elements
- it is a purposeful human organization created by people of various attitudes, motives and education
- it is an open system which means that it has no strict limits and does not care only of itself
- it deals with information of essential importance
- it is built of subsystems, which makes flow and control of information possible
- feedbacks applied in it make its control and optimisation possible
- it is so designed as to achieve targets by using various methods.

Man is an important element of fire safety system. During ship repair, ship's crew is incomplete and a number of people not permanently connected with the ship, e.g. shipyard workers, co-operators, supervisors and others, increases. For this reason the incomplete crew is not capable of controlling the situation on the ship. After working hours many crew members leave their ship and only watch remains on duty. Worth adding that fire accidents occur mostly in the night.

The above presented four-stage system may be iterated repeatedly. A number of iterations depends on frequency and range of changes made in a given technical object and its environment and it also depends on effectiveness of improvement actions. Return to the identification stage is performed after rational assessment of the object's operation. It is not a return to the starting point because the knowledge gained from the preceding identification stage, has been enriched with observations made during the preceding cycle.

Quantification of fire hazard level of a given ship area consists in determining fire progress depending on characteristics of particular elements of the area. It depends especially on

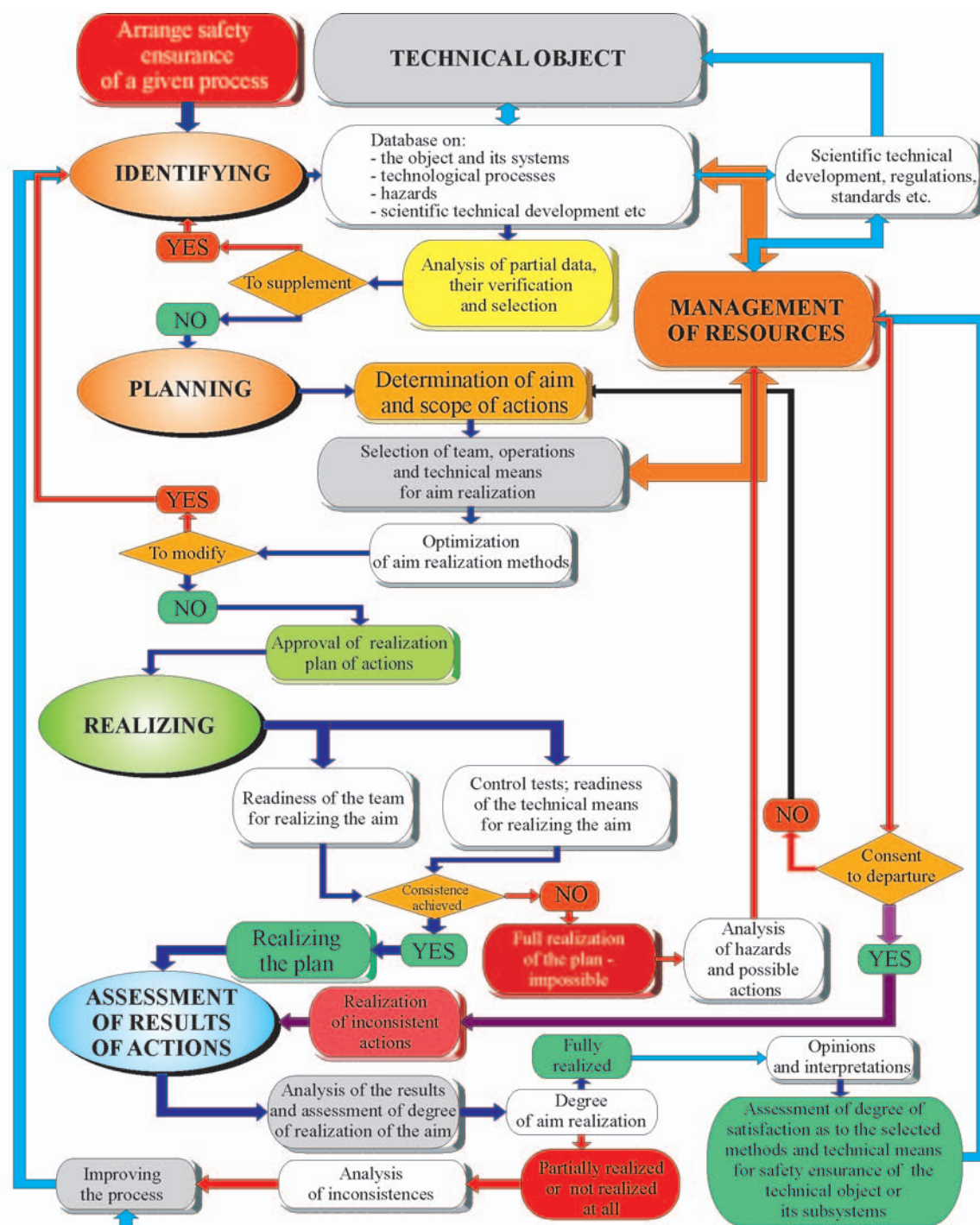


Fig. 4. Algorithm of the system of analysis and evaluation of effectiveness of applied safety measures

controllable features which constitute decisive parameters. Threshold analysis methods are useful to solve problems connected with safety of whole ship or its components. Barriers in safety systems may have control-informative function in the case of unwanted energy outflow, or protective function for technological process or state of technical object prior to occurrence of such outflow. If selection of an effective barrier cannot be made because of technological reasons or excessive costs, an administrative procedure should be elaborated for managing the level of defined and accepted hazard.

Fire progress control is possible in pre-ignition phase [1, 2] if the disposable heat abstraction intensity \dot{q}_{sd} of the endangered area (Fig. 5) is higher than the heat release rate of burning materials and thermal power of external ignition sources:

$$\dot{q}_{sd}(t) \geq \dot{q}_{poz}(t) = \dot{q}(t) + \dot{q}_z(t) - \dot{q}_s(t)$$

where:

- \dot{q}_{poz} - fire power [kW]
- \dot{q} - heat release rate of the process of thermal decomposition and burning the materials embraced by the fire [kW]
- t - time [s]
- \dot{q}_z - thermal power of external ignition sources [kW]
- \dot{q}_s - loss of heat per unit of time [kW].

The fighting with fully spread fire (i.e. rescue actions) is undertaken in a failure stage of an object or its components which is out of control. It indicates that the applied safety systems have not been capable of controlling the progress of the failure stage of the object.

There are many situations which favour fire ignition when a ship is under repair. These are such processes as: the repairing and changing of installations and ship devices, maintenance

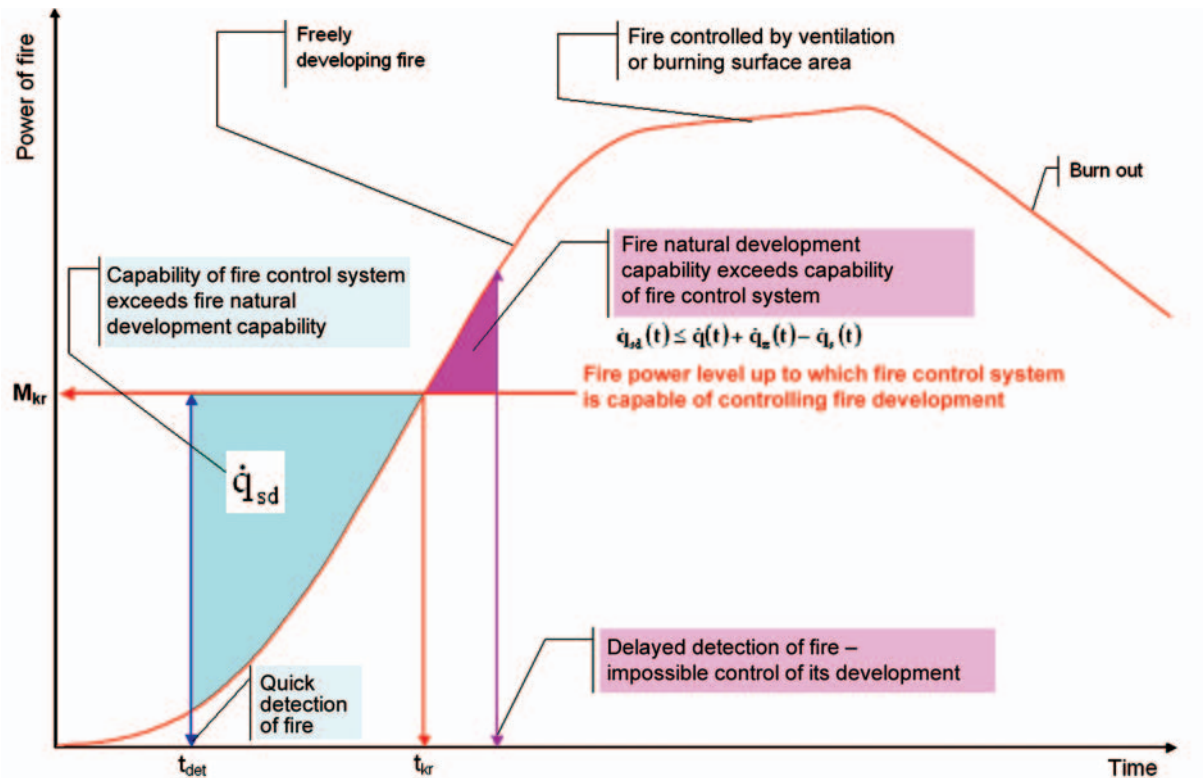


Fig. 5. Schematic diagram of the relation between fire progress and capability of fire control systems

and other operations associated with a potential fire hazard, e.g. welding, metal element gas cutting, metalworking, painting and maintaining work etc. The dismantling of many installations carried out on a ship or its disable state resulting from its stay in shipyard or from performed survey may lead to fire hazard; for example, the abnormal functioning of ship devices may be a reason for some improvisations and provisional starting the substitute devices. During repair work certain necessary flammable materials, such as: paints, wood, insulation materials, stuffing, oils and solvents and other flammable agents for rinsing the mechanisms are usually brought into the ship. When ship is under repair many wastes, garbage, parts of dismantled devices, spilled liquids and dirt are produced. The littering generates fire hazard as it favours starting a fire.

EXAMPLE SELECTION OF ACTIONS AND MEASURES TO ENSURE SAFETY DURING REPAIR WORK

An analysis of all possible fire hazards during ship repair is not included in this study. This part of the study is devoted to presentation of an example selection of actions and measures to ensure safety during repair work (welding) carried out in the bottom oil fuel tank located in the refrigerated hold no. 1 of a refrigerated vessel of old type, shown in Fig. 6.

It is necessary to identify all flows of unwanted energy or mass not only with regard to safety of people and technical object but also regarding operational costs of a given technological process or the whole technical object. Quantitative values of energy and mass flow rates, either known or potential, must be determined experimentally. Then on this basis their limit values must be defined, and devices intended for preventing the outflow and a system for minimizing the effects of unwanted energy outflow, have to be selected.

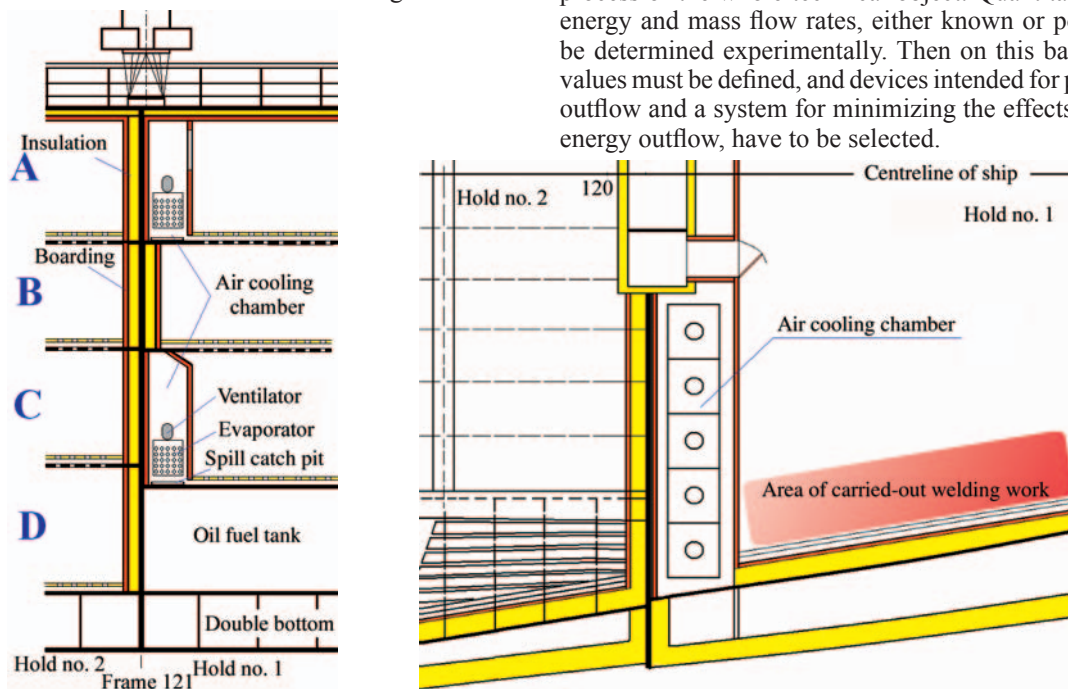


Fig. 6. Location of welding work carried out in oil fuel tank of the example refrigerated ship

The welding work carried out on the bottom of the hold no. 1 generates serious fire hazard. The temperature of oxyacetylene torch flame exceeds 1500°C. It is an essential possible cause of fire accident. Heating the burning metal, spread of metal particles dropping off the cutting gap, and dripping drops of fused metal are a potential source of ignition of flammable materials. Metal particles are also blown in direction of operating flame due to high pressure of gas at the torch outlet. All the things generate fire hazard for (Fig. 6.):

- ⇒ the starboard hold wall, made of flammable lacquered plywood
- ⇒ the polyurethane thermal insulation placed behind the hold wall
- ⇒ the air ventilation and cooling chamber.

The system in question is characterized by such advantages as completeness, objectivity and selectiveness [1, 2]. On the basis of ship technical specification a graphical network of connections between causes and effects is created at all connection levels. For each possible pair of the network nodes

(Fig. 7) a hazard level analysis is conducted with regard to effectiveness of the applied measures for passive and active fire protection.

Fire hazard to the boarding and thermal insulation of the hold no. 1 and 2 is introduced by fire characteristics of lacquered water-resistant hard plywood, hard polyurethane foam and inflammable mineral wool of low value of permissible temperature for its application. It is also caused by specific construction of hardly accessible spaces (Fig. 1 and 8) resulting from the adjustment of refrigerated holds to shipping the palletised cargo.

The cross-section area of hardly accessible spaces varies between 0 ÷ 2 m² depending on hull curvature of refrigerated vessel. Such spaces located between holds are separated by steel bulkheads. That is why the fire can be transferred from one hold to another by heat conduction. Moreover the air circulation is used to dry the thermal insulation in hardly accessible spaces in order to prevent a decrease of its insulation features. It means that the set of hardly accessible spaces connected with the air ventilation system of the holds favours fire progress on the ship (due to developed flue draft).

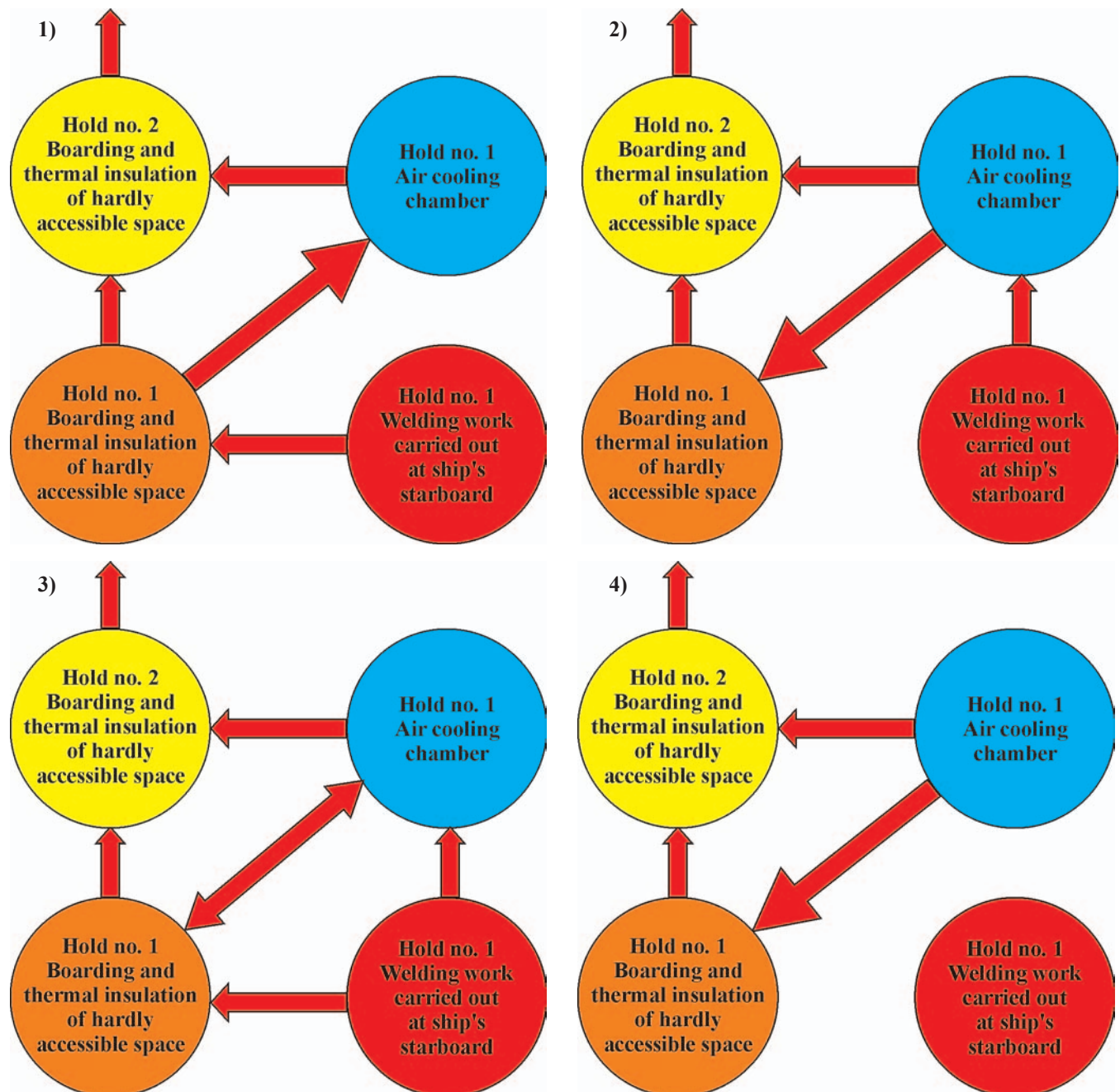


Fig. 7. Probable variants of fire progress

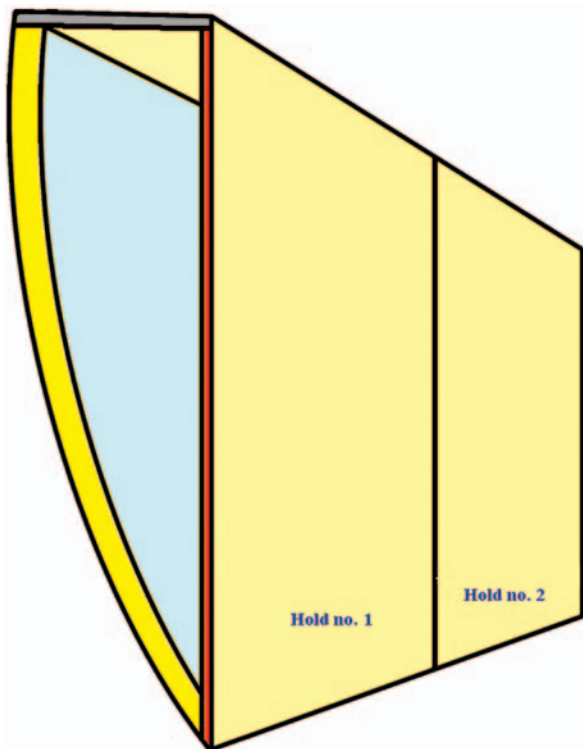


Fig. 8. Schematic cross-section of hardly accessible side spaces

FIRE CHARACTERISTICS OF TYPICAL MATERIALS WHICH CAN CONTRIBUTE TO FIRE PROGRESS

The determining of fire characteristics of typical materials which can contribute to fire progress in its initial, pre-ignition phase is an important element in predicting the fire progress.

Tests on fire characteristics of thermal insulation and boarding materials was carried out with the use of the methods complying with the International Code for Application of Fire Test Procedures (IMO FTP Code) [3] and ISO standards. Various materials applied to refrigerated vessel were tested. Out of all measured parameters and their derivatives, only the parameters which influence hard polyurethane foam behaviour in the initial phase of fire progress in the refrigerated hold, are presented in this study. They represent first of all influence of the conditions for thermal decomposition and combustion of hard polyurethane foam on heat release intensity, oxygen demand, smoke emission intensity and mass emission of oxygen and carbon dioxide.

The test results revealed that only the mineral wool can be deemed fully inflammable (Tab. 1).

Tab. 1. Test results of mineral wool fire characteristics according to the method given in Part 1 of IMO FTP Code [3]

Duration of sustained flaming	0.00	s
Rise of furnace temperature above the final furnace temperature	6	°C
Surface temperature above the final furnace temperature	5	°C
Rise of temperature in the centre of the specimen	2	°C
Loss of weight of specimen	7.98	%

The disadvantage of mineral wool used for thermal insulation is its low limiting temperature for use as the mineral wool melts in the temperature of 750 °C creating glassy mass of

a small volume. When shrinking it creates a free space behind the boarding, that favours development of flue drafts and gas exchange in the space (Fig. 9). This feature may contribute to fast fire progress in the space behind the shoring.



Fig. 9. The view of mineral wool sample before and after the fire tests

According to [3] the laminated plywood and hard polyurethane foam are flammable materials hence flames propagate fast on their surface (Tab. 2 and 3).

Tab. 2. Test results on surface flammability rate of lacquered water-resistant plywood of 20 mm in thickness, according to the method given in Part 5 of IMO FTP Code [3]

Critical flux at extinguishment	12.74	kW/m ²
Heat for sustained burning	1.50	MJ/m ²
Peak heat release rate	4.20	kW
Total heat release	4.88	MJ
Fall of heavy drops	it does not occur	

Tab. 3. Test results on surface flammability rate of hard polyurethane foam according to the method given in Part 5 of IMO FTP Code [3]

Critical flux at extinguishment	3.65	kW/m ²
Heat for sustained burning	0.20	MJ/m ²
Peak heat release rate	5.44	kW
Total heat release	1.08	MJ
Fall of heavy drops	it does not occur	

Besides, the tests showed that boarding made of lacquered water-resistant plywood, due to its thermal potential and the average constant heat release intensity of 50 kW/m², will intensify fire progress from thermal insulation.

The value of heat of combustion of the hard polyurethane foam, determined according to the method of ISO 1716, amounts to 26.80 MJ/kg.

The hard polyurethane foam is an intensively smoke emitting material (Tab. 4) according to the requirements of Part 2, IMO FTP Code [3]. During thermal decomposition of the polyurethane foam an intensive smoke emission appears first, then its flame combustion occurs (Fig. 10). It means that the flameless intensive smoke emission is a symptom of fire.

Tab. 4. Test results on smoke-producing rate of hard polyurethane foam, according to the method given in Vol. 2 of IMO FTP Code [3]

Time of sample ignition	1.10	s
Maximum optical specific density	590.70	-
Maximum speed of changes of optical specific density	21.99	1/s

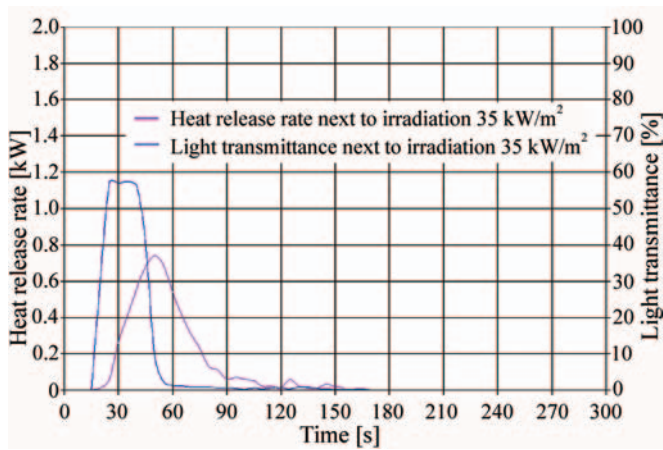


Fig. 10. Relationship between heat release intensity during thermal decomposition and combustion of hard polyurethane foam and transmittance of light passing through the layer of combustion products and time, recorded during the tests carried out according to the ISO 5660-1 method, at 35 kW/m² heat flux intensity on sample surface

Sparks formed during welding belong to the group of low-power ignition sources. For this reason, tests on ignitability were performed according to the method of PN-EN ISO 11925-2. Hard polyurethane foam lit in vertical position first ignites and then the burning dies down spontaneously after several tens of seconds. Besides, hard polyurethane foam is not characterized by progressive incandescence. It means that the foam applied to the insulation system of refrigerated hold, if ignited by welding spark or gas torch flame, will not transfer fire behind the boarding. It does not show the drop fall-off which is typical for plastics. Tests on surface flammability rate prove occurrence of this feature (Tab. 3). The value of the heat flux critical for the tested foam amounts to 3.65 kW/m². The critical heat flux is a measure of ignition source thermal power necessary for starting self-sustaining process of combustion of the material. Such behaviour results from a specific chemical structure of this group of plastics. Polyurethanes are polymers which are formed in the process of poly-addition of poly-functional organic isocyanates (two- and higher functional) with two- or higher functional compounds containing hydroxyl groups connected with aliphatic carbon atoms (glycols and polyols). Polyesters (prepared from adipic acid and ethylene, methylene, propylene glycol and also polyhydric alcohols) or poly-ethers (there are usually additive connections of propylene oxide with polyhydric alcohols); also, ricinus oil

and its derivatives are often used. Hydrogen chloride content in products of thermal decomposition and combustion (Tab. 5) points to halohydrocarbon frothing agent.

On the basis of the presented test results of fire characteristics of the following system of materials: metal plate, hard polyurethane foam, laminated plywood, it was stated that the fire is unlikely to be transferred behind the boarding. However, occurrence of combustion of the boarding due to external flame is always possible.

Fire hazard to the ventilation air cooling block is mainly produced by:

- the flammable boarding made of lacquered water-resistant hard plywood, used for the partitions of the air cooling chamber
- the fact that the chamber is a hardly accessible space
- the flammable tarry and dusty contamination of the chamber's internal surfaces, which always occurs during operation of the ventilation systems; in air cooling systems such contaminations settle in lower part of the compartment
- the oil contamination of the air cooling chamber's internal surfaces (Fig. 11 and 12), which may be formed when an unsealing of the cooling installation occurs (up to 10% of oil is contained in circulating refrigerant); a water content in oil accelerates oil deterioration and other negative effects including acid formation, which leads to corrosion of metals
- short-circuit in the electrical system may create an ignition source for flammable materials.

Summing up, probability of fire accident in the analyzed air cooling chamber is very high. Fire ignition sources may be produced by the heat metal particles created during cutting, blown into a cooling ventilation blowing gap in the direction of gas torch flame as a result of high gas pressure at its outlet, or a short-circuit in the electrical system. The fire initiated in the cooling chamber may progress invisibly for a long time because, when the hold ventilation is switched off during ship repair, the air will enter the air cooling chamber through a blowing gap at the floor, and fire products will propagate along ventilation ducts of the system, including air freshening ones installed in the hold. Smoke produced during cutting with the use of oxyacetylene torch will favour this process. Such fire will be revealed in its ignition phase or when the next of hardly accessible spaces will be under fire. Fire will appear always in a certain distance from its source. It may cause extinguishing

Tab. 5. Test results on mass emission of toxic products of thermal decomposition and combustion of hard polyurethane foam according to the method of PN-B-02855 standard

Decomposition temperature		Specific emission of toxic products					
		CO	CO ₂	HCN	NO ₂	HCl	SO ₂
		[mg/g]	[mg/g]	[mg/g]	[mg/g]	[mg/g]	[mg/g]
450°C	Specimen no 1	14.06	41.74	0.23	0.01	1.09	0.00
	Specimen no 2	22.92	54.84	0.31	0.01	2.04	0.00
	Specimen no 3	22.92	54.84	0.27	0.01	1.55	0.00
	Average	18.49	48.29	0.27	0.01	1.56	0.00
550°C	Specimen no 1	153.39	284.41	6.06	0.01	29.73	0.00
	Specimen no 2	169.53	326.97	6.11	0.01	31.09	0.00
	Specimen no 3	169.53	326.97	6.03	0.01	30.25	0.00
	Average	161.46	305.69	6.08	0.01	30.41	0.00
750°C	Specimen no 1	41.41	1097.95	1.71	0.03	4.17	0.00
	Specimen no 2	83.59	1057.85	1.43	0.02	9.54	0.00
	Specimen no 3	83.59	1057.85	1.60	0.02	6.54	0.00
	Average	62.50	1077.90	1.57	0.02	6.86	0.00

measures to be directed to an area where only fire products are revealed.



Fig. 11. Oil contamination visible on the walls of cooling chamber



Fig. 12. Open ducts of air cooling system (the view after fire accident)

During this time the heated metal bulkhead which divides the holds, will transfer the fire to the next hold as a result of heat conduction.

The presented hazard identification with regard to the specificity of the construction and equipment of the hold of the refrigerated vessel of old type, during the repair carried out in oil fuel tank in the hold no. 1, indicates that selection of fire safety actions and technical measures should be so performed as to prevent fire to ignite in hardly accessible spaces behind the boarding of hold walls and in air cooling chambers because, due to flue drafts, the fire may very fast propagate to the next holds and compartments of the ship.

Fire in air cooling chambers is very dangerous due to its possible dynamics. Contamination and oiling-up internal surfaces of the boarding of such spaces accelerate fire propagation over the surfaces, increasing this way its power.

THE APPLIED FIRE SAFETY MEASURES AND FINAL REMARKS

The measures selected to reach the optimum solution of the example fire safety problems associated with the repairing of oil fuel tank in the refrigerated hold no. 1 of the ship in question, are as follows :

- ❖ the detailed knowledge of the ship's technical documentation with special regard to specificity of construction and equipment of the area where maintenance and repair work are planned to be carried out
- ❖ the opening of the hardly accessible spaces by removing all the boarding of the hold walls in the area of the planned welding work
- ❖ the cleansing of the exposed internal surfaces of the air cooling chamber off the contaminations
- ❖ the making of inspection holes to monitor adjacent hardly accessible spaces over all the height of the hold because the ship's technical documentation may not include all existing air flow ducts
- ❖ the hazard level evaluation
- ❖ the selecting of a team, operating actions and technical measures, to perform the task
- ❖ the continuous monitoring of neighbouring hardly accessible spaces during repair work, on all height levels of the hold under repair and the neighbouring holds
- ❖ the usage of local extinguishing equipment to extinguish possible local ignitions of residues of flammable materials in the repair work area and hardly accessible spaces.

Internal fire extinguishing requires special techniques. Extinguishing activities must slow down the process of thermal decomposition and combustion of flammable materials by limiting oxygen inflow and by heat abstraction. Insulation features of the boarding made of lacquered water-resistant (non-absorbable) plywood make the internal fire extinguishing low efficient when using water stream directed to the external surface of this boarding. The extinguishing agent must be put inside these spaces. It requires to prepare an appropriate number of holes to make control of hardly accessible spaces possible before beginning the repair work and in case of fire; extinguishing measures such as, for example, a fire-extinguishing foam which limits fire propagation, must be used

Slowing down the fire progress in pre-ignition phase results from the applied barriers hence their properties should be so selected as to comply with object's operational conditions. The barriers are: passive or active screens, extinguishing systems, fire-resistant features of materials and construction, systems for control of dynamics of fire progress and propagation of its products, procedural and administrative requirements, etc.

A traditional approach to fire safety, which consists in removing the boarding and thermal insulation only from the area of immediate spread range of welding sparks, has turned out to be inefficient fire protection of repair work, in practice. The presented example fire accident on the refrigerated vessel during repair covered three holds out of four, causing significant financial losses.

The quantitative evaluation of fire hazard level is the basic measure of the policy of ship fire safety. This measure, instead of "curing" the fire damage effects, is focused on the complex approach to ship fire safety and on the preventing of possible negative effects of fire hazards. Therefore, to properly select such measures the possibly comprehensive description of ship environment, its complexity and the prediction of its changes resulting from fire hazard effects, is necessary.

Basic tasks of fire safety engineering of technical objects include:

- ☆ prediction of possible fire hazards and limiting them at the planning stage of object operation
- ☆ selection of appropriate fire safety systems and technical devices, and their technical and operational parameters, as well as the principles for operational procedures which ensure safety for operators of such objects and their systems, and minimize possible hazard to the environment.

BIBLIOGRAPHY

1. Sychta Z.: *The slowing down of the process of thermal decomposition and combustion of materials – the basic condition for fire safety of technical objects* (in Polish). Szczecin University of Technology, Prace naukowe (Scientific reports), No.570, 2002
2. *Quantification problems of fire-safety level of marine object*. Polish Academy of Sciences, Branch in Gdańsk Marine Technology Transactions. Vol.16, 2005
3. *International Code for Application of Fire Test Procedures*. International Maritime Organization. London 1998

CONTACT WITH THE AUTHORS

Zygmunt Sychta, Prof.
Faculty of Marine Technology,
Szczecin University of Technology
Al. Piastów 41
71-065 Szczecin, POLAND
e-mail : zygmunt.sychta@ps.pl

Removal of oxidable contaminations contained in submarine atmosphere

Ryszard Kłos, Assoc. Prof.
Polish Naval Academy



To remove flammable contaminations from submarine atmosphere, devices for their oxidation and chemical absorption of products resulting from the chemical reaction¹, can be applied. In this paper a catalytic system designed for hydrogen and carbon monoxide oxidation and its tests are presented.

ABSTRACT

Keywords: breathing atmosphere contaminations, submarine, catalytic reaction

KINDS AND SOURCES OF SUBMARINE ATMOSPHERE CONTAMINATIONS

Contamination of breathing medium due to components which generate toxic action to the human body is always undesirable. The contaminations of the air in an ecologically closed atmosphere can be split into three groups: those coming from the air itself, those coming from technical means being in contact with breathing medium², and those emitted by the human body.

Typical air contaminations are the following: carbon dioxide, hydrocarbons, carbon oxide etc. The contaminations emitted by the human body are similar as to their kind but of a much greater amount as a rule. For the designing purposes of life preservation systems in habitats, mean values of contaminations emitted by the human body are determined [1]. The ship classification societies provide typical kinds of contaminations coming from technical means and their maximum permissible concentrations [1]. The data concerning safe concentration values of the contaminations in submarine breathing atmosphere can be found also in military manuals and standards, e.g. [2]. On board submarine, apart from those hazardous for human health, also other contaminations which create fire hazard such as hydrogen released as a result of electric battery gassing, can be found.

HYDROGEN OXIDATION PROCESS

A prototype device for hydrogen catalytic burning was comprised of a metal reactor filled with a catalyst. For the tests was applied the catalyst in the form of 0.5%_m platinum placed

on alumina bars of 3 mm diameter, made by Johnson Matthey Ltd. When operating, the reactor with all its content was heated from outside with the use of a heating tape and simultaneously cooled³ from inside with water, through a membrane, Fig. 1a and b. The reactor's prototype was fitted with a set of measuring instruments intended for the monitoring of pressure, flow rate and temperature, as well as an analyzer for the measuring of hydrogen content in after-reaction mixture⁴. In Fig. 2 an overall view of the reactor placed on the test stand is presented.

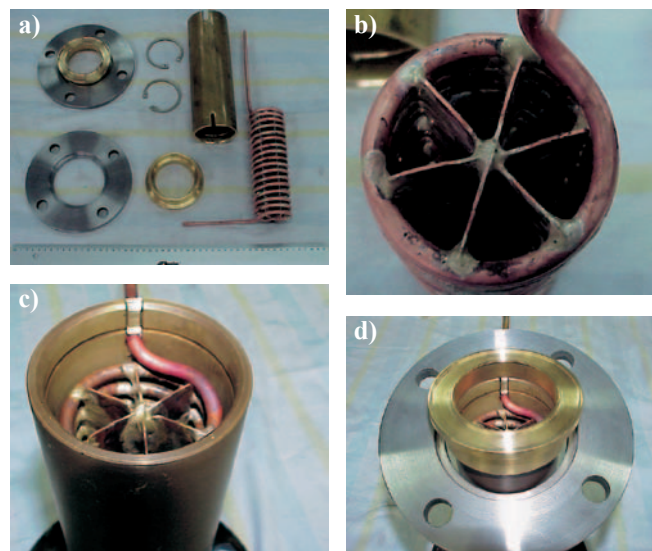


Fig. 1. Elements of the hydrogen combusting device: **a)** elements of the reactor; **b)** ribbing of the cooler; **c)** way of assembling the attachment; **d)** the ready-to-use attachment

¹ combustion products are usually water vapour and carbon dioxide

²e.g. volatile components of paints, thermal insulation materials, maintenance means, etc.

³if necessary

⁴after leaving the reactor

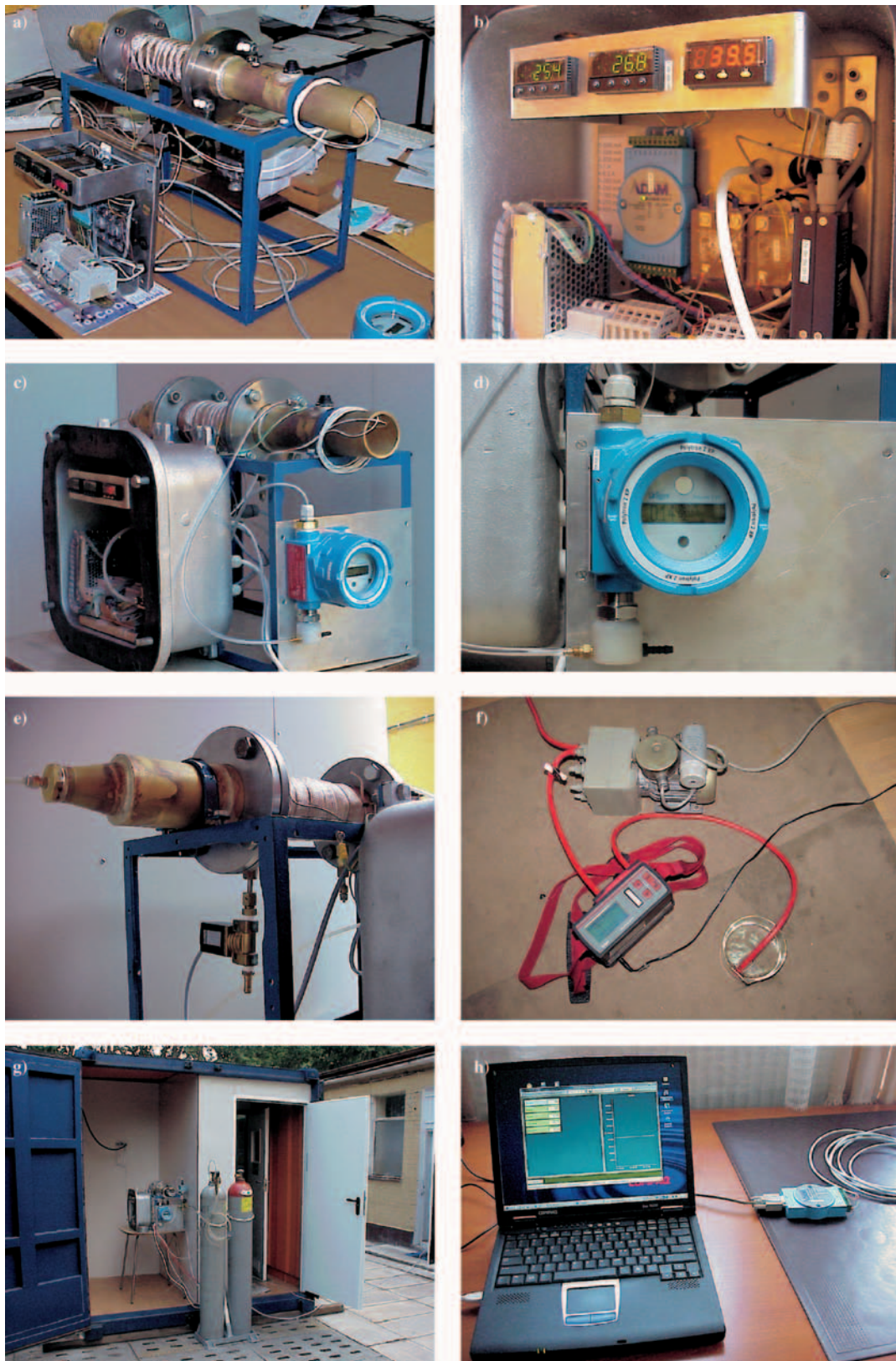


Fig. 2. The test stand and reactor's instrumentation: a) reactor and control panel; b) control panel; c) testing system; d) POLYTRON 2XP analyzer; e) inlet of gas for reaction; f) suction pump and MULTIWARN multi-channel analyzer; g) test stand; h) recording system for test results

THE TESTS

To the hydrogen content measuring the Polytron 2XP analyzer of the Dräger firm⁵ was used, Fig. 2d. Its gauge was connected with the input terminal of the ADAM4517 A/C converter of the ADVANTECH firm, Fig. 2b, then through the RS485/RS232 converter – with the computer, Fig. 2h. This way

the recording of measurement results with the use of a special software was made possible.

The measuring and control of heating tape temperature was performed by means of the i3253 NEWPORT module, Fig. 2b. Temperature inside the reactor was also measured by means of two additional i3253 NEWPORT modules⁶. To the tests was applied 2%_v hydrogen mixture in synthetic air, whose

flow was maintained at the rate of about $40 \text{ dm}^3 \cdot \text{min}^{-1}$. Before starting the tests the reactor was heated up to about 100°C . The rise of temperature inside the reactor above 150°C triggered the tap water membrane cooling to start. The mixture - after passing through the reactor⁷ - was directed to the Polytron 2XP hydrogen content analyzer, Fig. 2d. Hydrogen content values were read in 30 s intervals, and the total duration time of the experiment did not exceed 2h. The reactor test results for different temperature values kept on the heating jacket are presented in Fig. 3. The hydrogen content never exceeded the value of $0.2\%_v$, that complied with the requirements for the submarine of KILO class.

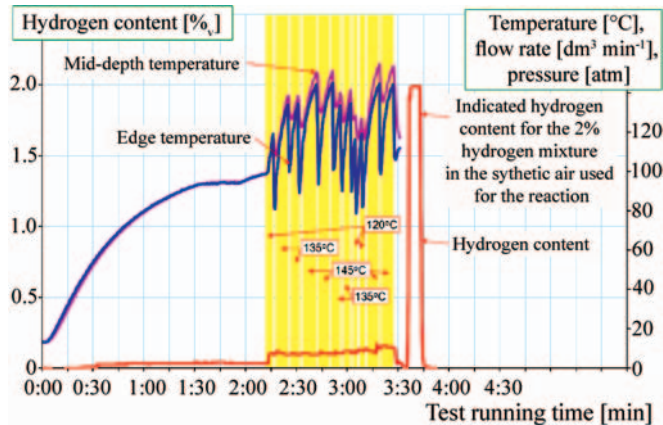


Fig. 3. Results of the hydrogen content measurements at the outlet from the reactor

THE CO OXIDATION REACTOR

The prototype of the device for CO catalytic oxidation is the same as that before described, however in this case its working temperature is different. Its tests were carried out in the same way as before with the exception of the reaction gas which was now $1.8\%_v$ CO mixture in the synthetic air. The tests showed that in this case a much higher temperature is necessary to carry out the reaction with a suitable effectiveness. For the measuring of CO content in the after-reaction mixture one of the channels of the MULTIWARN analyzer⁸, was used, Fig. 2f. From the test results shown in Fig. 4 it can be stated that the CO after-burning process down to the CO content of $0.02\%_v$ is possible.

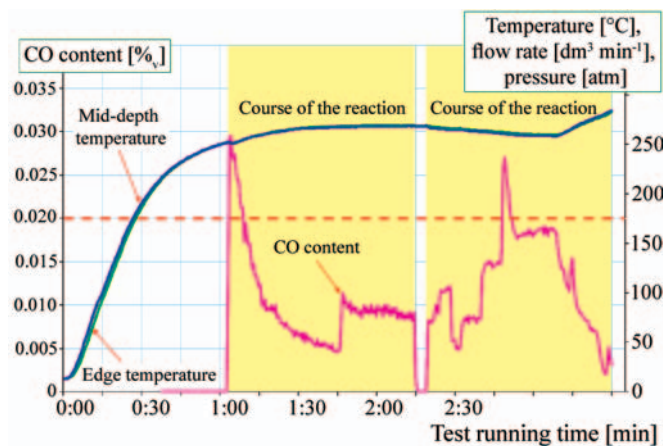


Fig. 4. Results of the measurements of temperature and CO content at the inlet from the reactor

Good correlation between the CO content in the after-reaction mixture and the reaction temperature was observed. On this basis it was concluded that the temperature should be maintained on the level of about 300°C , Fig. 5.

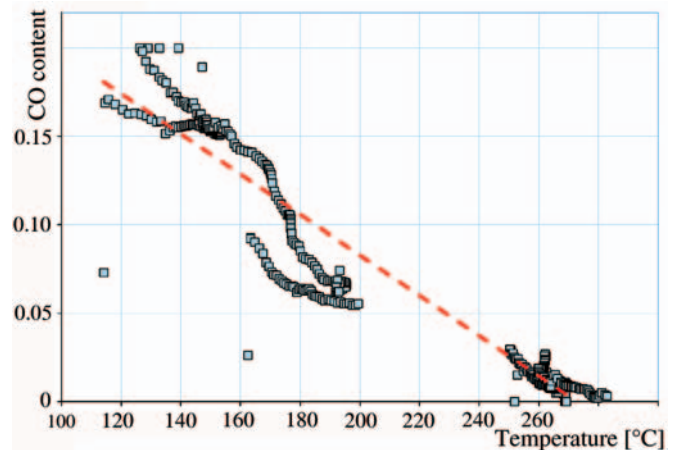


Fig. 5. The relation between carbon oxide concentration in after-reaction mixture and reaction temperature

And, the effectiveness tests of oxidation process of hydrocarbon vapours was also performed. From the tests it results that working conditions of such reactor should be similar to those for carbon oxide oxidation.

CONCLUSIONS

The elaborated prototype device meets the requirements put for the similar hydrogen after-burning device installed on board the submarine of KILO class. However the novel device is 50 times smaller than that compared and is additionally capable of burning carbon oxide and hydrogen vapours.

Additional note

This project has been financially supported by The Polish Ministry of National Defence (MON), (Contract No. 20/DPZ/3/OTM/S/WR/MON/2002/706)

BIBLIOGRAPHY

1. Kłos R.: *Diving devices fitted with breathing mixture regeneration* (in Polish), Publ. by KOOPgraf, Poznań 2000
2. *Руководство по борьбе за живую часть подводной лодки РБЖ-П/Л-82* (in Russian): Военное Издательство (Military Publishing House), Moscow 1983
3. STANAG 1301: *Minimum conditions for survival in a distressed submarine prior to escape or rescue*. NATO Standardization Agency, Brussels 2003

CONTACT WITH THE AUTHOR

Ryszard Kłos, Assoc. Prof.
Department of Diving Technology
and Underwater Activities
Polish Naval Academy
Śmidowicza 69
81-103 Gdynia POLAND
e-mail: skrzyn@wp.pl

⁵ of the measurement range: $0 \div 4\%_v \text{H}_2$, and the declared maximum relative measurement error: $\pm 5\%$

⁶ and the module for measuring the reactor's inside temperature controlled also the electromagnetic valve of water cooling system

⁷ in which the hydrogen after-burning process was performed

⁸ of the measurement range of $0 \div 200 \text{ ppm CO}$, and the declared maximum relative measurement error of $\pm 1\%$

Simulation method for determination of human reliability function taking stress into consideration

Mieczysław Hann, Prof.
Szczecin University of Technology

ABSTRACT



Application of computer simulation method for determination of the reliability function of a human being treated as an element of the system was presented in the paper. A method of considering the influence of the incidental random events occurring in the technical system or surroundings on committing faults by a human in the condition of stress was discussed. Computer code and examples of the results were also presented.

Keywords: human factor, reliability, computer simulation

INTRODUCTION

Macrosystem human-being – technology – marine environment is considered in the analysis of reliability and safety seeking the probability of appearance of a damage eventually followed by the accident.

Groups of functions performed by human can be distinguished in operations of machinery and marine systems similarly to the other branches of technology. Typically, the groups are:

- ☆ crew (seaman, steersman, carpenter etc.)
- ☆ supervisors (captain, officer, boatswain, inspector, insurance agent, owner)
- ☆ operator (of crane, decompression system, drilling system etc.)
- ☆ worker (diver, borer, assembler, underwater welder etc.).

Features of a human as an element of the macrosystem are difficult to define due to individual differences and complex external influences. The problem is addressed to e.g. in [3, 9, 14, 15, 17].

In the present paper an attempt is made to estimate analytically the influence of the technical system and marine environment on the human reliability in the aspect of the stress arising in the conditions of threat being the result of random events occurring in the technological system and environment.

In the human reliability analysis it is necessary to treat the surroundings of the object and cooperating teams in the way similar to treating the object. Sea-wave or abyssal stream and an operator or diver are also elements of the system, they are only subjected to different rules.

Features of a human-being as an element of the macrosystem are particularly difficult to define. The problem is addressed to in [1, 2, 3, 7, 8, 9, 11–14, 15, 17]. Attempts to define the human organism as a system are known [4] as well as attempts to describe the influence of the psychical condition [10], or health condition and training on efficiency of acting in the macrosystem. However, they do not provide a well-justified description of the reliability as an element of the analysed macrosystem.

A proposition of description of the human reliability is presented hereafter which leads to the real results of the analyses confirming the well-known truth that a man is often the weakest link of the macrosystem. The proposition is derived from the earlier works [5, 6]. A reason for commencing the investigation is resignation from treating a human as an element of the macrosystem which is often encountered approach. This can be explained by the lack of a method coherent with the methods of the analyses of the systems.

Human faults can be divided into three groups:

- A. Faults made independent of action of the technical system and surroundings. Such faults occur when the system acts correctly and no threats from the surroundings exist. Probability of occurrence of these faults depends on factors such as education or training, age, health condition, fatigue and exhaustion and similar factors dependant on the performed task.
- B. Faults dependant on the action of the technical system and threats emitted by surrounding. They arise in the result of stress caused by damages initiating events and impacts of surroundings dangerous for a man.
- C. Technical devices are operated in time T_c (Fig.1), relatively long comparing to time T_c suitable for analysis of human

faults. Time T_e is typically a few to several years while time T_c can be a few hours (e.g. time of a one shift, watch, flight etc.). A method of determination of the function defining human reliability $R_{HE}(t)$ in the scale of operational time T_e is given below. The method is based on the simulation of probability R_c of not committing a fault by the human in each time interval T_c after random time t_1 . Simulation analysis is performed in the area of systematic and incidental faults taking into consideration the influence of stress caused by undesirable events in the analysed macrosystem.

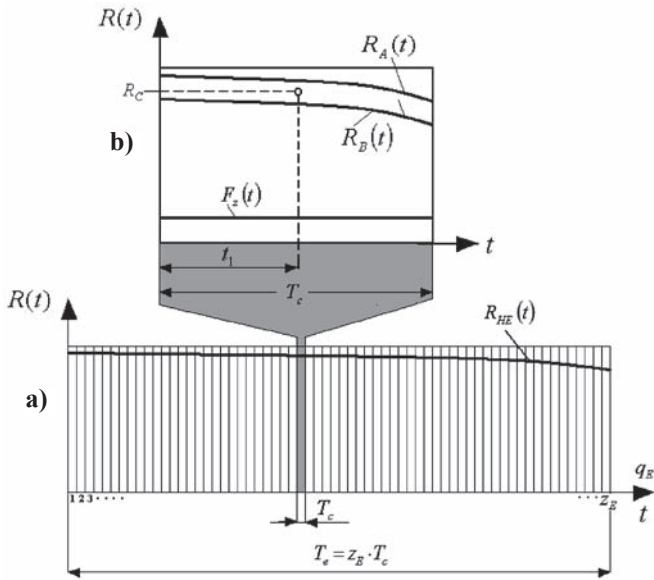


Fig. 1. Principle of analysis of human reliability a) scale of time T_e of operating technical system and fault analysis T_c b) area of incidental faults

Let us assume that probability of occurrence of the faults belonging to group A is given by the distribution function based on corresponding histogram. Cumulative distribution function allows to define reliability function $R_A(t)$ which yields the probability that a human fault will not occur in the period to required time. The function will be called **efficiency function**. By assumption, the probability density function of distribution of the faults can be truncated in zero, so the initial value of the cumulative distribution function $F_A(0) > 0$ and efficiency function $R_A(0) < 1$. It is the effect of occurrence of group A faults already in the beginning of the period of the shift.

The question arises how to determine analogical function $R_B(t)$ taking into consideration group B faults. Reaction of a man to stress depends on his individual features. People reacting to stress violently commit more faults qualified to group B. An area can thus be identified where incidental faults due to stress are located. A reason of stress is to be a random event occurring in the technical system or surroundings. It is illustrated by the event tree in Fig. 2 where intermediate events Z are indicated being the reason of human stress whose fault is one of initiating events IE denoted by $C1$.

Random distributions of the initiating events presented e.g. in the forms of reliability functions $R_{IE}(t)$ of the system elements where the events occur are known. It is thus possible to determine probability density function $f_z(t)$ of events Z influencing the human stress (Fig.2). Selected initiating events defined by function can also be considered as such events. Function $f_z(t)$ can be determined using a computational method – in the case when simple functors are present in the tree or a computer simulation method – in the case when conditions are present in the system prohibiting application of the Boolean algebra. [1]. Functions $f_z(t)$ and cumulative

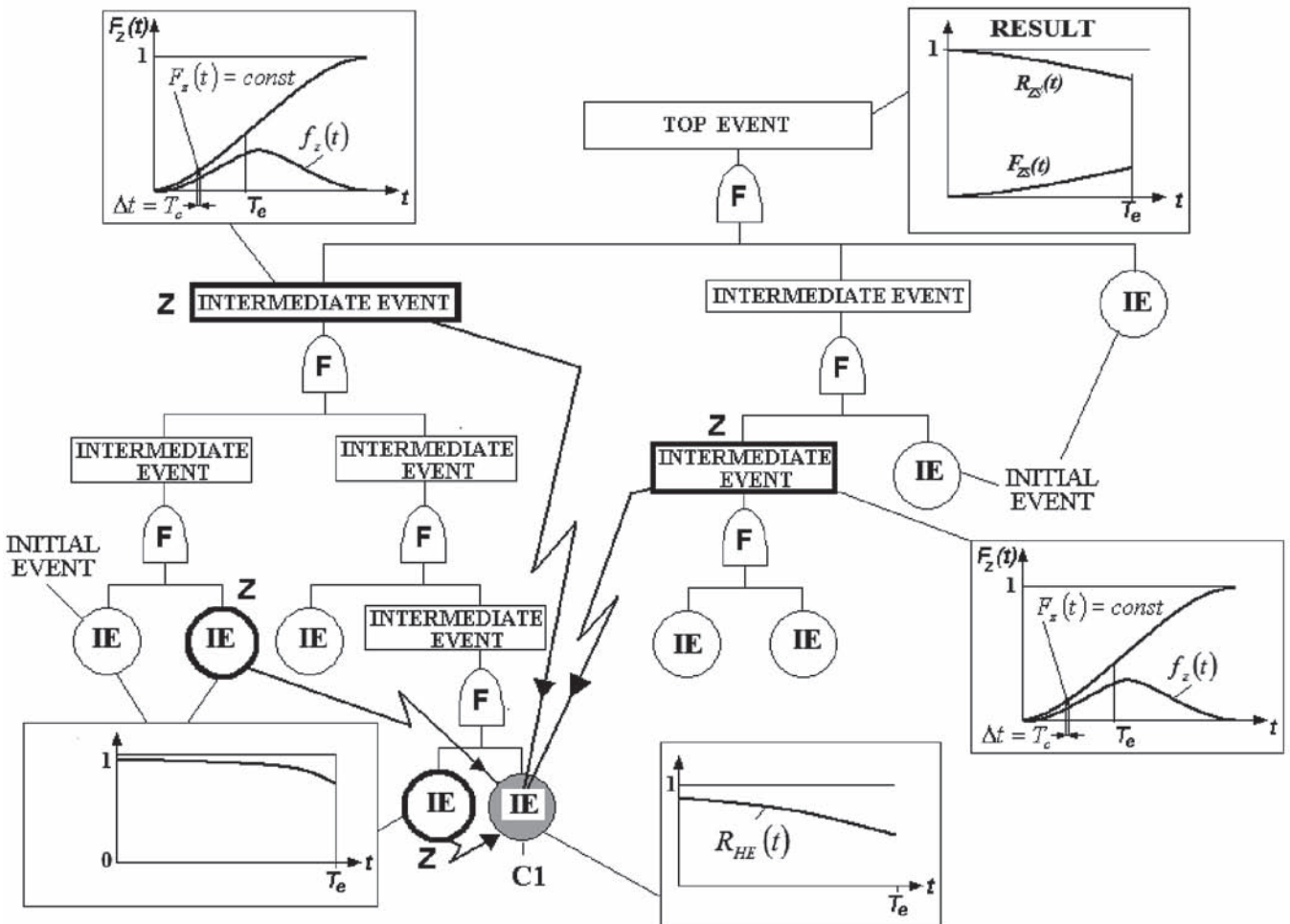


Fig. 2. Principle of action of events generating stress. IE – initiating events, F – logical functors, C1 – human fault due to stress, Z – events generating stress

distribution function $f_z(t)$ are determined in operational time T_c . Probability of occurrence of an event generating stress in given time interval Δt is:

$$p_z(t) = f_z(t) \cdot \Delta t \quad (1)$$

Since time T_c of one shift is negligibly small comparing to operational time T_c , it can be assumed $\Delta t = T_c$ what means that the probability of occurrence of an event generating stress in the period of one shift given by:

$$p_z(t_1) = f_z(t) \cdot T_c \quad (2)$$

is constant.

For the purpose of the computer analysis it means that the time increment should be taken not greater than time T_c . Since $T_c \ll T_c$ it can be assumed that:

$$p_z(t_1) = p_z = \text{const for } 0 < t_1 \leq T_c \quad (3)$$

Value of the cumulative distribution function for period $0 \div T_c$ is also constant:

$$F_z(t_1) = \text{const} \quad (4)$$

Assuming that the event generating stress implies fault due to stress, what corresponds to the absolute stress flexibility, can be given by **limit function of stress** $R_B(t)$. Single event from group A or B is enough to cause occurrence of a human error. The function is thus given by:

$$R_B(t) = 1 - R_A(t) \cdot [1 - F_z(t)] \quad (5)$$

If there is more than one incidental event generating stress the probability range of making fault due to stress increases. If we assume that for occurrence of stress one of the selected events is satisfactory, the limit stress function is written in the following form:

$$R_B(t) = 1 - R_A(t) \cdot \prod_{i=1}^k [1 - F_{z_{ii}}(t)] \quad (6)$$

where:

k – number of events generating stress.

Occurrence of stress does not imply making stress by a human. There is certain probability p_b of such an event. Let us assume that the probability is proportional to the human flexibility level to stress and that the flexibility can be measured using a scale. Let the scale have range $0 \div \eta$ where:

$$\eta = R_A(t) - R_B(t) \quad (7)$$

The scale can be e.g. 10-grade.

The probability of the event that a given person is flexible to stress at the given grade of the introduced scale can be estimated based on the results of the simulation investigation for a group of persons. Let us assume that the probability is independent of time but depends on the personality. If the random distribution of the stress flexibility e.g. in Fig. 3 is known, the probability can be evaluated:

$$p_b = p_b(t) = f(\eta) \cdot \Delta \eta \quad (8)$$

where:

$\Delta \eta = 1$ – section of the scale of the stress flexibility.

To evaluate a random value of the human reliability the computer simulation method can be applied. The idea of the method is presented in Fig. 4

The purpose of the simulation is to determine the probability that the fault does not happen in the random period of time $0 - t_1$ in the period of human activity in time T_c (e.g. first shift). Since cumulative distribution function of stress fault time distribution $F_B(t)$ is known – the simulation of time of occurring the event t_1

can be done using the well-known method of generating random numbers of homogenous distribution L_1 . Note that the ordinate of cumulative distribution function $F_z(t)$ (Fig. 1b) is different for various periods of time from range $0 - T_c$. Then cumulative distribution function of the distribution of the human flexibility to stress $F(\eta)$ in the range of the scale η is applied to sampling of random value of human reliability $R_c(t_1)$ using the homogenous distribution (random number L_2). If the operational period is divided into z cycles (Fig. 1) with time T_c , it is possible in the way of multiple repetition of the simulation for each cycle to obtain human reliability function $R_{HE}(t)$.

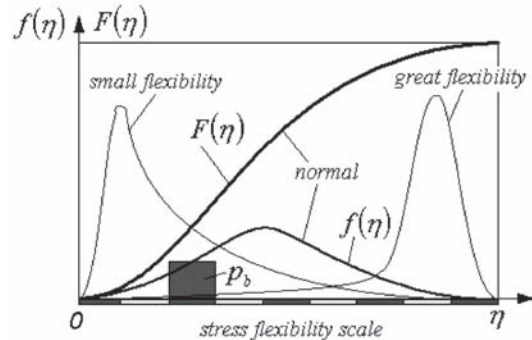


Fig. 3. Typical random distribution of human flexibility to stress

If the human fault is an initiating event (C1 – Fig.2) in the other branch of the event tree than event **Z** generating stress the analysis should be first performed in the limited area of the tree so that function $F_z(t)$ is determined. It is then possible to evaluate the human reliability. If the situation is contrary and the human fault impacts the random distribution of the events generating stress (**Z1**-Fig.2), the method of successive approximation can be applied assuming in the first step human reliability function being equal to 1.

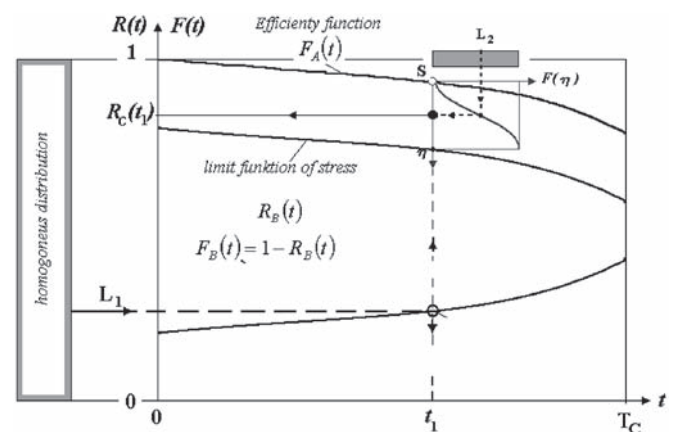


Fig. 4. Principle of computer simulation of single realisation of human reliability

Function of human efficiency and stress function as well as all reliability function of elements of technical system can be described employing the relationship useful for computer analysis [10]:

$$R(t) = e^{K \left(\frac{t}{T_c} \right)^b} - c \quad ; \quad K = \ln(a) \quad (9)$$

where:

- a – final value of the efficiency function (for $t = T_c$)
- b = 0 ÷ 13 – coefficient determining the curve shape
- c – initial value for $t = 0$.

Limit function of stress $R_B(t)$ can be determined according to Eq. (6) employing Eq. (9). Since Eq. (9) defines reliability

function $R(\eta)$, cumulative distribution function $F(\eta)$ (Fig.3) can be defined using Eq. (9) as:

$$F(\eta) = 1 - R(\eta) \quad (10)$$

Determination of the stress function is easy in the case when the stress generates another initiating event. Then the cumulative distribution function of this event is the cumulative distribution function of the event generating stress.

COMPUTER CODE FOR HUMAN RELIABILITY ANALYSIS

To present the results of the considerations given above computer code RELBOOL2 was developed. Logical dependencies between the events were limited to the events defined using symbols „AND” and „OR”. Thus

code RELBOOL2 analyses only simple trees employing dependencies typical for the Boolean algebra.

Total operational time T_c is divided into z_E time intervals and the time coordinate t is replaced by a coordinate of interval number q_E (Fig.1). This part of the code provides a possibility of very fast analysis of multi-element but simple fault trees and is obviously applied not only to human reliability analysis. For this analysis an initiating or intermediate event Z is selected which generates stress and remembers their characteristics $f_z(q_E)$ and $F_z(q_E)$.

In the next part of the code the procedures are launched for the reliability analysis of a human acting in conditions of possibility of stress induced by the intermediate events in the technical system and surroundings. The procedures compute ordinates of limit stress function $F_B(q_E)$ in the operational time loop ($q_E = 1 - z_E$) and sample in the range $t = 1 \div T_c$ ($q_C = 1 \div z_C$)

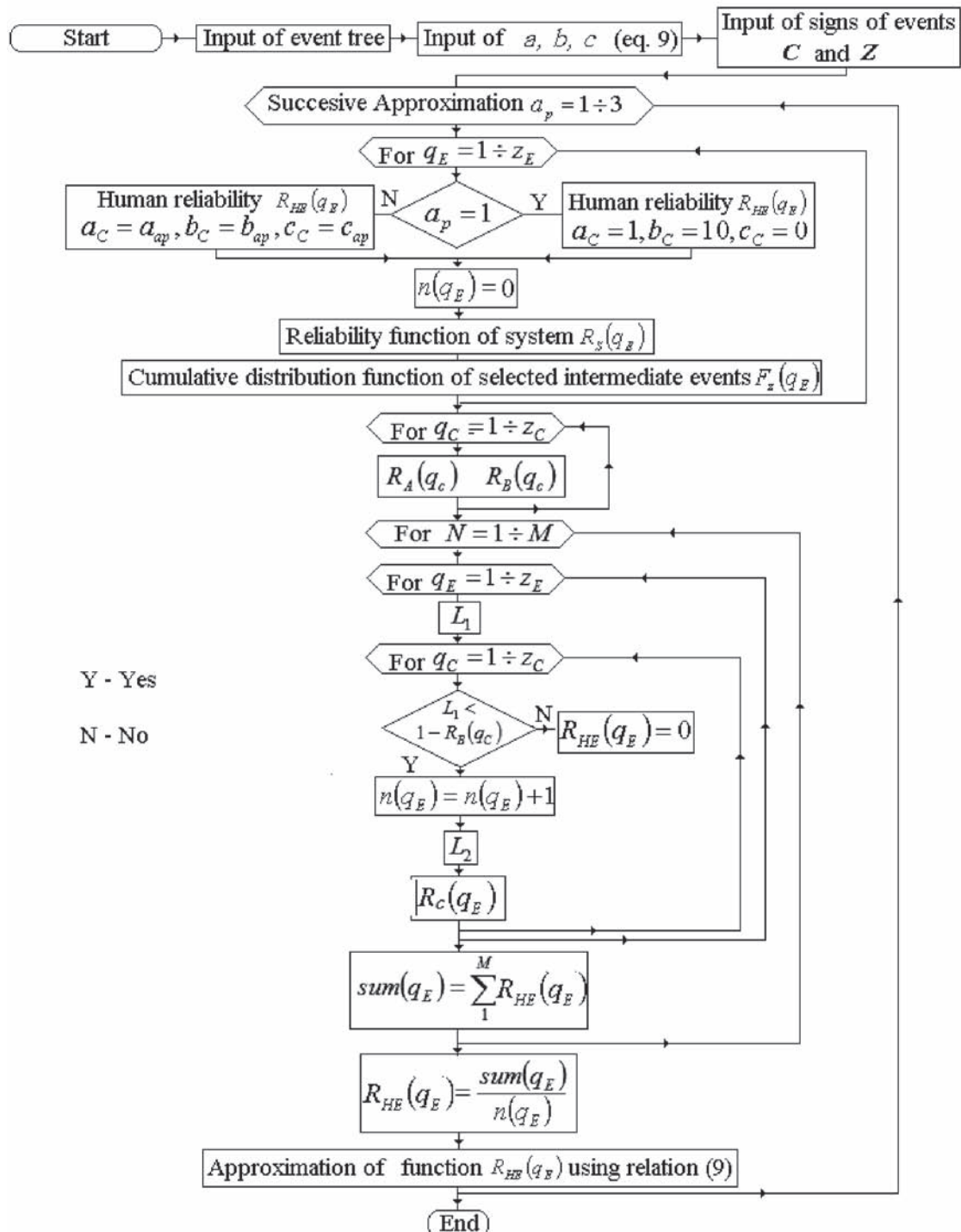


Fig. 5. Flowchart of code RELBOOL2

time t_i of fault occurrence and then sample value $R_c(q_E)$ of human reliability. The computations are repeated in the loop: $i = 1 - M$ times, and for each time interval q the mean value of the reliability obtained from M simulations. Values $M = 1 \cdot 10^4$ or greater are applied to obtain smooth reliability curves.

EXAMPLES OF HUMAN RELIABILITY ANALYSIS

Example P1

For clear presentation of applicability of the presented approach a simple example of the system is given (Fig. 6). In the system the divers are lowered in the diving bell using the single hoisting rope L fixed at the bell with bolt S .

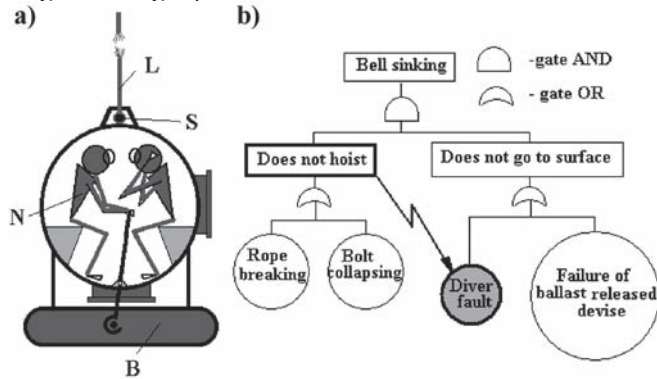


Fig. 6. Example P1 of simple diving system: a) scheme of the system, b) fault tree

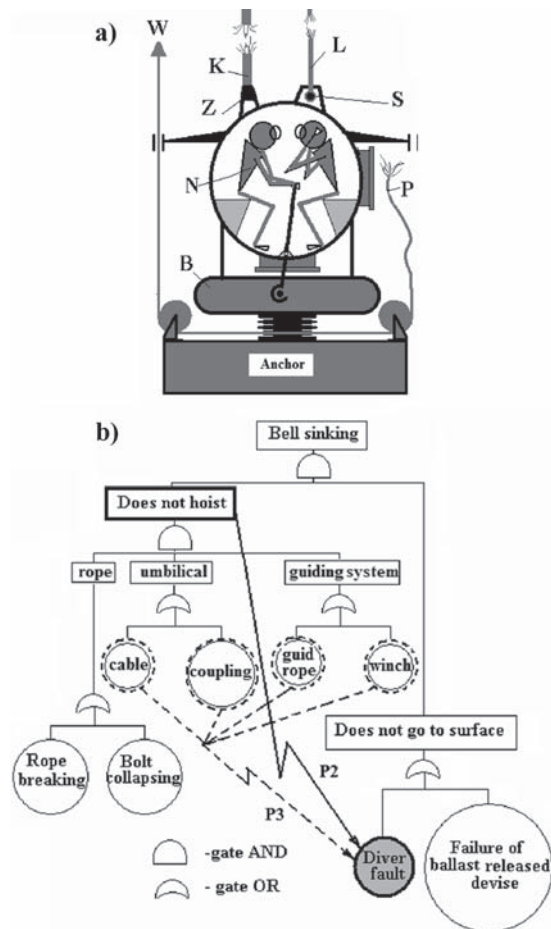


Fig. 7. Complex diving system (example P2 and P3): a) scheme of the system, b) fault tree

In the case of breaking the rope or collapsing the bolt in shear one of the divers (bell operator N) must release ballast

B to allow the bell to rise to the surface. The task is performed in stress induced by breaking the rope what can cause the fault and the ballast is not released. The same effect can appear due to failure of the technical subsystem releasing the ballast. The event tree for this scenario is presented in Fig. 6a. Intermediate event 1 “DOES NOT HOIST” as denoted as event Z inducing stress and the fault of diver „ N ”.

The following data were taken for the determination of the reliability function according to Eq. (9):

Rope: $a = 0.95$ $b = 5$ $c = 0$

Bolt: $a = 0.95$ $b = 5$ $c = 0$

Diver: $a = 0.95$ $b = 5$ $c = 0.02$ – efficiency function $R_A(q_C)$

Ballast: $a = 0.95$ $b = 5$ $c = 0$ (release system).

Example P2

For illustration of the influence of the structural quality, the system was analysed presented in Fig. 7. It is a significantly better system as it is equipped with umbilical (cable) K and guide rope P . The cable hose is fitted to the bell using connection Z . Other denotations in the scheme are similar to those used in Example 1. During regular operation the umbilical supplies energy and the other life support means to the diving bell. It is equipped with the internal strands made of carbon fibres which are load-carrying elements allowing to hoist the bell to the surface. Guide rope are normally loaded by the ballast anchor situated on the bed and strained by the controlled force to move the bell correctly if the bell is subject to side hydrodynamic thrust. In the emergency condition the cables hoist the bell with ballast above the water surface. Releasing ballast is definitely the last way to rise the bell in emergency. Thus there are three independent ways to rise the bell using the strands and self-acting rising to the surface.

Let us assume the following scenario: Breaking the load-carrying cable or the bolt connection with the bell and breaking the umbilical or its coupling and simultaneous (in the same period of time q) breaking the umbilical or failure of the hoisting winch W make hoisting the bell using the cables impossible. Then diver N subject to stress makes the fault disabling releasing ballast B or the ballast release system failure disables self-acting rise to the surface. The fault tree corresponding to this scenario is presented in Fig. 7.

The following data were taken for Example 2:

All elemens: $a = 0.95$, $b = 5$, $c = 0$.

Diver: $a = 0.95$, $b = 5$, $c = 0.02$ – efficiency function $R_A(q_C)$.

Elements which appeared in Example 1 have the same reliability.

Example P3

The data are taken as for Example 2. The scenario has been changed comparing to the Example 2 assuming that the stress is generated not due to one intermediate event „DOES NOT HOIST” but is an effect of four events: „CABLE” (breaking), “COUPLING”, “GUIDE ROPE” (breaking) and “WINCH”. It was thus assumed that the diver does not react with stress to event “DOES NOT HOIST” but reacts with increasing stress to four consecutive events.

Diagrams of the limit stress functions for previously presented examples P1, P2 and P3 are presented in Fig. 8. The functions are determined for a single cycle in the latest operational period that is for $q_E = z_E$. For the remaining periods the area between efficiency and stress functions is less what is reflected by the distribution function curve. (e.g. Fig. 14 curve P1). In example P2 the structure of the system is so reliable,

that the distribution function of the event influencing stress is close to zero. The effect of this situation is that the efficiency and stress functions are identical. Comparison of examples P1 and P3 is also interesting. It is evident that the assumption of susceptibility to stress caused by as many as four events can eliminate positive influence of structure on human reliability.

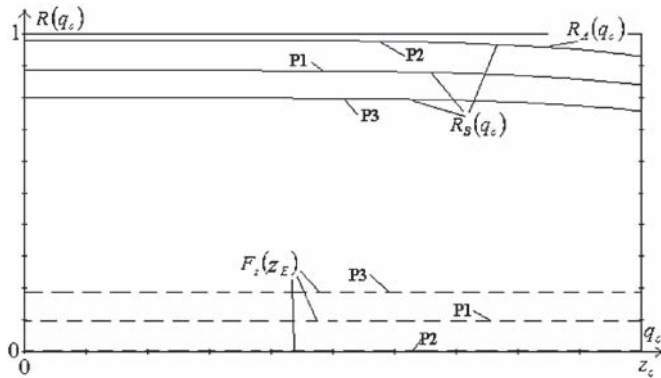


Fig. 8. Limit stress functions for examples P1, P2 and P3

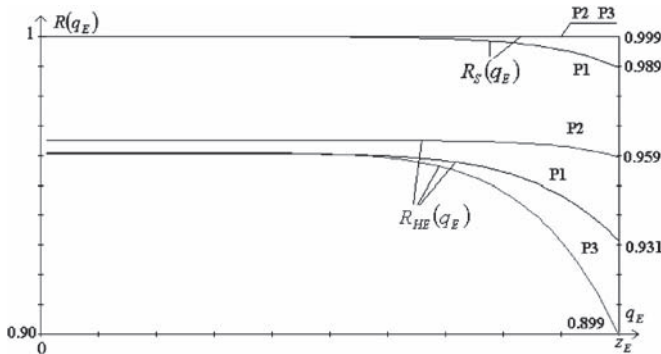


Fig. 9. Functions of human reliability $R_{HE}(q_E)$ and system reliability $R_S(q_E)$ for examples P1, P2 and P3

Functions of human reliability $R_{HE}(q_E)$ and system reliability $R_S(q_E)$ obtained for the presented examples are given in Fig. 9. The influence of the structure on human reliability and influence of the number of events causing stress on human reliability for the whole operational period.

Example P4

A transshipment system was considered (Fig. 10) using the crane traveling on the gate bridge. Hitting bumper B with full speed after passing the terminal position is one of the hazards for the safety of transshipment. It can occur if the system of electrical braking EBS or control system does not work. Passing the terminal position can also occur if sensor S controlling the crane position or the terminal switch ES fails. A system of the emergency braking is designed in which operator OP presses button STOP SB starting mechanical brakes MBS in the case signalization SG informs that the crane passed the terminal position. Operator acts in the stress caused by passing the terminal position or failure of the controller D and can commit a fault of not pressing button SB on time. Operator's action can be inefficient if button SB is damaged or signalization SG fails.

Function of efficiency of a human and all elements was taken to have identical values as in example P2.

Example P5.

Structure and event tree and human efficiency function are identical as in P4 while the reliability of other elements was taken to have less values:

- a = 0.8
- b = 5
- c = 0.

Fig. 12, analogically to Fig. 8, presents the limit stress functions and efficiency function for examples P4 and P5. Deterioration of quality of technical elements while the operator efficiency function remains unchanged is observed.

Functions of system reliability $R_S(q_E)$ and human reliability $R_{HE}(q_E)$ in the whole operational period are given in Fig. 13. It is not only the structure of the technical system which influences the human reliability (examples P1 and P2) but also the quality of the elements. The influence becomes more significant as the operational time increases what results from the distribution function of the damage process presented in Fig. 14.

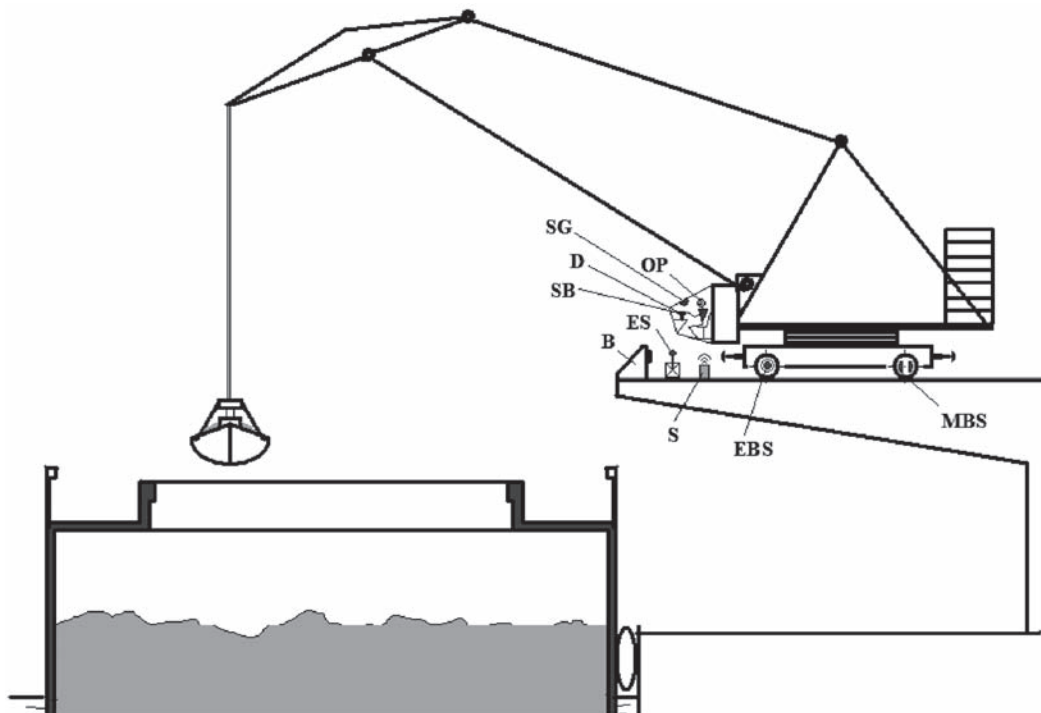


Fig. 10. Scheme of transshipment system

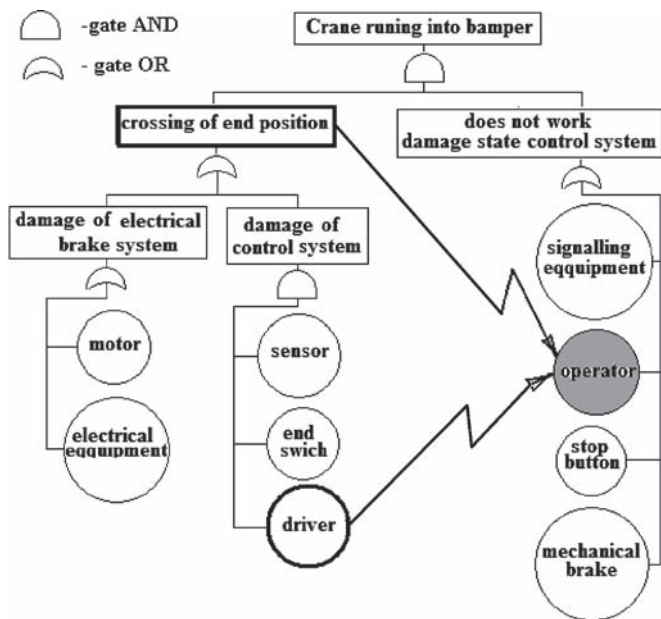


Fig. 11. Damage tree for examples P4 and P5

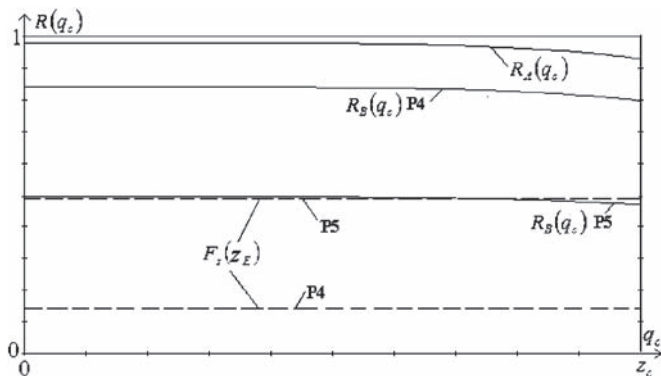


Fig. 12. Limit stress functions for examples P4 and P5

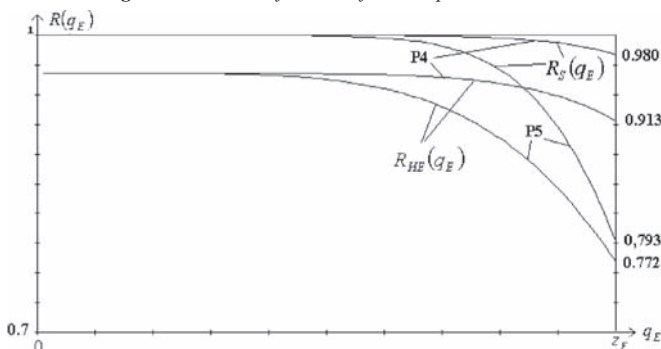


Fig. 13. Functions of human reliability $R_{HE}(q_E)$ and system reliability $R_S(q_E)$ for examples P4 and P5

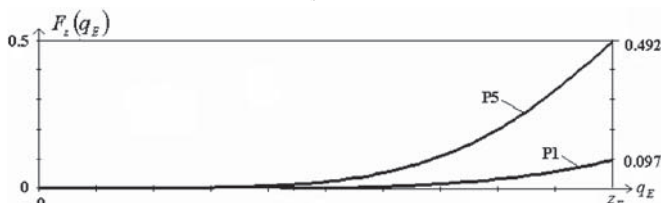


Fig. 14. Cumulative distribution functions of event „DOES NOT HOIST” for examples P1 and P5

CONCLUSIONS

- The proposed method allows to take into account the influence of the technical system on the human reliability in the reliability analyses.

- The human reliability functions based on the analysis of his faults in a short period of time (e.g. one watch) obtained using the presented approach can be referred to the whole system of operation of a technical system in the given macrosystem.
- Further research on the function which is referred to as human efficiency function in the present paper is advisable
- Application of the proposed approach to the algorithms for simulation computer codes taking into consideration complex dependencies between the events is advisable.

BIBLIOGRAPHY

1. Bareith A., Borbley S., et.: *Treatment of human factors for safety improvements at the pacs nuclear power plants*. ESREL'96 – PASM-III, vol.2, Crete, Greece, 1996
2. Bobrowski D.: *Mathematical modelling of system technical object-human being*. Proceedings of workshop Reliability of “system technical object-human being” (in Polish). KBM PAN Warszawa 1984
3. Dougherty E.M. Jr., Fragola J.R.: *Human reliability analysis*. John Wiley and Sohns, New York, 1998
4. Girtler J., Kitowski Z., Kuriata A.: *Safety of ships at sea – system-like approach* (in Polish). WKL, Warszawa 1995
5. Hann M.: *Computerised analysis of reliability and safety of ship machinery and structures subject to rolling* (in Polish). “Okretnownictwo i Żegluga” Sp. z o.o., Gdańsk 2001
6. Hann M., Rosochacki W.: *Threats during marine crane operation* (in Polish). PMR, Z. 19, 2002
7. Harms-Ringdahl L.: *Safety analysis. Principles and practice in occupational safety*. Elsevier Applied Science, London, UK, 1993
8. Kosmowski K.T.: *Issues of the human reliability analysis in the context of probabilistic studies*. International Journal of Occupational Safety and Ergonomics 1995
9. Kosmowski K.T.: *Integrated approach to probabilistic modelling and analysis of safety of anthropocentric systems belonging to certain class* (in Polish). Proceedings of VI Symposium of Safety of Systems, Kiekrz, 1996
10. Kuriata A.: *Selected methods for identification of “personality psychology”* (in Polish). ITWL, Proceedings of VI Symposium of Safety of Systems, Kiekrz, 1992
11. Morawski M.: *Analysis and estimation methods of reliability of human-machine systems* (in Polish). Proceedings of Conference Winter School 79, Katowice, 1979
12. Oziemski S.: *Efficiency of machine operation. Technical and economical basis* (in Polish). Wyd. ITE Radom, 2000
13. Oziemski S.: *Searching method for estimation of evaluating quality of machines* (in Polish). Proceedings of V Conference Shipbuilding and Marine Engineering, Międzyzdroje, 2000
14. Park K.S.: *Human reliability*. Elsevier, Amsterdam, 1987
15. Rouse W.B.: *System engineering models of human – machine interaction* (in Polish). North Holland, New York 1980
16. Semenov J.N.: *Managing risk in maritime economics* (in Polish). Vol. 1., Wydawnictwo PS, Szczecin 2003
17. Smalko Z., Jaźwiński J.: *Influence of human factor on correct behaviour of transportation systems* (in Polish). Proceedings of Conference EXPLO-SHIP'99. Międzyzdroje 1999.

CONTACT WITH THE AUTHOR

Prof. Mieczysław Hann
 Faculty of Marine Technology,
 Szczecin University of Technology
 Al. Piastów 41
 71-065 Szczecin, POLAND
 e-mail : kliet@ps.pl

The multidimensional approach to marine industry development

Part I.

Obstacles and willingness to the EU marine industry reengineering

Iouri N. Semenov, Prof.
 Szczecin University of Technology

ABSTRACT



The paper consists from two parts and generalizes traditional approaches to innovative transformations in various sectors of the EU marine industry. It is shown that shipping companies should permanently adapt and keep their business in sync with marketable changes and be ready to competitive struggle within the global economy. The critical solutions are determining the functional parameters of merchant ships at earliest stages of theirs structural designing, as and reengineering. Author offers a conceptual framework of the co-evolutionary approach to reengineering maritime transport. This problem-solving approach examines targeted ships in topological aspect as the multilayered configurations composed of various-of-a-kinds components, and in functional aspect as multicoalitional compositions. Basic attention focuses on identification of various constrains to innovative activity and choice of improvement strategies, for turning the European marine industry into the high competitive system. For completeness, in paper are presented three particular measures for an estimation of maritime transport success.

Keywords: European marine industry, maritime technology, obstacles to innovative activity, overcoming barriers strategy

INTRODUCTION

The increasing globalization is bringing in more competition in the market. In the European Union's Member States some of the shipbuilding enterprises and shipping companies operate under high overhead costs, such as labor wages, and find

themselves faced with tough price-oriented competition from low-cost producers in Asia [13, 15, 16].

The ability growth of maritime transport to navigation and operation is impossible without innovative transformations (Tab. 1). However, the globalization does not bring in only challenges but also presents an opportunity to internationalize

Table 1. Basic innovations in history of the maritime transport

Milestone event	Basic innovation	Period	Examples
The floating vehicles moving by man-power	Primitive raft constructed of the cane (ancient Mesopotamian)	3500 B.C. – 2700 B.C.	<ul style="list-style-type: none"> – Ships distinguished by a carvel-built wooden hull with constructive fastening – Ships distinguished by double hull out of high-strength steel – Ship's hull with changing configuration – Ship's hull out of a smart materials created under nanotechnologies
	Timber boat powered by oar (ancient Scandinavian)	3000 B.C. – 500 A.D.	
The floating vehicles moving by nature-power	Ship propelled by sail and constructed of the wooden (ancient Egypt, Viking)	2700 B.C.– 1900 A.D.	
The floating vehicles moving by engine-power	Ship propelled by steam- engine and constructed of the iron	1770 A.D. – 1915A.D.	
	Ship propelled by low-speed or medium-speed diesel (gas-turbine) & constructed of steel	1915 A.D.– 2030A.D.	
	Ship hull from super-light alloys differing by: ✓ renewable energy engine ✓ hull with changing geometry	2030 A.D. –	

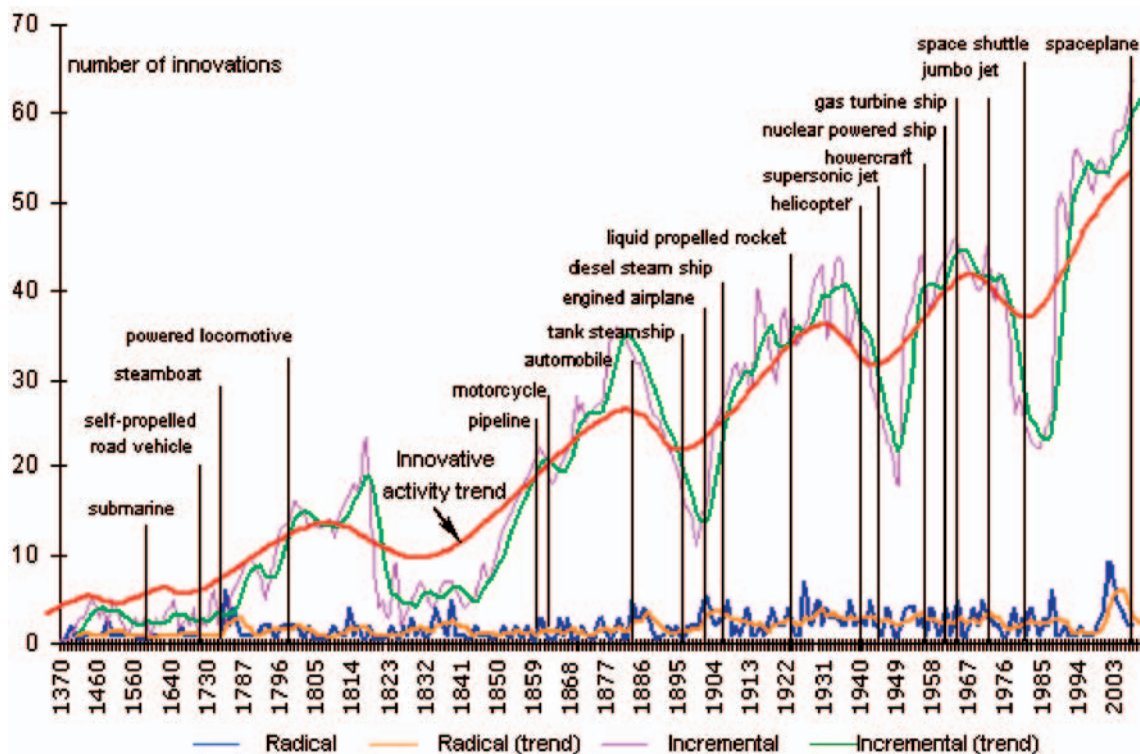


Fig. 1. Long-term cycles and short-term changes of European transport development

sales in new, rapidly growing maritime markets and thereby to generate additional revenues [27, 28].

Therefore among the European important problems within the next few years is the rapid development of energy-saving vessels and risk-free shipping technologies; implantation of ship's propulsion systems differing by high hydrodynamic efficiency, as well as improvement of onshore management techniques.

Tools towards these goals are increased partnerships both in the "knowledge triangle" – research, education, innovation and in the "innovativeness triangle" – idea, development and implementation [2]. A comprehensive investigation of business activities demonstrates that the EU Member States are important players in market, putting innovative solutions into practice by various ways [20, 21].

Herewith, in a number of the European Regions the world experience of innovative development is generalized and made use to improvement of various modes of the EU transport. Such tendency takes place for a long time (Fig. 1). Today numerous European Regions make use of world experiences of innovative development as part of their strategies for multi-purpose renovation of various sectors of staple industries, including marine industry [10, 12]. In a number of cases European Regions are focusing attention to commercial viability of various new solutions by the analysis of utility and profitability, but with less attention to quality of innovative activity. Unfortunately, some of the Regions do not take significant steps in the implementation of innovation availability evaluation although they recognize its importance. A serious threat for the economies of such Regions is a lack of innovations as a result of scanty investment into RDI (Research, Development and Innovation), and poor cooperation of domestic researchers and various enterprises of the marine industry, as well as government and regional authorities. Developed European Regions are focused on large-scale reengineering of harbours' infrastructure as key commerce hubs, and improving of navigation activity as vital transport mode. Herewith, on the one hand takes into account social opinions about risk-free and eco-efficient shipping technologies, and on the other

hand the estimation of future market demands and profitability forecast of innovative transshipment technologies. This gives an indisputable advantage as it allows the following:

- ✦ to make timely solutions with regard to the large-scale modernization of maritime transport, through the technical achievements and shipowners' wishes
- ✦ to adapt the production of the European shipyards to a large-scale commercialization, taking into account interest of freight forwarders, as well as passengers preferences.

Therefore, today's active debate is devoted to the analysis of an innovative policy and interpretation of transformation results both into various transport modes, and into shipbuilding industry [2, 12, 14]. The European Commission is key player in this area. The special attention of the EC is focused on quick adaptation of verified innovations into the European marine industry. In the author's opinion single and multipoint sources of the constrains to successful implantation of innovative solutions can take place both in the process of converting new ideas into lighthouse projects, and later into robust transportation systems. Such variety requires a systematization of these obstacles and definite proposals of efficacious strategies to their overcoming. Usually researchers are contented by the limited number of barriers, including [8, 9]:

- ✦ Lack of ability to use new technology
- ✦ Expensive human resources
- ✦ Lack of skilled human resources
- ✦ High interest rates
- ✦ Problems with access to finance
- ✦ Hard to protection intellectual property
- ✦ Lack of market demand for innovation
- ✦ Did not plan to innovation.

Such approach essentially constricts range of problems. Fig. 2 shows the importance degree of the above-listed obstacles to innovative activity for the EU enterprises on basis [8, 9, 15, 22]. The more detailed barriers classification to innovative activity follows in Tab. 3.

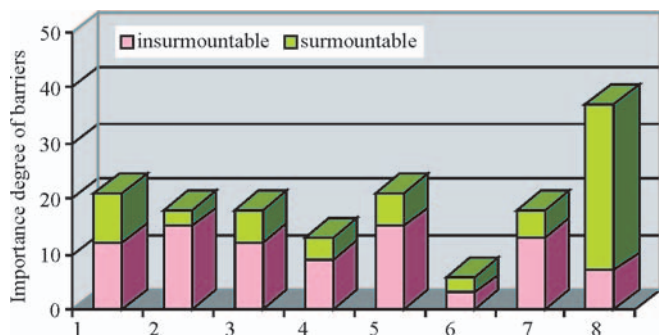


Fig. 2. The main constraints to innovative activity in the EU-27

First let's analyze modernization features of the European Union's marine industry.

MODERNIZATION FEATURES OF THE EU MARINE INDUSTRY

The marine industry is a complex and diverse branch of international economy with many sectors, which are confronted with an increasing international competition on all market shares. The worldwide economic cycles are very important to the European marine industry development too [24, 25]. It is typical for all sectors of the marine industry including shipbuilding, maritime transport, marine tourism, fishing, as well as maintenance and transshipment of various ships. A leading position in the European trade still is identified with merchant fleet and passengers' conveyance. Centuries-old experience reveals that both cargo carriers and cruise ships are complex engineering systems. As rule, each ship belongs to a shipping company, which is supercomplex socio-technical system, and consequently can be classified by various attributes. Such systems classify according to their topological space, as well as to functional parameters, e.g., [6].

In context with the problem of presented article, technical systems can be classified through their structural features, which determine occurrence of those or other obstacles to the subsequent modernization of these systems:

- ☆ structurally linear systems; an obstacles to their modernization are cumulative (the predictable) barriers;
- ☆ structurally nonlinear system, i.e., system which does not satisfy the principle of superposition; an obstacles to their modernization are both cumulative barriers and unpredictable synergetic barriers¹.

Any enterprises of the marine industry can be considered as multilayered systems including several levels. Then, full number of indivisible components, including both the units of standard-based equipment and the units of innovative equipment determine the bottom layer (the mini-level) of such enterprises. Some number of the standard equipment and the innovative equipment can be coalesced into target coalitions. These coalitions determine the average layer of the enterprise (the middle-level). Set of the targeted coalitions represents the higher hierarchical layer (the meta-level). For example, a shipyard as multicoalitional system includes the slipways, dry-docks, the productions lines to fabricate engine rooms etc. Principle of shipyard modernizations assumes that the top-managers beginning to improve one or a few coalitions, first of all should identify eventual barriers; to introduce only profitable decisions, and also they should step-by-step overcome all barriers to innovative changes in shipbuilding

activity, as well as keep shipyard's production balance. On the first step, structural composition of the modified shipyard will be a poorly-compatible. At the next stage of modernization such enterprise should be transformed to a mature-compatible composition by significant improvement of compatibility between standard-based equipment and the new embedded coalitions through overcoming internal and external barriers, and as result, reconfigurations of intercoalitions connections. Analogical sequence of equally likely events is characteristic for modernization process of any enterprises including shipping companies.

Every next effort of the top-managers should be focusing to maximum increase in interoperability of the modernized enterprise with its business environment. Any firm of the marine industry is called a highly-compatible enterprise, if it does not contain a redundant coalition or component, as well as if works performs without errors or inconsistencies. In the author's opinion, only such companies should be target of the top-managers because of their resilience to global market influence. One more status of any future-oriented enterprise is theoretically possible, namely so-called ideally-compatible state, if it's impeccably cooperates with every business share, and always ready to overcoming various barriers even under asymmetric influences (market, inflationary expectations, restrictive laws etc.). Therefore, can be formulated the following substantive recommendations relating to successful modifications of enterprises of the marine industry into highly-competitive companies:

- to meet of market requirements, including a freight forwarders' needs and a shipowners' wishes, as and to identify critical barriers to implantation of new solutions
- to promote of verified and proven innovations, as well as risk-based techniques focused to overcoming eventual barriers
- to use technique SWOT or method CBA for comprehensive assessment of opportunities and vulnerabilities of possible strategies of the planned changes, and at last
- to systemic reorganization of the enterprise's infrastructure through implementing advanced software, hardware and orgware for efficiently planning, control and development.

Modernization of the EU maritime transport

Maritime transport systems are supercomplex systems, characterizing by dual logic. On the one hand, such systems require stability for maintenance of users' enthusiasm, but on the other hand, realization of effectual innovative policy. For reduction of this self-contradiction, the author has offered new approach to the innovative support of maritime transport systems. This approach unifies the methodological basis for investigations of change/conservation rate and describes by parameter "Dimensions of Systems' Renovation". Further in the article, this methodology is referred as DSR approach. Under condition that dimensions number more than one ($N \geq 2$) such approach increases both simulation veracity of renovation of engineering systems, including maritime transport systems, as well as identifies best way to convertibility of the new ideas. Let's explain this thesis.

Early methods in the design of engineering systems and their subsequent modernization were based upon the use of informal procedures obtained empirically. Obvious disadvantages of taking cut-and-dried decisions on the basis of an empirical approach have led to development of the deterministic

¹ The word "synergy" originates from the Greek language and is composed of the word "syn", which means "together", and "ergon" meaning "work" [17].

approach. Such approach considers the designed system as a structurally-stable composition of various components. At that, each of these components is a discrete indivisible element and adaptive interactions between them are linear and weak. In a general sense the deterministic approach was developed on basis of formalized procedures for solving such problems as screening of structural compositions of simple engineering systems, e.g. single hull tankers or tramp bulk carriers (1960-70 years); reducing of an informational uncertainty, e.g. of shipping management (in succeeding years); and at last, problem of large-scale standardization of decision-making and the solutions verification.

It tries to predict the properties of a revised system under very limiting conditions, and under only one control variable, most often variable “*Components Number*” (the informational measure of system’s renovation), and as the result, reflects readiness of top-managers for overcoming situational barriers (Fig. 3). Therefore, the deterministic approach is called

DISR (the one dimension of system’s renovation) according classification offered by author. The each maritime transport system has a unique nature because it consists of various coalitions [26].

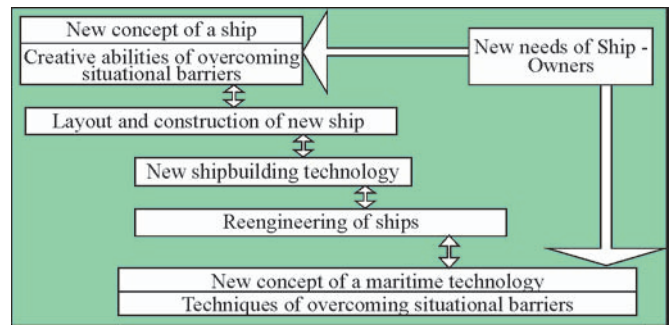


Fig. 3. Deterministic approach (DISR) to development of a new ship's concept

Table 2. Compound-chain of converting new idea-into-product

Stage	Activities in an innovative reengineering	Results
Basic research	– identification of market demand, including of shipowners needs	Lighthouse project
	– definition of reengineering problem and eventual barriers	
	– research of critical barriers to maritime transport reengineering	
Applied researches (lighthouse project)	– estimation of worldwide experience in reengineering	Experimental development
	– definition of problem that aimed at the application of innovative idea into reengineering process	
	– analysis of eventual barriers to maritime transport reengineering	
	– definition of complete and unambiguous set of functional & legislative requirements for activities in an innovative reengineering	
	– identification necessary resources for overcoming barriers, taking into account funds, personal skill, public opinion	
	– conceptual view and planning process of reengineering, taking into account of shipowners' needs and eventual barriers	
	– problem and data structuring	
	– development of applicable requirements sufficient to enable satisfactory performance of the targeted system's life-cycle activities, taking into account informational compatibility	
	– choice of innovative solution, taking into account structural and functional compatibility as a verification results of it practicality	
	– development of the analytical model and design-making tools	
Experimental development	– identification of real barriers and tools for their overcoming using historical experience, as well as integrated analysis of best practice and cumulative knowledge	Decision-making about realization of innovative project
	– revision and correction of the reengineering conception, taking into account extent of its conformity to market's trends	
	– converting of new idea into the prototype model and its testing	
	– identification of the weak points of the novelty prototype, as well as probable barriers at the future realization of innovative project	
	– revision and modification of the prototype, taking into account conformity extent of the prototype to ideally-compatible model	
Implementation	– definition and description of requirements to competencies and working environment, e.g. for crew of new ship	Decision-making about large-scale production
	– forecast how the required technical, quality, and human-centered activities will be fitted into the life-cycle of maritime transport	
	– maritime transport of demanding	
Large-scale production	– creation of the in-line documentation and training procedures for overcoming barriers to large-scale commercialization of new object	Wide expansion of new ships or technologies
	– development of the strategy for large-scale commercialization, taking into account maturity and readiness extent of a business environment to implantation of maritime transport	
	– commercial production of the targeted object, e.g. top-class ships	
	– realization of selected strategies for competitiveness support of the new ships during period of large-scale commercialization	
	– standardization of new solutions for the EU maritime transport	

Unfortunately on initiative stage of renovation process, new coalition embedded into the modernized transport system rarely will improve its quality; similarly new qualities' giving to such system of isn't always accompanied by positive functional effects. The author proposes the following sequence of converting new idea into a new shipbuilding product or putting maritime technology (Tab. 2).

In the middle of XX century for study of engineering systems as a whole, including both its complexity and development dynamics was proposed systemic approach by L. von Bertalanffy [1]. This approach integrates a synthetic and the analytic methods, taking into account the informational and topological measures of systems design (the second dimension of system's renovation), as and enables to investigate the cumulative internal and external barriers. Therefore, the systemic approach should be called D2SR according to classification offered by author (Fig. 4). Later investigations allow formulating the so-called principle of co-evolutionary development. Its earliest use was connected with research by biologists and concerned the analysis of community evolution and the reciprocal aspects of interaction between organisms of different species in nature. Subsequently the co-evolutionary dimension began to be used by scientists from the other scientific domains.

The qualitative modernization of the EU industry sectors requires the multilevel compatibility and interoperability of approved innovations through multilateral adaptation of standard and innovative solutions, taking into account both the interactions diversity and the eventual barriers to innovative changes, i.e. evolutionary measure of system design (the third dimension of system's renovation). The combination of the evolutionary measure with structural and informational measures (the first & the second dimensions) enables a modernization of transport system through the so-called Three-Dimensional (D3SR) approach. Such approach allows use of various tools, covering numerous aspects of systems modernization, e.g., increase of safety and competitiveness, as well as an amplification of operational and economic efficiency through integration of transportation modes into the local, regional or global maritime transport systems distinguished by a user-friendly, environmentally sustainable development and stable resistance to critical failures. The D3DA focuses on process research of converting in the "from-idea-to-product" chains, using:

- ◆ unified designing space for conjoint analysis of transformed maritime transport systems via structural, informational and evolutionary measures
- ◆ the integrated index of conformity degree of innovation with the ideally-compatible model for estimation of renovation decisions' efficiency, taking into account various positive effects as a consequence of innovative activities.

This process include the basic and applied researches, an experimental and implementation phases, as well as diffusion phase of a standardized solution, which covers the improvement actions. Let's consider this assumption in details:

- ★ the first stage is all attention on initial choice of innovative solutions satisfying to modernization requirements of the maritime transport systems; as a rule, on this stage make up a complete multitude of verified and proven innovations, as well as identification of critical barriers to their using. These barriers have cumulative nature
- ★ at the second stage is paying attention on the embedding of innovative coalitions into the maritime transport systems with permanent verification of inter-coalitional compatibility; as a rule, this stage leads to formation of targeted system, characterizing by partial compatibility in view of existence of a latent barriers. These barriers have synergetic nature
- ★ the third stage is focused on improvement of inter-coalitional compatibility; as a rule, this stage leads to targeted system, characterizing by mature internal compatibility on the one hand, but on the other hand, requiring the further improvement through overcoming residual barriers. These barriers have synergetic nature, as and cumulative nature
- ★ at the fourth stage is focused on overcoming barriers to implantation of the improved maritime transport system into a business environment; this process allows to increase compatibility of inter-system up to greatest possible level, and at last
- ★ the fifth stage is listening carefully consequences of diffusion of the improved maritime transport system, as well as it's prepare to subsequent standardization, i.e. creation of regulative barriers for widening life-cycle of the modernized system.

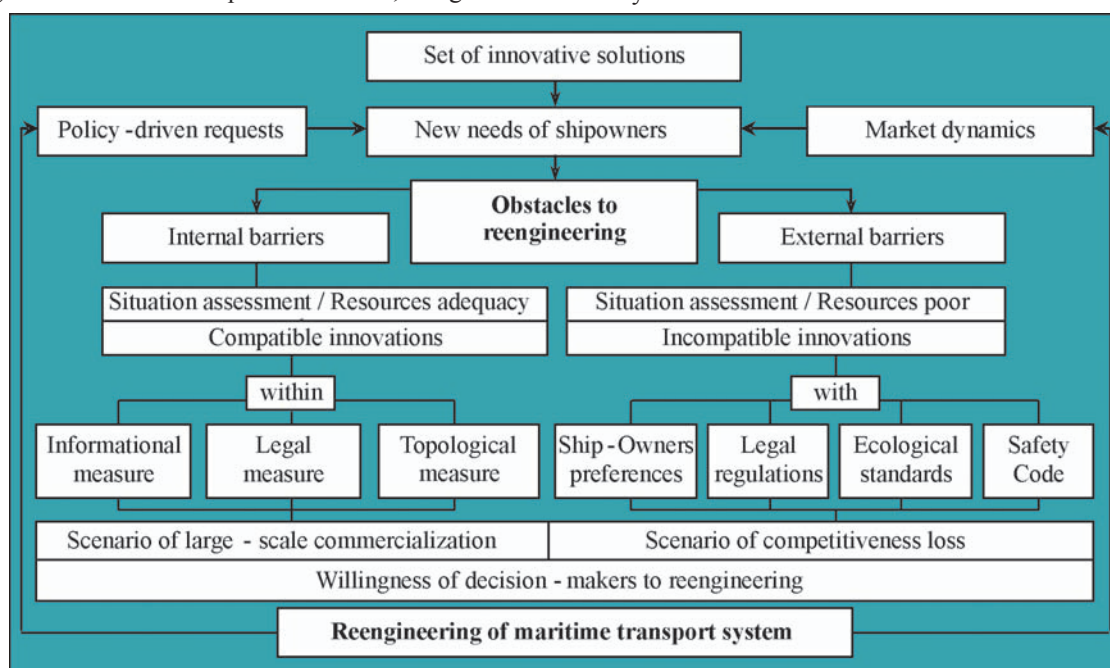


Fig. 4. Two-Dimensional Approach (D2SR) to choice of investment strategy

The three initial stages represent the pre-commercial period. Decision-makers identify the targeted transport system, as well as choose, correct, test and develop appropriate technologies and techniques within the context of the innovative problem. At the same time, they develop quantitative and qualitative measures for close estimation of innovative solutions' potential influence on intra-system compatibility. The goal of these stages is to support innovative transformations using necessary resources, strategies and tools, as and timely decision making to overcoming of various barriers. Therefore, the outcomes of third stage will help decision-makers identify shortcomings, evaluate risks, and invest in the best combination of innovative strategies, minimizing influence of eventual barriers, and as result, to increase competitiveness for improved transport system, as well as help to estimate the resulting benefit from the innovative idea.

The fourth and fifth stages represent the commercialization's period. At the fourth stage, decision-makers correct the plan of activity, considering the obtained results of estimation at the third stage. The market penetration strategy develops, taking

into account marketing research, the regional market condition and the competitors' profiles. The goal of this stage is to evaluate the potential of the innovation and ability of its adaptation to changeable wishes of consumers. At the fifth stage, decision-makers take steps to the complete standardization of the novelties. The main goal of this stage is large-scale market expansion.

Barriers to innovative activity within the EU marine industry

The RDI activities are keys to renewing economic growth, strengthening competitiveness and boosting employment. Successful implementation of innovative knowledge-based products with enhanced utility and profitability may help for the EU shipping companies, on the one hand, raise both service quality and environment safety, and as result to achieve a domestic promotion, and on the other hand strengthen their competitive position in global market through overcoming various barriers [11, 17, 29]. Author offered new classification of barriers to innovative activity, shown in Tab. 3.

Tab. 3 Barriers classification to innovative activity on the European-wide scale

Barriers to innovative activity					
Positive barriers		Negative barriers			
		Bi-criterion classification			Multi-criterion classification
		Subjective	Objective		
<i>Individual barriers:</i>	<ul style="list-style-type: none"> • Threat of economic collapse • Individual ethical code 	<i>Labor obstacles:</i> <ul style="list-style-type: none"> • Skills shortages of a staff • A high level of intra-staff conflicts • Staff passivity to innovative changes • Workers unwilling-ness to retraining 	<i>Business environment obstacles:</i> <ul style="list-style-type: none"> • Economical cycles (economic recession) • Market uncertainty • Limited potential of domestic market • The peculiar regional environment 	<i>By source localization</i>	Internal
					External
<i>Social barriers:</i>	<ul style="list-style-type: none"> • Public moral code • Multi- aspect liability to future generations: <ul style="list-style-type: none"> - ecological - living conditions - architecture & historic protection - landscape preservation -safety etc. 	<i>Individual obstacles:</i> <ul style="list-style-type: none"> • Lack of entrepreneurial spirit • Lack of intelligence & creativity • Lack of task awareness • Prejudice against innovative changes • Undisciplined behaviour • High level of informational uncertainty, as result of lack of firsthand knowledge 	<i>Regulative obstacles:</i> <ul style="list-style-type: none"> • Restrictive laws and government regulations • Long certification procedures • Universal service obligation 	<i>By number sources</i>	Single
			<i>Administrative obstacles:</i> <ul style="list-style-type: none"> • High level of bureaucracy • Long external decision -making processes • Strong requirements to novelty submission • Disconnect between science and business • Unawareness of support importance of new initiative 		Surmountable
			<i>By ability to overcoming</i>	Partial surmountable	
<i>Regulative barriers:</i>	<ul style="list-style-type: none"> • Antitrust rules • Obligatory ecological assessment • Obligatory safety testing; • Intellectual property rights 	<i>Organizational obstacles:</i> <ul style="list-style-type: none"> • Corporate culture does not encourage innovativeness • Lack of innovator - decision maker contact • Undue centralization • Formalism, long inte-rnal decision-making processes • A low level of imple-mentation control; • Incorrect business-plan / master-plan 	<i>Industrial obstacles barriers:</i> <ul style="list-style-type: none"> • Three-dimensional complexity of innovative changes • Conflict for resources; • Bundling (high interdependency) of technology 	<i>By mechanism</i>	Cumulative
			<i>Financial obstacles:</i> <ul style="list-style-type: none"> • Lack of funds • High innovation costs • Inflation risk • Exchange rate risk • High credit rate 		Synergetic

This necessitates efforts to bring new and more profitable products into the consumer market. Experience shows, that identification and research of critical barriers to an innovation are important, but creation of strategies and tools to overcoming barriers to innovative process has even more values. The most investigations of innovative process are focused on two types of barriers to converting of new ideas into new products. First of all, it is internal and external barriers to innovative transformations. Secondly, ones are so-called business environment barriers forming under of market fluctuations [3, 5, 7].

In author's opinion such classification of eventual barriers is adequate, if an innovative process is described for structurally linear systems. On basis of many investigations [18, 20], and author's researches, we can contend that for structurally nonlinear systems main obstacles to rapid achievement of total success are connected with poor encouraging motivations for innovative actions, as and lack of systemic approach to leveling or removing of various barriers to implementing novelties. Properly, the dominant barriers to European innovative activity can be divided into ten groups: financial, labour, administrative, industrial, regulative, business environment, organizational, operational, individual and natural barriers. Fig. 5 and 6 shows the importance degree of barriers to innovative activity in the EU, on basis [4, 8, 9, 15, 16, 22, 23].

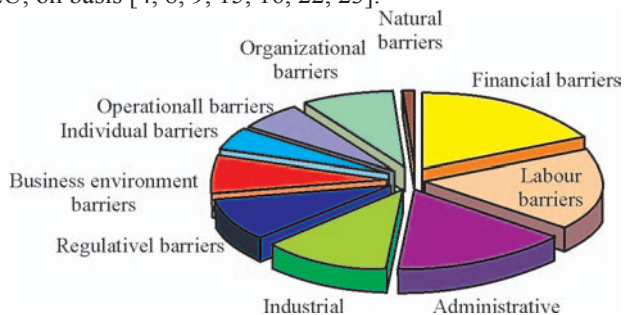


Fig. 5. Main obstacles to the European innovative activity

Otherwise additional classification of such barriers is required, considering the sources forming mechanisms, a surmountableness level, etc. Also the author classifies barriers to innovative activity by one more criterion, namely by predictability:

⇒ The predictable cumulative barriers. These barriers foresee at the early design stages of any engineering systems. These are divided into predictable positive barriers including external and internal, as well as, predictable negative barriers.

The nature of the predictable positive external barriers lays in aspiration for the support of public and ecological safety as well as in liability to future generations. The predictable positive internal barriers, i.e. barriers within the organization, focuses on identification and development of promising innovations through demand to the innovator to give a detailed suggestion of the innovative changes or a business plan which shows the way to commercialization. The nature of these barriers lays in aspiration for the avoidance of additional expenditure. The high moral standards and professional ethics of personnel are the positive internal barriers too, e.g., refusal to novelties use without intellectual property rights.

⇒ Unpredictable synergetic barriers. Generally, the nature of these barriers is closely connected with resonance phenomenon induced by multidimensional innovative changes. In most cases this phenomenon generating structural, information and evolutionary complexities, and as result critical obstacles to end-to-end innovative process. According to numerous investigations [6, 29]:

- ♦ structural complexity is a measure of topological features produced by differentiation and integration in the spatial dimension of the improving system. It is determined by extent of structural compatibility through mapping intra-coalitional level, inter-coalitional level, and inter-system. Structural compatibility within inter-coalitional level implies spatial compatibility between both innovative and standard coalitions embedded into improved system. Structural compatibility within inter-system level implies spatial compatibility between updated maritime transport and business distinguished by administrative, regulative and/or market barriers
- ♦ information complexity is a measure of conceptual features of targeted system and its conformity extent to market's expectations. It is described both by basic characteristics and distinguishing features of the updated system, as well as by groups of conformity between these descriptions. Information complexity is determined by informational compatibility which means an opportunity of legal, language, and/or knowledge barriers, and
- ♦ evolutionary complexity is a measure of transformations features carried out within the system's modernization. It is determined by integration of all changes in the temporal dimension through three aforementioned systems levels. Evolutionary complexity within intra-coalitional level implies age-related barrier between all elements embedded into each coalition. Evolutionary complexity within inter-coalitional level implies operational barrier between coalitions embedded into renovated system, which is determined by timeliness of replacement of outdated coalitions by innovative coalitions. Evolutionary complexity within inter-system level implies advancement barrier between consumers' demands and supply, which is determined by maturity and readiness of a business to implantation of new solutions.

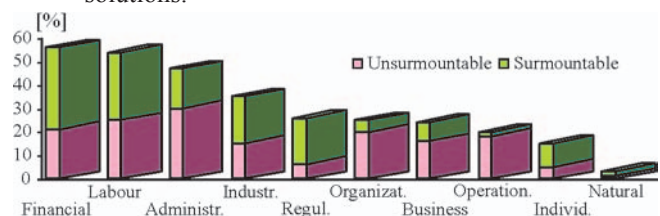


Fig. 6. Percentage composition of main barriers to reengineering of the European marine industry

All barriers should be divided by positive barriers and negative barriers. Positive barriers play a vital part in an attempt both to the environmental protection and the maintenance of operational safety. Negative barriers are obstacles in development. Such barriers are the responses of obsolete systems to innovative solutions. Some reasons for this opposition are unwillingness of top management to changes, lack of creativity, a low level of motivation, aspiration for the avoidance of high economic risks as consequence of market uncertainty high level and lack of pressure from customers.

The multilevel contradictions between innovative activity obstacles generate the so-called Domains of Incompatibility (DoIs). The mini-level contradictions lead to forming the intra-coalitional DoIs and to the drop in competitiveness of separate shipping company. The middle-level contradictions lead to forming the inter-coalitional DoIs and to the reduction of regional economic activity. The meta-level contradictions lead to recession in the marine industry and to the drastic growth of market uncertainty, and as result, to the pressing

need of various tools and resources to overcoming predictable and unpredictable barriers, forming into various the European Regions. The marine industry is very important part of the EU economy. Let's discuss some facts. First of all, in 2006 years, the European shipbuilding was characterized by [10, 13, 15]:

- approx 9 000 production and supply enterprises, with more than 350 000 workforce
- an annual turnover of more than € 35 billion, more than half of it through exports
- stable positions on global market in sophisticated shipbuilding production, particularly fast ferries, chemical tankers, cruise ships, megayachts, FPSO
- nearly 10% of turnover spent on Research, Development and Innovation (RDI) activities.

At the same time, the European maritime transport plays major role in the international and internal trade of the EU. In 2005/2006 years, key data of this sector of marine industry were:

- ◆ almost 90 % of the European Union's external trade (imports and exports combined) is transported by seaways, in particular that relating to bulky and low value goods
- ◆ more 40 % of the internal trade between the EU Member States is realized by the maritime transport and inland waterways
- ◆ more 4,000 mln tones of a freight loaded/unloaded in the European Union harbours.

The level of risk factor plays an essential part in acceptance of new technique or technology by any shipping company or shipyard. Quite enough one tragic event, so that the freighters or shipowners' preferences have been radical changed, and their DoIs are extended.

Enlargements of an individual dissatisfactions of permanent participants of innovative process (e.g. eventual freighter/shipowner) takes place as a consequence of the enduring increase

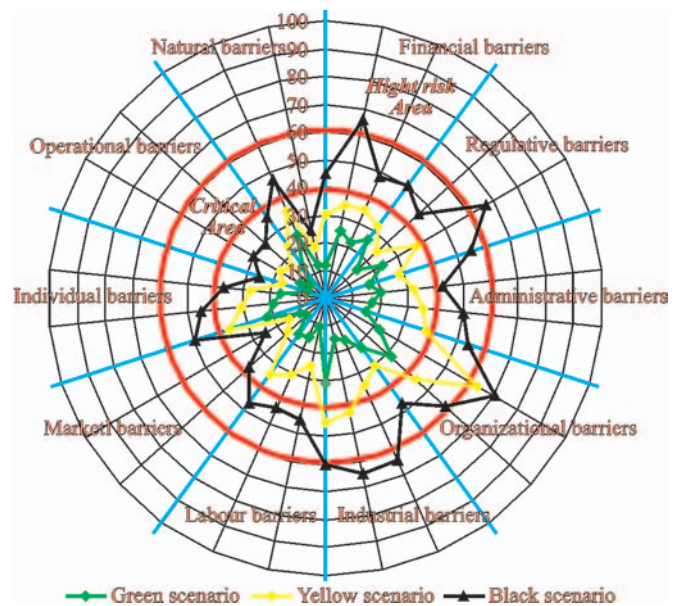


Fig. 7. Risk-mapping of the barriers' impacts to the innovative activity within the EU maritime industry

of the various requirements to a risk level of investments, to the transportation quality etc. Best tool for investigation of DoIs is risk-mapping techniques (Fig. 7). Therefore, critical goal of each innovative process is choice of high-quality strategy for rapid growth of the European economy (Tab. 4).

Forecast of the barriers impacts to the innovative activity through creation of various scenarios are necessary before the beginning of innovative changes with the purpose of the negative results' minimization. This problem is very important for the Polish maritime industry too. Therefore Part II of this paper will be devoted to the multi-objective analysis of the obstacles in the Polish maritime industry development.

Table 4. The basic strategies for European Regions development through overcoming barriers to innovations

Key strategy	Convergence Regions	Phasing – in Regions	Competitive Regions
The policy of main Regional barriers overcoming	Upgrading of regional economy through use of world experiences of innovative development	Intensification of regional economy through incremental innovations	Strengthening position of regional economy in global knowledge economy
The strategy of Regional barriers in marine industry overcoming	<ul style="list-style-type: none"> – increase co-operation between inventors and sea-port authorities – increase innovative capabilities of shipping companies – implant of “catching up learning” techniques 	<ul style="list-style-type: none"> – wide innovative activity – new sectors of marine industry – implant new ideas in sea transportation systems – establish of joint-ventures companies 	<ul style="list-style-type: none"> – enlargement of bases of knowledge – embedded of radical innovative solutions – enhance interaction of regional industry and decision-makers on new market shares
The strategy of Regional barriers in education systems overcoming	<ul style="list-style-type: none"> – build up medium level skills – co-operation increase between shipowners and High Schools, Maritime Academies 	<ul style="list-style-type: none"> – build up new skills required – inter-regional mobility schemes through co-operation shipowners and Universities 	<ul style="list-style-type: none"> – set up both Universities and High Schools for growth specialized abilities – increase attraction of new skills
The strategy of Regional barriers in knowledge networks overcoming	<ul style="list-style-type: none"> – creation of a permanent links between innovative firms for transfer knowledge inside the Region – preference to the demand-led approach to development of Regional knowledge networks 	<ul style="list-style-type: none"> – stimulation of activity of knowledge networks – support to new technologies on National and International horizons – encourage interfaces between researchers and marine industry 	<ul style="list-style-type: none"> – all possible assistance of creation and development of knowledge networks – promote Regional networks among shipping companies

CONCLUSIONS

- The innovative activity is required to be designed on the basis of assessment results of their expediency and opportuneness, i.e. research of real market demands, as well as utility of planned changes and resources necessary for its execution.
- Early identification of cumulative barriers, as and the forecast of synergetic barriers to required innovative changes are very important.
- Creation of effective strategies, helpful resources and instruments for overcoming barriers before beginning of improvement process plays a key role to the innovative project's success as whole.
- The more carefully innovative project is elaborated, the barriers to successive modernization of maritime transport are less, and at last the risk of a misfortune is lower.
- It is necessary to remember that the increase of uncertainty in free resources raises the probability of the unpredictable barriers' evolvement to the modernization process of maritime transport.
- Simulation of innovative process is required to be executed under condition that the black scenario of shaping of negative effects during barriers overcoming takes place.
- It is recommended to choose decisions to overcoming barriers to the modernization process using risk-mapping techniques.

Acknowledgment

This paper was supported by the Polish State Committee for Scientific Research. 2008

BIBLIOGRAPHY

1. Bertalanffy, L. *The theory of Open Systems in Physics and Biology*. Science, 111, 1950
2. Borg J. *Role of the future EU maritime policy in shaping new standards of maritime education and employment*. Inter. Consultation Conf. from Education to Employment - How to create a Successful Image of Seafaring in Europe. Sopot, 22 February, 2007
3. Bharadwaj, S.; Menon, A.: *Making Innovation Happen in Organizations: Individual Creativity Mechanisms, Organizational Creativity Mechanisms or Both?* Journal of Product Innovation Management, Volume17, issue 6, 2000
4. Birla M. *FedEx: How the World's leading Shipping Company keeps innovating and Outperforming the Competition*, Wiley, John & Sons, 2005
5. Boutellier, R., Gassmann, O., and von Zedtwitz, M.: *Managing Global Innovation: Uncovering the Secrets of Future Competitiveness*, 2nd ed., Springer, Berlin, 2000
6. Braha, D., Maimon, O. *The Measurement of a Design Structural and Functional Complexity*. IEEE Transactions on Systems, Man and Cybernetics, Part A: Systems and Humans, Volume 28, issue 4, 1998
7. Dougherty, D.; Hardy, C.: *Sustained product innovation in large, mature organizations: Overcoming innovation-to-organization problems*, Academy of Management Journal, Volume 39, No. 5, 1996
8. EC: *Observatory of European SMEs: Analytical report*, Eurobarometer, №196, The Gallup Organization, 2007
9. EC: *Observatory of European SMEs: Technical and Evaluation report*, Eurobarometer, №196, The Gallup Organization, 2007
10. EC: *Attitudes on issues related to EU Transport Policy: Analytical report*, Eurobarometer, №206b, The Gallup Organization, 2007
11. EC: Commission staff working document: *European maritime transport space without barriers reinforcing the internal market for intra-European maritime transport*. Brussels, SEC 2007
12. EC: *Defining the future of the shipbuilding of the European shipbuilding and shiprepair industry*, 2003
13. EC: *Europe in figures. Eurostat yearbook 2006-07*, Luxembourg: Office for Official Publications of the European Communities, 2007
14. EC: *Improving the competitiveness, safety and security of European shipping*, Directorate-General for Energy and Transport, Brussels, 2006
15. EC: *Key figures on Europe. Statistical Pocketbook*, Luxembourg: Office for Official Publications of the European Communities, 2006
16. EC: *Panorama Transport EU. Statistical book*, Luxembourg: Office for Official Publications of the European Communities, 2007
17. Freel, M. (2000): *Barriers to product innovation in small manufacturing firms*, in: International Small Business Journal, Volume18, № 2, Jan. 2000
18. Galende, J.; de la Fuente, J.M.: *Internal factors determining a firm's innovative behaviour*, Research Policy, Volume 32, issue 5, pp. 715-736, 2003
19. Gallin C. *Synergy in ship propulsion- a CODMAE plant for efficient, flexible, and redundant operation*. The Naval Architect, UK, March, 2003
20. Hekkert, M.P., Suurs, R.A.A., Negro, S.O., Kuhlmann, S., and Smits, R.E.N.M. *Function of innovation systems: A new approach for analyzing technological change*. Technological Forecasting and Social Change, Volume 74, issue 4, 2007
21. Hulfactor M. *Overcoming Barriers to Market Understanding: Achieving Innovative Technology Product and Service Success*. Decision Trend Research LLC, Feb., 2006
22. *Knowledge for growth: Role and Dynamics of Corporate R&D*. Proc. of the 1st European Conf., Seville, 2007
23. Pearce R.: *Globalization of R&D: key features and the role of TNCs*, Proceedings of the Expert Meeting *Globalization of R&D and Developing Countries*, United Nations Conference on Trade and Development, Geneva, 2005
24. Robinson, J.E. *Waves of Change*. Published by The Nautical Institute, London. 2007
25. Schumpeter, J. *Business Cycles: A Theoretical, Historical and Statistical Analysis of Capitalist Process*. McGraw-Hill, New-York. 1939
26. Semenov, I., N: *The multivariable co-evolutionary approach to modeling innovative vehicles*. Part I and Part II., PAS, Marine Technology Transactions, Vol.16, 2005
27. *UNCTAD survey on the internationalization of R&D: Current patterns and prospects on the internationalization of R&D*, Occasional Note, United Nations Conference on Trade and Development, Geneva, 2005
28. U.S. Department of Transportation. *US Marine Transportation System: A Vision for the 21st Century*, Washington, November, 2007
29. Zaltman, G.; Duncan, R.; Holbek, J. (1973): *Innovations and Organizations*, Wiley & Sons, 1973.

CONTACT WITH THE AUTHOR

Prof. Iouri N. Semenov
Faculty of Marine Technology
Szczecin University of Technology
AL. Piastów 41,
71-065 Szczecin, POLAND
e-mail: jusiem@ps.pl

Application of expert systems in diagnostics, management and logistics

Zbigniew Korczewski, Assoc. Prof.
Polish Naval University

ABSTRACT



There has been demonstrated base terms concerning expert systems and analysis of their organisation structure. Some possibilities of the expert knowledge codification worked out on the basis of different application of the object-attribute-value triplets have been presented as well.

Keywords: diagnostics, expert systems, logistics, management, power plants, simulate human behaviour

INTRODUCTION

Since the Second World War was finished the British and American research workers who dealt with computer technique have tried to develop research methods which would enable the computers to simulate human behaviour. As a result of such activities a new interdisciplined science domain arised. Nowadays the domain is called artificial intelligence. Within the artificial intelligence expert systems develop in especially dynamical way. They are viewed as intelligent computer programmes that are able to solve complex medical, technical, economic and organisation problems by means of proper usage of available utility knowledge [3, 4, 5, 8]. The solved problems usually need significant human expertise. From such a point of view a generated expert model belonging to the best practitioners as well as implemented infer procedures represent a necessary knowledge to perform an ordered decision task.

Contemporary expert systems posses a lot of merits thanks to which they may supplement perfectly action of „alive” expert. They might be even more reliable in some circumstances. It results from imperfection of human being that characterises:

- ★ tendency, lack of consequence and flexibility in estimation of real situations
- ★ lengthened reaction time on quick changeable events and facts
- ★ difficulties in formulating logical conclusions in case of uncertain and incomplete information
- ★ frequent weariness, insufficient concentration, limited possibilities in reminding themselves a big number of date, that are deepened in difficult, stressful situations.

Additionally, growing popularity of the expert systems results from organisation regards and as a consequence imperfection of the reality surrounded us:

- ✦ personnel rotation within expert cluster
- ✦ high service charges, the higher expert class and complex (expensive) diagnose object the higher service charges are
- ✦ limited possibilities of transporting “alive” experts.

ORGANISATION STRUCTURE OF AN EXPERT SYSTEM

The expert knowledge represents the base of the organisation structure of each expert system [1]. The knowledge consists of following elements:

- ⇒ facts – standing for information matter of an expert object that is commonly available and arranged by the expert of the considered domain
- ⇒ heuristics (rules) – being in the majority of cases personal, in some circumstances subjective and discussible rules of proper interpretation of the possessed facts. The facts are consequently adjusted according to probable, possible to acceptation reasoning and characterise decision taken by the expert in the determined detail level depending, of course, on the extent of the knowledge possessed.

For instance, technical state evaluation of a device by means of an expert system application is carried out by the particular way i.e. mainly on the basis of characterising symptoms occurred during its improper running, observed by the user. The system gathers the knowledge about a technical shape of the device by means of inquiring the user (directly). The answers are selected in an operating memory of the system [4, 6, 7]. The knowledge depends on subjective, often suggestive estimation done by the user who must carefully stare at and listen to the device’s running before starting work with computer-expert. That is why the knowledge is sometimes “washed away” and even uncertain.

The user should be also able to answer the questions asked by the computer program at once.

Computer – expert taking into consideration appropriate confidence factor (CF), formulates diagnosis. Its correctness depends on information incorporated into the knowledge base. The base represents a main junction of the expert system, besides deduction mechanism – Fig. 1. An operating memory is coupled to the knowledge base. It contains current information about the expertised object, obtained from the consultations

Some subsystems are coupled to the deduction mechanism:

- knowledge acquisition
- explanations
- user's interface.

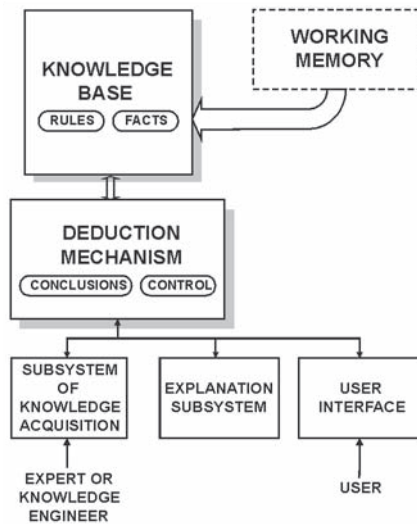


Fig. 1. Organisation structure of an expert system

The deduction mechanism contains deduction strategy and controllers the expert used while manipulating with facts and rules.

The problem of knowledge representation consists in finding such a method of figurative expert knowledge codification which reflects precisely what the expert knows and subsequently – transforming the knowledge into computer language. The specialists constructing the expert systems (having the knowledge base as a ground) deal with foregoing problem. The main task of the computer, that is viewed as the system device relies on efficient manipulating with this knowledge.

Building the semantic networks represents the most frequent method of an expert knowledge representation. Deduction rules are the main link of the networks. They have following form:

„If CONDITION, then CONCLUSION.”

where:

- ☆ **CONDITIONS** – define a determined requirement (requirements) that must be fulfilled in order to apply the given rule
- ☆ **CONCLUSIONS** – determine statement (statements) or activities, that should be done in case while the condition has been fulfilled.

Expert's diagnostic activities are very often connected with (because of various reasons) illogical, imprecision observations and data or even their lack, moreover the gathered information (from expert interviews) are often subjective and difficult to univocal interpretation [1, 2]. Thus the sensible deduction mechanism should be equipped with confidence factors defining a level of correctness for each deduction rule. They

are assigned to the conditions as well as the conclusions within deduction rules, implying scopes of their permissible values and connected with them, a probability of the existence within the scopes. The confidence factor defines accordingly, that is to say, the boundary conditions, that univocally determine what value of the confidence factor is able to activate the determined deduction rule. According to the most common, familiar approach towards the deduction issue there is a classic, double value Boole's algebra [2], where only two value of the confidence factor is distinguished:

- ☆ CF = 0 ("NO"), it means - false
- ☆ CF = 1 ("YES"), it means - true.

Widening the deduction mechanism by i.e. “washes away” reasoning there is distinguished fractional values of the confidence factor given from the scope between 0 and 1 or from the scope between -100 and +100 [3,4]. The confidence factor represents, in this case, probability of choice (expertise) existence on condition that the particular attributes of the expertise object take determined values. They are defined by means of the probability p_{bk} within the successive deduction rules, n . The confidence factor may be determined from the following formulas:

- as an average value of the probabilities:

$$CF = \frac{\sum_{k=1}^n p_{bk}}{n} \quad (1)$$

- as dependent probabilities:

$$CF = \prod_{k=1}^n p_{bk} \quad (2)$$

- as independent probabilities:

$$CF = 1 - (1 - p_{b1})(1 - p_{b2})(1 - p_{b3}) \dots (1 - p_{bk}) \quad (3)$$

OBJECT – ATTRIBUTE – VALUE RELATIONS

The most common way of writing the expert system knowledge is fact's representation by means of OBJECT-ATTRIBUTE-VALUE relations. Within such a notation the particular ATTRIBUTES (features) having particular values are assigned to the OBJECT. The OBJECT may be viewed as a physical unite (concrete, thing), like: human being, technical device or a notion unit, like: a fact of device's purchase as well as a selection of the company manager. In general the ATTRIBUTES are characteristics or features connected with the OBJECT. Dimensions or physical chemistry features stand for typical ATTRIBUTES to the physical OBJECTS. For instance, the purchase price or income tax (VAT) may be the ATTRIBUTE for an events of the device purchase. The OBJECT-ATTRIBUTE constraint is a “have” type.

A VALUE that defines precisely a character or nature of the ATTRIBUTE during especial situation of the evaluation process, represents particular, the last one element of the characteristic triple of the expert knowledge notation. The ATTRIBUTE-VALUE constraint is a “be” type. For instance, a human high may be “tall” or an income tax of the purchase price may amounts “7%”.

In the Fig. 2 we can see an example of the facts representation for expert system by using OBJECT-ATTRIBUTE-VALUE relations. In the analysed case, a flow path of a gas turbine engine stands for the OBJECT. A technical state of flow passages is one of the flow path's ATTRIBUTES. It is possible to attribute VALUE “fouling” to the “technical state of flow passages”.

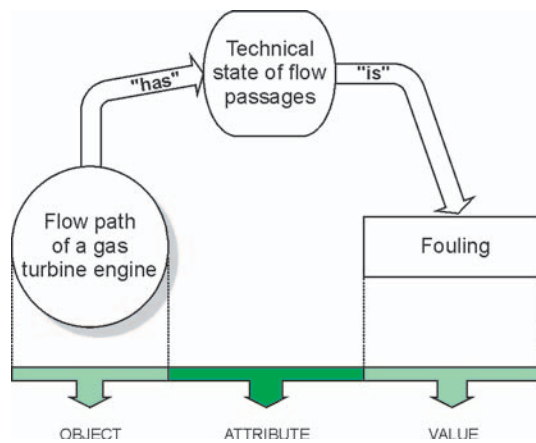


Fig. 2. Object-attribute-value relation

Diagnostic applications

Engineering

Expert systems are very useful, commonly applied diagnostic „tools” for assessing the operation shape of complex technical objects. A necessary expert knowledge is gathered in the form of “failure-symptom” correlations incorporated as a result of:

- ✦ experimental examinations carried out on the real objects,
- ✦ simulation experiments carried out on computer programmes which are especially built for this purpose (if there is no possibilities to examine a real object) [4, 6, 7].

An example of object-attribute-value relation applied within diagnostic evaluation is presented in Fig. 3. The diagnostic evaluations concerns a compressors unit of the naval gas turbine. Diagnosing process relies on the analysis of thermogasdynamic parameters of the air flow along the considered unit. The parameters’ alterations are observed during the engine’s unsteady processes: acceleration and deceleration of the engine shafts.

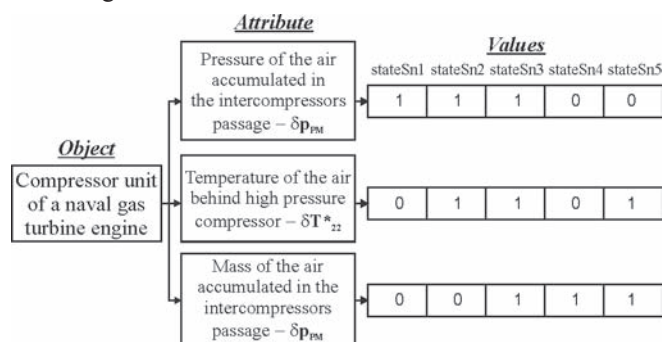


Fig. 3. Object-attribute-value relations within the expert system for diagnostic purposes of the compressors unit of a naval gas turbine engine: „1” – diagnostic parameter δx_j reacts to the unserviceability state S_{ni} by 10% exceedance of the tolerance field limits, „0” – diagnostic parameter does not react to the unserviceability state.

The presented relations results from the simulation experiments worked out on the adequate mathematic model. The following unserviceability operation states of the analysed compressor unit were introduced into the simulation model [7]:

- S_{n1} – fouling the low pressure compressor’s flow passages
- S_{n2} – the simultaneous intensive fouling the inter-blade passages of both the compressors mating in series
- S_{n3} – the air leakage from the intercompressor passage

- S_{n4} – the leakage of one out of two air bleeder valves behind high pressure compressor
- S_{n5} – the defect of the automatic fuel supply system of the engine, resulting in engine acceleration process (it was assumed that the time of the air pressure increase behind the high pressure compressor shortened).

Measurable symptoms of the technical state alterations that put up maximum quantity of gained information about simulated unserviceability states represent the object’s attributes [7]. It is relevant from the data in figure 3 that the observed values of the respective diagnostic parameters enables performing a univocal identification of considered failures of the compressors unit.

Medicine

Diagnosing optic nerve illnesses as well as illnesses of subsequent sections of the optic way represent vulnerable area for an expert system implementation. While the optic nerve is damaged the significant handicap of sight eye or even total blindness of the particular eye may occur. Such disturbances result, among the others, from trauma, optic nerve, inflammation, ishaemia, tumour press or because of atrophy. This is possible to localise focuses that damage the optic way. It may be achieved on the basis of analysing anatomic data of the optic way and disturbances within visual field correlated to the optic way. Precise examinations of a visual field are carried out by means of computer perimeter [9]. Every one of registered lack of display legibility within visual field correspond to particular localisation of damage’s focus. Possible cases of disturbances within visual field have been presented in Fig. 4.

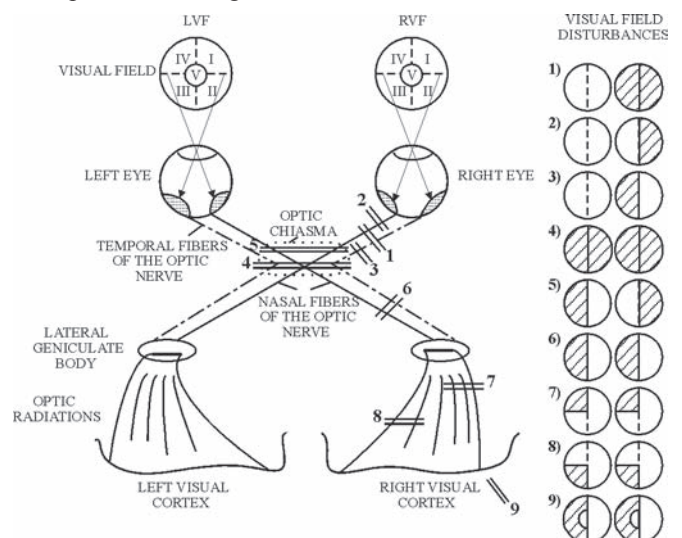


Fig. 4. Visual field disturbances. I, II, III, IV, V – sections of visual field, LVF, RVF – respectively: left and right visual field, 1 – right eye ipsilateral blindness, 2 – loss of temporal (external) part of the right eye visual field, 3 – loss of nasal (internal) part of the right eye visual field, 4 – total blindness, 5 – bitemporal hemianopsia, 6 – left hemianopsia, 7 – left superiol quadrantanopsia, 8 – left inferiol quadrantanopsia, 9 – homonymous hemianopsia with macula saved

Arab numerals denote possible places where optic way’s damages may occur and responding to them disturbances of the visual fields:

Example 1. Entire damage of the optic nerve of the right eye before the optic chiasma gives right eye ipsilateral blindness.

Example 2. Partial, medial damage of the right optic nerve gives loss of temporal (external) part of the right eye visual field.

Example 3. Partial, external damage of the right optic nerve gives loss of nasal (internal) part of the right eye visual field.

Example 4. Entire damage of the optic chiasma gives total blindness.

Example 5. Partial, medial damage of the optic chiasma gives bitemporal hemianopsia.

Example 6. Entire damage of the right optic nerve behind the optic chiasma gives left hemianopsia.

Example 7. Partial, external damage of the right optic radiations gives left superior quadrantanopsia.

Example 8. Partial, medial damage of the right optic radiations gives left inferior quadrantanopsia.

Example 9. Partial damage of the right optic cortex causes homonymous hemianopsia with macula saved. There is possible that the quadrantanopsia may also appear among damages of the optic cortex.

In order to improve diagnostic inferring process concerning physiopathological state of the optic nerve, that bases on a digital notation registered by computer perimeter, it should be firstly defined an adequate set of object-attribute-value expert relation within neurological knowledge that is supported by appropriate results of clinical examinations.

In Fig. 5 there has been proposed the simplest 0-1 (Boole's algebra) approach to the codification of the estimation relations with reference to considered cases of visual field disturbances. It is relevant from the numerical data ascribed to the particular attributes of the examined object that it is possible to define synonymously the state of optic nerve physiopathology. For instance, it can be concluded, when analysing the set of the diagnostic parameters, that a right eye ipsilateral blindness (Sfp1 physiopathological state) happens, if the result of {0000011111} appears during the diagnostic investigation. No identical result appears elsewhere.

It is worth pointing out that disturbances within visual field shown in Fig. 4 represent a significant simplification and occur rarely in so typical manner. In daily experience we usually deal with lacks in visual field that are much more varied, less regular, difficult repeatedly to univocal interpretation. In such a situation result (display) of clinical examination might be characterised by "washes away" values of optic nerve's attributes. As a consequence one test result may correspond to several focuses damaging the optic way.

Managing applications

Very often in our profession there is a necessity to evolve the best candidate for managing position between the company workers. In all the cases this is a very complex and responsible managing task that decides about a father development of the determined organisation cell. Getting to the realisation of the task there should be considered following organisation issues with many-sided way:

- ✧ How to define vital criteria (attributes) for estimation of personal-professional features of the intended manager of an organisation cell?
- ✧ Which personal values (rational and irrational) should be assigned to the respective candidates?
- ✧ Which one out of destined features are especially vital and which one have less meaning?

In order to obtain proper answers for such a way formulated questions (and similar) there should be performed multi-repeated simulation experiments on possible selections of the candidate that are worked out by means of the expert system.

In the first stage of an estimation process there should be properly written a knowledge of the company expert-manager. The knowledge should be written in the form of object-attribute-value relations. In Fig. 6 there has been

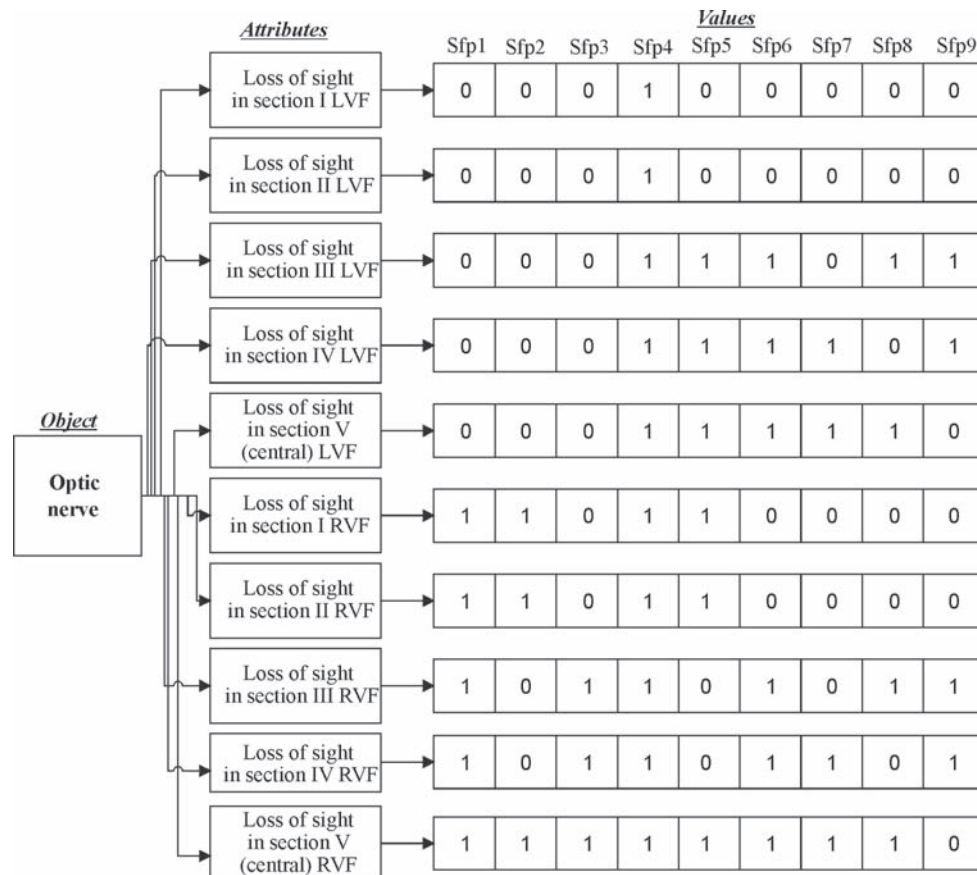


Fig. 5. Object-attribute-value relations within the expert system for estimation of optic nerve physiopathological state Sfp1,...Sfp9 – successive optic nerve physiopathological state – known and recognisable cases of visual field disturbances „1” – registered (computer perimeter) loss of sight, „0” – correct sight

demonstrated an example of such a notation in relation to maritime university.

Perennial organisation experiences encountered from maritime university activity have given possibility to elaborate a wide list of attributes in the considered case of personal-professional features of the created manager of an organisation cell. They represent a psycho-physical portrait of the intended candidate. The silhouette of the potential manager involves professional qualifications as well marked out personality features that the candidate should possess.

Following values have been assigned to the defined attributes:

- ZPwW – much more above requirements – the range of suitability coefficient: (+90)÷(+100),
- PwW – above requirements - the range of suitability coefficient: (+70)÷(+90),
- SW – fulfils requirements - the range of suitability coefficient: (0)÷(+70),
- PnW – below requirements - the range of suitability coefficient: (0)÷(-70),

ZPnW – much more below requirements - the range of suitability coefficient: (-70)÷(-90),

NSW – does not fulfil requirements - the range of suitability coefficient: (-90)÷(-100).

Four candidate have been subjected to the estimation procedure. They have been maritime university lectures. Respective values of the attributes, that influence the worked out professional duties have been assigned to the candidates. The main aim of the expert system consists in carrying out the estimation of the competence for each one candidate and pointing out which candidate is the best choice for the future manager

Logistics applications

An adequately created expert system is able to support the choice and purchase processes concerning different products. The heart of its usage consists in estimation: which one from considered objects is the most suitable to the user's needs. In order to work out such a formulated expert task there should

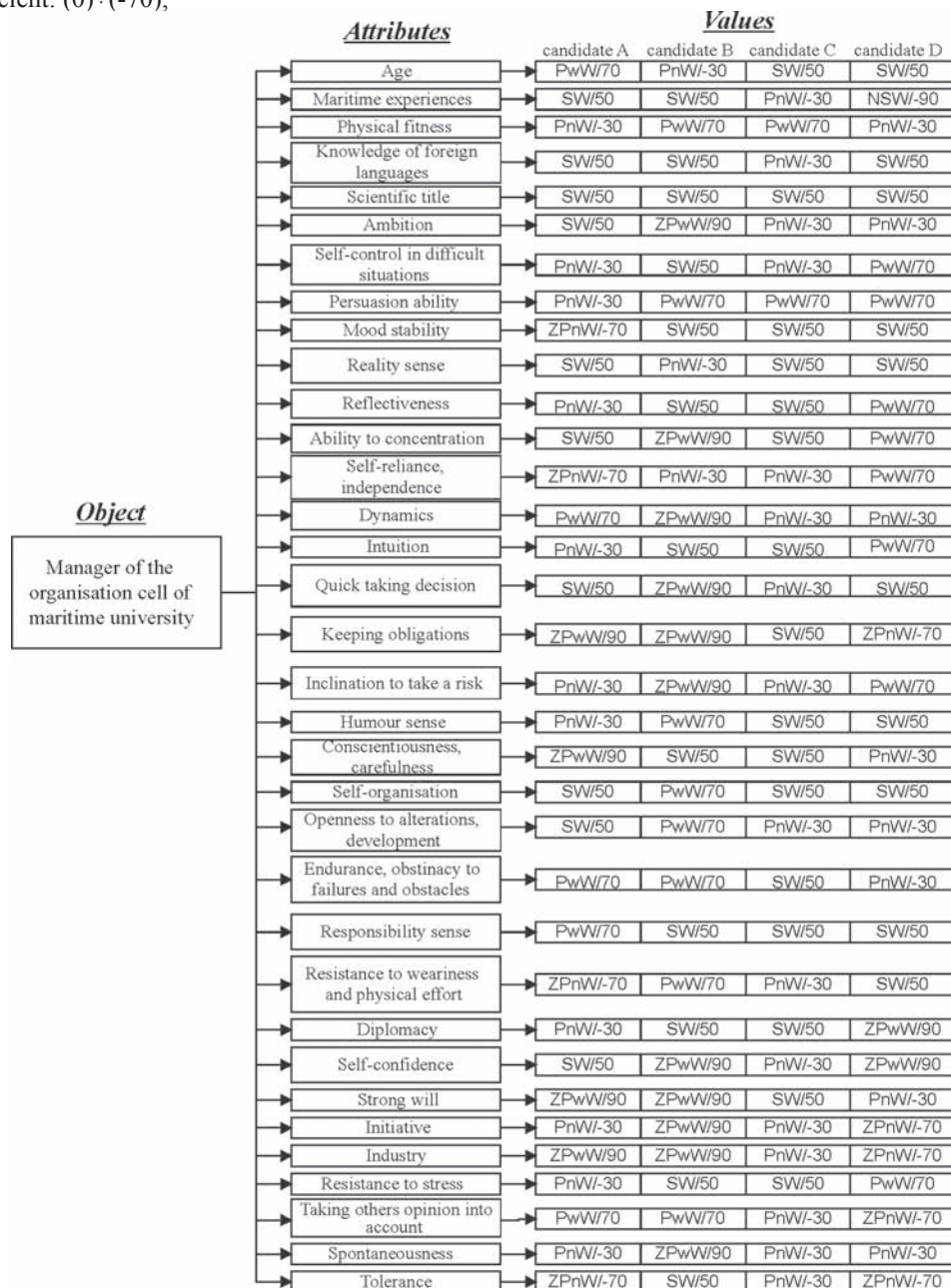


Fig. 6. Object-attribute-value relations within the expert system for estimation of personal-professional features for the selection purpose of the competent manager of an organisation cell of an organisation cell. Company manager decides personally about desirable values of the personal-professional features that potential candidate should possess

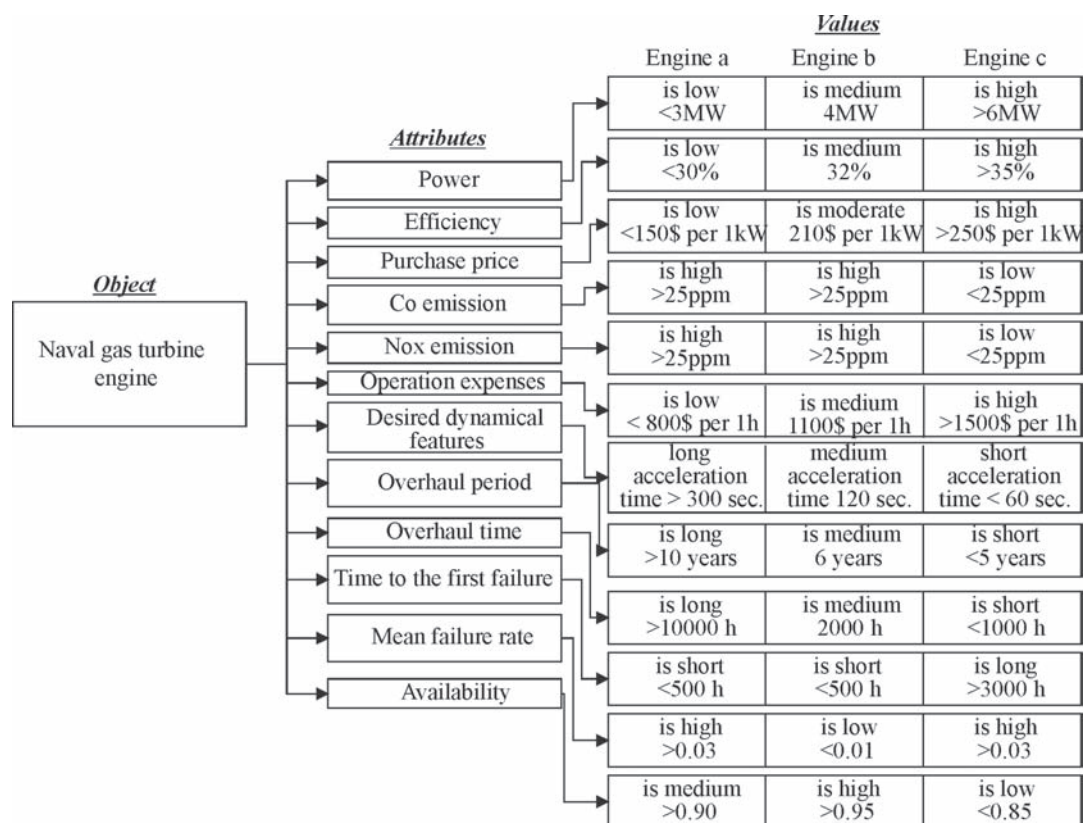


Fig. 7. Object-attribute-value relations within the expert system for choice and purchase a gas turbine engine of the vessel's propulsion

be precisely defined the estimation criteria, and consequently respective measures and values should be assigned to the established criteria.

In marine practise there are often taken decisions concerning a selection of the „most appropriate” type of the main engine for propelling propulsion system. In all the cases the issue needs carrying out universal techno-economical analysis within the world engine market. The performed analysis should be supported with penetrating estimation of the geopolitical situation of the producer's country.

As a result the list of familiar units is coming into existence. It helps to restrict a quantity of the products taken into consideration. We usually dispose several or even more types of propelled engines. Their usefulness for the application is determined with the values of the earlier defined estimation magnitudes. In Fig. 7 there has been demonstrated a trial of the expertise expression of such a task. The expert knowledge is written down by means of object-attribute-value relations. Within considered case the solved problem consists in selection of naval gas turbine engine destined as a cruise engine in twin-shaft COGAG propulsion system.

The attributes of the purchased object represent technical parameters of the estimated engines as well as general purchase and operation expenses. Within demonstrated case there have been only taken into consideration fundamental estimation magnitudes. Their values results from subjective Author's opinion and thus their are controversial and left for Readers to think their over.

CONCLUSIONS

For last several years there has been observed a tendency to more and more interest of the human being with possibilities that a development of the wide-understood computerisation puts up. Expert systems develop stormily confirming their high usefulness to solve complex decision problems. They

are created on the base of more and more perfect computer hardware. The examples of writing the expert system knowledge in the form of object-attribute-value relation shown within the paper demonstrate only a piece of possible applications. They represent for the Author an introduction for further works concerning different way of formulating the conclusion rules, as a base link for every expert system.

BIBLIOGRAPHY

1. Bolc L., Cytowski J.: *Metody przeszukiwania heurystycznego*. PWN, Warszawa 1989.
2. Bolc L., Borodziejewicz W., Wójcik M.: *Podstawy przetwarzania informacji niepewnej i niepełnej*. PWN, Warszawa 1991.
3. Chadwick M., Hannah J.: *Expert systems for microcomputers. An introduction to artificial intelligence*. TAB BOOKS Inc., USA 1996.
4. Cholewa W., Pedrycz W.: *Systemy doradcze*. Skrypt Politechniki Śląskiej, Gliwice 1987.
5. Harmon P., King D.: *Expert systems. Artificial Intelligence in Business*. A Wiley Press Book, New York USA 1985.
6. Kiciński J.: *Systemy komputerowe w budowie i eksploatacji maszyn - stan i perspektywy rozwoju*. XXVII Ogólnopolskie Sympozjum „Diagnostyka Maszyn”, Węgierska Górka 2000.
7. Korczewski Z.: *Identyfikacja procesów gazodynamicznych w zespole sprężarkowym okrętowego turbinowego silnika spalinowego dla potrzeb diagnostyki*. Wydawnictwo monograficzne. AMW Gdynia 1999.
8. Mulawka J.: *Systemy ekspertowe*. WNT Warszawa 1996.
9. Prusiński A.: *Podstawy neurologii klinicznej*. PZWL Warszawa 1989.

CONTACT WITH THE AUTHOR

Assoc. Prof. Zbigniew Korczewski
Mechanic-Electric Faculty,
Polish Naval University
Śmidowicza 69
81-103 Gdynia POLAND
e-mail: zkorczewski@wp.pl

Algorithm for searching out similar ships within expert system of computer aided preliminary design of ship power plant

Maria Meler-Kapcia, Ph. D.
Gdansk University of Technology

ABSTRACT



This paper presents an algorithm for searching out similar ships, implemented in a hybrid system for aiding preliminary design of ship power plant, based on new similarity functions as well as those adapted from literature sources. For searching out similar ships a multi-criterial optimization method of weighed profits was applied.

Keywords: artificial intelligence, neural networks, expert systems, similarity functions, CBR method, multi-criterial optimization, ship design aiding

INTRODUCTION

The elaborated algorithm of searching out similar ships was implemented in a hybrid system of aiding preliminary design of ship power plant with application of selected tools of artificial intelligence such as: Exsys Developer expert system with applied fuzzy logic. Access relational database as well as artificial neural network of back-propagation of errors. It is intended for aiding preliminary ship design process in which designs of similar existing ships are as a rule used.

To this end, the algorithm for searching out similar ships on the basis of introduced similarity functions (rectangular, trapezoidal, triangular, Gaussian) and those adopted from literature sources (that with lower limit, identity test, and fuzzy logic), was elaborated. For searching out similar ships a multi-criterial optimization method of weighing profits was applied.

Models for multi-criterial assessment of design solutions should be described by means of functions containing main ship design parameters.

If it is given the n -dimensional vector of searched parameters, x :

$$x = [x_1, x_2, \dots, x_n]^T \in R^n, n \in N \quad (1)$$

which is assessed according to the m -dimensional vector of criteria (objective functions), $f(x)$:

$$f(x) = [f_1(x), f_2(x), \dots, f_m(x)]^T \in R^m, m \in N \quad (2)$$

and under assumption that the coordinates of the criterial vector are profit functions, then the multi-criterial optimization problem can be defined as the task of multi-criterial maximization of the profit vector:

$$\max_x f(x) \quad (3)$$

In the optimum design process the following decisions can be taken:

- to select one solution and assume it the best
- to select a subset of solutions out of the set of optimum solutions
- to rank all solutions in the order from the best to the worst, i.e. to made their ranking list.

The multi-criterial optimization methods can be divided into:

- classical ones
- ranking ones.

The classical methods consist in integration of many criteria into one. Among other, the weighed criteria method belongs to the classical multi-criterial optimization methods.

The weighed criteria method consists in reducing the multi-criterial optimization to that one-criterial by introducing a substitute criterion in the form of the weighed sum of criteria:

$$Z = \sum_{q=1}^M [w_q \cdot f_q(X)] \rightarrow \text{MIN} \quad (4)$$

where:

$$0 \leq w_q \leq 1 \quad (5)$$

$$\sum_{q=1}^M w_q = 1 \quad (6)$$

In the method a problem is to select a priori values of weighing factors of particular criteria, that may lead to differing solutions.

DESCRIPTION OF THE ALGORITHM FOR SEARCHING OUT SIMILAR SHIPS

The problem of searching out similar ships can be reduced to the task of multi-criterial optimization. Out of the available methods of solving multi-criterial optimization tasks the classical method of weighed profits was implemented. In the method the coordinates of vector of profits (partial similarities) are aggregated into one function of profits (summary similarity) by means of the following transformation:

$$pg(is) = w * pcz(is) \quad (7)$$

where:

- pg(is) – summary similarity
- pcz(is) – vector of partial similarities
- w – normalized row vector of weighing factors:
 $[w_1, w_2, \dots, w_{ip}, \dots, w_{lp}], w_{ip} \in <0,1>$ and $\sum w_{ip} = 1$
- is – ship identifier
- ip – index of ship parameter
- lp – number of ship parameters
- * – scalar product

The process of searching out similar ships begins from the determination of:

- ☆ parameters (database fields) of designed ship
- ☆ lower and upper limits and standard parameters: (P_G, P_D, O_G, O_D) .

The searching out is realized on the basis of ship parameters considered as input data to the algorithm. Number of the parameters is limited and may be contained in the range from one to a few dozen.

Fig. 2 presents the example schematic diagram of the algorithm for searching out similar ships, in which the following blocks can be distinguished:

- ⇒ block of similarity functions (rectangular, trapezoidal, triangular, Gaussian or that with lower limit)
- ⇒ block of threshold functions which determine minimum similarity limit for a given phase of searching process. Threshold value should be greater than zero and smaller than 1, (8)
- ⇒ block of products for realization of the weighed sum $pg(is) = w * pcz(is)$
- ⇒ block of settings of similarity function parameters: kind of function, $S(x)$, upper standard deviation (O_G) and lower one (O_D), lower limit deviation (P_D), and upper one (P_G)
- ⇒ block of settings of the thresholds $Pr[ip]$ and output control. In the case when any of the ship parameters is of a value below the assumed threshold then the considered ship is neglected
- ⇒ block of determination of vector of parameter weighing factors.

Between values of partial similarities and the block of setting threshold values a feedback mechanism is applied to limit number of found similar events (ships) having too low similarity.

The elaborated algorithm for searching out similar ships was based on the application of the following similarity functions:

➔ Rectangular function

In the case of finding the ships identical with the designed ship, design solutions of one of them are used for the design project under elaboration. The function is presented in Fig.1a. If in the database is no identical ships then other functions are applied to calculate similarity in the following

sequence: trapezoidal, triangular, Gaussian, or that with lower limit – for numerical parameters, as well as the identity test (zero-one method) – for text parameters (such as e.g.: (type of main engine, name of its producer or type of screw propeller).

➔ Trapezoidal function

For less stringent design requirements the algorithm can be started by assuming the trapezoidal function as an initial similarity function, shown in Fig. 1c, where: $(P_G - O_G) > (O_D - P_D)$. The similarity in the interval from O_D to O_G is assumed equal 1, and linearly changing - below and over the interval.

➔ Triangular function

The trapezoidal function can be transformed to the triangular one, either symmetrical or non-symmetrical $(P_G - p_p) > (p_p - P_D)$, by assuming values of standard deviations equal zero, see Fig.1b. In the diagrams of trapezoidal and triangular functions different values of upper and lower deviations are assumed in order to show possible choice of asymmetry of the functions in question.

➔ Gaussian function

The Gaussian function, in which asymmetry is also applied, provides the widest range of searching similar objects. It is presented in Fig. 1d.

➔ Threshold function

It determines a minimum limit of similarity for a given phase of searching out process. Value of the threshold Pr should be greater than zero and smaller than 1 (Fig. 1f).

$$H(p_z) = p_z * H(p_z - Pr)$$

where:

$$0 < Pr < 1, H(p_z) - \text{unit jump function} \quad (8)$$

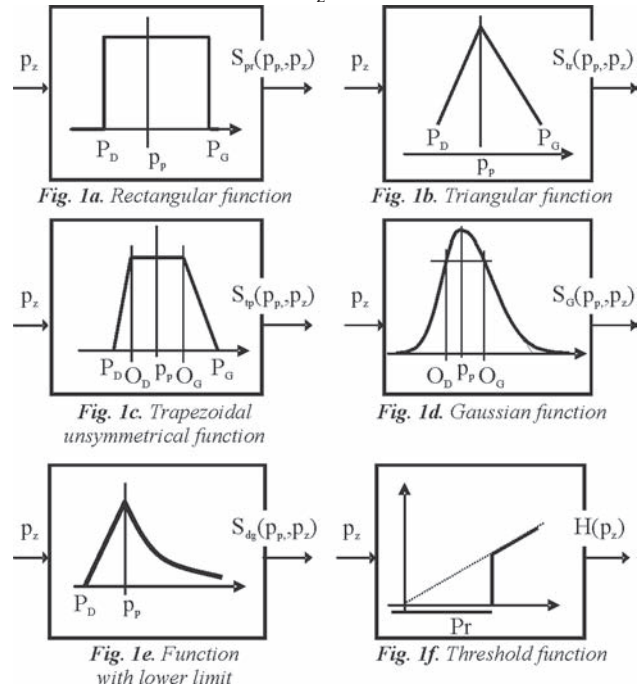


Fig. 1. Functions used in the algorithm for calculation of similarity of ships

where:

- p_p – value of designed ship parameter
- p_z – current value of existing ship
- P_D – lower limit of value of the parameter p_p
- P_G – upper limit of value of the parameter p_p
- O_D – lower standard parameter
- O_G – upper standard parameter

as well as percentage values of deviations of these parameters:

$$\Delta P_D = (p_p - P_D) / p_p * 100\% \text{ - lower limit deviation,}$$

$$\Delta P_G = (p_p - P_G) / p_p * 100\% \text{ - upper limit deviation,}$$

$$\Delta O_D = (p_p - O_D) / p_p * 100\% \text{ - lower standard deviation,}$$

$$\Delta O_G = (p_p - O_G) / p_p * 100\% \text{ - upper standard deviation.}$$

The searching out of a similar ship is performed in the following phases:

- ✦ Ships identical with the designed one are searched out by using the rectangular similarity function. If the set of similar ships is empty the phase 2 is realized.
- ✦ In the case of no identical ships the searching out process by using the triangular similarity function with decreased threshold values of threshold functions, is triggered. This can result in: the empty set of similar ships (then the phase 3 is realized) or the set containing from one to many similar ships.
- ✦ In the case of no similar ships the searching out process based on the trapezoidal similarity function is realized. If many similar ships are found then the threshold values of threshold functions are increased and the searching out process is repeated so as to reduce number of found ships down to a few at the most.
- ✦ When no similar ships are found the Gaussian similarity function is applied for further calculations and if it does not provide a result the phase 5 is realized.
- ✦ The similarity function with lower limit is applied. It is characterized by the feature that in searching out similar ships it takes into account broader and broader range of values of ship parameters over design value.

In the successive phases of the algorithm the similarity functions are called in the same sequence, shown in Fig. 2.

The above specified phases of searching out process are initiated automatically, however the designer is allowed to interfere in each of them.

The schematic diagram of the algorithm is presented in Fig. 3.

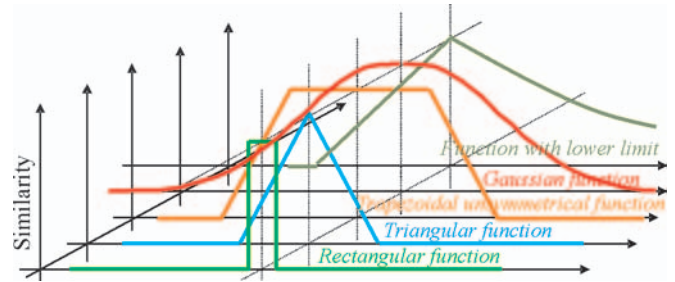


Fig. 2. Ship similarity functions called in successive phases of the ship searching out algorithm

IMPLEMENTATION OF THE ALGORITHM FOR SEARCHING OUT SIMILAR SHIPS

The main function of the elaborated algorithm is to search similar ships out of the database. Number of such ships can be very different: from one to even a few dozen. The number results from applied similarity function as well as from size and content of the database and assumed design parameters such as ranges and thresholds of similarity function. The parameters are determined in advance by the designer before initiation of the process of searching out similar ships. Next, name of database file and designed ship's data should be put in. Then the process of calculation of similarity of particular parameters, such as main engine's power and its rotational speed, and of similarity of threshold function, is started. Final similarity of a parameter is obtained by calculating the weighed similarity of the parameter. The calculation process of weighed similarities of particular parameters is ended when all introduced ship parameters are taken into account, and their weighed sum constitutes a partial similarity (of main propulsion system, for example). Sum of the partial similarities constitutes the total

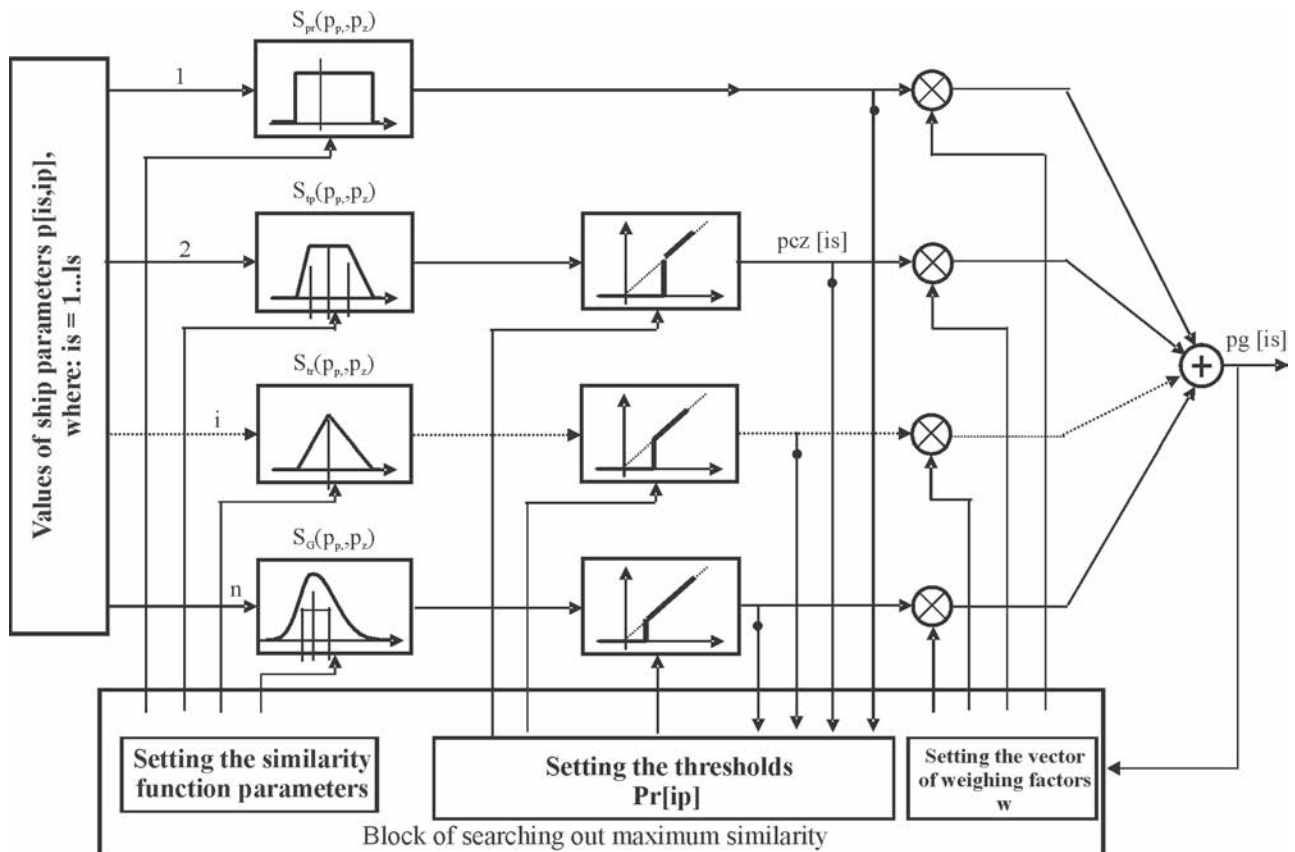


Fig. 3. Schematic diagram of the algorithm for searching out similar ships

weighed similarity of entire ship, on the basis of which similar ships are searched out.

For practical reasons it has been assumed that in the algorithm of searching out similar ships percentage values of deviations of parameters of most similar ships, from their input values, as well as p_p value, are applied, as shown in Tab. 2. To obtain real values of the parameters the following formulae are used:

$$P_D = p_p - \frac{p_p * \Delta P_D}{100} \quad (9)$$

$$O_D = p_p - \frac{p_p * \Delta O_D}{100} \quad (10)$$

$$P_G = p_p + \frac{p_p * \Delta P_G}{100} \quad (11)$$

$$O_G = p_p + \frac{p_p * \Delta O_G}{100} \quad (12)$$

where:

$\Delta P_D = (p_p - P_D) / p_p * 100\%$ – lower limit deviation,
 $\Delta P_G = (p_p - P_G) / p_p * 100\%$ – upper limit deviation,
 $\Delta O_D = (p_p - O_D) / p_p * 100\%$ – lower standard deviation,
 $\Delta O_G = (p_p - O_G) / p_p * 100\%$ – upper standard deviation.

In Tab. 1 example values of more important parameters of the main propulsion system of designed ship are given.

Tab. 1. Values of design parameters of the ship main propulsion system (NG)

Ship	Number of main engines (ME)	Type of ME	Producer of ME	ME output power [W]	Rotational speed of ME [rpm]	Number of propellers
BXXX	1	6RTA76	SULZER	16500	110	1

The elaborated functions for similarity calculation are presented and tested on the basis of two numerical parameters, i.e. ME output power and rotational speed. The analysis was performed for example values of the limit and standard deviations of the parameters as well as example values of their weighing factors, given in Tab. 2;

Tab. 2. Values of weighing factors of design parameters of main propulsion system (NG)

(Variant 1)

ME output power [W]	Rotational speed of ME [rpm]	Number of main engines (ME)	Type of ME	Number of propellers	Producer of ME
0.3	0.2	0.2	0.1	0.1	0.1

as well as the limit and standard deviations, given in Tab. 3.

Tab. 3. Values of limit and standard deviations of design parameters of main propulsion system (NG)

Parameter	P_p	ΔP_D %	ΔO_D %	ΔP_G %	ΔO_G %
Power [kW]	16500	20	10	20	10
Rot. speed [rpm/min]	110	20	10	20	10

The summary similarities calculated by means of the database application according to particular functions, for assumed values of weighing factors, limit and standard deviations, are given in Tab. 4.

Tab. 4. Summary similarities of numerical parameters of main propulsion system (NG)

Ship	Power [kW]	Speed [rpm/min]	Pod NG with lower limit	Pod NG trapezoidal	Pod NG Gaussian	Pod NG triangular
124	18 160.00	110.00	0.47	0.50	0.31	0.35
41	18 160.00	110.00	0.47	0.50	0.31	0.35
60	18 160.00	110.00	0.47	0.50	0.31	0.35
18	17 400.00	122.00	0.46	0.48	0.28	0.31
109	17 400.00	122.00	0.46	0.48	0.28	0.31

The combined similarities of the NG obtained from summation of similarities of numerical and non-numerical parameters (calculated by using identity test method), are presented in Tab. 5.

Tab. 5. Combined similarities of main propulsion system (NG)

Ship	Pod NG non-numerical	Pod with lower limit	Pod trapezoidal	Pod Gaussian	Pod triangular
60	0.30	0.77	0.80	0.61	0.65
41	0.30	0.77	0.80	0.61	0.65
124	0.30	0.77	0.80	0.61	0.65
109	0.30	0.76	0.78	0.58	0.61
18	0.30	0.76	0.78	0.58	0.61

Values of limit and standard deviations as well as weighing factors are of an example character and have been assumed arbitrarily on the basis of the designer's decision supported by his experience and practice. However the elaborated algorithm for calculation of ship similarity is of a versatile character and can be applied to arbitrary values of design parameters.

SUMMARY AND CONCLUSIONS

The functioning of the algorithm was analyzed on the basis of three example cases:

Case 1. Assumed symmetrical values of limit and standard deviations of numerical parameters (ME output power and rotational speed)

Case 2. Assumed greater values of upper limit deviation and upper standard deviation of both parameters in question

Case 3. Assumed symmetrical values of limit and standard deviations of one parameter (ME output power), and smaller values of lower limit and standard deviations, than those of upper ones, of other parameter (ME rotational speed).

On their basis the following detail conclusions can be drawn:

- In Case 1 symmetrical values of the limit and standard deviations of the considered numerical parameters (ME output power and rotational speed) were assumed. The applied increase of values of weighing factors of the selected non-numerical parameters (ME number and type) and the simultaneous decrease of values of the weighing factors of the selected numerical parameters, resulted in:
 - the increase of values of the summary similarity of the non-numerical parameters,
 - the significant decrease of the summary similarity of the numerical parameters as well as the decrease of values of the combined similarity, most in the case of application of the trapezoidal method, and least – in the case of Gaussian method. The same similar ships were searched out.
- In Case 2 the assumption of greater values of the upper limit and standard deviations and smaller values of the lower deviations of both selected parameters (ME output power and rotational speed) resulted in a relatively large decrease of the similarity values for all analyzed similarity calculation methods, however it was the greatest in the case of the triangular method, and the least – in the case of Gaussian one. This did not result in a change in searching out similar ships: the same similar ships were found.
- In Case 3 where symmetrical values of the limit and standard deviations of one parameter (ME output power) and smaller values of the lower limit and standard deviations, than upper values of other parameter (ME rotational speed), were assumed, the following was observed:
 - almost the same decrease of similarity value in the case of application of the trapezoidal and triangular functions,
 - the greatest decrease of similarity value in the case of application of Gaussian function,
 - no change of similarity value in the case of the function with lower limit. In the Case 1 a greater number of similar ships was selected than in the Case 1 and 2.

The above presented example cases illustrate that the algorithm is flexible in searching out similar ships. The

designer, by choosing values of weighing factors, is capable of searching out ships having one, strictly defined feature, or some purposefully emphasized.

Also, by correcting values of the standard and limit deviations, increasing or decreasing tolerance of calculated results can be achieved.

It is also possible, by proper choice of similarity function, to assess similarity within a given range of values, as well as to obtain distributions of sample size of ships.

BIBLIOGRAPHY

1. Kowalski Z., Meler-Kapcia M., Zieliński S.: *A method for determining similarity of ships in the process of selecting automation systems for power systems* (in Polish). Scientific Bulletins of Mechanical Faculty, Koszalin University of Technology, No. 27 (Zeszyty Naukowe Wydż, Mechanicznego Politechniki Koszalińskiej), Miłno 2000.
2. Kowalski Z., Arendt R., Meler-Kapcia M., Zieliński S.: *An expert system for aided design of ship systems automation*. Expert Systems with Applications, No. 3, Vol. 20, 2001.
3. Kowalski Z., Meler-Kapcia M., Zieliński S.: *Choice of methods for calculation of similarity of ships in aiding ship power plant automation design* (in Polish). Proc. of The Technical Scientific Conference „Automation 2000” (Materiały Konferencji Naukowo-Technicznej Automation 2002), PIAP, Warszawa 2002.
4. Lee D., Lee K. H.: *An approach to case-based system for conceptual ship design assistent*. Expert Systems with Applications, No. 2, Vol. 16, 1999.
5. Meler-Kapcia M., Zieliński S., Kowalski Z.: *On application of the Case-Based Reasoning methods in ship automation design*. Polish Maritime Research, No. 2, 2003.
6. Meler-Kapcia M., Zieliński S., Kowalski Z.: *The aiding of ship power plant automation design by means of CBR method* (in Polish). Proc. of The Technical Scientific Conference „Automation 2004” (Materiały Konferencji Naukowo-Technicznej Automation 2004), PIAP, Warszawa 2004.
7. Meler-Kapcia M., Zieliński S., Kowalski Z.: *On application of some artificial intelligence methods in ship design*. Polish Maritime Research, No.1, 2005.
8. Reich Y, Barai S. V.: *A methodology for building neural networks models from empirical engineering data*. Engineering Applications of Artificial Intelligence, Vol. 13, 2002.
9. Zbroja S.: *Case-Based Reasoning in data and knowledge bases – selected aspects of formal case representation* (in Polish). 2nd Domestic Conference on Computer Methods and Systems in Scientific Research and Engineering Design (II Krajowa Konferencja: Metody i systemy komputerowe w badaniach naukowych i projektowaniu inżynierskim). Kraków, October 1999.

CONTACT WITH THE AUTHOR

Maria Meler-Kapcia, Ph. D.
Faculty of Ocean Engineering
and Ship Technology
Gdansk University of Technology
Narutowicza 11/12
80-952 Gdansk, POLAND
e-mail : mariola@pg.gda.pl